Electronic Thesis and Dissertation Repository

11-29-2011 12:00 AM

Reactivity of Dimethylplatinum (II) Complexes

Muhieddine A. Safa, *The University of Western Ontario*

Supervisor: Dr. Richard J. Puddephatt, *The University of Western Ontario*
A thesis submitted in partial fulfillment of the requirements for the Doctor of Philosophy degree in Chemistry

REACTIVITY OF DIMETHYLPLATINUM(II) COMPLEXES

(Thesis Format: Monograph)

by

Muhieddine Ahmad Safa

Department of Chemistry

Submitted in partial fulfilment

of the requirements for the degree of

Doctor of Philosophy

The School of Graduate and Postdoctoral Studies

The University of Western Ontario

London, Ontario

November, 2011

THE UNIVERSITY OF WESTERN ONTARIO

THE SCHOOL OF GRADUATE AND POSTDOCTORAL STUDIES

CERTIFICATE OF EXAMINATION

Chief Advisor

Dr. Richard J. Puddephatt
_____

Advisory Committee

Dr. Kim M. Baines
_____

Dr. Yang Song
_____

Examining Board

Dr. Paul J. Ragogna
_____

Dr. John F. Corrigan
_____

Dr. Ulrich Fekl
_____

Dr. Jose E. Herrera
_____

The thesis by

Muhieddine Safa

entitled

Reactivity of Dimethylplatinum(II) Complexes

is accepted in partial fulfilment of the

requirements for the degree of

Doctor of Philosophy

Date _____

Dr. Margaret J. Kidnie
_____

Chairman of Examining Board

ii

ABSTRACT

This thesis describes a study of dimethylplatinum(II) and dimethylplatinum(IV) complexes containing bidentate nitrogen donor ligands. This work deals with oxidative addition, and reductive elimination chemistry, and it focuses on synthesis, characterization, and reaction mechanisms in studies of these complexes.

The compound [PtMe$_2$(bpe)], bpe = 1,2-*bis*(2-pyridyl)ethane, is easily oxidized to give octahedral organoplatinum(IV) complexes and the subsequent chemistry is profoundly influenced by the accompanying strain induced in the 7-membered Pt(bpe) chelate ring. On reaction of [PtMe$_2$(bpe)] with HCl, the initial product [PtHClMe$_2$(bpe)] undergoes reductive elimination of methane to form [PtClMe(bpe)]. In contrast, methyl iodide reacts with [PtMe$_2$(bpe)] to give [PtIMe$_3$(bpe)], and this decomposes by loss of the bpe ligand to give the cubane [(PtIMe$_3$)$_4$] and not by reductive elimination. Finally, a new class of platinum(IV) double cubane clusters was obtained on oxidation of complex [PtMe$_2$(bpe)] with either hydrogen peroxide to give [Pt$_4$(μ-OH)$_4$(μ_3-OH)$_2$Me$_{10}$], as a mixed complex with [PtMe$_2$(CO$_3$)(bpe)], or with oxygen in methanol to give [Pt$_4$(μ-OH)$_2$(μ-OMe)$_2$(μ_3-OMe)$_2$Me$_{10}$].

The oxidation of the complex [PtMe$_2$(bps)], bps = bis(2-pyridyl)-dimethylsilane, by oxygen, hydrogen peroxide or dibenzoyl peroxide in the presence of water or alcohol gives the complex cation, [PtMe$_3$(κ^3-N,N,O-HOSiMe(2-C$_5$H$_4$N)$_2$)]$^+$, in a reaction involving easy cleavage of a methylsilicon bond. Treatment of the complex [PtMe$_2$(bps)] with B(C$_6$F$_5$)$_3$ in trifluoroethanol in air gives the complex [Me(bps)Pt-OSiMe(2-C$_5$H$_4$N)$_2$PtMe$_3$]$^+$ [B(OCH$_2$CF$_3$)(C$_6$F$_5$)$_3$]$^-$. The unique binuclear platinum complex is formed via the competitive methyl platinum group cleavage from [PtMe$_2$(bps)] by the acid H[B(OCH$_2$CF$_3$)(C$_6$F$_5$)$_3$] to give

the platinum(II) fragment and oxidation by air to give the platinum(IV) fragment. Combination of the two units then gives the binuclear complex which involves a very easy methylsilicon group cleavage reaction.

The platinum(II) complexes containing five-membered heterocyclic imidazole ligands show high reactivity to a broad variety of alkyl halides, peroxides, and halogens forming stable platinum(IV) complexes. The dimethylplatinum(II) complex [PtMe$_2${(mim)$_2$C=CH$_2$}], (mim)$_2$C=CH$_2$ = 1,1-bis(1-methylimidazole-2-yl)ethene reacts with dichloromethane to give the dimethylplatinum(IV) complex [PtCl(CH$_2$Cl)Me$_2${(mim)$_2$C=CH$_2$}]. The product exists as a mixture of two isomers, the *cis* isomer as the kinetic product and the *trans* isomer as the thermodynamic product.

The dimethylplatinum(II) complex [PtMe$_2$(DECBP)], DECBP = 4,4'-diethoxycarbonyl-2-2'-bipyridine], undergoes easy oxidative addition to the corresponding platinum(IV) complexes. The reactions of the complex [PtMe$_2$(DECBP)] with alkyl bromides RCH$_2$Br, which have hydrogen bond donor or acceptor functional groups, result in the formation of stable platinum(IV) complexes. Those complexes self-assemble in the solid state to form supramolecular polymers via the intermolecular OH•••O=C, N-H•••Br, OH•••BrPt, interactions, with other predicted interactions such as the π-stacking, and the C(H)•••BrPt secondary weak interactions.

Keywords: Platinum complexes, oxidative addition, reductive elimination
bidentate nitrogen donor ligands, NMR spectroscopy, X-ray
crystallography, H-D exchange.

ACKNOWLEDGEMENT

I would like to express my deepest appreciation to my supervisor, Dr. Richard J. Puddephatt, for his patience, encouragement, and guidance during the course of this work.

I would like to express my sincere thanks to Drs. Jennings, Payne and Popov for their crystallographic expertise. Special thanks to Dr. M. Jennings, Dr. G. Popov, Dr. Benjamin Cooper, and Mrs. Aneta Borecki for solving the X-ray structures.

Many thanks are also extended to Dr. Mathew Willans, who has provided excellent NMR service. I would also like to acknowledge Doug Hairsine for his help with mass spectrometry.

I would like to thank faculty, graduate students and staff for their help and support during the course of this work.

I would also like to express my gratitude for the friendships formed among the graduate students. In particular I would like to mention Anas Lataifeh, Matthew McCready, Mohammad Afifi, Kyle Pellarin and Shawn Robinson.

Most of all, I would like to thank my family for their support, patience and understanding throughout the course of my studies. I couldn't have done it without them.

To my Family

TABLE OF CONTENTS

LIST OF TABLES

LIST OF FIGURES

ABBREVIATIONS

a, b, c, α, β, γ = unit cell parameters

A = absorbance

Å = Ångstrom = 10^{-8} meters

Anal Calcd = analysis calculated

Ar = aryl

bipy = 2,2'-bipyridyl

dpe = 1,2-bis(2-pyridyl)ethane

bps = bis(2-pyridyl)dimethylsilane

br = broad

^{t}Bu = *tert*-butyl

^{o}C = degrees centigrade

δ = chemical shift

DECBP = 4,4'-diethoxycarbonyl-2-2'-bipyridine

d = doublet

dd = doublet of doublet

dt = doublet of triplets

DPK = di-2-pyridyl ketone

Et = ethyl

Et_2O = diethylether

Eq = equation

g = gram

$\Delta G^{\ddagger}$ = free energy of activation

h = Planck's constant

hv = electromagnetic radiation

Hz = hertz

IR = infra-red

J = coupling constant

^{x}J(AB) = coupling constant between nuclei A and B through X number of bonds

J = joule

K = degrees kelvin

L-L/N-N = bidentate diimine ligand

MS = mass spectrometry

m = meta

Me = methyl

MHz = megahertz

min = minutes

mL = millilitre

mmol = millimole

MW = molecular weight in g/mol

M = molarity or metal center, depending on the context

mol = mole

m = multiplet

nm = nanometre

NMR = nuclear magnetic resonance

N = Avogadro's number

o = ortho

p = para

ppm = parts per million

Ph = phenyl

Py = pyridyl

PN = 2-(di-tert-butylphospinomethyl)pyridine

q = quartet

R = ideal gas constant or alkyl/aryl, depending on the context

s = singlet

S_N2 = bimolecular nucleophilic reaction

t = triplet

T = temperature

Tc = coalescence temperature

tert = tertiary

UV = ultraviolet

VT-NMR = variable temperature-NMR (^{1}H unless otherwise stated)

X = halogen (unless otherwise stated)

Z = number of formula units in unit cell

CHAPTER 1

General Introduction

1.1 The History of Platinum

Platinum, from the Spanish "platina" is translated as little silver, is a metal with many unique properties. Later on it became known as Platina del Pinto, which is a small river near Popayan in New Granada, and then known as "oro blanco", white gold, or "juan blanco". Local archives had the first reference of platina in 1707, where it had been used to adulterate the gold.[1] The metal was intriguing to many people due to its high melting point and corrosion resistant properties, so platinum was used for lining crucibles used in the production of special glasses. It was first introduced to Europe by Ulloa, the Spanish explorer of Colombia. The first samples of platinum to reach Europe were brought by Charles Wood, a British metallurgist in 1741.[2] Two centuries later, the Europeans realized that platina was actually a mixture of elements: platinum, palladium, rhodium, iridium, osmium, and ruthenium. Today, platinum is found in ores from Canada, China, Colombia, South Africa and Russia. These ores tend to contain nickel and copper along with platinum too.

1.2 Platinum in Organometallic Chemistry

Organometallic complexes are compounds containing at least one chemical bond between a carbon atom and a metal atom. Zeise's salt was the first organometallic compound, prepared in 1827 by Zeise.[3] He produced the salt by boiling a solution of potassium hexachloroplatinate in ethanol, obtaining the complex, $K[Pt(C_2H_4)Cl_3].H_2O$. Ever since that time, organoplatinum chemistry has been of major interest to chemists. The chemistry of platinum metal is dominated by three major oxidation states, 0, +2, and +4. Also known are the +1, +3, +5, and +6 oxidation states. Furthermore, formal negative oxidation states for platinum have been reported in platinum carbonyl cluster complexes.[4] Organoplatinum complexes can easily undergo two-electron

oxidation and reduction among the three dominant oxidation states, via oxidative addition and reductive elimination reactions, which typically involve the two-electron transfer between the ligands and platinum center.[5]

Organoplatinum complexes can exist in many different geometries. Platinum(0) complexes usually favor tetrahedral geometry as in the case of $[Pt(PF_3)_4]$,[6] or trigonal planar geometry as for $[Pt\{Sn(NR_2)_2\}_3]$.[7] Square planar geometry is preferred by platinum(II) complexes as for $[PtMe_2(bipy)]$, bipy = 2,2'-bipyridyl, while platinum(IV) complexes favor octahedral geometry such as in $[PtIMe_3(bipy)]$, bipy = 2,2'-bipyridyl.[8] Platinum has three principal non-radioactive isotopes ^{194}Pt, ^{195}Pt, and ^{196}Pt, which exist with roughly equal natural abundance. The isotope ^{195}Pt is particularly significant in organometallic chemistry. Platinum compounds are typically studied using NMR spectroscopy due to the presence of the spin active isotope ^{195}Pt, which has a nuclear spin of ½ and is found in 33.7% natural abundance. In compounds of platinum, the ^{195}Pt atoms can couple with other NMR active nuclei such as ^1H, creating unique patterns in the NMR spectrum. The compounds of third-row transition metals such as platinum often react more slowly than first and second row transition metals in reactions such as ligand substitution, which makes platinum complexes ideal for the characterization of reaction intermediates and the study of reaction mechanisms.[9] The main focus in this thesis is on square planar platinum(II) and octahedral platinum(IV) complexes.

1.3 Oxidative Addition[10]

Oxidative addition is a class of reaction, which is a very important process in organometallic chemistry that proceeds via several mechanistic pathways. This type of reaction involves the oxidation of a metal via the addition of a substrate X-Y, which increases the coordination number and the formal oxidation state by two units due to the formation of two new bonds M-X and M-Y. The term is usually used to describe a two-electron oxidation, but one-electron oxidative addition reactions are also known. In two-electron oxidative addition the formal charge of the metal increases by 2, and two electrons are removed from its d-electron configuration (Equation 1.1). While in one-electron oxidative addition the formal oxidation state increases by 1, and one electron is removed from the d-electron configuration (Equation 1.2). In both cases, there is an overall two-electron change, $M^{(n)}$ to $M^{(n+2)}$ or $2M^{(n)}$ to $2M^{(n+1)}$, and an increase in the coordination number of the metal center.

$$M^{(n)} + \text{X-Y} \rightleftharpoons \underset{X-M^{(n+2)}}{\overset{Y}{|}} \qquad\qquad (1.1)$$

$$2M^{(n)} + \text{X-Y} \rightleftharpoons X-M^{(n+1)} + Y-M^{(n+1)} \qquad\qquad (1.2)$$
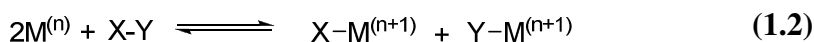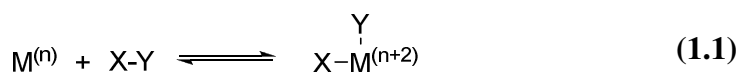
Oxidative addition reactions are common for 16-electron square planar platinum(II) complexes, and lead to the formation of 18-electron octahedral platinum(IV) complexes. These reactions could often occur in an 18-electron complex, where a two-electron site must be opened in the complex by the loss of a ligand. There are three different classes of substrates for oxidative

addition. Class A substrates which are non-polar or have low polarity (e.g., H_2, R-H, B-H, and R$_3$Sn-H) usually react via two different oxidative addition mechanisms, *cis* oxidative addition (concerted), and homolytic bond activation. Reagents with polar bonds (class B substrates), such as alkyl halides (R-X), often undergo oxidative addition through formal one-electron or two-electron mechanisms. There are two categories of one-electron mechanisms, the free radical chain mechanism, and the free radical non-chain mechanism. Formal two-electron oxidative addition proceeds usually via bimolecular S_N2 type mechanism. The mechanism of reaction of the class C substrates, such as O_2 and epoxides, are similar to class B substrates.

1.3.1 Three-Centre Concerted Mechanism

Substrates for oxidative addition reactions which are non-polar or have low polarity such as H_2 and alkanes usually react by a three-center, or concerted, oxidative addition mechanism as shown in Scheme 1.1. Class A substrates are often very difficult to activate, so the oxidative addition of this category of reagents to platinum(II) complexes is not widely represented. The reaction mechanism involves the formation of a three-centred transition state between the metal center and the X-Y substrate, which then proceeds to form the product of *cis* addition. Coordinative unsaturation is necessary for the reaction to proceed, and retention of configuration at chiral carbon is expected. Class A substrates rarely undergo oxidative addition via homolytic bond activation and two metal centers are needed (Scheme 1.2).

$$M^{(n)} + \text{H-H} \longrightarrow \left[M \overset{H}{\underset{H}{\cdots}} \right]^{\ddagger} \longrightarrow \text{H}-\overset{\overset{H}{|}}{M}^{(n+2)}$$

Scheme 1.1

5
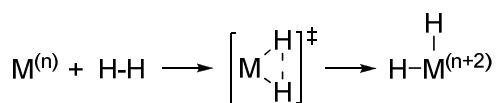
$$2\,M^{(n)} + H\text{-}H \longrightarrow \left[\begin{array}{c} M \underset{H}{\overset{H}{<}} M \\ \text{or} \\ M\text{-}H\text{--}H\text{--}M \end{array} \right]^{\ddagger} \longrightarrow 2\,H\text{--}M^{(n+1)}$$
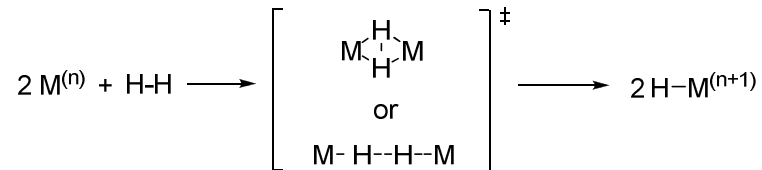
Scheme 1.2

Concerted three center oxidative addition is initiated by an associative substitution reaction. The intramolecular oxidative addition of a C-H bond is achievable upon using an electron rich platinum(II) complex such as $[PtMe_2\{PhCH=N(CH_2)_2NMe_2\}]$.[11] The reaction follows first-order kinetics, and it proceeds via a concerted C-H oxidative addition to form a five-coordinate intermediate (Chart 1.1a), which is followed by the reductive elimination of CH_4. By the use of specially designed ligands, the *ortho*-metallation can occur in which C-H bond undergoes a secondary bonding with the platinum center.[12] Chart 1.1 shows some of the proposed five coordinate intermediates which would lead to the intramolecular oxidative addition of C-H bonds.

(X = H, F)

(a)   (b)

Chart 1.1

6
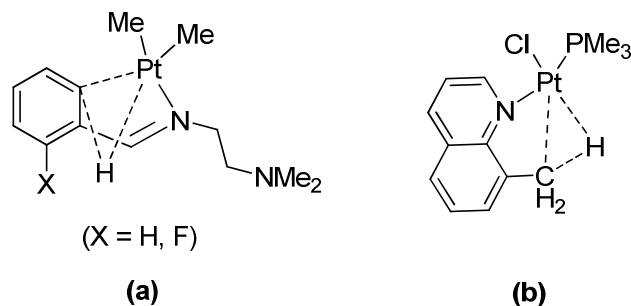
1.3.2 Bimolecular S$_N$2 Mechanism

Reagents with polar bonds often undergo oxidative addition by the S$_N$2 mechanism (Scheme 1.3). The oxidative addition of an alkyl halide to a metal complex proceeds via the attack from a nucleophilic metal at the carbon center to break the C-X (X = I, Br, Cl, F) bond in the substrate. The S$_N$2 mechanism is found in the addition of methyl, allyl, and benzyl halides. The reaction kinetics are second order, and the reaction involves an inversion of configuration at a chiral electrophilic carbon of the substrate. The rate of the reaction is accelerated using polar solvents, and the alkyl halides show greater reactivity in the order Me > primary > secondary >> tertiary, and I > Br > Cl >> F. In some cases, oxidative addition occurs through coordination of an anion to a neutral metal complex, which proceeds to generate an anionic complex prior to the oxidative addition of the C-X bond via S$_N$2 mechanism (Scheme 1.4).

X = Cl, Br, or I
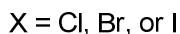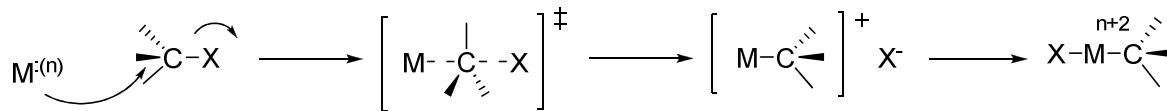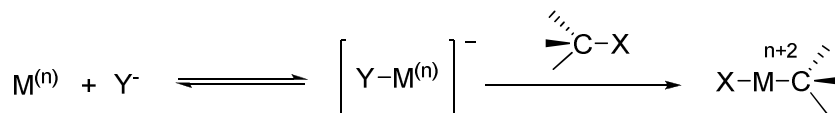
Scheme 1.3

Scheme 1.4

Another related mechanism is known in reactions with hydrogen halides, which proceeds via the dissociation of hydrogen halides in solution, and then the anion and the proton add to metal complexes in different steps. Usually, the metal complex is basic enough to be protonated, and then the anion coordinates to give the final product. If the initial complex has a net positive charge, the reaction often proceeds by coordination of the halide ion, followed by the protonation of the intermediate complex. The formation of a cationic intermediates were proposed for the reaction of methyl iodide with the platinum(II) complex $[PtPh_2(bipy)]$, which was observed in polar solvents such as CD_3CN at low temperatures using ^{1}H-NMR spectroscopy. That process is then followed by the rapid substitution of the charged species to produce the platinum(IV) complex $[PtIMePh_2(bipy)]$.[13]

1.3.3 Radical Non-chain Mechanism

Radical mechanisms in oxidative addition often lead to mixtures of products.[14] The free radical non-chain mechanism is shown in Scheme 1.5, where the alkyl halide R-X is the substrate oxidatively added to the metal center. The reaction mechanism proceeds through the coordination of the R-X substrate to the metal center, which is then followed by the electron transfer from the metal to R-X to form a solvent-caged radical pair. The reaction then could collapse to form the oxidative addition product, or the radical pair could escape forming free radicals R$^•$, which reacts further forming side products. The oxidative addition product from this pathway is the same as that formed from the S_N2 pathway, except that racemization instead of inversion of the stereochemistry is usually observed. The reaction mechanism is faster the more basic the metal, and the substrates follow the reactivity order of R-I > R-Br > R-Cl. The reaction also goes faster as the alkyl radical becomes more stable and easier to form, thus giving rise to

reactivity order of $3^o > 2^o > 1^o > Me$. Scheme 1.6 shows a proposed free nonchain radical

mechanism which operates in the addition of alkyl halides R-X, to $Pt(PPh_3)_3$ (R = Me, Et; X = I;

R = PhCH$_2$; X = Br).

$$M^{(n)} + R-X \rightleftharpoons \left[\overset{(n+1)}{M} \ RX^- \cdot \right]_{cage}$$

escape

collapse

$$R-R \longleftarrow \overset{(n+1)}{M}\!-\!X + R\cdot \qquad \overset{(n+2)}{R-M-X}$$

$$M^{(n)}$$

$$\cdot \overset{(n+1)}{M}\!-\!R$$

Scheme 1.5

$$PtL_3 \xrightarrow{\text{fast}} PtL_2$$

$$PtL_2 + R\text{-}X \xrightarrow{\text{slow}} \cdot PtXL_2 + R\cdot$$

$$\cdot PtXL_2 + R\cdot \xrightarrow{\text{fast}} RPtXL_2$$

Scheme 1.6

9
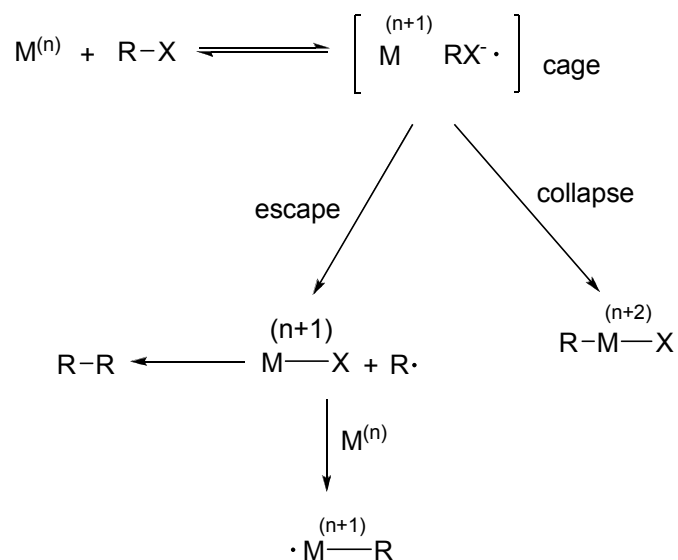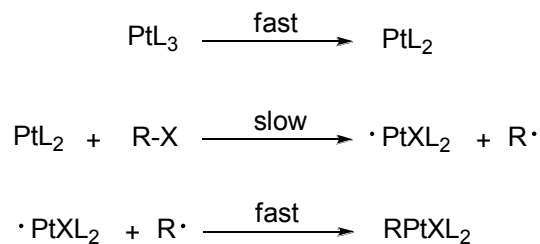
1.3.4 Radical Chain Mechanism

Another type of oxidative addition of organic halides through radical intermediates could occur via radical chain mechanisms, which usually has an induction period (Scheme 1.7). This type of reaction requires a coordinatively unsaturated metal center, and a radical initiator, In•. The reactions shown in Scheme 1.6 could sometimes lead to chain mechanism if the formed radicals could escape from the cage without combination; otherwise a radical initiator is required to start the process. Free radical chain mechanisms are often slowed down through the presence of radical inhibiters, and are identified via the racemization at chiral carbon.

$$In\cdot \ + \ R-X \longrightarrow \ R\cdot \ + \ In-X \qquad \Big\} \ \text{initiation}$$

$$R\cdot \ + \ M^{(n)} \longrightarrow \ R-M^{(n+1)}$$
$$R-M^{(n+1)} + \ R-X \longrightarrow \ R-M \overset{(n+2)}{\text{—}} X \ + \ R\cdot \qquad \Big\} \ \text{propagation}$$

$$\left. \begin{array}{c} R\cdot \ + \ M\cdot \\ 2R\cdot \end{array} \right\} \longrightarrow \ \text{side products} \qquad \Big\} \ \text{termination}$$

Scheme 1.7

10
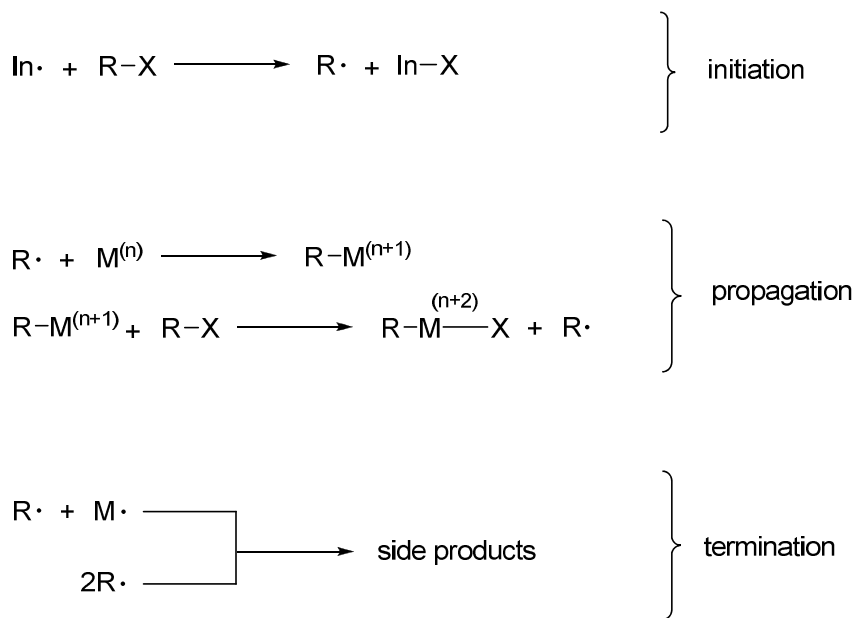
A study conducted by Hill and Puddephatt proposed a free radical chain mechanism of the photochemically-initiated oxidative addition of isopropyl iodide to [PtMe$_2$(bpy)].[15] The reaction is initiated by photochemical MLCT to form [PtMe$_2$(bpy)]*, which has a primarily triplet character. The intermediate then abstracts an iodine atom, thus generating an alkyl radical. The reaction mechanisms are shown in Scheme 1.8.
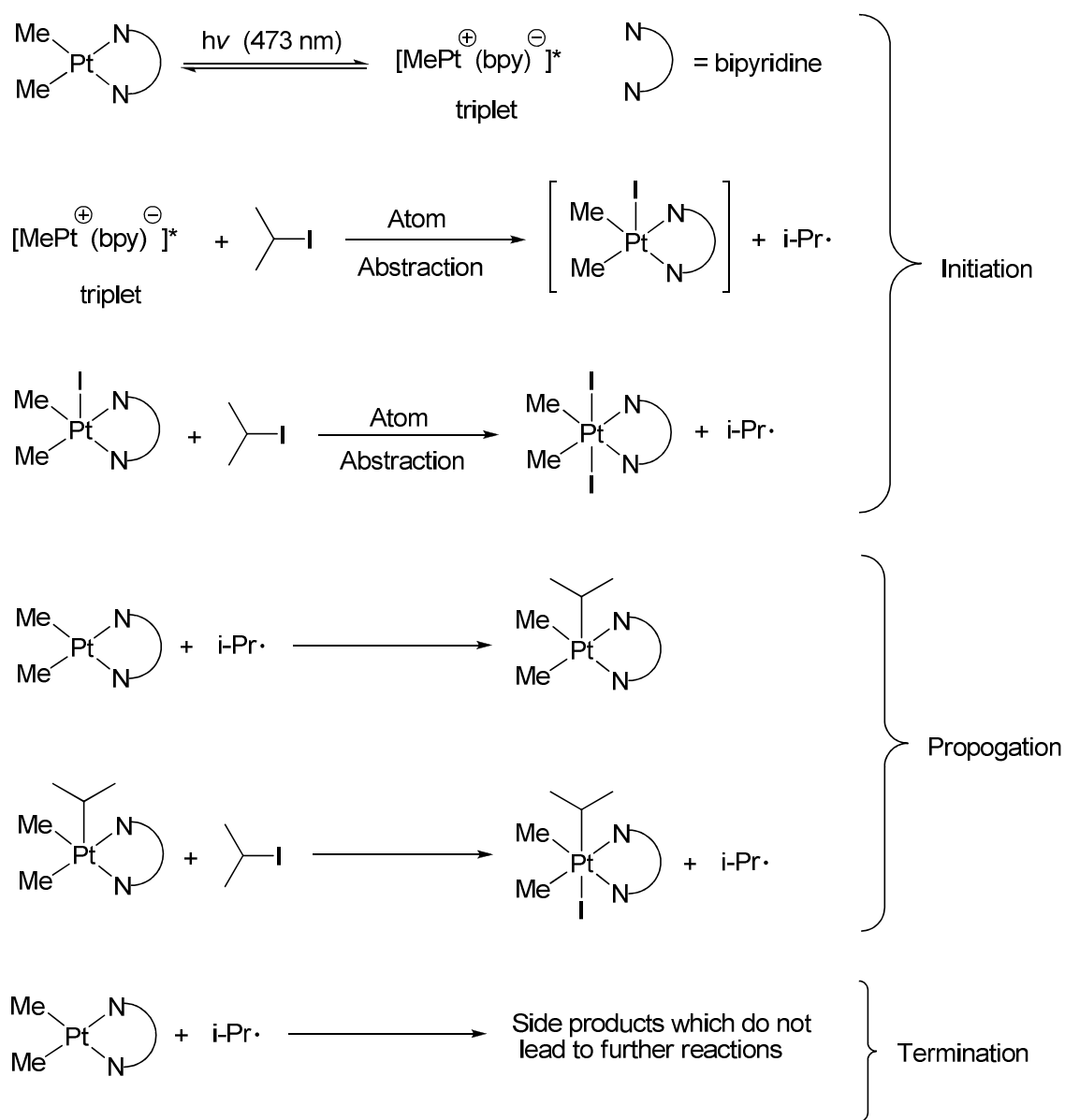
Scheme 1.8

1.4 Reductive Elimination[10]

The reductive elimination reaction is the reverse process of oxidative addition. This reaction is observed in complexes with electron deficient transition metals in high oxidation states, and the formal oxidation state of the metal is reduced by two. Reductive elimination often forms products from the coupling of two covalent ligands at single metal center, or two ligands at two different metal centers (Scheme 1.9). The reductive elimination in a mononuclear system decreases the oxidation state at the metal center from n + 2 to n, and it increases the number of electrons in the metal d-configuration by 2. On the other hand, the process in systems containing two different metal center decreases the oxidation state at each metal center from n + 1 to n, and it increases the number of electrons in the d-electron configuration by 1. The reaction is well known for d^6 metal ions, such as Pt(IV), Pd(IV), and Ir(III). The ligands must be cis to each other in order for concerted reductive elimination to occur, and so, in these examples, a prior isomerization has to occur for ligands that are initially $trans$ to each other. Steric and electronic properties play a big role in the rate of reductive elimination process.

$$L_nM \langle \begin{matrix} A \\ B \end{matrix} \longrightarrow L_nM \ + \ A\text{-}B$$

$$\begin{matrix} A & B \\ | & | \\ L_nM\text{—}ML_n \end{matrix} \longrightarrow L_nM{=}ML_n \ + \ A\text{-}B$$

$$2 \, L_nM\text{—}A \longrightarrow L_nM\text{—}ML_n \ + \ A\text{-}A$$
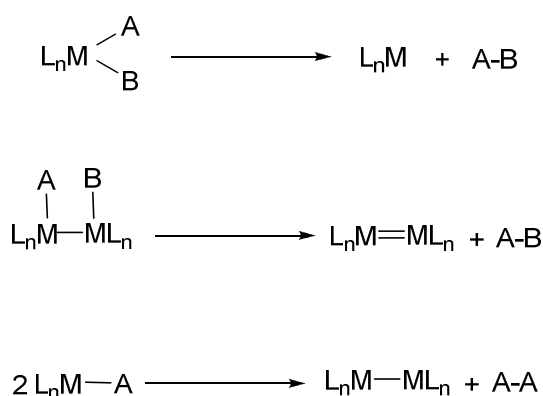
Scheme 1.9

Electron deficient transition metal centers in octahedral d^6 complexes of platinum(IV) and palladium(IV) usually undergo the reductive elimination process, but prior to that often a 5-coordinate intermediate is formed. A proposed mechanism by the Goldberg group for complex [PtMe$_3$I(PPh$_2$-C$_2$H$_4$-PPh$_2$)] showed that the octahedral d^6 platinum(IV) complex undergoes reductive elimination thus producing the square planar d^8 platinum(II) complex (Scheme 1.10).[16] Other side products were observed such as methyl iodide, and ethane. The reductive elimination proceeds through the formation of less rigid 5-coordinate intermediates. The elimination of two methyl groups *cis* to each other produces ethane, while methyl iodide is produced through the iodine attack on the methyl group *trans* to the open site.

Scheme 1.10

13
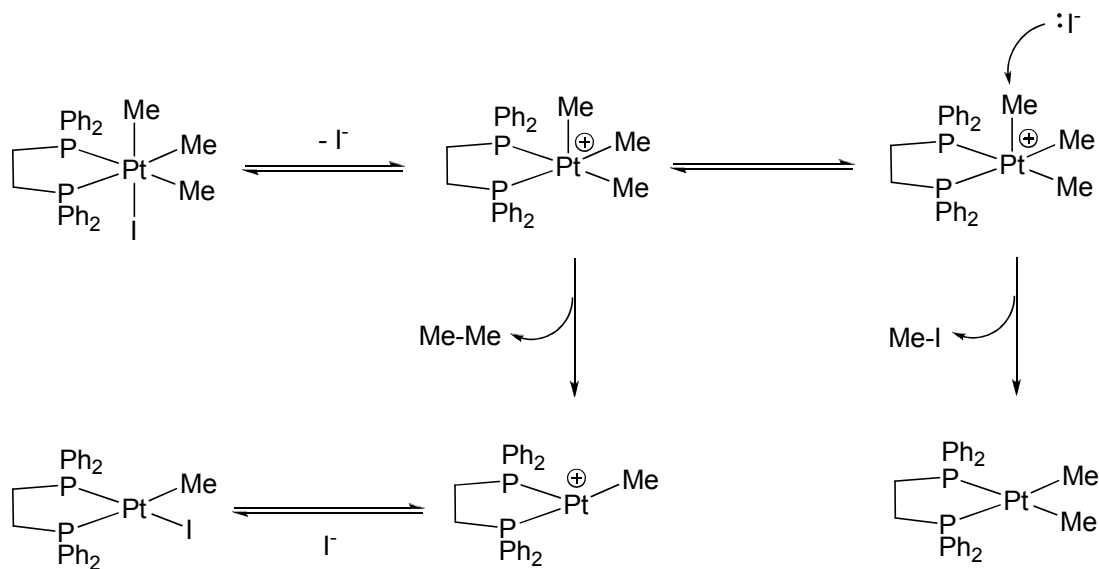
1.5 Activation of Inert Bonds

In recent years extensive research efforts have been aimed at the selective functionalization of alkanes by transition metal complexes. Thus many examples of the inter- and intramolecular C-H bond activation have been discovered.[17] However, only a few of these discoveries lead to actual functionalization.[18] Selective C-H bond functionalization is considered to be a very valuable approach for synthesis in areas ranging from fuels and commodity chemicals to pharmaceuticals.[16,19] The selective transformation of alkanes leading to oxygenated petrochemicals such as alcohols is essential for improved utilization of petroleum and natural gas resources. The activation of C-H bonds by platinum(II) complexes has been gaining a lot of interest since the discoveries of Shilov during the late 1960's and 70's, when he demonstrated that solutions of platinum(II) salts were capable of activating and functionalizing normally unreactive hydrocarbon C-H bonds (Scheme 1.11).[16-20] Shilov's discoveries have attracted much interest due to the mild reaction conditions and the air stability of the system. The reactions are carried out in water, and they are catalytic in platinum(II) complexes.
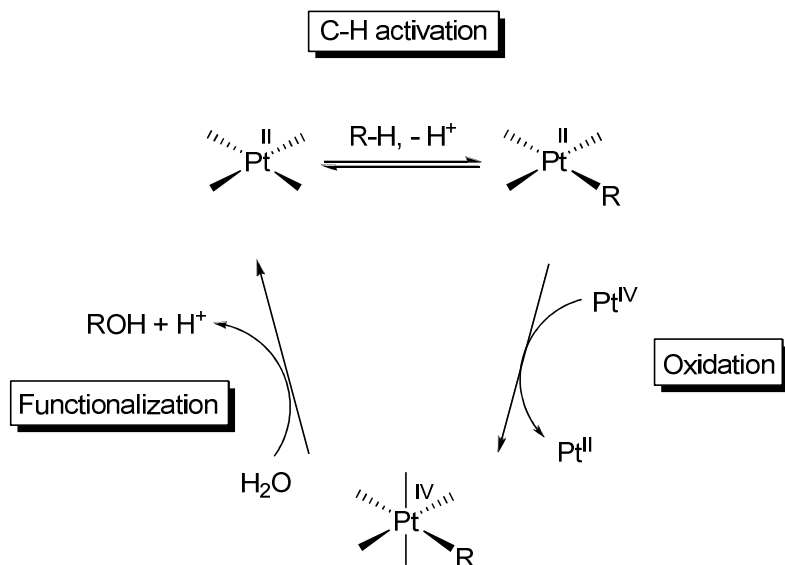
Scheme 1.11

Only few practical processes exist on converting alkanes or saturated hydrocarbons directly to valuable products.[19b] Methane is used in industry to produce methanol that is vital in the production of several essentials such as paint and plastics. A potential mechanism of converting methane gas into methanol using platinum(II) complexes is shown in Scheme 1.12.[20] According to the proposed mechanism by Shilov the first step in the catalytic formation of methanol from methane involves the coordination of methane to the platinum(II) complex through displacement of a weakly coordinating water ligand. Then oxidative addition of methane via C-H bond activation proceeds to form the electrophilic methylplatinum(IV) complex. The platinum(IV) complex undergoes reductive elimination by proton loss to give the more stable platinum(II) complex. The platinum(II) intermediate is then oxidized to platinum(IV) in the presence of oxygen and water, which helps in functionalizing the methyl group. Finally, the reductive elimination proceeds to produce methanol, and regenerate the platinum(II) starting material.
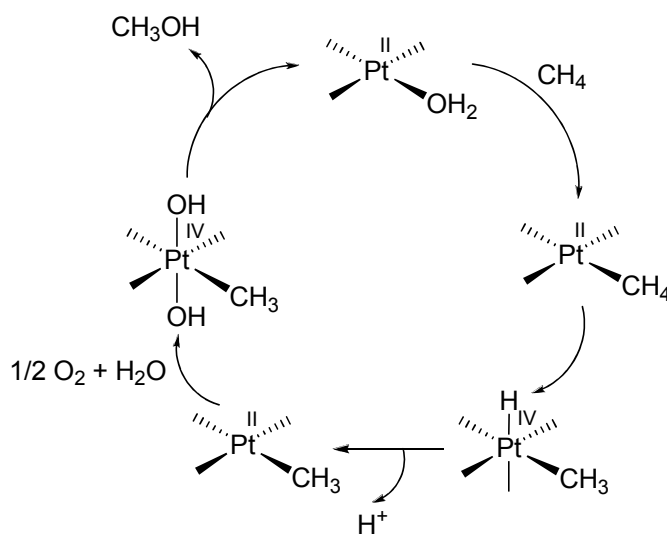
Scheme 1.12

The oxidant used by Shilov was a platinum(IV) salt and not dioxygen, and the system was not industrially useful.[20c] In recent years, developments have occurred in the area of mechanistic understanding of the Shilov system, which helped in speeding up the process in utilizing this system in functionalizing alkanes. It is especially important to use cheaper oxidants such as O_2.[21] Monaghan and Puddephatt reported in 1984 the oxidation of platinum(II) dialkyls (Chart 1.2a) via alcohols or water, which proceeded to form the platinum(IV) alkoxides (Chart 1.2b).[22] The work was done in an aerobic system, and extra studies on the same system by Rostovtsev and Bercaw in 1998 proved that the oxidation happened via O_2 as oxidant.[23]
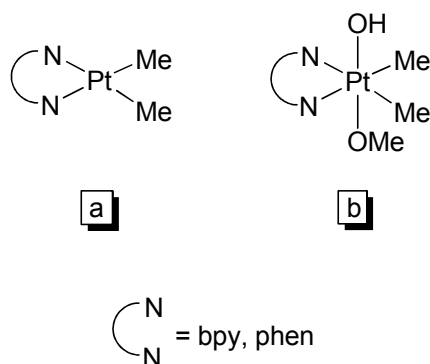
Chart 1.2

The research group of Britovsek showed the insertion of dioxygen in a platinum(II)-methyl bond.[24] The platinum(II) complex was reacted with oxygen in polar solvent acetonitrile at room temperature in the presence of light, which proceeded to form the final product via O_2 insertion according to Equation 1.1. The presence of light played a vital role in the rate of the dioxygen insertion reaction, and the reaction proceeded within minutes. Recently Grice and

16

Goldberg reported similar results on the platinum(II) complex [PtMe$_2$(PN)], PN = 2-(di-tert-butylphospinomethyl)pyridine, where insertion reaction of dioxygen into the platinum(II)-methyl bond occurred easily at room temperature in the presence of light.[25] The complex [PtMe$_2$(PN)] could be reacted in CD$_2$Cl$_2$ or C$_6$D$_6$ in 5 atm of O$_2$, and monitoring the reaction via ^{1}H-NMR showed the presence of a platinum methylperoxo complex, which formed through the insertion of dioxygen in the Pt-Me bond (Equation 1.2).

1.1

1.2
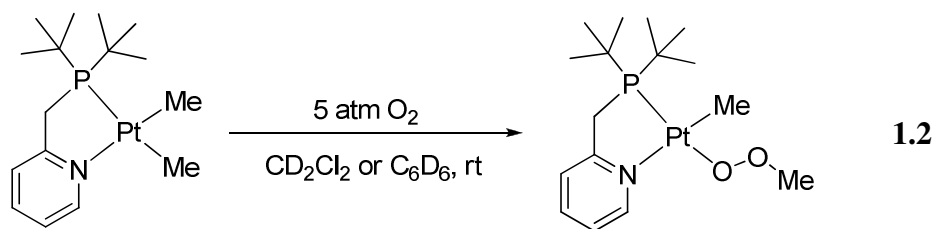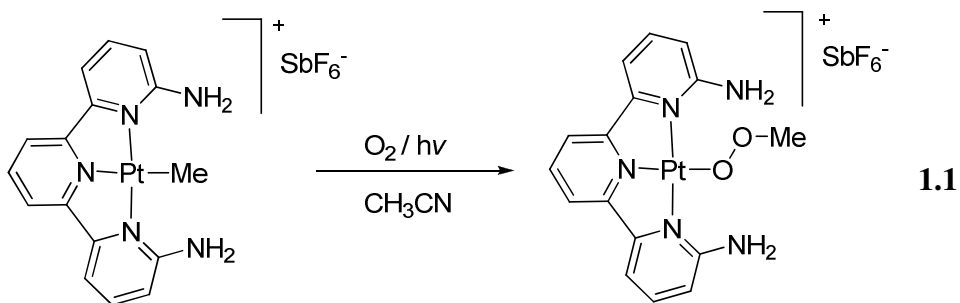
1.6 Supramolecular Chemistry

Supramolecular chemistry is simply known as the chemistry of multicomponent molecular assemblies in which the component structural units are typically held together by a variety of weaker (non-covalent) interactions.[26] This field has developed rapidly over recent years. The notion "supramolecular chemistry" was first introduced in 1978 by Jean-Marie Lehn[27] who understood, "Just as there is a field of molecular chemistry based on the covalent bond, there is a field of supramolecular chemistry, the chemistry of molecular assemblies and of the intermolecular bond." Supramolecular chemistry has a more concise definition such as "chemistry beyond the molecule" or "the chemistry of non-covalent bonds" which are regularly utilized to describe the rapidly growing field.[28]

Supramolecular compounds result from the connection of two or more molecules through intermolecular interactions.[29] These interactions are typically non-covalent in nature and include metal ion coordination, hydrogen bonding, electrostatic forces, π-π stacking interactions and van der Waals interactions.[28] There is continuing interest in self-assembly of polymers and networks using simple coordination complexes as building blocks to give functional molecular materials. This extensive field uses the combination of inorganic and organometallic synthetic pathways with self-assembly through hydrogen bonding to produce a variety of unusual polymeric and network matertials.[30] Self-assembly is usually defined as the process by which a supramolecular species forms spontaneously from its components. Molecular compounds are typically synthesized via the formation of covalent bonds between suitable precursors, while supramolecular compounds are produced by self-assembly of the precursor molecules.[31]

Hydrogen bonds can be considered to represent a special type of electrostatic interaction. A simple description is that it is an attractive interaction between a proton donor and a proton acceptor.[26, 28] Pimentel and McClellan defined a hydrogen bond as follows: "A hydrogen bond exists between a functional group A-H and an atom or a group of atoms B in the same or a different molecule when (a)there is evidence of bond formation, (b)there is evidence that this new bond linking A-H and B specifically involves the hydrogen atom is already bonded to A."[32] Usually both the donor (A) and the acceptor (B) atoms have electronegative character, with the proton involved in the hydrogen bond being shared between the electron pairs on A and B, and the hydrogen then acting as a bridge between them. A hydrogen bond could be abbreviated as A-H•••B (A = donor, B = acceptor) and described in terms of r, d, D, θ, ϕ, where the hydrogen atom is the bridge between both A and B as shown in Figure 1.1.
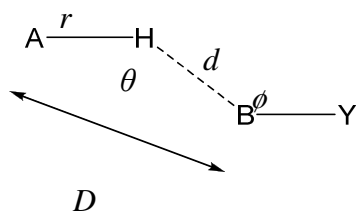
Figure 1.1. Graphical definition of the terms r, d, D, θ, ϕ in a hydrogen bond A-H•••B-Y.

Hydrogen bonds can vary in strength from being very weak to being the strongest of the intermolecular interactions.[26-29] Several spectroscopic and structural methods are typically used to study hydrogen bonding and investigate the several types. The energy of hydrogen bond varies from 14-40 kcal/mol (strong) to 4-15 kcal/mol (moderate) to < 4 kcal/mol (weak).[33] Table 1.1 shows some properties of strong, moderate, and weak hydrogen bonds.[33a] Some of the most common hydrogen bonding motifs reported in the literature are of the type O-H•••O, N-H•••O, O-H•••N and N-H•••N, and are formed via interactions between functional groups such as NH_2, OH, CO_2H, $CONH_2$ and CONHR.

Table 1.1. Properties of strong, moderate, and weak hydrogen bonds.[33a]

	Strong	Moderate	Weak
A-H•••B interaction	mostly covalent	mostly electrostatic	electrostatic
Bond lengths	A-H ≈ H-B	A•••H > H•••B	A•••H >> H•••B
H•••B Å (d)	~ 1.2 – 1.5	~ 1.5 – 2.2	2.2 – 3.2
A•••B Å (D)	2.2 – 2.5	2.5 – 3.2	3.2 – 4.0
Bond angles (θ)	$175 – 180^o$	$130 – 180^o$	$90 – 180^o$
Bond energy (kcal/mol)	14 – 40	4 – 15	< 4
Examples	Acid salts	Acids	C-H•••O/N
	HF complexes	Alcohols	O/N-H•••π bonds

Hydrogen bonding in organometallic complexes has played an important role in supramolecular chemistry. In recent years, attention has been aimed at the role of organoplatinum complexes in self-assembly through hydrogen bonding, π-stacking, and other weak secondary bonding.[34] Much of research has been aimed at the formation of porous organometallic materials that have potential as size-selective catalysts.[34b] Supramolecular organometallic chemistry has slowly developed, because many metal-carbon complexes are incompatible with the functional groups NH and OH that are usually used in self-assembly through hydrogen bonding. The ability to understand the intermolecular interactions controlling the organization of molecules or ions in the solid state is essential prerequisite for the construction of materials with predefined chemical and physical properties.[34a] There have been exciting advances in supramolecular chemistry recently, where the first polymeric organometallic double helix has been synthesized by self-assembly through hydrogen bonding using organoplatinum(IV) complexes.[35] Two different cationic organoplatinum(IV) complexes were synthesized containing carboxylic acid groups and amides as hydrogen bond acceptors and donors. The dicationic complexes are shown in Chart 1.3. The complex shown in Chart 1.3a formed zigzag one dimensional polymer through hydrogen bonding between the carboxylic acid groups. The dicationic complex shown in Chart 1.3b formed a one dimensional polymer chain through hydrogen bonding between carboxylic acid groups, but the flexible ligand N,N-bis(pyridine-4-ylmethyl)oxalamide induced the formation of long range helicity.
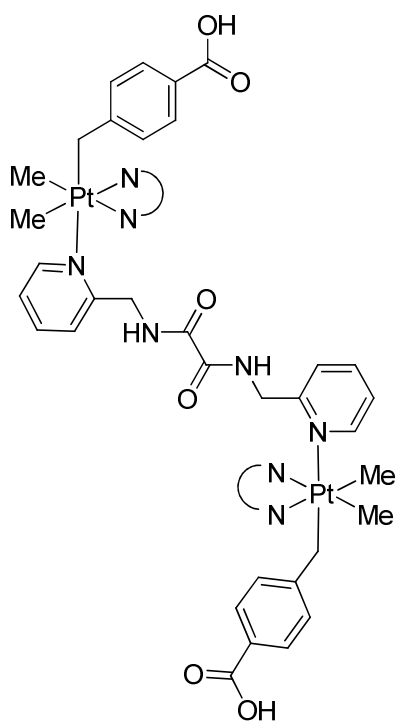
a
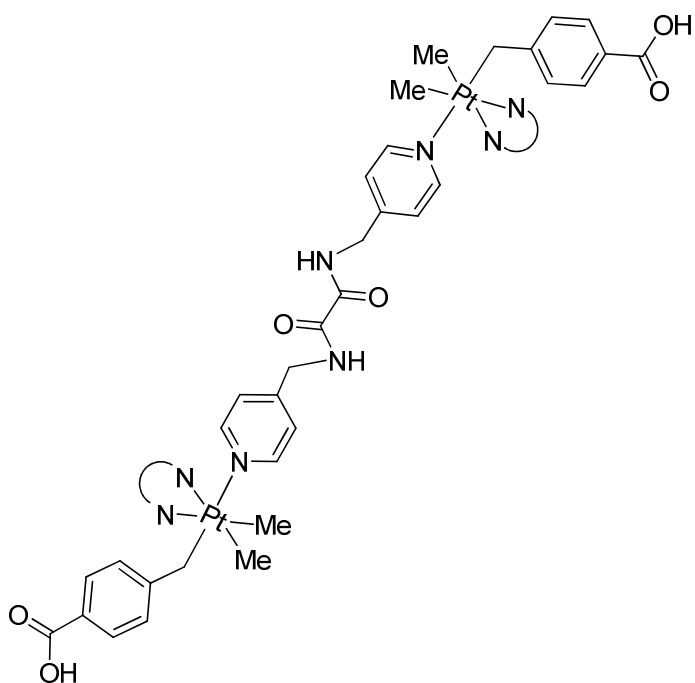
b

NN = 4,4'-di-*t*-butyl-2,2'-bipyridine

Chart 1.3

1.7 A Description of the Thesis

In general, this thesis is concerned with reactions of dimethylplatinum(II) complexes containing bidentate nitrogen donor ligands with main group reagents. In this thesis, efforts have been focused on understanding the mechanism of oxidative addition reactions which are relevant to catalysis, and isolating the products of new reactions.

Recent discoveries in the activation of C-H bonds of arenes using platinum(II) complexes containing bidentate nitrogen donor ligands with 6-membered chelate ring encouraged us to attempt activation of inert bonds, like Si-C and C-H bonds, using a ligand system with 7-membered chelate ring.[36] Chapter 2 is concerned about the reaction of the new dimethylplatinum system with various organic reagents. Chapter 2 also covers the reactions of [PtMe$_2$(dpe)], dpe = 1,2-di-2-pyridylethane, with hydrogen peroxide and methanol which give [{PtMe$_3$OH·PtMe$_2$(OH)$_2$}$_2$][PtMe$_2$(CO$_3$)(dpe)]$_2$, in which the central cluster has an unexpected structure based on a face-bridged double cubane. The mechanisms of these reactions are discussed in detail, and the products are fully characterized.

Chapter 3 deals with the oxidative addition of organic compounds to [PtMe$_2$(bps)], bps = bis(2-pyridyl)dimethylsilane. The main focus is the detection of intermediates, the isolation and characterization of products, and the investigation of the mechanism for the various organoplatinum complexes. This chapter also covers easy oxidatively induced silicon-carbon bond activation using the platinum(II) complex [PtMe$_2$(bps)].

Chapter 4 elaborates on the use of the classical bidentate nitrogen donor ligands, by using a range of related bidentates containing 1-methylimidazol-2-yl rings as ligands. Platinum(II) complexes containing these ligands are shown to be very reactive to organic compounds, and solvents via oxidative addition.

Chapter 5 in this thesis is concerned with the supramolecular chemistry using platinum(IV) complexes containing nitrogen donor ligands with 5-membered chelate rings. The crystal engineering of organoplatinum(IV) complexes was achieved through introducing various hydrogen bond donors and acceptors. The complex [PtMe$_2$(DECBP)], DECBP = 4,4'-diethoxycarbonyl-2-2'-bipyridine, is reacted with various alkyl bromide and benzyl bromide reagents containing amide, ester, alcohol functional groups. Finally, general conclusions are given in chapter 6.

NMR spectroscopy is a powerful method of characterizing all of the complexes discussed in this project. The presence of the spin (I) = ½ isotopes ^{1}H, ^{13}C, ^{19}F, and ^{195}Pt provides an easy way to characterize all the complexes by NMR spectroscopy. The relative abundances of these nuclei are: ^{1}H 100%, ^{13}C 1.1%, ^{19}F 100%, and ^{195}Pt 33.7. In this work ^{1}H NMR spectroscopy is used extensively, and couplings of ^{1}H to ^{13}C, ^{19}F, and ^{195}Pt provide valuable chemical information that can be used to identify the nature of the novel species in solution. Also, X-ray crystallography and mass spectrometry are used in the characterization of the work conducted through the whole project.

1.8 References

1. McDonald, D.; Hunt, L. B. *A History of Platinum and its Allied Metals*; Johnson Matthey, London, **1982**, Chapter 1.

2. Cotton, S. A., *Chemistry of Precious Metals*, Blackie Academic and Professional, New York, **1997**, P. 173-174.

3. Zeise, W. C. *Ann. Phys.*, **1827**, 9, 932.

4. Wilkinson, G; Stone, F. G. A.; Abel, E. W. *Comprehensive Organometallic Chemistry*, Vol. 6, Pergamon Press, Oxford, **1982**, P. 478.

5. Shriver, D. F.; Atkins, P.; Langford, C. H. *Inorganic Chemistry*, 2nd Ed.; W. H. Freeman and Company, New York, **1994**, P. 649.

6. Marriot, J. C.; Salthouse, J. A.; Ware, M. J.; Freeman, J. M. *Chem. Commun.*, **1970**, 595.

7. Hitchcock, P. B.; Lappert, M. F.; Misra, M. C. *J. Chem. Soc., Chem. Commun.*, **1985**, 863.

8. Zhang, F.; Broczkowski, M. E.; Jennings, M. C.; Puddephatt, R. J. *Can. J. Chem.*, **2005**, 83, 595.

9. Shriver, D. F.; Atkins, P.; Langford, C. H. *Inorganic Chemistry*, 2nd Ed.; W. H. Freeman and Company, New York, **1994**, P. 247.

10. a) Collman, J. P.; Hegedus, L. S.; Norton, J. R.; Finke, R. A. *Principles and Applications of Organotransition Metal Chemistry*, 2nd ed.; University Science Books: Mill Valley, California, **1987**. b) Rendina, M. L.; Puddephatt, R. J. *Chem. Rev.*, **1997**, 97, 1735. c) Crabtree, R. H. *The Organometallic Chemistry of the Transition Metals*, 5th Ed.; John Wiley, **2009**, Chapter 6. d) Hartwig, J. F. *Organotransition Metal Chemistry*, University Science Books, Sausalito, California, **2010**, Chapters 6, 7, and 8.

11. a) Anderson, C. M.; Puddephatt, R. J.; Ferguson, G.; Lough, A. J. *J. Chem. Soc.*, *Chem. Commun.*, **1989**, 1297. b) Anderson, C. M.; Crespo, M.; Jennings, M. C.; Lough, A. J.; Ferguson, G.; Puddephatt, R. J. *Organometallics*, **1991**, 10, 2672.

12. Puddephatt, R. J. *Coord. Chem. Rev.*, **2001**, 157.

13. Jawad, J. K.; Puddephatt, R. J. *J. Organomet. Chem.*, **1976**, 117, 297. b) Jawad, J. K.; Puddephat, R. J. *J. Chem. Soc., Dalton Trans*, **1977**, 1466.

14. Peloso, A. *J. Chem. Soc.*, *Dalton Trans*, **1976**, 984.

15. Hill, R. H.; Puddephatt, R. J. *J. Am. Chem. Soc.*, **1985**, 107, 1218.

16. a) Fekl, U.; Kaminsky, W.; Goldberg, K. I. *J. Am. Chem. Soc.*, **2001**, 123, 6423. b) Fekl, U.; Goldberg, K. I. *Adv. Inorg. Chem.*, **2003**, 54, 259.

17. a) Zhong, H. A.; Labinger, J. A.; Bercaw, J. E. *J. Am. Chem. Soc.*, **2002**, 124, 1378. b) Arndtsen, B. A.; Bergman, R. G.; Mobley, T. A.; Peterson, T. H. *Acc. Chem. Res.*, **1995**, 28, 154.

18. a) Waltz, K. M.; Hartwig, J. F.; *J. Am. Chem. Soc.*, **2000**, 122, 11358. b) Chen. H. Y.; Schlecht, S.; Semple, T. C.; Hartwig, J. F. *Science*, **2000**, 287, 1995.

19. a) Williams, T. J.; Caffyn, A. J.; Hazari, N.; Oblad, P. F.; Labinger, J. A.; Bercaw, J. E. *J. Am. Chem. Soc.*, **2008**, 130, 2418. b) Labinger, J. A.; Bercaw, J. E. *Nature*, **2002**, 417, 507.

20. (a) Goldshlegger, N. F.; Eskova. V. V.; Shilov, A. E.; Shteinman, A. A. *Zhur. Fiz. Khim.*, **1972**, 46, 1353. (b) Shilov, A. E. *Activation of Saturated Hydrocarbons by Transition Metal Complexes*; D. Reidel Publishing: Dordrecht, **1984**. c) Lersch, M.; Tilset, M. *Chem. Rev.*, **2005**, 105, 2471.

21. a) Vedernikov, A. N. *Chem. Commun.*, **2009**, 4781. b) Rostovtsev, V. V.; Henling, L. M.; Labinger, J. A.; Bercaw, J. E. *Inorg. Chem.*, **2002**, 41, 3608.

22. Monaghan, P. K.; Puddephatt, R. J. *Organometallics*, **1984**, 3, 444.

23. Rostovtsev, V. V.; Labinger, J. A.; Bercaw, J. E. *Organometallics*, **1998**, 17, 4530.

24. Taylor, R.; Law, D.; Sunley, G.; White, A.; Britovsek, G. *Angew. Chem. Int. Ed.*, **2009**, 48, 5900.

25. Grice, K. A.; Goldberg, K. I. *Organometallics*, **2009**, 28, 953.

26. Lindoy, L. F.; Atkinson, I. M. *Self-Assembly in Supramolecular Systems*. **2000**, 3.

27. Lehn, J.-M. *Pure Appl. Chem.* **1978**, 50, 871.

28. Lehn, J.-M. *Supramolecular Chemistry; Concepts and Perspectives, VCH: Weinheim*. **1995**.

29. Steed, J. W.; Atwood, J. L. *Supramolecular Chemistry,* John Wiley & Sons Ltd.*,* **2000**.

30. Au, R. H. W.; Jennings, M. C.; Puddephatt, R. J. *Organometallics*, **2009**, 28, 3734.

31. a) Espinet, P.; Esteruelas, M. A.; Oro, L. A.; Serrano, J. L.; Sola, E. *Coord. Chem. Rev*., **1992**, 117, 215. b) Collin, J. P.; Gavina, P.; Heitz, V.; Sauvage, J. *Eur. J. Inorg. Chem.*, **1998**, 14.

32. Pimentel, G. C.; McClellan, A. L. *The Hydrogen Bond*, Freeman, San Francisco, **1960**.

33. a) Jeffrey, G. A. *An Introduction to Hydrogen Bonding*. Oxford University Press: New York, **1997**. b) Atwood, J. L.; Steed, J. W. *Encyclopedia of Supramolecular Chemistry*, Marcel Dekker: New York, **2004**.

34. a) Braga, D.; Grepioni, F.; Desiraju, G. *J. Organomet. Chem.*, **1997**, 548, 33. b) Zhang, F.; Jennings, M. C.; Puddephatt, R. J. *Chem, Commun.*, **2007**, 1496. c) Au, R. H. W.; Jennings, M. C.; Puddephatt, R. J. *Organometallics*, **2009**, 28, 3754. d) Au, R. H. W.; Jennings, M. C.; Puddephatt, R. J. *Organometallics*, **2009**, 28, 5052.

35. Fraser, C. S. A.; Eisler, D. J.; Jennings, M. C.; Puddephatt, R. J. *Chem, Commun.*, **2002**, 1224.

36. Zhang, F.; Kirby, C. W.; Hairsine, D. W.; Jennings, M. C.; Puddephatt, R. J. *J. Am. Chem. Soc.*, **2005**, 127, 14196.

CHAPTER 2

Synthesis, Characterization and Reactions of the

Complex [PtMe$_2$(1,2-di-2-pyridylethane)]

2.1 Introduction

Organoplatinum complexes are significant molecules due to their well established roles in catalysis and photochemistry.[1] Platinum(II) complexes containing nitrogen-donor ligands are typically highly reactive in oxidative addition reactions.[1,2] This high reactivity plays a major role in the activation of normally inert chemical bonds such as C-H bonds. Oxidative addition reactions of organic halides, and halogens to platinum(II) compounds have been studied thoroughly during recent years.[1] These reactions are essential in many industrially important catalytic reactions, and typically occur via the S_N2 mechanism, involving a second order rate law.[1,3]

The oxidative addition of a wide variety of reagents to platinum(II) complexes [PtMe$_2$(LL)], LL = 2,2'-bipyridyl or its derivatives have been studied intensively, since such reactions are vital in the activation of inert bonds. The dimethylplatinum(II) complex [PtMe$_2$(DPK)], DPK = di-2-pyridyl ketone, has been reported to undergo easy oxidative addition to give platinum(IV) complexes. The platinum(II) complex contained a six membered chelate ring, which resulted in distortion from planarity, thus playing a significant role in the reactivity.[2] Platinum(II) complexes containing 2,2'-bipyridyl give five-membered chelate rings that are planar, and this geometry appears to be unsuitable in the activation of C-H bonds.

Few studies exist on catalytic reactions of platinum(II) complexes containing bidentate nitrogen donor ligands that form seven membered chelate rings. It was revealed that the chelate ring size of bis-pyridine ligands plays a major role in C-H activation of arenes (Chart 2.1).[4] Square planar platinum(II) complexes that formed five membered chelating rings with bipyridine ligands failed to activate the C-H bonds in hydrocarbons, probably due to the steric effects caused by the *ortho* hydrogen atoms on the pyridine rings, but the non planar platinum(II)

complexes that formed six membered chelating rings with bis-pyridine ligands were successful in activating C-H bonds in arenes, because the *ortho* hydrogens on the bowed pyridine rings are out of plane, and cause less steric effect.[2]
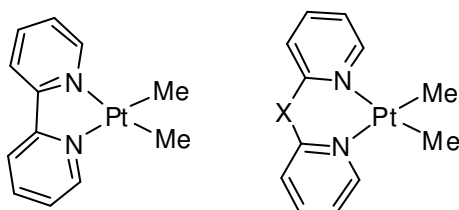
X = CO, NH, and CH$_2$

Chart 2.1

In this chapter, a new platinum(II) complex containing the bidentate nitrogen donor ligand 1,2-di-2-pyridylethane is reported. The dimethylplatinum(II) complex contained a seven membered chelate ring, which resulted in unusual products with exciting molecular structures. The main goal was to activate C-H bonds in alkyl or aryl groups. This goal was not achieved due to the unanticipated lability of the platinum ligand bonds. This labile bond feature caused the ligand to exchange rapidly or to dissociate from platinum to produce unique structures such as [{PtMe$_3$X)(PtMe$_2$X$_2$)}$_n$], X = OH, or OMe upon the reaction with hydrogen peroxide or methanol. These structures are based on a face-bridged double cubane with two vertices missing. We were able to activate the C-H bond in the ligand 1,2-bis(2-pyridyl)ethane (dpe) through the oxidative addition of iodine to the platinum(II) complex. Other oxidative addition and reductive elimination reactions, which helped in understanding the features of this system, are reported.

2.2 Results and Discussion

2.2.1 Synthesis and Characterization of [PtMe$_2$(dpe)]

The ligand 1,2-bis(2-pyridyl)ethane, **2.1**, was prepared using a modified procedure of Quagliotto *et al.*[5] and isolated as an oily product. The complex [PtMe$_2$(dpe)], **2.2**, was synthesized readily by the reaction of the ligand dpe with the precursor [Pt$_2$Me$_4$(μ-SMe$_2$)$_2$],[6] in diethyl ether solution (Equation 2.1). Complex **2.2** was precipitated as a white solid, and was characterized by its ^{1}H-NMR spectrum. The methyl platinum groups give a resonance at $\delta =$ 0.60, with coupling constant $^2J_{Pt-H} = 88$ Hz. The doublet resonance of the *ortho* hydrogen atoms of the pyridine ring also shows a coupling to platinum with $^3J_{Pt-H} = 18$ Hz (Ar-H$_{ortho}$). A broad singlet resonance for the two CH$_2$ groups of the dpe ligand was observed at $\delta = 4.01$ ppm. The presence of the broad resonance suggests that the platinum(II) complex is non planar, and the two site system is undergoing exchange at room temperature. The ^{1}H-NMR parameters for the dpe ligand of complex **2.2**, were similar to those for [PtCl$_2$(dpe)],[7] with differences as expected in the coupling constants of the *ortho* protons due the higher *trans* influence of the methyl groups in complex **2.2**, compared to the chloro groups in [PtCl$_2$(dpe)]. The ^{1}H-NMR spectrum of complex **2.2** is shown in Figure 2.1.

Chemical Shift (ppm)
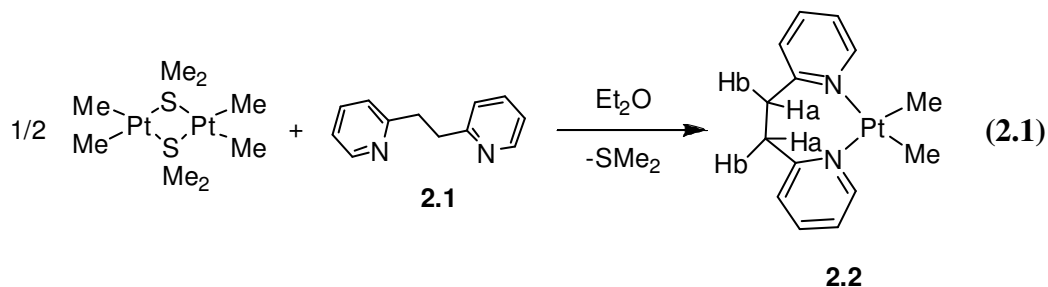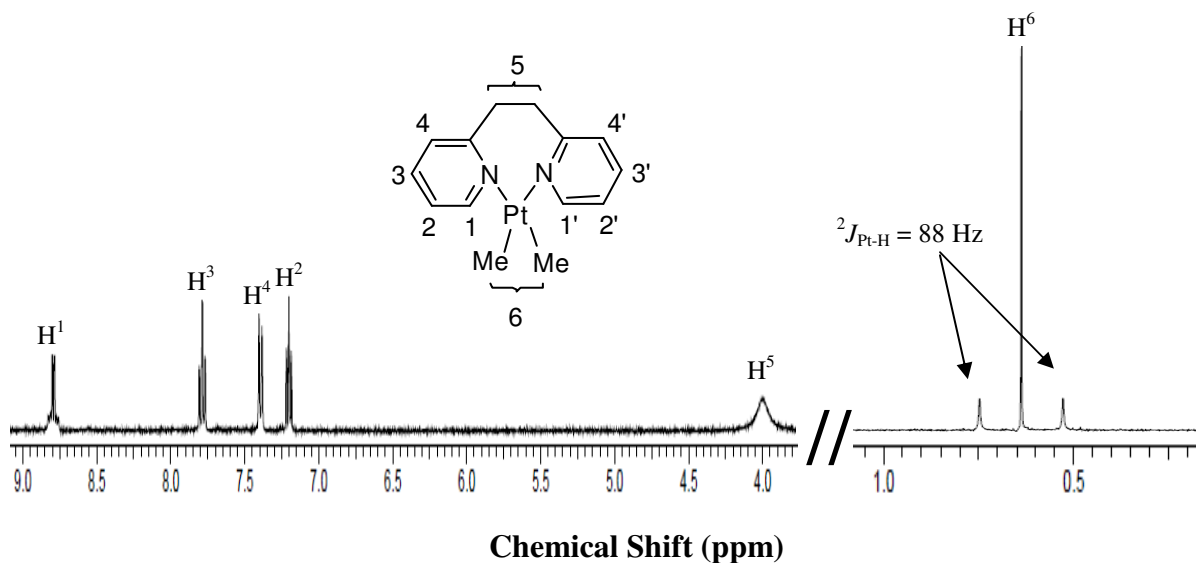
Figure 2.1. The ^{1}H-NMR spectrum (400 MHz, acetone-d$_6$) of complex **2.2**, [PtMe$_2$(dpe)].

A variable temperature NMR study was needed to calculate the energy of exchange, $\Delta G^{\ddagger}$, between the protons H^a and H^b. The NMR spectra were recorded at 20 ^{o}C intervals between -80 and +20 ^{o}C (Figure 2.2). The resonance for the CH$_2$ protons is broad at room temperature due to the fast exchange, and two resonances are observed at -80 ^{o}C. The coalescence temperature, T$_c$= -20°C, is then used to calculate the free activation energy using Equation 2.2.

$$\Delta G^{\ddagger} = RT_c \ln \frac{RT_c\sqrt{2}}{\pi \cdot N \cdot h \left| \nu_A - \nu_B \right|} \qquad \textbf{(2.2)}$$

The calculated value for the free activation energy $\Delta G^{\ddagger}$ is 47 ($\pm$1) kJ·mol^{-1}. In the above equations h is Planck's constant in J·s, N is Avogadro's number in mol^{-1}, R is the value for the

gas constant in $J \cdot K^{-1} \cdot mol^{-1}$, T_c is the coalescence temperature in Kelvin, and $\nu_A - \nu_B$ is the frequency difference in Hz between the two observed proton resonances.
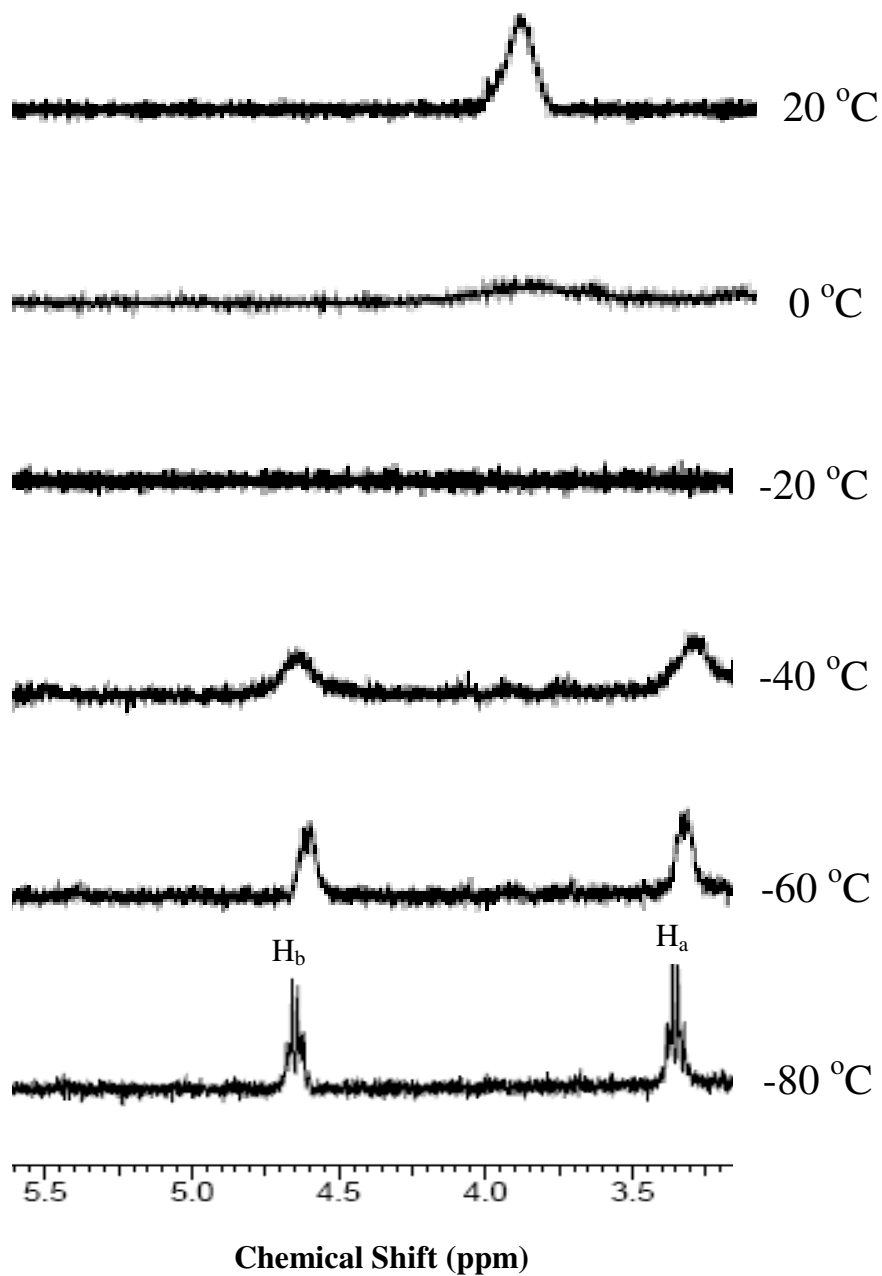
Figure 2.2. The VT-NMR spectra (400 MHz, acetone-d_6) of complex **2.2,** [PtMe$_2$(dpe)].

2.2.2 Reaction of [PtMe$_2$(dpe)] with Methyl Iodide

Complex **2.2** reacts rapidly with MeI to form a yellow solid compound **2.3**, which was identified as the known complex [(PtIMe$_3$)$_4$] by its ^{1}H NMR spectrum [$\delta_{(Me\text{-}Pt)}$ = 1.81 ppm, $^2J_{(Pt\text{-}H)}$= 80 Hz].[8] The ^{1}H NMR spectrum also showed the presence of the uncoordinated dpe ligand, so the reaction occurred according to equation 2.3.

$$(2.3)$$
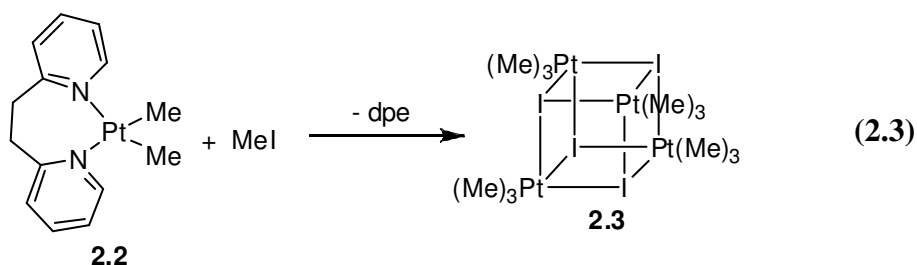
A variable temperature ^{1}H NMR experiment was obtained to investigate the reaction of CD$_3$I with complex **2.2** in acetone-d_6. The reagents were mixed at -80 ^{o}C and spectra were recorded at 20 ^{o}C intervals between -80 ^{o}C and 20 ^{o}C (Figure 2.3). At -80 ^{o}C it was observed that the CD$_3$I reacted with **2.2** via oxidative addition to give a mixture of the intermediates **A** and **B** in ~1:2 ratio (Scheme 2.1). The resonance of [(PtI(CD$_3$)Me$_2$)$_4$], **2.4**, at δ = 1.81, started to appear at -20 ^{o}C. At 0 ^{o}C, the separate resonance for the CH^{a}H^b protons and the methyl platinum protons of **A** and **B** coalesced. This reaction shows that complex **2.2** is reactive to oxidative addition, but that the dpe ligand is easily displaced from platinum(IV). The coalescence temperature T$_c$= 0 ^{o}C, which is used to calculate the free activation energy. The calculated value for the free activation energy ΔG‡ for the axial and equatorial methyl groups using Equation 2.2 is 49 ($\pm$1) kJ·mol^{-1}.

Scheme 2.1

Δ:Me^{eq}(A+B)
□:Me^{ax}(B)
O:Me^{eq} + Me^{ax}

Acetone-d_6

Δ

□

2CH$_2$

-80 ^{o}C

$^2J_{\text{Pt-H}}$ = 72 Hz

-60 ^{o}C

Coordinated dpe

$^2J_{\text{Pt-H}}$ = 69 Hz

-40 ^{o}C

Complex **2.4**
[{PtIMe$_2$(CD$_3$)}$_4$]

-20 ^{o}C

Free dpe

2.4

0 ^{o}C

2.4

o

20 ^{o}C

Chemical Shift (ppm)
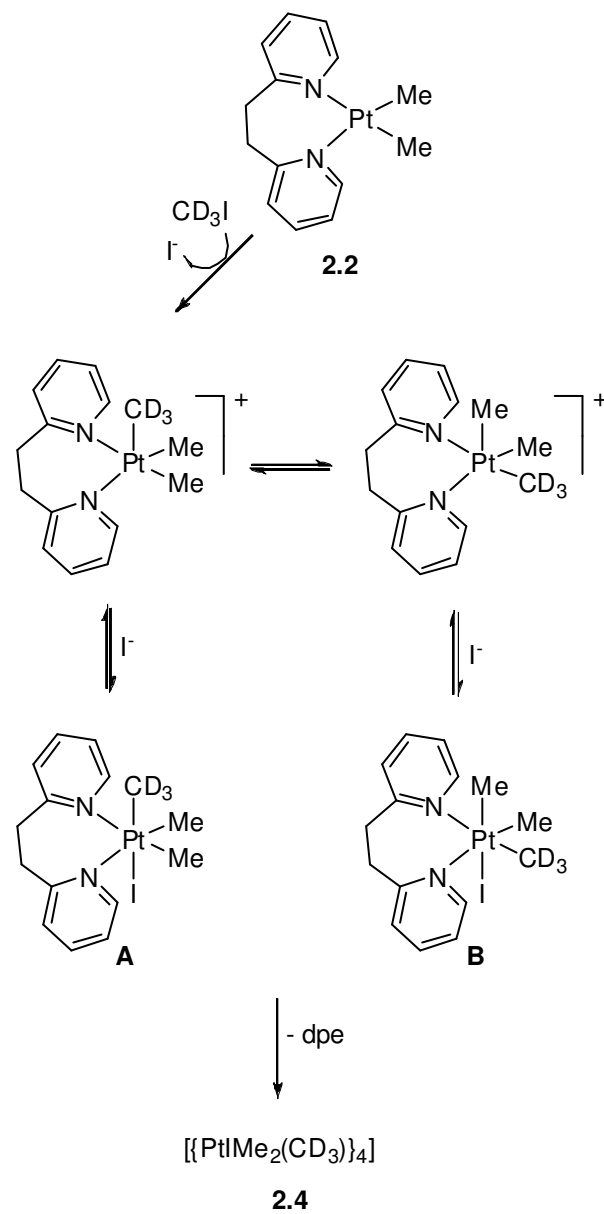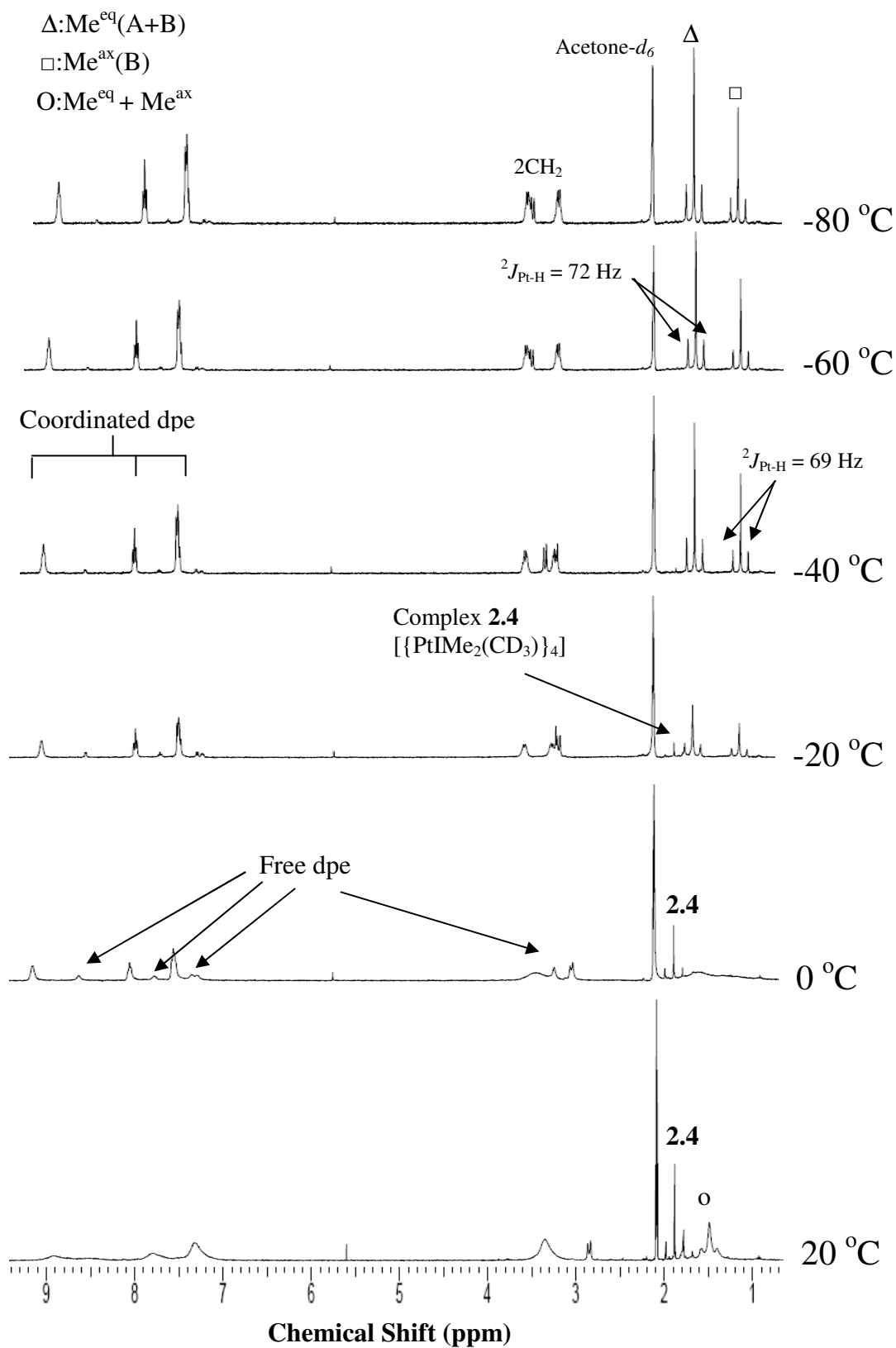
Figure 2.3. The VT-NMR spectra (400 MHz, acetone-d$_6$) for the reaction of CD$_3$I with **2.2**.

2.2.3 Reactions of [PtMe$_2$(dpe)] with Halogens, X$_2$ (X = Br, I)

The complex [PtMe$_2$(dpe)], **2.2**, reacted rapidly with bromine in a dry methylene chloride solution at room temperature to give *trans*-[PtBr$_2$Me$_2$(dpe)], **2.5a**, which was isolated as a red solid. The platinum(IV) complex **2.5a** is the product of the *trans* oxidative addition. Complex **2.5a** is not stable, and it decomposed slowly through the reductive elimination of MeBr forming the platinum(II) complex [PtBr$_2$(dpe)], **2.6**, according to Scheme 2.2. The ^{1}H-NMR spectrum in Figure 2.4 shows that the methyl platinum resonance for **2.5a** occurred δ = 2.24, with coupling $^2J_{\text{Pt-H}}$ = 72 Hz. The complex **2.5a** gave a single set of pyridyl resonances, with the *ortho* pyridyl protons δ = 8.89, with coupling $^3J_{\text{Pt-H}}$ = 23 Hz, and both the chemical shift and coupling constant are typical of a platinum(IV) complex with a pyridyl group *trans* to a methyl group.[2] A single CH$_2$ resonance was observed at δ = 3.48. Equation 2.4 shows the reaction of complex **2.2** with Br$_2$ at room temperature. Complex **2.6** was characterized by the absence of any methyl platinum proton resonances in the ^{1}H NMR spectrum, and the presence of one set of pyridyl resonances as expected for a symmetrical complex. The *ortho* pyridyl proton resonance for **2.6** was observed at δ = 9.13, with coupling constant $^3J_{\text{Pt-H}}$ = 33 Hz, which is higher than the 23 Hz observed in the complex **2.5a**, indicating that the pyridyl groups in **2.6** are *trans* to a ligand with a low *trans* influence such as bromine, similar to the complex [PtCl$_2$(dpe)].[7] Two quartets were observed at δ = 3.44 and 4.82 due to the proton resonances of the CH$_2$ groups.
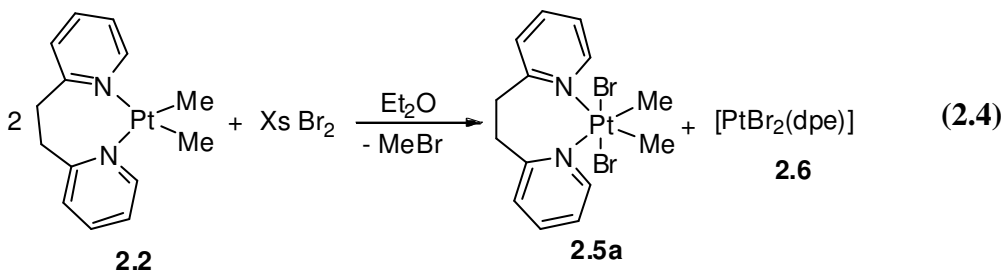
The course of the reaction was monitored by low temperature ^{1}H-NMR spectroscopy (Figure 2.5). Bromine was added at -80 °C to a solution of [PtMe$_2$(dpe)], **2.2**, in CD$_2$Cl$_2$. At -80 °C the reaction proceeded by the *trans* oxidative addition of bromine to **2.2** to give **2.5a.** At -60 °C the platinum(IV) complex isomerizes from the *trans* to the *cis* isomer, **2.5b**, which was characterized by two new methyl platinum resonances at δ = 1.99 and 2.49, with $^2J_{Pt-H}$ = 76 and 78 Hz respectively. The methyl platinum group with the higher coupling constant is the one *trans* to the bromide ligand, because halogens have a lower *trans* influence than nitrogen.[7] Then at -40 °C, the methyl platinum resonance reappeared at δ = 2.24, with $^2J_{Pt-H}$ = 72 Hz. At that temperature of -40 °C the *cis* product **2.5b** is the major, and the *trans* product **2.5a** is the minor product. At -20 °C, the *cis* complex is the minor product, and the *trans* complex is the major. At 20 °C, the resonances for **2.5b** were broad while those of **2.5a** remained sharp. Scheme 2.2 shows the ^{1}H-NMR spectra from 20 °C to -80 °C for the reaction of **2.2** with bromine.
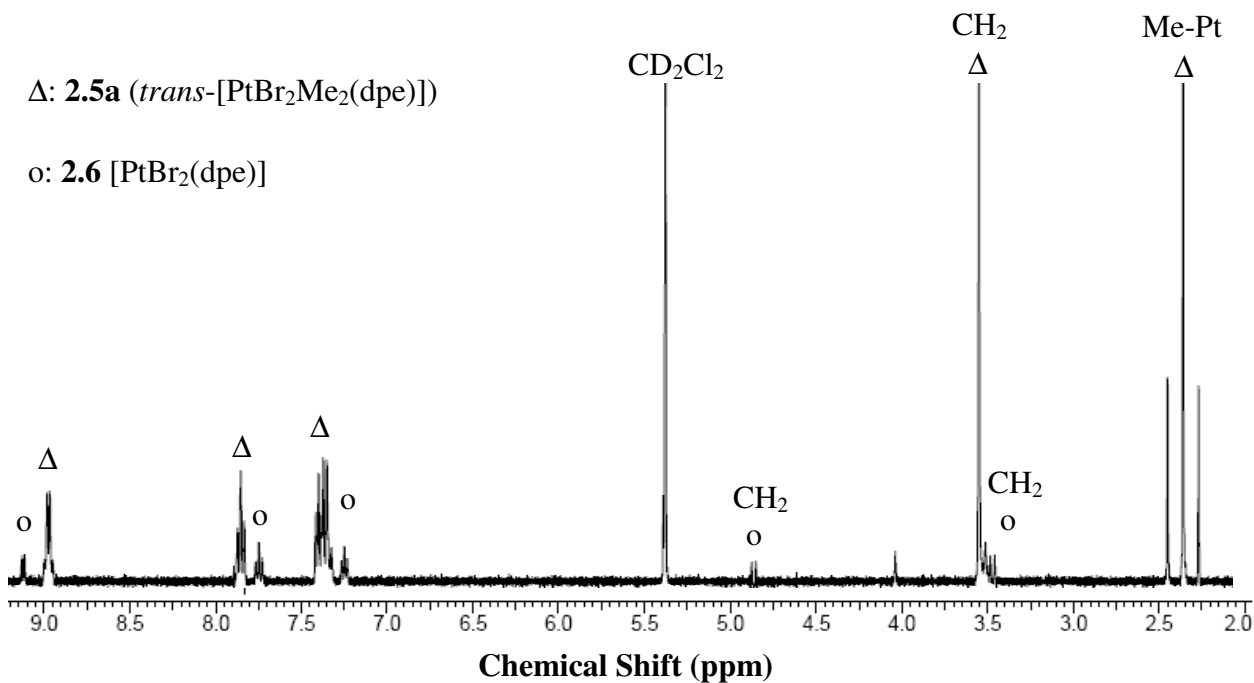
Figure 2.4. The ^{1}H NMR spectrum (400 MHz, CD$_2$Cl$_2$) for the reaction of complex **2.2** with bromine at room temperature.

Scheme 2.2

2.5a (*trans*): Δ

2.5b (*cis*): o

MeBr: Ө

CD₂Cl₂

CH₂ Δ

CH₂ o

Me-Pt
Ө Δ

o Δ o o Δ o Δ

20 °C

Δ

0 °C

Δ
o o

-20 °C

Δ

-40 °C

-60 °C

o o

-80 °C

10.0 9.5 9.0 8.5 8.0 7.5 7.0 6.5 6.0 5.5 5.0 4.5 4.0 3.5 3.0 2.5 2.0

Chemical Shift (ppm)
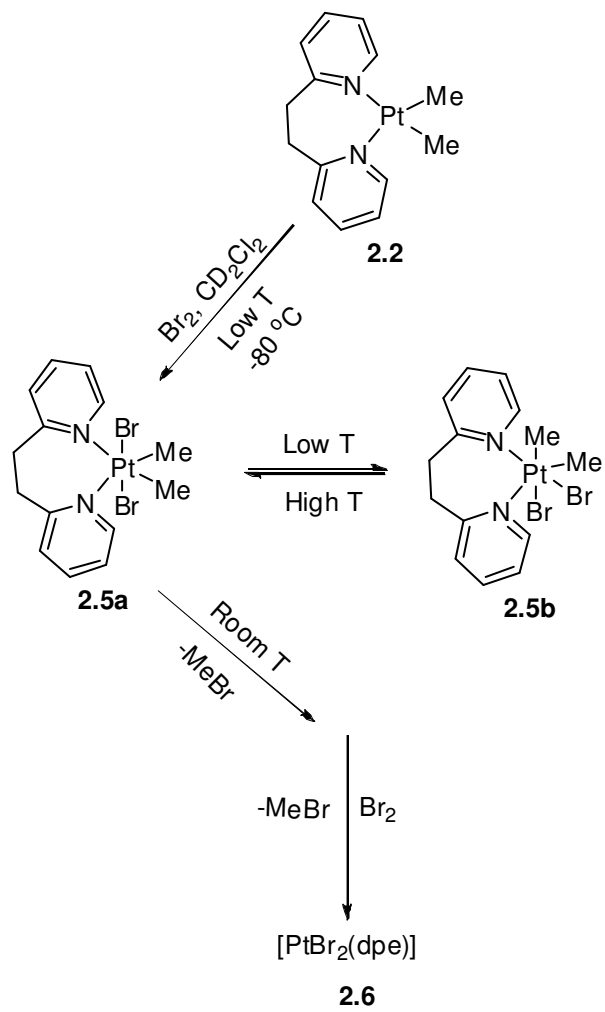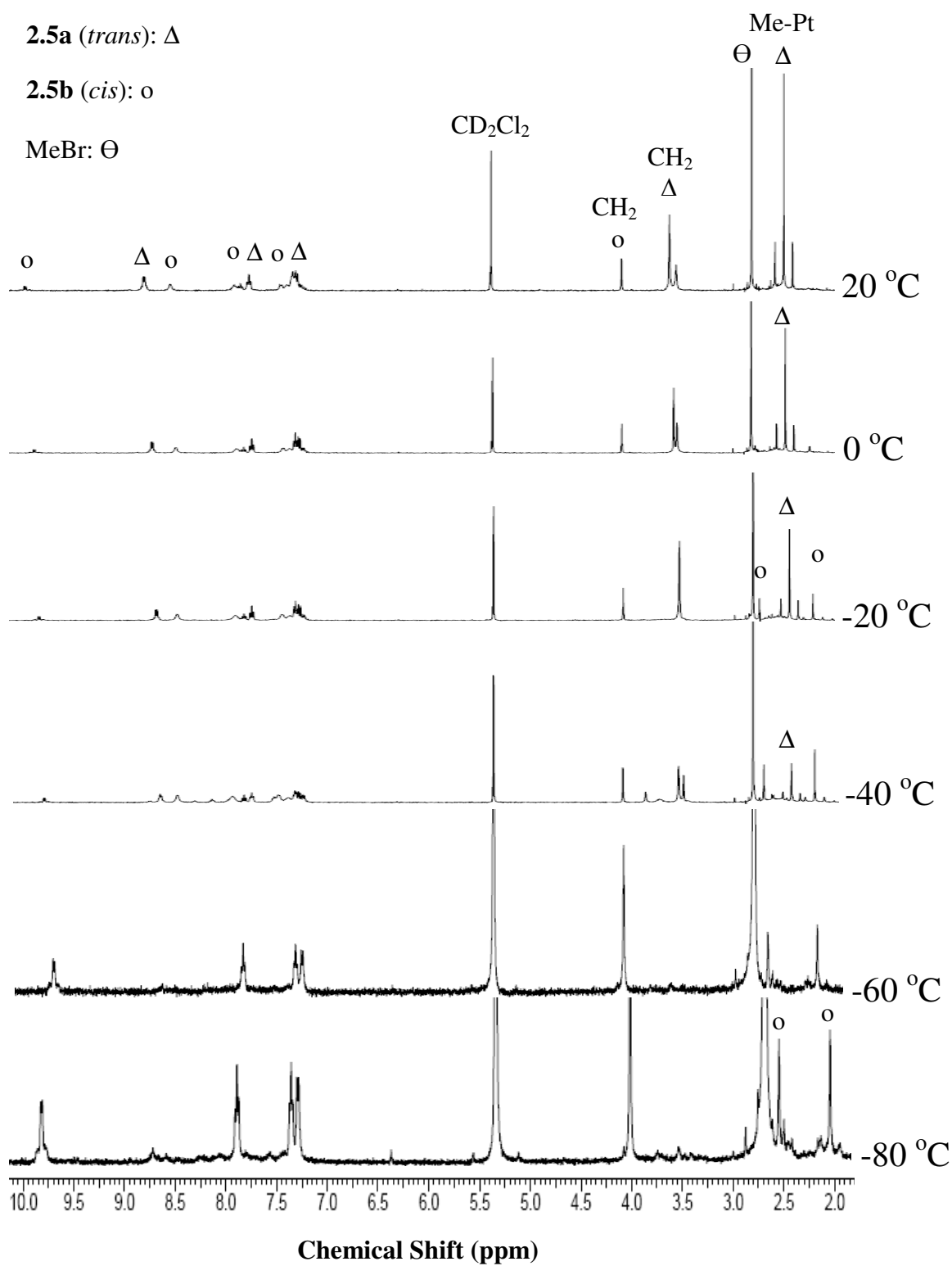
Figures 2.5. The ^{1}H NMR spectra (400 MHz, CD₂Cl₂) at -80 °C to 20 °C
for the reaction of **2.2** with bromine.

These results indicate that the oxidative addition of bromine occurs with *trans* stereochemistry, but that there is an easy equilibrium between *cis* and *trans* isomers at temperatures above -60 $^{\circ}$C. At low temperature, the equilibrium favors **2.5b** while at higher temperature the equilibrium favors **2.5a** (Scheme 2.2). At room temperature, methyl bromide was released by a reductive elimination step in the platinum(IV) complex.

A day later the reaction mixture was cooled down to –80 ^{0}C, the *trans* product **2.5a** isomerized to the *cis* product **2.5b** at lower temperature. This indicates that the *cis-trans* isomerization reaction is reversible. A similar form of isomerism was observed for the product of iodine oxidative addition to platinum(II) phosphine complexes.[9] The same experiment (Scheme 2.2) was repeated under the same conditions and procedures, and it showed reproducibility.

Complex **2.2** reacted at room temperature with iodine in a solution of CH_2Cl_2 to give $[PtI_2(dpe)]$, **2.7**, which was isolated as an air stable dark red solid. The complex **2.7** was characterized spectroscopically, and its structure was confirmed crystallographically (Figure 2.6). Table 2.1 shows selected bond lengths and angles. The ^{1}H NMR spectrum of **2.7** contained no methyl platinum groups in the high field region. In the low field region of the spectrum only one set of pyridyl resonances was observed, which means that the pyridyl groups were equivalent. The *ortho* pyridyl resonance was observed at $\delta = 9.09$, with coupling $^{3}J_{Pt-H} = 38$ Hz. The coupling constant in complex **2.7** is higher than typical platinum(II) complexes with a methyl group *trans* to a pyridyl, which means that the pyridyl group is *trans* to a ligand with a low *trans* influence such as iodine. Two quartets were observed at $\delta = 3.41$ and 4.72 due to the proton resonances of the bridging CH_2 groups. Complex **2.7** is the product of the double

oxidative addition of iodine, and then the double reductive elimination of methyl iodide, so a low

temperature ^{1}H-NMR experiment was needed to investigate the reaction.

Table 2.1. Selected bond lengths [Å] and angles [°] for [PtI$_2$(dpe)], **2.7**.

Pt-N(11)	2.036(9)	Pt-N(24)	2.067(9)
Pt-I(1)	2.583(8)	Pt-I(2)	2.602(9)
N(11)-C(12)	1.343(1)	N(11)-C(16)	1.351(2)
C(19)-N(24)	1.349(1)	C(23)-N(24)	1.361(1)
C(16)-C(17)	1.506(2)	C(17)-C(18)	1.528(2)
C(18)-C(19)	1.494(2)	C(15)-C(16)	1.387(2)
N(11)-Pt-N(24)	85.3(3)	N(11)-Pt-I(1)	174.2(3)
N(24)-Pt-I(1)	89.1(2)	N(11)-Pt-I(2)	91.7(3)
N(24)-Pt-I(2)	175.8(2)	I(1)-Pt-I(2)	93.9(3)
C(16)-C(17)-C(18)	123.7(1)	C(19)-C(18)-C(17)	113.8(9)
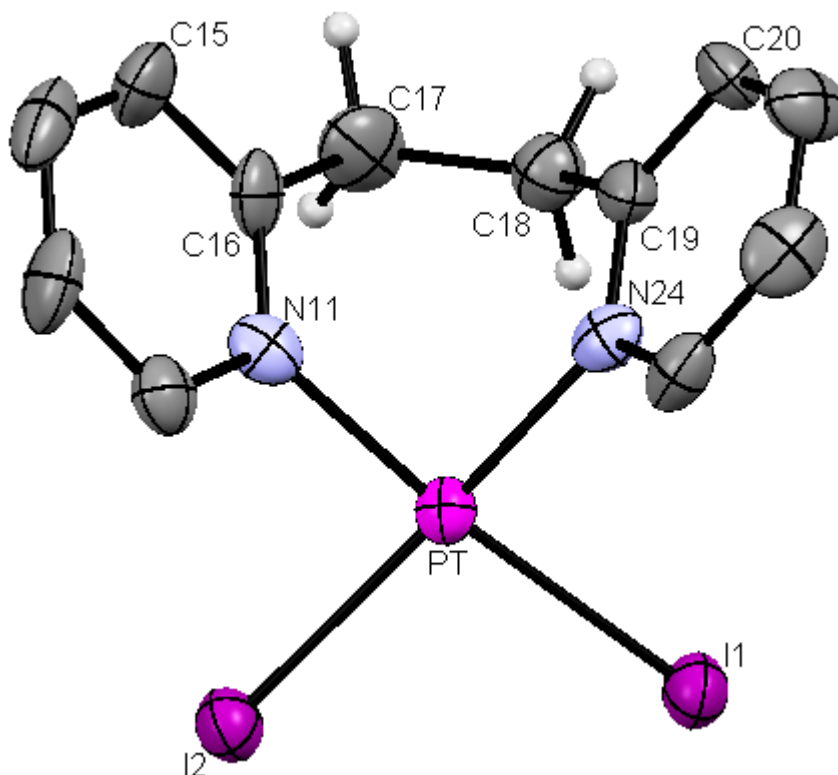
Figure 2.6. The structure of the complex [PtI$_2$(dpe)], **2.7**.

Complex **2.7** does not adopt the expected square planar platinum(II) geometry, and the pyridyl groups are twisted out of the plane by 56°. Figure 2.7 shows a view of the primary supramolecular polymer structure of **2.7** which was formed via self-assembly of weak CH•••IPt, with I(1)•••H(13A) = 3.14 Å, and I(1)•••H(20A) = 3.05 Å. The complexes were stacked via another type of secondary bonding between carbons of pyridyl groups and the adjacent bridging H-CH, with C•••H = 2.87 Å. All these relatively weak secondary bonding helped in the formation of the supramolecular structure.
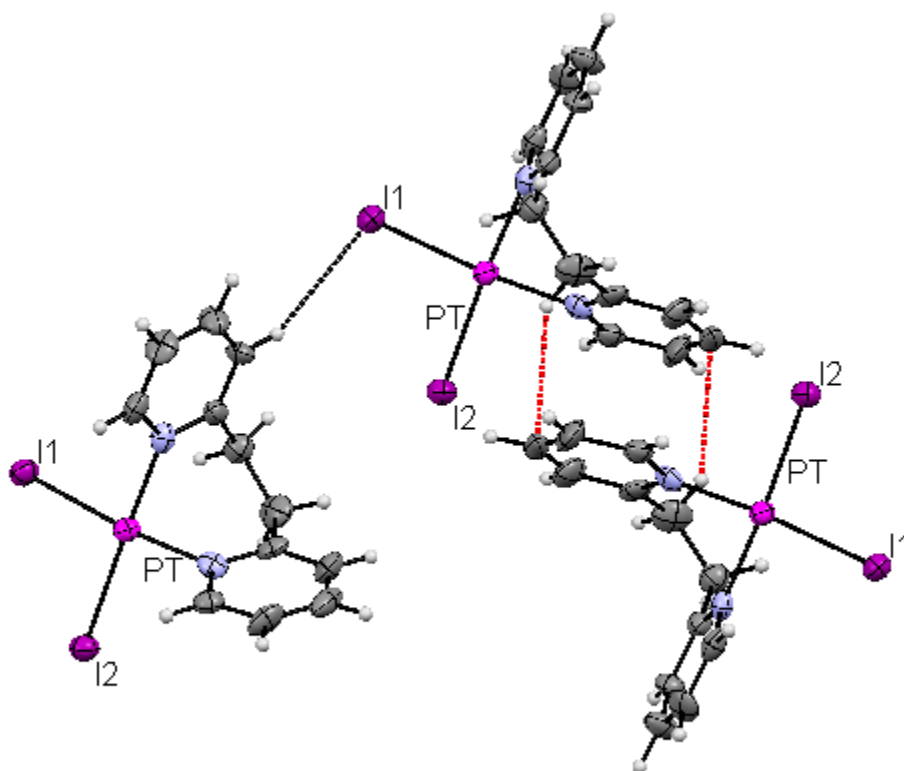
Figure 2.7. A view of the molecular structure of complex **2.7**.

Reacting complex **2.2** and I_2 in CD_2Cl_2 at -60 °C (Figure 2.8) showed the immediate formation of the complex *trans*-[PtI$_2$Me$_2$(dpe)], **2.8**, which started to disappear slowly upon warming to room temperature to produce the complex [PtI$_2$(dpe)], **2.7**, along with the release of MeI. In complex **2.8**, the two methyl platinum groups have a proton resonance at $\delta = 2.54$, with coupling $^2J_{Pt-H} = 72$ Hz, which is typical for platinum(IV) complexes. The *ortho* pyridyl proton resonance was observed at $\delta = 8.81$, with coupling $^3J_{Pt-H} = 20$ Hz, which is lower than the observed value in complex **2.7**. The CH$_2$ groups for **2.8** have a singlet proton resonance at $\delta = 3.33$, instead of two quartets observed in **2.7**. Also a single MeI proton resonance at $\delta = 2.16$ was seen. Three days later in the reaction mixture, red and transparent crystals started to form in the solution. These insoluble crystals were found to be the new chiral platinum(IV) complex [PtMe$_2$I$_2$\{κ^2-N,C-(2-C$_5$H$_4$N)CH$_2$CH(2-C$_5$H$_4$NMe)\}], **2.9** (Figure 2.9), which formed via complex **2.8**. This complex appears to be formed by the C-H bond activation of the ligand dpe. Table 2.2 shows selected bond lengths and angles for **2.9**. Complex **2.9** is not soluble in any organic solvent, so neither ^{1}H NMR spectrum nor regular mass spectrum was obtained for complex **2.9**. The identity of **2.9** was supported by the results of the MALDI mass spectrometry, which showed peaks at m/z = 550, and 676 corresponding to [PtMe$_2$I\{κ^2-N,C-(NC$_5$H$_4$)CH$_2$CH(C$_5$H$_4$NMe)\}]$^+$, and [PtMe$_2$I$_2$\{κ^2-N,C-(NC$_5$H$_4$)CH$_2$C(C$_5$H$_4$NMe)\}]$^+$, respectively. Scheme 2.3 shows the reaction of complex **2.2** with I_2 in CD_2Cl_2 at variable temperatures.

Δ: **2.8** (*trans*-[PtI$_2$Me$_2$(dpe)])

o: **2.7** [PtI$_2$(dpe)]

(a)　　ɵ: MeI

CD$_2$Cl$_2$

Me-Pt　ɵ

CH$_2$

CH$_2$

Δ

o Δ　o

CH$_2$

o

CH$_2$

o

o Δ
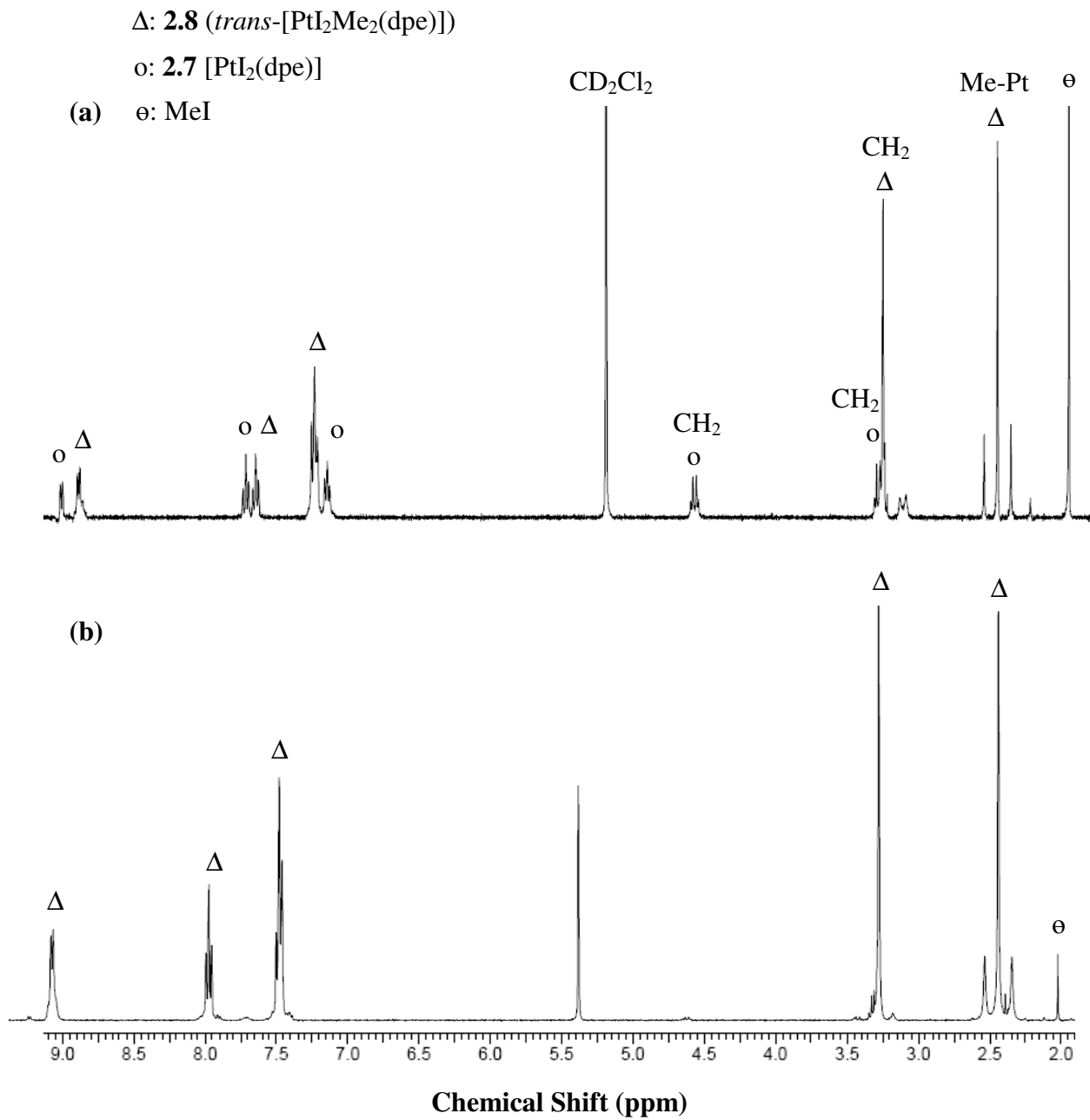
Figure 2.8. ^{1}H NMR spectra (400 MHz) for the reactions of complex **2.2** with I$_2$ in CD$_2$Cl$_2$ at (a) 20 ^{o}C; and (b) -60 ^{o}C.
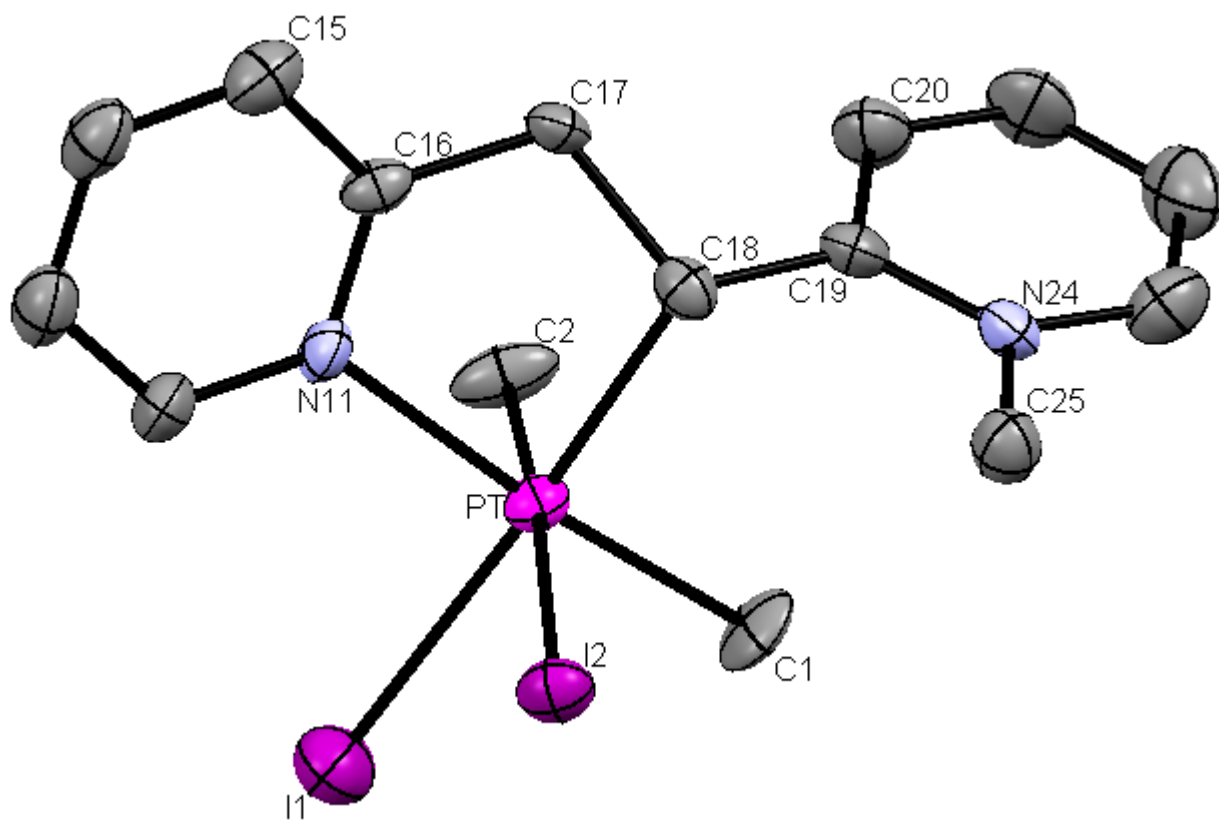
Figure 2.9. The molecular structure of complex **2.9**.
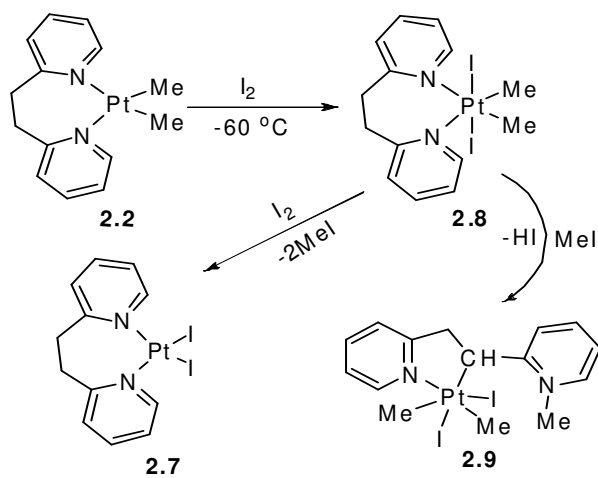
Scheme 2.3

Table 2.2. Selected bond lengths [Å] and angles [°] for [PtMe$_2$I$_2$(μ-{(NC$_5$H$_4$)-CH$_2$CH(C$_5$H$_4$NMe)}], **2.9**.

Pt-C(2)	2.060(1)	Pt-C(1)	2.092(1)
Pt-C(18)	2.126(1)	Pt-N(11)	2.168(8)
Pt-I(1)	2.723 (1)	Pt-I(2)	2.794 (8)
C(16)-C(17)	1.495(2)	C(17)-C(18)	1.543(1)
C(2)-Pt-C(1)	86.6(5)	C(2)-Pt-C(18)	92.5(5)
C(1)-Pt-C(18)	95.2(5)	C(2)-Pt-N(11)	92.4(4)
C(1)-Pt-N(11)	174.8(5)	C(18)-Pt-N(11)	79.7(4)
C(2)-Pt-I(1)	85.3(4)	C(1)-Pt-I(1)	86.7(4)
C(18)-Pt-I(1)	176.9(3)	N(11)-Pt-I(1)	98.4(3)
C(2)-Pt-I(2)	175.6(5)	C(1)-Pt-I(2)	95.0(4)
C(18)-Pt-I(2)	91.4(3)	N(11)-Pt-I(2)	86.3(2)
I(1)-Pt-I(2)	90.8(3)	C(16)-C(17)-C(18)	110.5(8)

The reaction was repeated, and the crystals of complex **2.9** again appeared after 3 days. The reaction was prepared in two different NMR tubes, the first tube was kept in the dark, and the second tube was exposed to light. There were no crystals observed for the tube kept in the dark, but crystals of compound **2.9** were formed in the tube exposed to the light. So an experiment was carried out using UV-visible spectroscopy to observe the behaviors of the both the ligand and complex **2.2** at different concentrations. The ligand on its own had a distinctive UV absorbance at wavelength of 263 nm. Similar spectra have been observed in the region of 280-290 nm for pyridine based ligands and the band was attributed to the π-π* transitions associated with the pyridyl fragment.[10] The UV absorbance for platinum(II) complex, **2.2,**

showed a band at 341 nm, in the region for a platinum(II) complex with a bis-pyridine ligand, and this absorbance is due to the metal to ligand charge transfer absorption.[10,11] Figures 2.10 and 2.11 show the absorbance of the ligand and complex **2.2** at five different concentrations. The absorbance vs. concentration plot of the free ligand fits to a straight line, while the plot for complex **2.2** deviates from linearity. This phenomenon of absorbance band shift is usually explained due to the aggregation and the presence of short Pt---Pt bonds.[10] In a UV cell, complex **2.2** and I_2 were mixed at 1:1 ratio in CD_2Cl_2, the UV absorbance showed a band at 257 nm. The same experiment was repeated but with 0.9 equivalent of iodine to prevent the strong absorbance of the halogen, an absorbance band shows at 504 nm. The ^{1}H-NMR was then checked and it showed the presence of [$PtMe_2I_2(dpe)$] and [$PtMeI(dpe)$].

Complex **2.7**, [$PtI_2(dpe)$], does not undergo fast exchange of the CH^aH^b protons. On the other hand, complex **2.9** is formed from complex **2.8**, [$PtMe_2I_2(dpe)$], which undergoes a reductive elimination to produce [$PtMeI(dpe)$]. The C-H activation reaction proceeds after the nucleophilic substitution reaction of the N in the dpe ligand with MeI produced via reductive elimination. Similar results were found in platinum phosphine complexes that were used in C-H bond activation.[12] The results for the platinum phosphine complexes showed that at a wavelength of 254 nm the ligand undergoes a C-H bond activation (Equation 2.5).

$$[(PPh_3)_2PtC_2H_4] \xrightarrow[\text{254 nm}]{hv} [(PPh_3)(Ph_2PC_6H_4)Pt(H)(C_2H_4)] \quad \textbf{2.5}$$
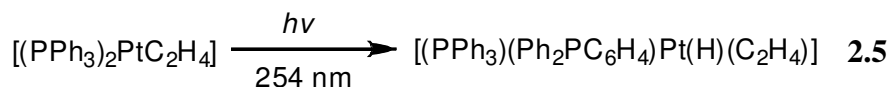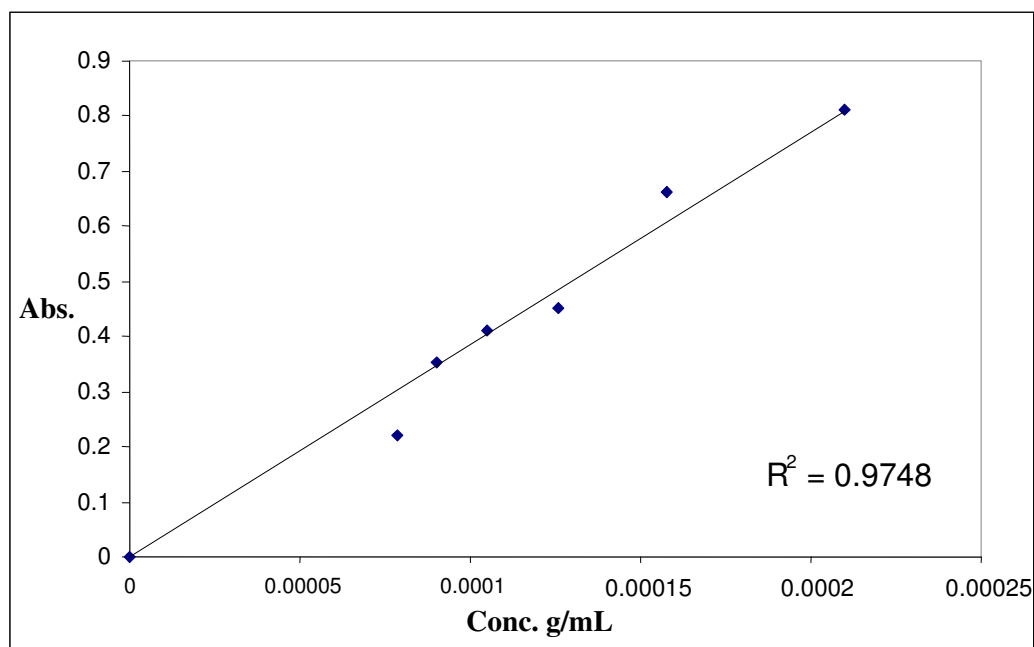
Figure 2.10. The absorbance of the ligand 1,2-di-2-pyridylethane as a function of concentration.
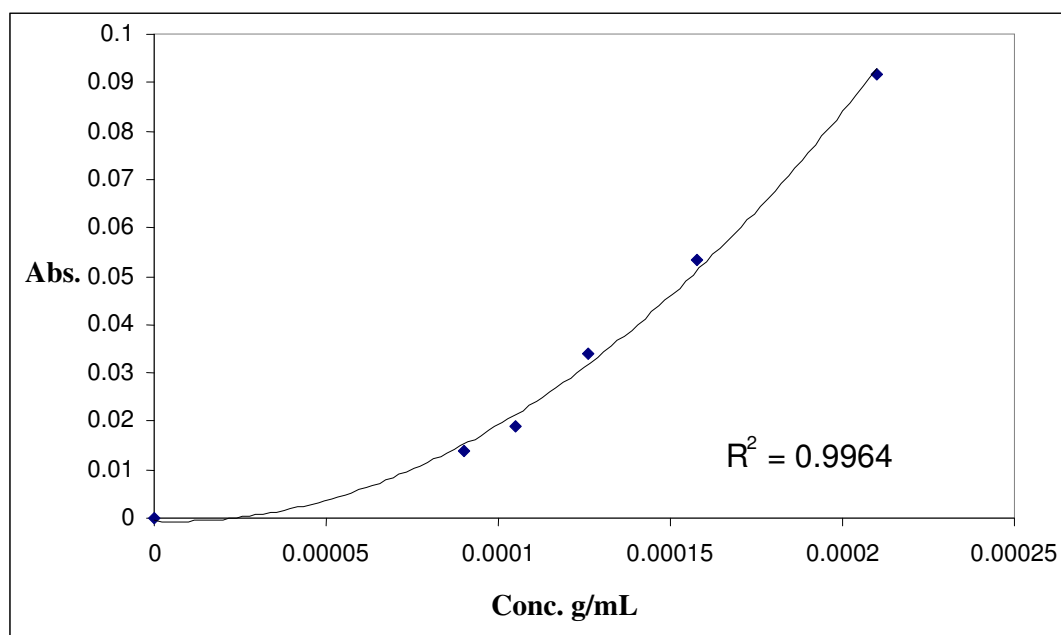
Figure 2.11. The absorbance of complex **2.2** as a function of concentration.

2.2.4 Reactions of [PtMe$_2$(dpe)] with Hydrochloric Acid

The complex [PtMe$_2$(dpe)], **2.2**, reacted with HCl at -60 $^{\circ}$C to produce [PtHClMe$_2$(dpe)], **10**, via *trans* oxidative addition. Complex **2.10** was characterized by its ^{1}H NMR spectrum at –60 $^{\circ}$C, which showed a methyl platinum proton resonance at δ = 1.15, with coupling $^{2}J_{\text{Pt-H}}$ = 67 Hz. Similar low values of $^{2}J_{\text{Pt-H}}$ were observed for platinum (IV) complexes.[2] The ^{1}H NMR spectrum contained a hydride resonance at δ = -20.6, with $^{1}J_{\text{Pt-H}}$ = 1609 Hz, in the range expected for a hydride *trans* to chloride.[13] The *trans* oxidative addition was also proved by observing the equivalence of the two pyridyl groups. The *ortho* pyridyl appeared at δ = 9.33, with coupling $^{3}J_{\text{Pt-H}}$ = 16 Hz. Also seen at δ = 0.18 is a small proton resonance due to methane. The reaction process for complex **2.2** with HCl in CD$_2$Cl$_2$ at variable temperatures is shown in Scheme 2.4.
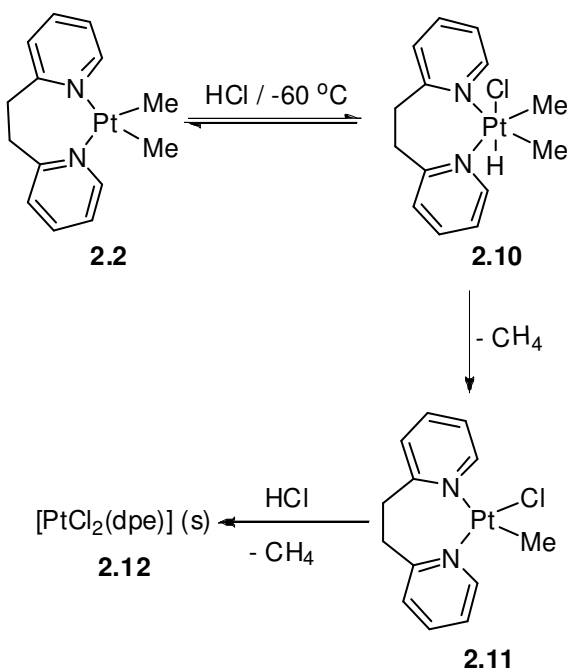
Scheme 2.4

Two proton resonances were observed at δ = 3.31, and 4.20 due to the CH_2 protons of **2.10**. At -20 ^{o}C, complex **2.10** started to disappear, and a new compound [PtMeCl(dpe)], **2.11** was produced via the reductive elimination of methane. Complex **2.11** was characterized by its ^{1}H NMR spectrum, which showed the presence of two different sets of pyridyl resonances due to the unsymmetrical structure. The methyl platinum group gave a proton resonance at δ = 0.81, with $^2J_{Pt-H}$ = 80 Hz. There were two *ortho* pyridyl proton resonances at δ = 8.63, and 9.06, with coupling $^3J_{Pt-H}$ = 36, and 17 Hz respectively. The coupling constant is higher for the proton resonance that is in the pyridyl group *trans* to the chloride ligand, due to its low *trans* influence. The two signals corresponding to the CH_2 protons appeared at δ = 3.31, and 3.81. At 0 ^{o}C, complex **2.10** disappeared totally, and the only product observed was [PtMeCl(dpe)], **2.11.** Using excess of HCl caused the precipitation of the known yellow complex [PtCl$_2$(dpe)], **2.12**. [7]

The V-T ^{1}H NMR experiment of complex **2.2** with HCl was repeated, but instead DCl was used to investigate for hydrogen/deuterium exchange. DCl was produced by reacting phosphorus pentachloride with D_2O. The reaction of **2.2** with DCl proceeded in a similar way to the previous experiment with HCl, but upon the reduction of methane gas, the proton resonances of all possible isotopomers CH_nD_{4-n} were seen in the ^{1}H NMR spectra (Figure 2.12). The singlet for CH_4, 1:1:1 triplet of CH_3D, and multiplets of CH_2D_2 and CHD_3 were all observed. The platinum methyl region of the ^{1}H NMR spectrum showed some evidence of deuterium incorporation into the methyl group. A singlet chemical shift was observed for Pt-CH_3 at δ = 0.81 ppm, with coupling $^2J_{Pt-H}$ = 79.7 Hz, also a 1:1:1 triplet for Pt-CH_2D was observed at δ = 0.79 ppm, with coupling $^2J_{H-D}$= 2.7 Hz. This shows that an H/D exchange occurs between the initial deuteride and the methyl ligands, also exchange is happening between the hydride ligand and the DCl.

These deuterium exchanges involve a methane complex intermediate. Scheme 2.5 shows the H/D exchange within the complex.
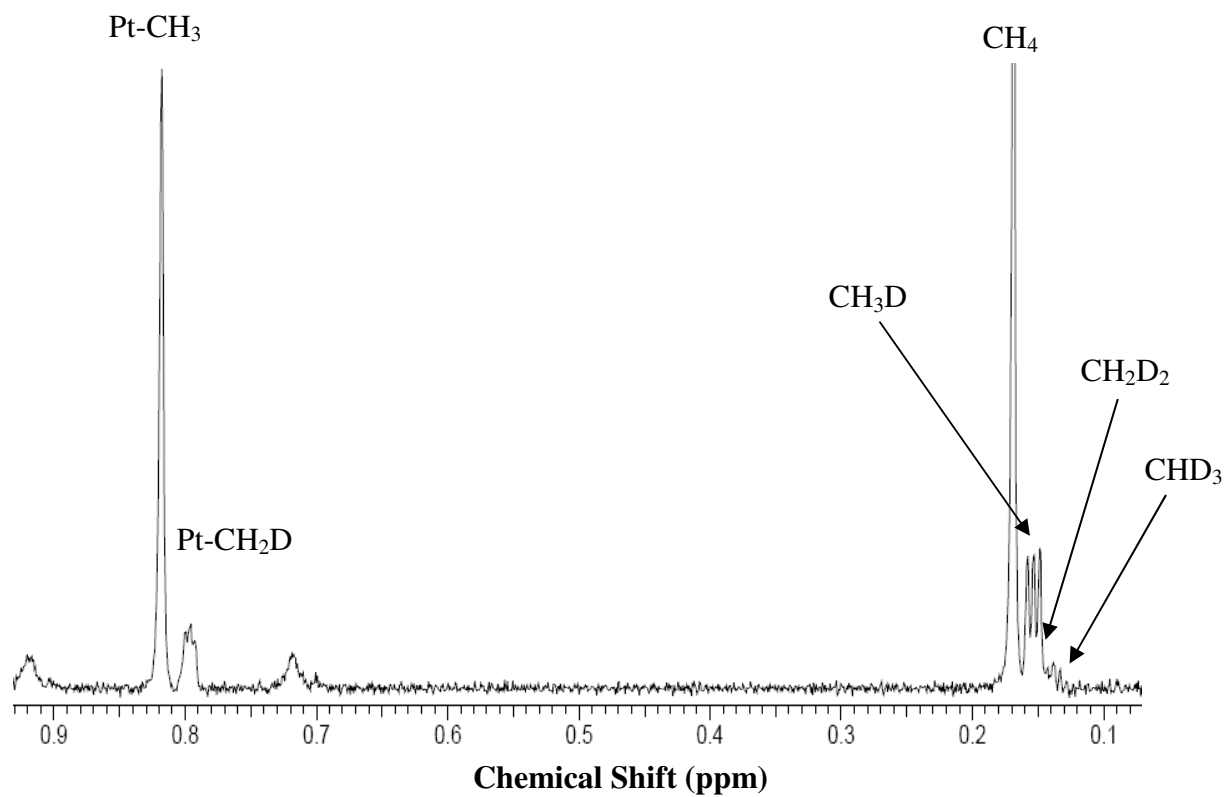
Figure 2.12. The ^{1}H-NMR spectrum (400 MHz, CD_2Cl_2) at room temperature in methylplatinum and methane regions for the reaction of **2.2** with DCl.
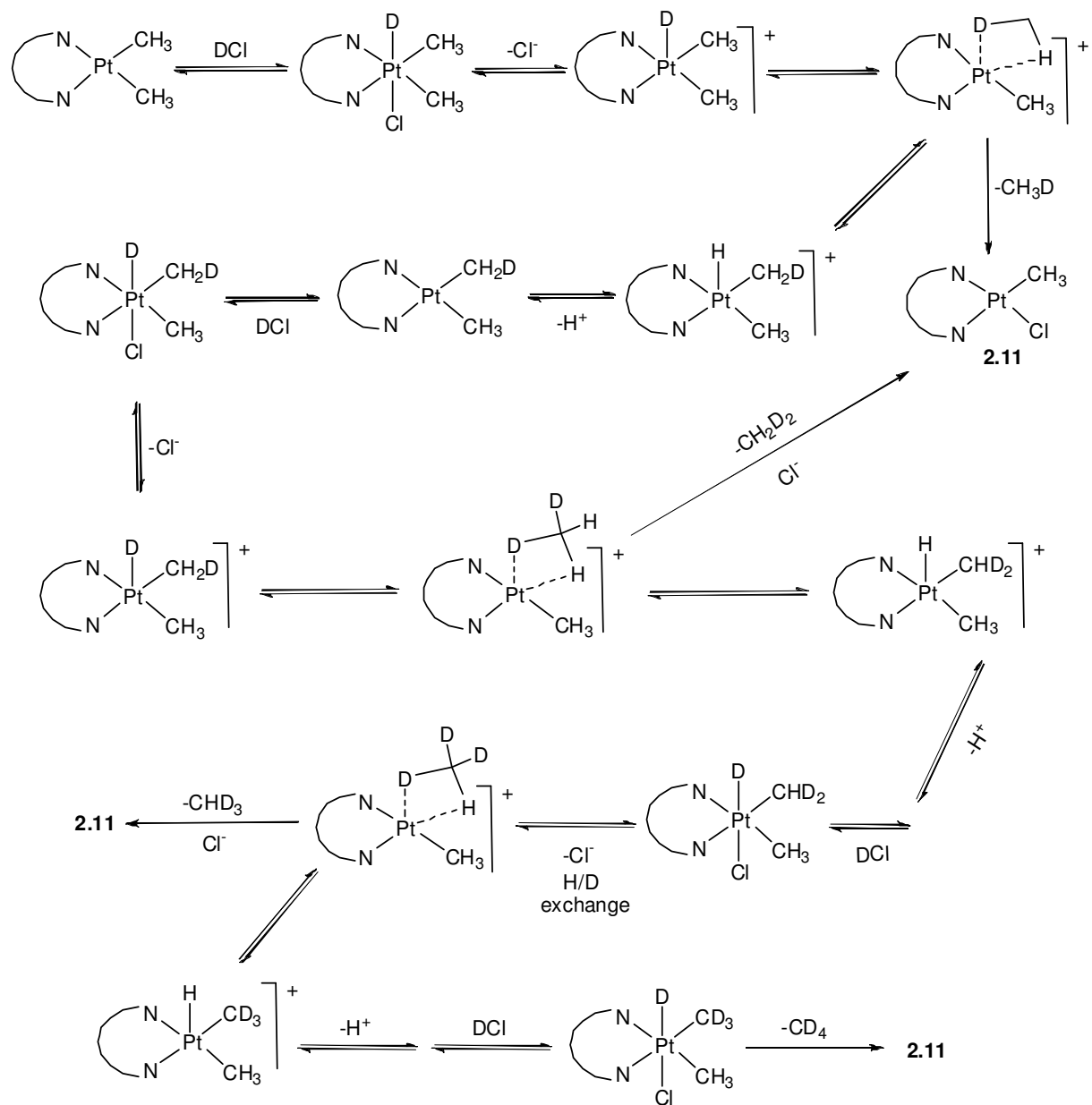
Scheme 2.5

2.2.5 Reactions of [PtMe$_2$(dpe)] with Hydrogen Peroxide

Reactions of complexes [PtMe$_2$(LL)], LL = diimine ligand, with hydrogen peroxide usually give the corresponding platinum(IV) complexes [PtMe$_2$(OH)$_2$(LL)] by oxidative addition.[2,14] However, in the case with LL = 1,2-di-2-pyridylethane, the oxidative addition of H$_2$O$_2$ to complex **2.2** was followed by easy ligand loss to give [{PtMe$_2$(OH)$_2$}$_n$], as a white precipitate (Scheme 2.6). The insoluble complex [{PtMe$_2$(OH)$_2$}$_n$], thought to be the sesquihydrate, has been prepared previously by hydrolysis of [{PtMe$_2$Br$_2$}$_n$].[15, 16] It is reported to dissolve in acidic aqueous solution to give the *cis*-[PtMe$_2$(OH$_2$)$_4$]$^{2+}$ ion, identified by a methylplatinum resonance in the ^{1}H NMR spectrum (Figure 2.13) at δ = 1.99, with $^2J_{(Pt-H)}$ = 75 Hz. [15, 16] Complex [{PtMe$_2$(OH)$_2$}$_n$], dissolved in D$_2$O acidified with sulfuric acid, gave identical parameters. However, when the reaction mixture of Scheme 2.6 in acetone was allowed to stand in air for several weeks, crystals of a new mixture which contained both a carbonatoplatinum(IV) complex [PtMe$_2$(CO$_3$)(dpe)], **2.13**, and the cluster complex [{PtMe$_3$(OH)•(PtMe$_2$(OH)$_2$)}$_2$], **2.14**, were slowly deposited. Complex **13** is evidently formed by the reaction of [{PtMe$_2$(OH)$_2$}$_n$] and the dpe ligand with atmospheric CO$_2$, while the formation of **2.14**, which contains both trimethylplatinum(IV) and dimethylplatinum(IV) units, requires methyl group transfer to give the PtMe$_3$OH units.
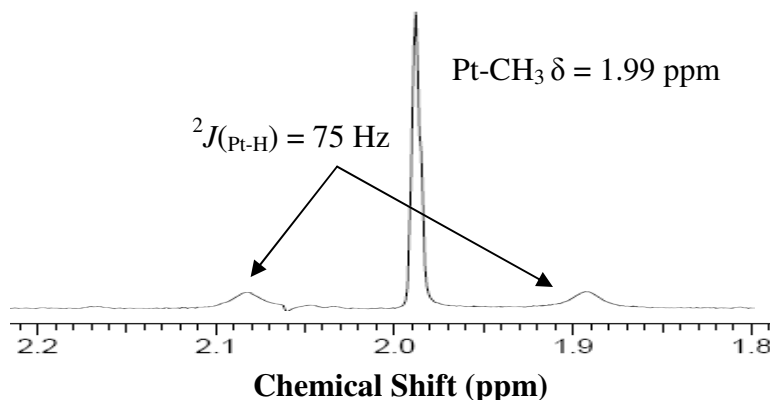
Figure 2.13. The ^{1}H NMR spectrum (600 MHz, D$_2$O) of the *cis*-[PtMe$_2$(OH$_2$)$_4$]$^{2+}$ ion.
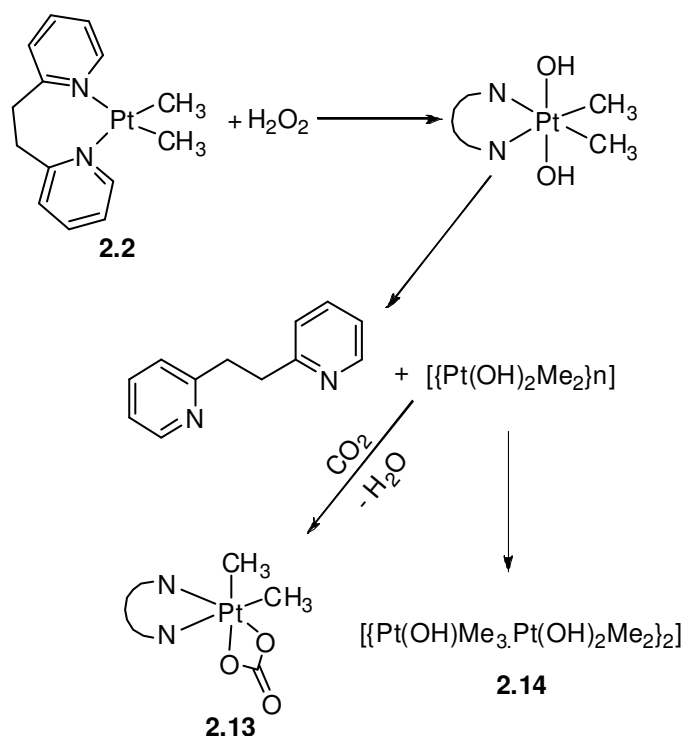
Scheme 2.6

The trimethylplatinum(IV) complexes [(PtMe$_3$X)$_4$], X = Cl, Br, I, OH *etc.*, were among the first alkyl complexes of transition metals to be prepared, and so they have particularly important place in organometallic chemistry.[17, 18] They have the cubane structure **A**, Scheme 2.7.[18] There are also complexes of formula [{(PtMe$_3$X)(PtMe$_2$X$_2$)}$_n$] and [(PtMe$_2$X$_2$)$_n$] whose compositions are well established but whose structures are less certain.[15,19] The compounds [{PtMe$_3$X)(PtMe$_2$X$_2$)}$_n$] are proposed to have cubane structures, **B** or **C** (Scheme 2.7), based mostly on vibrational spectroscopy and by analogy to **A**.[19] The reaction of complex **2.2** with H$_2$O$_2$ shows that the complex [{(PtMe$_3$X)(PtMe$_2$X$_2$)}$_n$], X = OH, actually has the structure **D** (Scheme 2.7), which is based on a face-bridged double cubane with two vertices missing.[20]

(A)   **(D)**

(B)   **(C)**
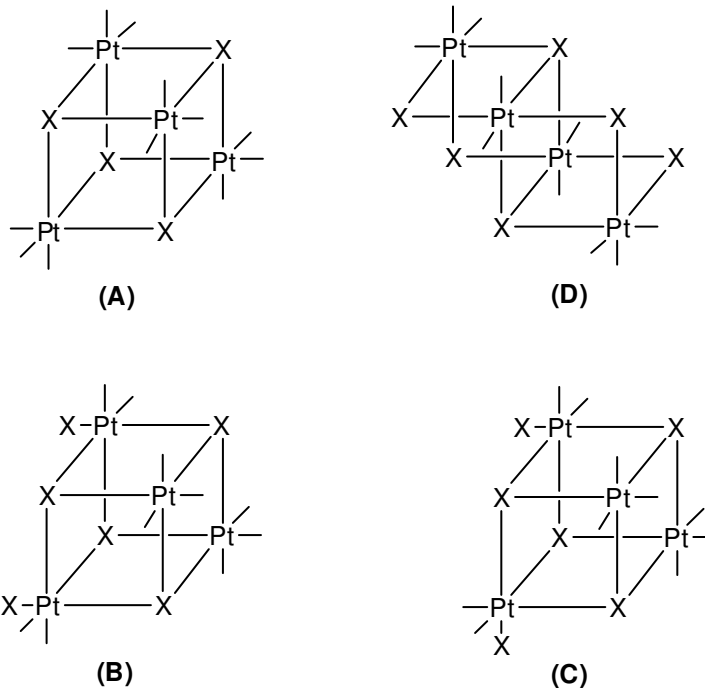
X = Cl, Br, I, or OH

Scheme 2.7

The characterization of the new mixture, of composition **2.13$_2$•2.14**, relies primarily on X-ray structure determination. The complex is sparingly soluble in organic solvents, and it does not survive dissolution. Thus, the ^{1}H NMR spectrum (Figure 2.14) in CD$_2$Cl$_2$ contained resonances for [{PtMe$_3$(OH)}$_4$] and for [PtMe$_2$(CO$_3$)(dpe)], **2.13**, but no resonances attributable to [PtMe$_2$(OH)$_2$] units were observed. This indicates that mixture breaks apart reversibly to give the component complexes **2.13**, [{PtMe$_3$(OH)}$_4$], and the insoluble [{PtMe$_2$(OH)$_2$}$_n$].[15, 19] Complex **2.13**, [PtMe$_2$(CO$_3$)(dpe)], was characterized by two methyl platinum resonances at $\delta = 1.54$ and 1.91, with $^2J_{Pt-H} = 71$ and 72 Hz respectively. The complex gave 2 sets of pyridyl resonances due to being unsymmetrical, with two *ortho* pyridyl protons resonances at $\delta = 8.11$ and 8.76, with

coupling $^3J_{Pt-H}$ = 32 and 18 Hz, respectively, the *ortho* pyridyl proton (*trans* to carbon) has a lower coupling constant due to the higher *trans* influence of the methyl ligand. Two resonances were observed for the two CH_2 groups at δ = 3.30 and 3.79. The complex [{PtMe$_3$(OH)}$_4$] was identified by a methyl platinum resonance at δ = 0.90, with $^2J_{Pt-H}$ = 80 Hz. After that, the solvent was removed under vacuum, and an IR experiment was run on the sample, and it showed intense bands at v(CO) = 1609 and 1655 cm^{-1}, due to the carbonate group.
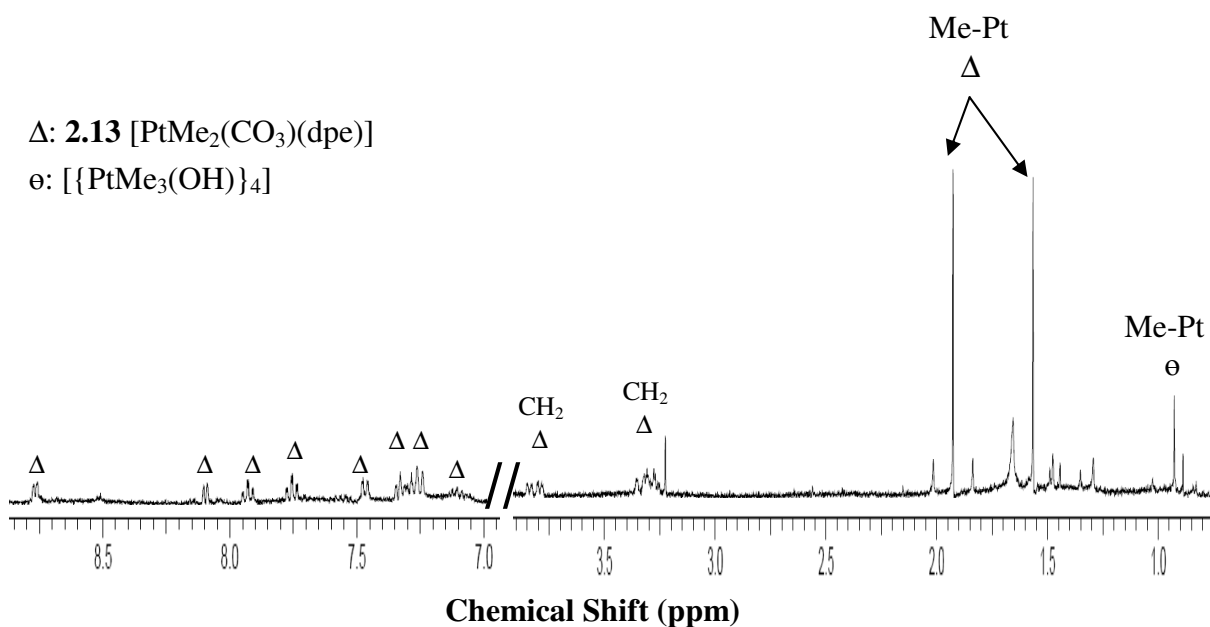
Figure 2.14. The ^{1}H NMR spectrum (400 MHz, CD$_2$Cl$_2$) of supramolecular mixture, which contained resonances for [{PtMe$_3$(OH)}$_4$] and for [PtMe$_2$(CO$_3$)(dpe)], **2.13**.

The structure of complex **2.13** is shown in Figure 2.15, and the structure of complex **2.14** is shown in Figure 2.16. Complex **2.13** has octahedral stereochemistry with the *cis,cis,cis* orientation of the dpe ligand, methyl and carbonate groups. The geometrical parameters of the platinum-carbonate group are similar to those in the chelating carbonate complexes [Pt(CO$_3$)L$_2$], L = phosphine,[21] but there is some distortion because of the high *trans*-influence of the methyl

group. Thus the Pt-O distances Pt-O(3) = 2.008(6) Å (*trans* to nitrogen) and Pt-O(4) = 2.197(5) Å (*trans* to carbon) can be compared to intermediate distances of 2.045(3) and 2.063(3) Å (*trans* to phosphorus) in [Pt(CO$_3$)PPh$_3$].[21] The Pt-N distances in complex **2.13** are also significantly different as a result of the higher *trans*-influence of methyl compared to carbonate. Thus, the distance Pt-N(24) = 2.256(6) Å (*trans* to carbon) is longer than Pt-N(11) = 2.028(7) Å (*trans* to oxygen). Although carbonate complexes of platinum are important in the bioinorganic chemistry of platinum drugs such as *cis*-platin, little is known about the structures and this appears to be the first structure determination of a platinum(IV) carbonate derivative.[22]
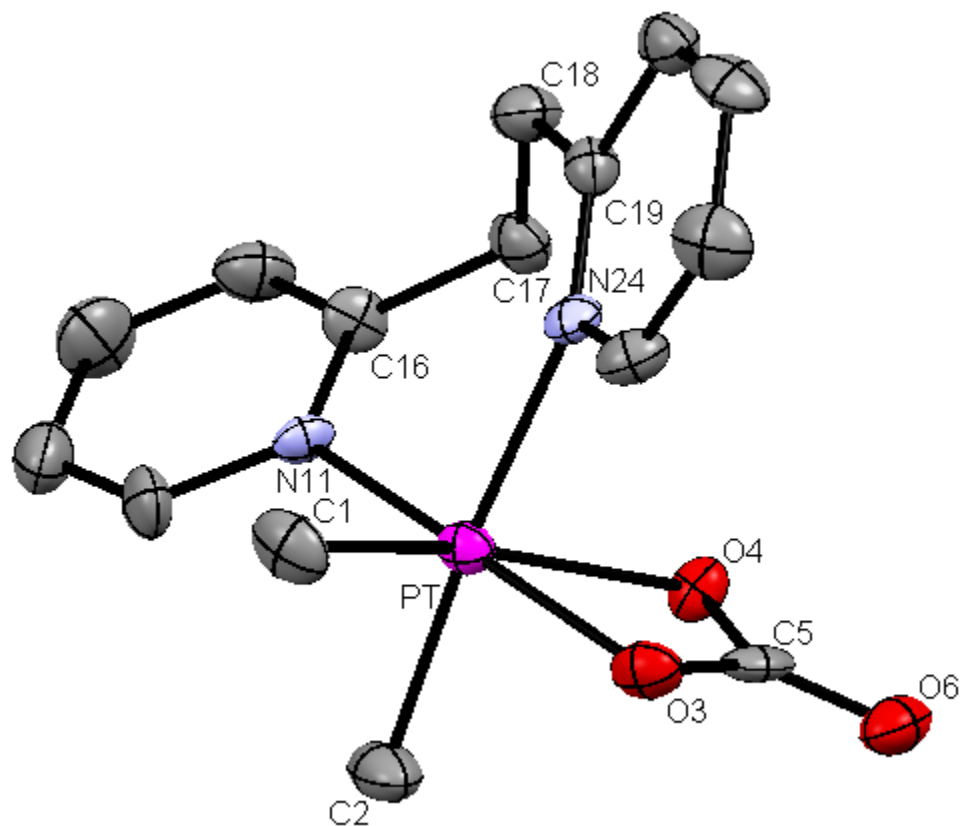
Figure 2.15. A view of the structure of complex **2.13**.
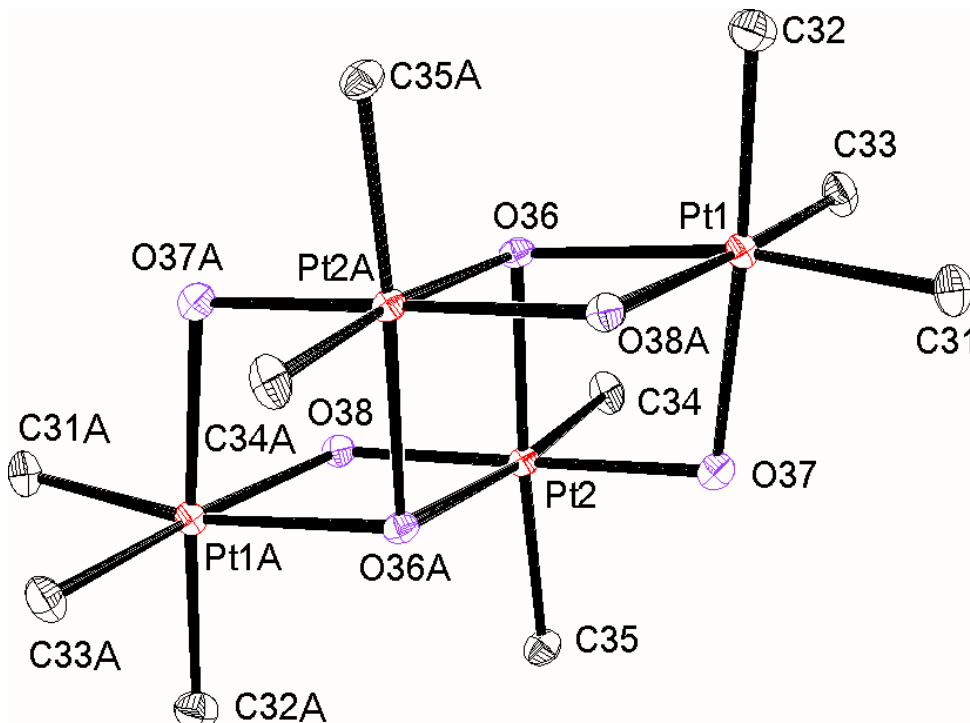
Figure 2.16. A view of the structure of complex **2.14**.

The structure of the cluster complex [{PtMe$_3$OH•PtMe$_2$(OH)$_2$}$_2$], **2.14**, is clearly shown in Figure 2.16 to be based on the structure **D** (Scheme 2.7), which is previously unknown in platinum(IV) chemistry. It can be described as having a face-bridged double cubane structure with two vertices missing.[20] Each platinum centre is 6-coordinate with octahedral stereochemistry. The two trimethylplatinum(IV) groups [Me$_3$Pt(1) and Me$_3$Pt(1A)] are at either end of the cluster and the two dimethylplatinum(IV) units [Me$_2$Pt(2) and Me$_2$Pt(2A)] are at the

centre. Two of the hydroxyl groups in **2.14** are triply bridging, μ_3-OH [O(36) and O(36A)] and the other four are doubly bridging, μ_2-OH [O(37), O(37A), O(38) and O(38A)].The triply bridging μ_3-OH [O(36) and O(36A)] are *trans* to carbon and the distances fall in the range 2.184(6)-2.216(6) Å, similar to the value in the classic cubane [{Pt(OH)Me$_3$}$_4$] with Pt-O = 2.205(4) Å.[18] However, the doubly bridging, μ_2-OH [O(37), O(37A), O(38) and O(38A)] are *trans* to both carbon and oxygen and the distances Pt(1)-O(37) = 2.204(6); Pt(1)-O(38A) = 2.209(6) Å *trans* to methyl are significantly longer than the distances Pt(2)-O(38) = 2.024(6); Pt(2)-O(37) = 2.037(6) Å *trans* to hydroxide. It is important to note that these short distances Pt(2)-O(38) and Pt(2)-O(37) are in the range expected for terminal Pt-OH groups.[14e, 23]

All of the hydroxo ligands of the cluster complex **2.14** are hydrogen-bonded to oxygen atoms of the carbonato ligands of complex **2.13**, as shown in Figure 2.17. The oxygen atom O(4) of complex **2.13** which is *trans* to methyl forms a hydrogen bond to the μ_3-OH group of **2.14**, O(4)•••H-O(36), with O(4)•••O(36) = 2.745(7) Å, and the carbonyl oxygen O(6) forms two hydrogen bonds to μ_2-OH groups with O(6)•••O(37) = 3.079(8) and O(6)•••O(38) = 2.777(8) Å. The carbonate oxygen atom O(3) which is *trans* to nitrogen, and so probably carries the least negative charge, does not take part in hydrogen bonding. It is probably this hydrogen bonding which favors formation of the supramolecular mixture with stoichiometry **2.13$_2$•2.14**.
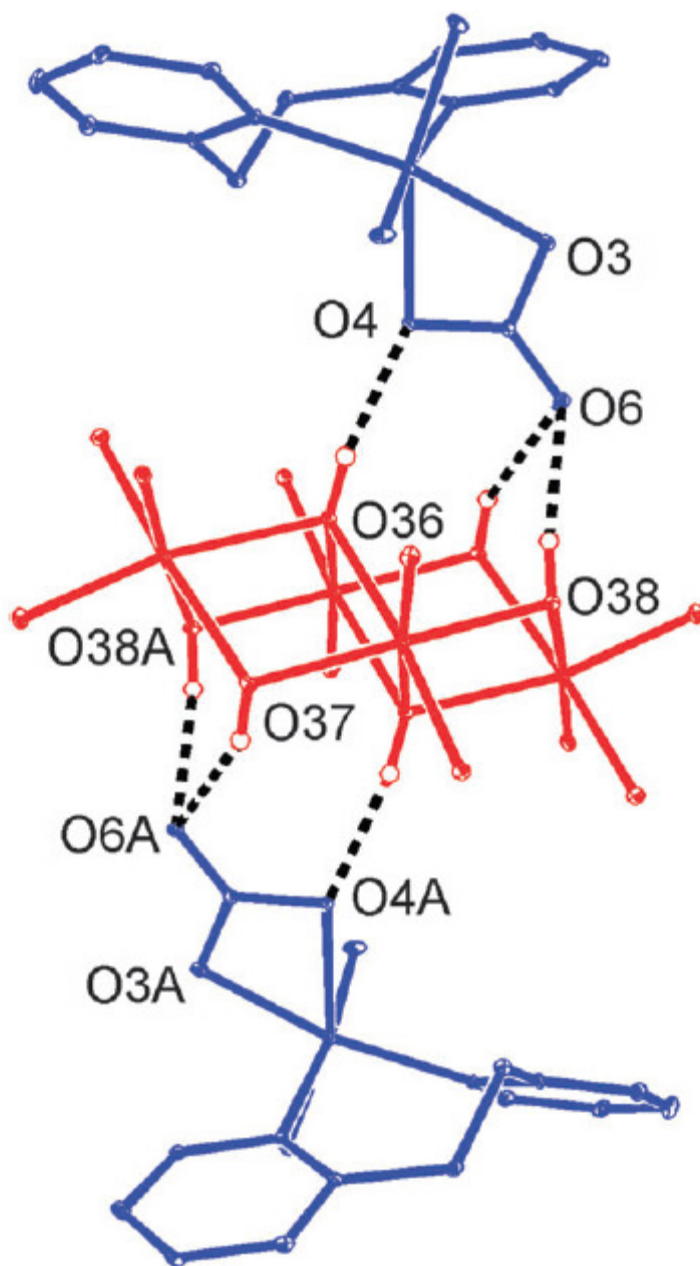
Figure 2.17. The hydrogen bonding between complexes **2.13** (top, bottom) and **2.14** (centre).

Table 2.3. Selected bond lengths [Å] and angles [°] for complexes **2.13** and **2.14**.

	Complex **2.13**		
Pt-O(3)	2.008(6)	Pt-O(4)	2.197(5)
Pt-N(11)	2.028(7)	Pt-N(24)	2.256(6)
Pt-C(1)	2.041(8)	Pt-C(2)	2.054(9)
O(3)-C(5)	1.334(1)	O(4)-C(5)	1.302(1)
C(5)-O(6)	1.226(1)	C(17)-C(18)	1.538(1)
O(3)-Pt-N(11)	169.5(3)	O(3)-Pt-C(1)	99.5(3)
N(11)-Pt-C(1)	90.1(3)	O(3)-Pt-C(2)	88.0(4)
N(11)-Pt-C(2)	87.2(4)	C(1)-Pt-C(2)	92.0(4)
O(3)-Pt-O(4)	62.5(2)	N(11)-Pt-O(4)	107.9(2)
C(1)-Pt-O(4)	162.0(3)	C(2)-Pt-O(4)	87.9(3)
O(3)-Pt-N(24)	85.3(3)	N(11)-Pt-N(24)	99.6(3)
C(1)-Pt-N(24)	87.3(3)	C(2)-Pt-N(24)	173.1(4)
	Complex **2.14**		
Pt(1)-C(31)	2.011(9)	Pt(1)-C(32)	2.023(9)
Pt(1)-C(33)	2.031(9)	Pt(1)-O(36)	2.216(6)
Pt(1)-O(37)	2.204(6)	Pt(1)-O(38A)	2.209(6)
Pt(2)-C(34)	2.035(8)	Pt(2)-C(35)	2.022(8)
Pt(2)-O(38)	2.024(6)	Pt(2)-O(37)	2.037(6)
Pt(2)-O(36A)	2.184(6)	Pt(2)-O(36)	2.193(8)

It is current conventional wisdom that complexes $[(PtR_3X \cdot PtR_2X_2)_n]$ and $[(PtR_2X_2)_n]$ have structures based on the closed cubane structure **A** (Scheme 2.7), which is firmly established for $[(PtR_3X)_4]$,[17,18] with either two or four alkyl groups R replaced by terminal halide or analogous groups X.[19,24] The relative energies were calculated using DFT for the complexes

[(PtMe$_3$X•PtMe$_2$X$_2$)$_2$] with X = OH, Cl, Br, or I, and the results are given in Table 2.4. It can be seen that the structure **D** (Scheme 2.7) is predicted to be more stable than either **B** or **C** in all cases. The primary evidence for the structure **B** or **C** is the observation of an infrared peak assigned to v(Pt-X) of a terminal Pt-X group for [(PtMe$_3$X•PtMe$_2$X$_2$)$_n$] with X = Br or I at 250 cm^{-1} or 175 cm^{-1}, respectively, along with lower energy peaks assigned to the bridging Pt$_3$(μ_3-X) groups.[19] The highest energy band, due to v(Pt-X), for structure **B** was calculated by DFT to be at 250 cm^{-1} or 182 cm^{-1}, for X= Br or I, in good agreement with the observed spectra.[19] However, the calculated spectra for structure **D** also contained a higher energy band at 235 cm^{-1} or 190 cm^{-1}, for X = Br, or I, also in reasonable agreement with the observed spectra.[19] These higher energy bands are assigned to v(Pt-X) for the mutually *trans* X-Pt-X groups, analogous to the O(37)-Pt(2)-O(38) unit of complex **2.14** (Figure 2.16), in which the Pt-X bonds are stronger than in all *trans* Me-Pt-X units.

Table 2.4. Calculated relative energies (kJ mol^{-1}) of structures **B**, **C**, and **D** (Scheme 2.7) for complexes [(PtMe$_3$X•PtMe$_2$X$_2$)$_2$] with X = OH, Cl, Br, or I

Structure	X = OH	X = Cl	X = Br	X = I
D	0	0	0	0
B	34	56	52	47
C	54	39	39	39

2.2.6 Reactions of [PtMe₂(dpe)] with Methanol
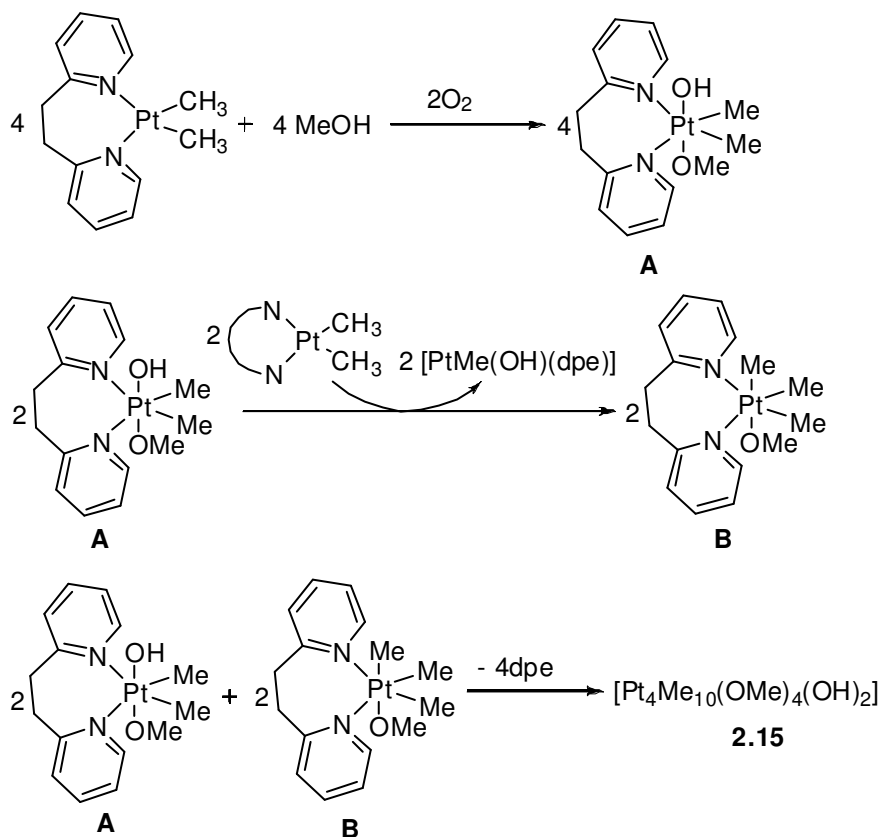
Scheme 2.8

The reaction of complex **2.2**, [PtMe₂(dpe)], with MeOH proceeded easily at room temperature to give complex **2.15**, [Pt₄Me₁₀(μ₂-OMe)₂ (μ₃-OMe)₂(μ₂-OH)₂] (Scheme 2.8), whose structure was determined and is shown in Figure 2.18. Complex **2.2** was stirred in methanol for 1 hour, and the solution was then allowed to stand at room temperature. Two days later, crystals of complex **2.15** precipitated out. The structure of complex **2.15** is similar to the structure of complex **2.14**, but the differences are that complex **2.15** has 4 bridging methoxy groups. Two of the methoxy groups are triply bridging and the other two are doubly bridging. The crystals of

complex **2.15** are soluble in methylene chloride, so complex **2.15** was characterized using ^{1}H and

NOESY NMR spectroscopy.
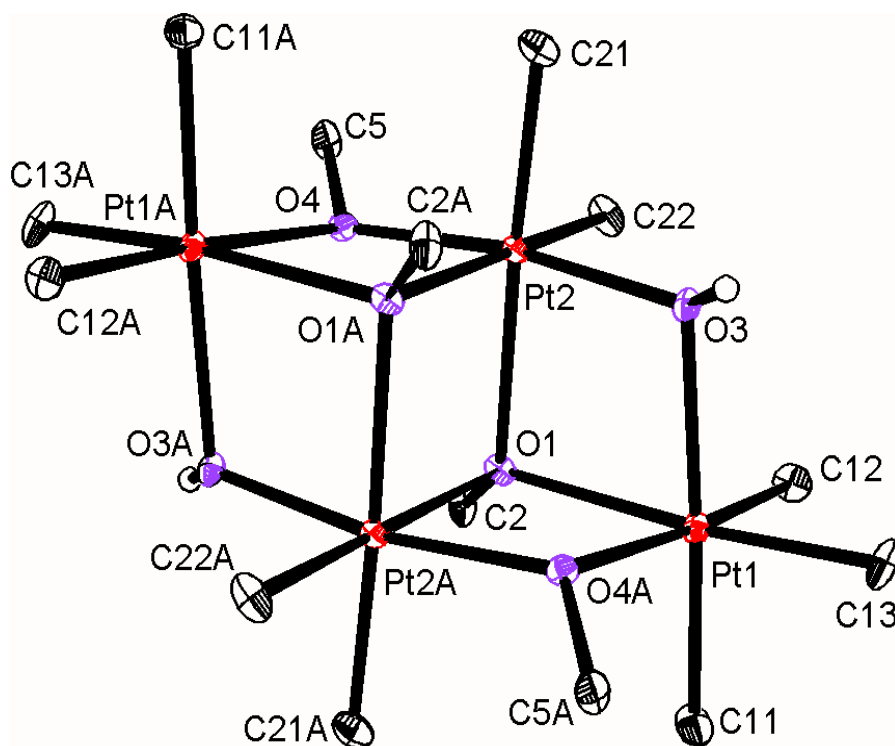
Figure 2.18. A view of the structure of complex **2.15**.

The ^{1}H NMR spectrum (Figure 2.19) showed a highly deshielded proton resonance at δ = -

1.20 which belongs to the hydroxyl groups. This OH proton resonance is broad due to fast

exchange, and upon monitoring the complex at low temperatures the peak became narrower.

Also, the ^{1}H NMR spectrum showed five different methyl platinum resonances at δ = 0.75, 0.92,

0.96, 1.67, and 1.73 ppm, with $^2J_{Pt-H}$ = 77, 76, 76, 77, and 77 Hz, respectively. The two doubly

bridging methoxy groups have a proton resonance at δ = 2.96 ppm, with $^3J_{\text{Pt-H}}$ = 13 Hz (*trans* to carbon), and $^3J_{\text{Pt-H}}$ = 38 Hz (*trans* oxygen), since carbon has a higher *trans* influence than oxygen. On the other hand, the two triply bridging methoxy groups have a proton resonance at δ = 3.86 ppm, with $^3J_{\text{Pt-H}}$ = 13 Hz (*trans* to carbon). The coupling constants values in complex **2.15** are similar to the results found in complex **2.13**. Also the Pt-O distances Pt-O (*trans* to carbon) = 2.198(7)-2.238(5) Å, and Pt-O (*trans* to oxygen) = 2.011(7) Å are similar to the Pt-O distances found in complex **2.14**. As in **2.14**, the Pt-O distances are longer for the hydroxyl or methoxy groups *trans* to methyl than for those *trans* to an oxygen-donor ligand (OH or OMe). Each molecule of complex **2.15** is connected to two neighboring molecules through hydrogen bonding, mediated by the methanol solvate molecules, to give a supramolecular polymer (Figure 2.20). Replacing methanol with CD$_3$OD showed similar results except for the loss of the two methoxy proton resonances.
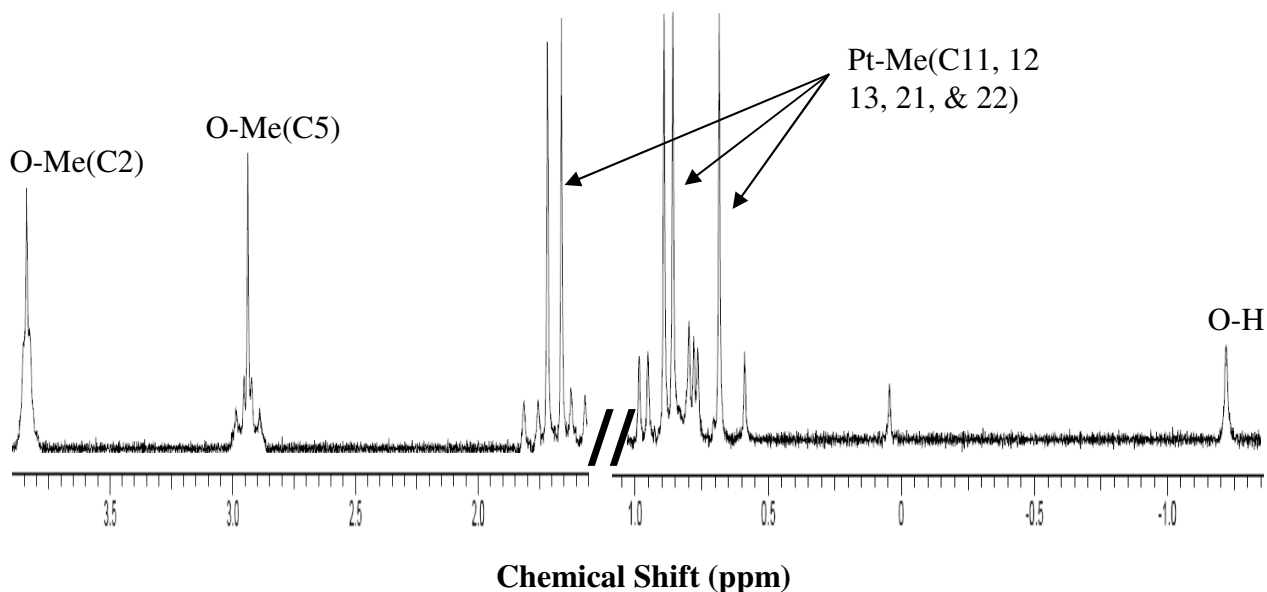
Figure 2.19. The ^{1}H NMR spectrum (400 MHz, CD$_2$Cl$_2$) of complex **2.15**.
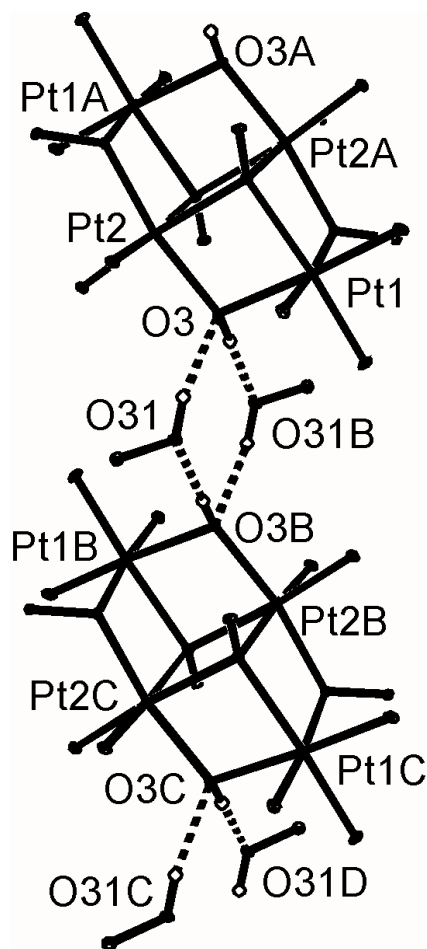
Figure 2.20. The hydrogen bonding between complexes **2.15** (top, bottom) and methanol.

Table 2.5. Selected bond lengths [Å] for complex **2.15**

Pt(1)-C(13)	2.020(1)	Pt(1)-C(12)	2.037(1)
Pt(1)-C(11)	2.048(1)	Pt(1)-O(4A)	2.200(7)
Pt(1)-O(3)	2.204(8)	Pt(1)-O(1)	2.220(8)
Pt(2)-O(3)	2.011(7)	Pt(2)-O(4)	2.012(7)
Pt(2)-C(21)	2.019(1)	Pt(2)-C(22)	2.048(9)
Pt(2)-O(1A)	2.198(7)	Pt(2)-O(1)	2.238(8)
O(1)-C(2)	1.415(1)	O(4)-C(5)	1.420(1)

2.3 Conclusions

The reaction of the ligand dpe with the precursor $[Pt_2Me_4(\mu\text{-}SMe_2)_2]$,[6] in diethyl ether proceeded easily at room temperature forming the 7-membered chelate ring complex $[PtMe_2(dpe)]$. The complex was isolated easily, and is stable for a short period of time at room temperatures. It should be stored at low temperatures and under nitrogen at all times, because the ligand dissociates easily. The reaction of complex **2.2**, $[PtMe_2(dpe)]$, with MeI formed the known complex $[(PtIMe_3)_4]$. The ^{1}H-NMR experiments for the reaction of MeI/CD_3I with **2.2** showed that complex **2.2** was reactive to oxidative addition, but that the dpe ligand was easily displaced from platinum(IV) at elevated temperatures.

The oxidative addition of bromine with the dimethylplatinum(II) complex $[PtMe_2(dpe)]$, occurs with *trans* stereochemistry, but that there is an easy equilibrium between *cis* and *trans* isomers at temperatures above -60 ^{o}C. At low temperature, the equilibrium favors **2.5b** while at higher temperature the equilibrium favors **2.5a**. At room temperature, methyl bromide was released by a reductive elimination step in the platinum(IV) complex. Reacting complex **2.2** with iodine proceeded at room temperature to give complex **2.7**, $[PtI_2(dpe)]$. The reaction was monitored using ^{1}H-NMR at lower temperatures, which showed the formation of the dimethylplatinum(IV) complex $[PtMe_2I_2(dpe)]$, that underwent reductive elimination of MeI at higher temperatures thus forming $[PtI_2(dpe)]$. A reaction of MeI with complex **2.2** produced crystals, which were found to be the new chiral platinum(IV) complex $[PtMe_2I_2(\mu\text{-}\{(NC_5H_4)\text{-}CH_2CH(C_5H_4NMe)\}]$, **2.9**. This complex is produced from the dimethylplatinum(IV) complex $[PtMe_2I_2(dpe)]$ via the C-H activation.

The reaction of HCl with **2.2** proceeded to give the hydrido-platinum(IV) complex at low temperatures, but at higher temperatures formed the dichloro-platinum(II) complex via the reductive elimination of methane. Also the reaction with DCl instead of HCl showed the presence of H/D exchange, and these reactions produced all possible isotopomers of methane and deuterium. These results demonstrate the ability of relatively simple systems to interact or even affect the C-H bonds.

The reaction of complex **2.2** with H_2O_2 or methanol and dioxygen gave the complexes $[\{PtMe_3X)(PtMe_2X_2)\}_n]$, X = OH or OMe, which are shown to have actually the structure **D**, which is based on a face-bridged double cubane with two vertices missing.

2.4 Experimental

All reactions were carried out under nitrogen using standard Schlenk techniques or using a drybox, unless otherwise specified. Solvents were dried and distilled under N_2 before use. NMR spectra were recorded on Varian Mercury 400 or Varian Inova 400 or 600 spectrometers. [1]H and ^{13}C chemical shifts are reported relative to TMS. The complexes cis/trans-[PtCl$_2$(SMe$_2$)$_2$] and [Pt$_2$Me$_4$(μ-SMe$_2$)$_2$] were prepared from K$_2$[PtCl$_4$] according to the literature.[6] Analytical data were obtained from Guelph Chemical Labs. The proton resonances of the pyridyl groups were assigned according to Chart 2.2. DFT calculations were performed by Dr. Richard Puddephatt using the Amsterdam Density Functional program based on the Becke-Perdew functional, with first-order scalar relativistic corrections.
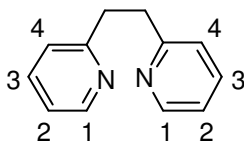
Chart 2.2

[1,2-di-2-pyridylethane], (dpe), 2.1. A modified procedure of Quagliotto *et al.*[5] was followed. Using a three-necked round bottom flask equipped with N_2 gas in a dry ice-acetone bath, a 2.5 M solution of butyllithium in pentane (50 mL, 0.125 mol) and anhydrous ethyl ether (150 mL) were added. Then at -20 °C 2-methyl pyridine (12.7 mL, 0.125 mol) was added dropwise, under stirring, giving a red orange solution. Then 1,2-dibromoethane (10.77 mL, 0.125 mol). The reaction mixture was allowed to react for 2 h at -20 °C, and then for 4 h at room temperature. The reaction was quenched by the dropwise addition of water (15 mL). The solution was extracted

with hydrogen chloride solution. The aqueous layer was separated and treated with sodium

hydroxide, until basic, when an orange–reddish oil separated. The oil was extracted three times

with ether. Then the organic layer was dried with anhydrous sodium sulfate, filtered, and

evaporated. The crude product was purified by distillation under high vacuum. Yield 59%. [1]H

NMR in CDCl$_3$: δ = 3.18 (s, 4H, 2CH$_2$), 7.02 (dt, 2H, $^3J_{\text{H-H}}$ = 5 Hz, $^3J_{\text{H-H}}$ = 6 Hz, Py{H^2}), 7.06

(d, 2H, $^3J_{\text{H-H}}$ = 7 Hz, Py{H^4}), 7.47 (dt, 2H, $^3J_{\text{H-H}}$ = 7 Hz, $^3J_{\text{H-H}}$ = 6 Hz, Py{H^3}), 8.49 (d, 4H, $^3J_{\text{H-}}$

$_{\text{H}}$= 5 Hz, Py{H^1}).

[PtMe$_2$(dpe)], 2.2. [Pt$_2$Me$_4$(μ-SMe$_2$)$_2$] (0.5 g, 0.869 mmol) was added to a stirring solution of

[1,2-di-2-pyridylethane], (0.32 g, 1.73 mmol) in ether (20 mL). After 10 minutes of stirring the

complex started to precipitate out of solution as a white solid. The product precipitated over a

period of 40 minutes. The reaction mixture was placed on ice for a period of 30 minutes. The

product was first separated from the solution by decanting most of the solvent. Then it was

precipitated in pentane and decanted again. It was washed with ether (3x2 mL) and pentane (3x2

mL), and then dried under high vacuum. Yield 85%. ^{1}H NMR in acetone-d$_6$: δ = 0.60 (s, 6H, $^2J_{\text{Pt-}}$

$_{\text{H}}$ =88 Hz, Pt-CH$_3$), 4.01 (broad, 4H, 2CH$_2$), 7.17 (dt, 2H, $^3J_{\text{H-H}}$ = 6 Hz, $^3J_{\text{H-H}}$ = 6 Hz, Py{H^2}),

7.35 (d, 2H, $^3J_{\text{H-H}}$ = 8 Hz, Py{H^4}), 7.75 (dt, 2H, $^3J_{\text{H-H}}$ = 8 Hz, $^3J_{\text{H-H}}$ = 6 Hz Py{H^3}), 8.73 (d, 2H,

$^3J_{\text{H-H}}$ = 6 Hz, $^2J_{\text{Pt-H}}$ = 18 Hz, Py{H^1}); Anal. Calcd. for C$_{14}$H$_{18}$N$_2$Pt (%): C 41.31, H 4.42, N 6.82.

Found: C 41.26, H 4.53, N 6.44.

[(PtMe$_3$I)$_4$], 2.3. Excess methyl iodide (0.025 mL) was added dropwise to a solution of complex

2.2 (0.05 g, 0.122 mmol) in acetone (15 mL). After 3 minutes the color of the solution changed

from orange to yellow. 20 minutes later after almost complete precipitation, the volume was

reduced to half and then placed overnight in the fridge. The next day solvent was removed by

decanting. The precipitate was washed with pentane (3x2 mL) and then dried under high vacuum. Yield 87%. ^{1}H NMR in acetone-d_6: δ = 1.81 (s, 36H, $^2J_{Pt-H}$ =80 Hz, Pt-CH$_3$).

[(PtMe$_2$(CD$_3$)I)$_4$], 2.4. Complex **2.2**, [PtMe$_2$(dpe)], (0.01 g, 0.0244 mmol) was dissolved in acetone-d_6 (1 mL). Then the solution was placed in an NMR tube. The NMR tube was then placed in the NMR machine (Inova 400 MHz), and the temperature of the probe was brought down to -80 ^{o}C. Then an excess chilled solution of CD$_3$I (0.008 mL, 0.122 mol) was added to the NMR, and the reaction was monitored via ^{1}H-NMR spectroscopy. The oxidative addition reaction proceeded very quickly, and the NMR proton resonances for both platinum(IV) complexes, *cis* and *trans* started disappearing upon warming up the probe to room temperature. ^{1}H-NMR in acetone-d_6 -80 to -20 ^{o}C: δ = 1.05 (s, 3H, $^2J_{Pt-H}$ = 69 Hz, *cis*-axial Pt-Me), 1.52 (s, 6H, $^2J_{Pt-H}$ = 72 Hz, *cis/trans*-equatorial Pt-Me). ^{1}H-NMR in acetone-d_6 at room temperature: δ = 1.81 (s, 24H, $^2J_{Pt-H}$ = 80 Hz, Pt-CH$_3$).

[PtBr$_2$Me$_2$(dpe)], 2.5, and [PtBr$_2$(dpe)], 2.6. To a solution of complex **2.2** (0.03 g, 0.073 mmol) in dry CH$_2$Cl$_2$ (15 mL) was added excess amount of bromine (0.02 mL). The color of the solution rapidly changed from orange to red. After 30 minutes the solvent was reduced to ~1mL, then pentane (2 mL) was added to precipitate the product as a red powder. The red precipitate was washed with pentane (3x2 mL) and ether (3x2 mL) and then dried under high vacuum. Yield 84%. ^{1}H NMR in CD$_2$Cl$_2$: *trans* (**2.5a**); δ = 2.34 (s, 6H, $^2J_{Pt-H}$ =72 Hz, Pt-CH$_3$), 3.48 (s, 4H, 2CH$_2$), 7.30 (d, 2H, $^3J_{H-H}$ = 7 Hz, Py{H^4}), 7.34 (dt, 2H, $^3J_{H-H}$ = 5 Hz, $^3J_{H-H}$ = 6 Hz, Py{H^2}), 7.79 (dt, 2H, $^3J_{H-H}$ = 7 Hz, $^3J_{H-H}$ = 6 Hz Py{H^3}), 8.89 (d, 2H, $^3J_{H-H}$= 5 Hz, $^2J_{Pt-H}$ = 23 Hz, Py{H^1}); *cis* (**2.5b**) at low temperatures; δ = 1.99 (s, 3H, $^2J_{Pt-H}$ = 76 Hz, Pt-CH$_3$), 2.49 (s, 3H, $^2J_{Pt-H}$ = 78 Hz, Pt-CH$_3$), 3.95 (s, 4H, 2CH$_2$), 7.22-9.92 (8H, pyridyl); complex (**2.6**); δ = 3.44 (m,

2H, $^3J_{\text{H-H}}$ = 6 Hz, $^2J_{\text{H-H}}$ = 16 Hz, CH$_2$C), 4.82 (m, 2H, $^3J_{\text{H-H}}$ = 6 Hz, $^2J_{\text{H-H}}$ = 16 Hz, CH$_2$C), 7.23-7.74 (6H, Py{H^2, H^3, H^4}), 9.13 (d, 2H, $^3J_{\text{H-H}}$= 5 Hz, $^2J_{\text{Pt-H}}$ = 33 Hz, Py{H^1}).

[PtI$_2$(dpe)], 2.7. To a stirred solution of [PtMe$_2$(dpe)] (0.038 g, 0.092 mmol) in dry CH$_2$Cl$_2$ (15 mL) was added excess iodine (0.012 g).Within 5 minutes the color of the solution turned from yellow to dark red. The reaction was kept stirring for 1 hour. Then the solvent was pumped off using a rotavap. A red precipitate remained in the bottom of the flask, which was washed pentane (3x3 mL) and ether (3x3 mL) and then dried under high vacuum. Yield 78%. ^{1}H NMR in CD$_2$Cl$_2$: δ = 3.39 (m, 2H, $^3J_{\text{H-H}}$ = 6 Hz, $^2J_{\text{H-H}}$ = 15 Hz, CH$_2$C), 4.70 (m, 2H, $^3J_{\text{H-H}}$ = 6 Hz, $^2J_{\text{H-H}}$ = 15 Hz, CH$_2$C), 7.16 (dt, 2H, $^3J_{\text{H-H}}$ = 6 Hz, $^3J_{\text{H-H}}$ = 7 Hz, Py{H^2}), 7.26 (d, 2H, $^3J_{\text{H-H}}$ = 8 Hz, Py{H^4}), 7.66 (t, 2H, $^3J_{\text{H-H}}$ = 8 Hz, $^3J_{\text{H-H}}$ = 7 Hz, Py{H^3}), 9.08 (d, 2H, $^3J_{\text{H-H}}$ = 6 Hz, $^2J_{\text{Pt-H}}$ = 35 Hz, Py{H^1}).

[PtMe$_2$I$_2$(dpe)], 2.8. Low temperature ^{1}H-NMR experiment for the reaction of [PtMe$_2$(dpe)] with I$_2$. [PtMe$_2$(dpe)] (0.005 g, 0.012 mmol) was dissolved in CD$_2$Cl$_2$ and then placed in an NMR tube. The temperature of the probe was brought down to -60 $^{\text{o}}$C, and then excess iodine was added to the NMR sample. The tube was shaked and then placed quickly back in the NMR machine to obtain the spectra at low temperatures. At low temperatures, the platinum(IV) complex **2.8**, was observed, and with time complex **2.7** was produced via the reductive elimination of MeI (δ = 2.16). ^{1}H-NMR of **2.8** in CD$_2$Cl$_2$: δ = 2.54 (s, 6H, $^2J_{\text{Pt-H}}$ = 72 Hz, Pt-Me), 3.33 (s, 4H, CH$_2$C), 7.30 (m, 4H, Py{H^2, H^4}), 7.77 (t, 2H, $^3J_{\text{H-H}}$ = 7 Hz, Py{H^3}), 8.81 (d, 2H, $^3J_{\text{H-H}}$ = 5 Hz, $^2J_{\text{Pt-H}}$ = 20 Hz, Py{H^1}).

[PtMe$_2$I$_2$\{κ^2-N,C-(NC$_5$H$_4$)CH$_2$CH(C$_5$H$_4$NMe)\}], 2.9. To a stirred solution of [PtMe$_2$(dpe)] (0.003 g, 0.007 mmol) in dry CH$_2$Cl$_2$ (5 mL) was added excess iodine. The mixture was stirred for 10 mintues, and then kept overnight in the fume hood. The next day complex **2.9** crystallized

out of the solution. The crystals of **2.9** are not soluble in any organic solvent, so we couldn't obtain ^{1}H NMR spectra, but the crystals were good to diffract X-rays, so the structure of **2.9** was determined crystallographically using x-ray. MALDI mass spectrometry was used to characterize the complex, which showed peaks at m/z = 550, and 676 corresponding to $[PtMe_2I\{\kappa^2\text{-}N,C\text{-}(NC_5H_4)CH_2CH(C_5H_4NMe)\}]^+$, and $[PtMe_2I_2\{\kappa^2\text{-}N,C\text{-}(NC_5H_4)CH_2C(C_5H_4NMe)\}]^+$, respectively.

[Pt(H)Me₂Cl(dpe)], 2.10, [PtMeCl(dpe)], 2.11, and [PtCl₂(dpe)], 2.12. Low temperature ^{1}H-NMR experiment for the reaction of [PtMe₂(dpe)] with HCl. [PtMe₂(dpe)] (0.005 g, 0.012 mmol) was dissolved in CD₂Cl₂ and then placed in an NMR tube. The temperature of the probe was brought down to -60 ^{o}C, and then excess HCl was added to the NMR sample. At low temperatures, the platinum(IV) complex **2.10**, and the platinum(II) complex **2.11** were observed. Upon warming up the probe, only complex **2.12** was observed, which was produced via reductive elimination. ^{1}H NMR in CD₂Cl₂: (**2.10**) δ = -20 (s, 1H, $^1J_{\text{Pt-H}}$ = 1609Hz, Pt-H), 1.15 (s, 6H, $^3J_{\text{Pt-H}}$ = 67, Pt-Me), 3.31 (m, 2H, $^3J_{\text{H-H}}$ = 7 Hz, $^2J_{\text{H-H}}$ = 16 Hz, CH₂C), 4.20 (m, 2H, $^3J_{\text{H-H}}$ = 7 Hz, $^2J_{\text{H-H}}$ = 16 Hz, CH₂C), 7.18-7.28 (4H, Py{ H^2, H^4}), 7.70 75 (t, 2H, $^3J_{\text{H-H}}$ = 7 Hz, Py{H^3}), 9.33 (d, 2H, $^3J_{\text{H-H}}$ = 6 Hz, $^2J_{\text{Pt-H}}$ = 16 Hz, Py{H^1}); ^{1}H NMR of (**2.11**): δ = 0.81 (s, 3H, $^3J_{\text{Pt-H}}$ = 80, Pt-Me), 3.31 (broad, 2H, CH₂C), 3.81 (broad, 2H, CH₂C), 7.05-7.71 (6H, Py{ H^2, H^3, H^4}), 8.63 (d, 1H, $^3J_{\text{H-H}}$ = 6 Hz, $^2J_{\text{Pt-H}}$ = 36 Hz, Py{H^1}), 9.06 (d, 1H, $^3J_{\text{H-H}}$ = 6 Hz, $^2J_{\text{Pt-H}}$ = 17 Hz, Py{H^1}); ^{1}H NMR of (**2.12**): δ = 3.35 (m, 2H, $^3J_{\text{H-H}}$ = 7 Hz, $^2J_{\text{H-H}}$ = 15 Hz, CH₂C), 4.80 (m, 2H, $^3J_{\text{H-H}}$ = 7 Hz, $^2J_{\text{H-H}}$ = 15 Hz, CH₂C), 7.16 (t, 2H, $^3J_{\text{H-H}}$ = 6 Hz, Py{H^2}), 7.22 (d, 2H, $^3J_{\text{H-H}}$ = 7 Hz, Py{H^4}), 7.65 (t, 2H, $^3J_{\text{H-H}}$ = 7 Hz, Py{H^3}), 8.95 (d, 2H, $^3J_{\text{H-H}}$ = 6 Hz, $^2J_{\text{Pt-H}}$ = 36 Hz, Py{H^1}).

H/D Exchange with 2.2. DCl was produced via the reaction of phosphorus pentachloride with D₂O. Then the produced DCl was bubbled in a solution of CD₂Cl₂ and cooled in dry ice.

Complex **2.2**, [PtMe$_2$(dpe)], (0.01 g, 0.024 mmol) was dissolved in CD$_2$Cl$_2$ and placed in an NMR tube. The NMR tube containing complex **2.2** was placed in the NMR machine (400 MHz), and the temperature of the probe was brought down to -60 ^{o}C. Then the chilled solution of DCl was added to the NMR tube, and the reaction was monitored by ^{1}H-NMR spectroscopy. As reductive elimination of methane progressed, the peaks for [PtCH$_{3-n}$D$_n$(dpe)] (n = 1, 2) began to appear as well as peaks for the isotopomers of methane. ^{1}H NMR in the methyl region of the different isotopomers CH$_n$D$_{4-n}$ produced upon reductive elimination: δ = 0.81 (s, 3H, $^2J_{Pt-H}$ = 79.7 Hz, Pt-Me), 0.79 (t, $^2J_{H-D}$= 2.7 Hz, Pt-CH$_2$D), 0.17 (s, CH$_4$), 0.15 (t, 2.7 Hz, CH$_3$D), 0.14 (m, CH$_2$D$_2$), 0.12 (m, CHD$_3$).

[PtMe$_2$(CO$_3$)(dpe)], 2.13, and [{PtMe$_3$(OH)•(PtMe$_2$(OH)$_2$)}$_2$], 2.14. To a stirred solution of [PtMe$_2$(dpe)] (0.02 g, 0.048 mmol) in acetone, was added excess H$_2$O$_2$. The solution was allowed to stir for 2 hours. The crystals of complexes **2.13** and **2.14** crystallized out if the solution in an NMR tube. The single X-ray crystallography analysis showed the presence of both complexes **2.13** and **2.14**, but the ^{1}H-NMR spectrum showed the presence of complex **2.14**, and [(PtMe$_3$OH)$_4$]$_2$ in 3:2 ratio. ^{1}H NMR in CD$_2$Cl$_2$: δ = 0.90 (s, 9H, Pt-Me), 1.54 (s, 3H, $^2J_{Pt-H}$ = 71 Hz, Pt-Me), 1.91 (s, 3H, $^2J_{Pt-H}$ = 72 Hz, Pt-Me), 3.30 & 3.79 (m, 4H, 2CH$_2$), 7.13-7.94 (6H, Py{H^2, H^3, H^4}), 8.11 (d, 1H, $^3J_{H-H}$ = 6 Hz, $^2J_{Pt-H}$ = 32 Hz, Py{H^1}), 8.76 (d, 1H, $^3J_{H-H}$ = 6 Hz, $^2J_{Pt-H}$ = 18 Hz, Py{H^1}).

[Pt$_4$Me$_{10}$(μ$_2$-OMe)$_2$ (μ$_3$-OMe)$_2$(μ$_2$-OH)$_2$], 2.15. [PtMe$_2$(dpe)] (0.02 g, 0.048 mmol) was dissolved in MeOH (mL). The solution was stirred for 1 hour. After two days the crystals of complex **2.15** precipitated out. The solvent was decanted out, and then the crystals were washed with pentane and ether. The product was dried under vacuum. Yield 68%. ^{1}H NMR in CD$_2$Cl$_2$: δ = -1.20 (b, 4H, O-H), 0.75 (s, 6H, $^2J_{Pt-H}$ = 77 Hz, Pt-Me), 0.92 (s, 6H, $^2J_{Pt-H}$ = 76 Hz, Pt-Me), 0.96

(s, 6H, $^2J_{Pt-H}$ = 76 Hz, Pt-Me), 1.67 (s, 6H, $^2J_{Pt-H}$ = 77 Hz, Pt-Me), 1.73 (s, 6H, $^2J_{Pt-H}$ = 77 Hz, Pt-Me), 2.96 (s, 6H, $^3J_{Pt-H}$ = 13 and 38 Hz, Pt-OMe), 3.86 (s, 6H, $^3J_{Pt-H}$ = 13 Hz, Pt-OMe).

X-ray Structure Determinations: X-ray data were obtained and solutions were determined by Dr. M. Jennings in this chapter. Suitable crystals were mounted on a glass fiber, and data were collected at low temperature (-123 °C) on a Nonius Kappa-CCD area detector diffractometer with COLLECT (Nonius B.V., 1997-2002). The unit cell parameters were calculated and refined from the full data set. The crystal data and refinement parameters for all complexes are listed in the following tables.

Table 2.6. Crystallographic data for [PtI$_2$(dpe)], **2.8**.

_____

[PtI$_2$(dpe)] • ½ CH$_2$Cl$_2$

_____

Empirical formula	C12.50 H12 Cl I2 N2 Pt
Formula weight	674.58
Wavelength	0.71073 Å
Crystal system	Monoclinic
Space group	C 2/c
Unit cell dimensions	a = 21.925(2) Å α= 90°
	b = 10.465(7) Å β= 124.06(3)°
	c = 17.416(1) Å γ = 90°
Volume	3310.8(4) Å^3
Z	8
Density (calculated)	2.707 Mg/m^3
Absorption coefficient (μ)	12.354 mm^{-1}
Crystal size	0.22 x 0.09 x 0.03 mm^3
Refinement method	Full-matrix least-squares on F^2
Goodness-of-fit on F^2	0.981
Final R indices [I>2sigma(I)]	R1 = 0.0452, wR2 = 0.1054
R indices (all data)	R1 = 0.0701, wR2 = 0.1156

Table 2.7. Crystallographic data for complex **2.9**.

	$[PtMe_2I_2(\mu-\{(NC_5H_4)CH_2CH(C_5H_4NMe)\}]$
Empirical formula	C15 H20 I2 N2 Pt
Formula weight	677.22
Wavelength	0.71073 Å
Crystal system	Monoclinic
Space group	P 2_1/c
Unit cell dimensions	a = 10.989(6) Å $\alpha = 90°$
	b = 10.958(8) Å $\beta = 105.78(4)°$
	c = 15.165(1) Å $\gamma = 90°$
Volume	1757.3(2) Å^3
Z	4
Density (calculated)	2.560 Mg/m^3
Absorption coefficient (μ)	11.492 mm^{-1}
Crystal size	0.25 x 0.25 x 0.08 mm^3
Refinement method	Full-matrix least-squares on F^2
Goodness-of-fit on F^2	1.050
Final R indices [I>2sigma(I)]	R1 = 0.0560, wR2 = 0.1509
R indices (all data)	R1 = 0.0680, wR2 = 0.1593

Table 2.8. Crystallographic data for complex **2.13•½2.14**.

$[PtMe_2(\mu\text{-}\{N_2C_{12}H_{12}\})(CO_3)] \bullet \frac{1}{2} [Pt_4Me_{10}(\mu\text{-}OH)_6]$	
Empirical formula	C20 H36 N2 O6 Pt3
Formula weight	985.78
Wavelength	0.71073 Å
Crystal system	Monoclinic
Space group	P 2_1/n
Unit cell dimensions	a = 11.314(4) Å $\alpha = 90°$
	b = 13.935(3) Å $\beta = 106.78(1)°$
	c = 16.666(5) Å $\gamma = 90°$
Volume	2515.53(13) Å^3
Z	4
Density (calculated)	2.603 Mg/m^3
Absorption coefficient (μ)	16.678 mm^{-1}
Crystal size	0.22 x 0.08 x 0.03 mm^3
Refinement method	Full-matrix least-squares on F^2
Goodness-of-fit on F^2	1.042
Final R indices [I>2sigma(I)]	R1 = 0.0364, wR2 = 0.0880
R indices (all data)	R1 = 0.0460, wR2 = 0.0919

Table 2.9. Crystallographic data for complex **2.15**.

$[Pt_4Me_{10}(\mu_2\text{-OMe})_2\,(\mu_3\text{-OMe})_2(\mu_2\text{-OH})_2]$	
Empirical formula	C16 H52 O8 Pt4
Formula weight	1152.94
Wavelength	0.71073 Å
Crystal system	Triclinic
Space group	P -1
Unit cell dimensions	a = 8.740(2) Å α= 70.96(3)°.
	b = 9.233(2) Å β= 64.90(3)°.
	c = 9.889(2) Å γ = 81.15(3)°.
Volume	683.0(2) Å^3
Z	1
Density (calculated)	2.803 Mg/m^3
Absorption coefficient (μ)	20.449 mm^{-1}
Crystal size	0.28 x 0.22 x 0.15 mm^3
Refinement method	Full-matrix least-squares on F^2
Goodness-of-fit on F^2	1.069
Final R indices [I>2sigma(I)]	R1 = 0.0454, wR2 = 0.1210
R indices (all data)	R1 = 0.0505, wR2 = 0.1248

2.5 References

1. (a) Shilov, A. E.; Shul'pin, G. B. *Chem. Rev.*, **1997**, 97, 2879. (b) He, Z.; Wong, W.; Yu, X.; Kwok, H.; Lin, Z. *Inorg. Chem.*, **2006**, 45, 10922. (c) Rendina, L. M.; Puddephatt, R. J. *Chem. Rev.*, **1997**, 97, 1735. (d) Song, D.; Sliwowski, K.; Pang, J.; Wang, S. *Organometallics*, **2002**, 21, 4978.

2. Zhang, F.; Broczkowski, M. E.; Jennings, M. C.; Puddephatt, R. J. *Can. J. Chem.*, **2005**, 83, 595.

3. (a) Baar, C. R.; Jenkins, H. A.; Vittal, J. J.; Yap, G. P.; Puddephatt, R. J. *Organometallics*, **1998**, 17, 2805. (b) Hoseini, S. J.; Nabavizadeh, S. M.; Jamali, S.; Rashidi, M. *Eur. J. Inorg. Chem.*, **2008**, 5099.

4. Zhang, F.; Kirby, C. W.; Hairsine, D. W.; Jennings, M. C.; Puddephatt, R. J. *J. Am. Chem. Soc.*, **2005**, 127, 14190.

5. Quagliotto, P.; Viscardi, G.; Barolo, C.; Barni, E.; Bellinvia, S.; Fisicaro, E.; Compari, C. *J. Org. Chem.*, **2003**, 68, 7651.

6. Hill, G.; Irwin, M. J.; Levy, C. J.; Rendina, L. M.; Puddephatt, R. J. *Inorg. Synth.*, **1998**, 32, 149.

7. McFarlane, A.; Lusty, J. R.; Fiol, J. J.; Terron, A.; Molins, E.; Miravittles, C.; Moreno, V. *Z. Naturforsch.*, **1994**, 49b, 844.

8. Kite, K.; Smith, J.; Wilkins, E. *J. Chem. Soc.*, **1966**, 1744.

9. Yahav, A.; Goldberg, I.; Vigalok, A. *Organometallics,* **2005,** 24, 5654.

10. He, Z.; Wong, W.; Yu, X.; Kwok, H.; Lin, Z. *Inorg. Chem.*, **2006**, 45, 10922.

11. Tu, C.; Wu, X.; Liu, Q.; Wang, X.; Xu, Q.; Guo, Z. *Inorg. Chim. Acta*, **2004**, 357, 95.

12. Boaretto, R.; Sostero, S.; Traverso, O. *Inorg. Chim. Acta*, **2002**, 330. 59.

13. Ong, C.; Jennings, M.C.; Puddephatt, R. J. *Can. J. Chem.*, **2003**, 81, 1196.

14. (a) Aye. K. T.; Vittal, J. J.; Puddephatt, R. J. *J. Chem. Soc., Dalton Trans.*, **1993**, 1835. (b) Zhang, F.; Jennings, M, C.; Puddephatt, R. J. *Chem. Commun.*, **2007**, 1496. (c) Thorshaug, K.; Fjeldahl, I.; Romming, C.; Tilset, M. *Dalton Trans.*, **2003**, 4051. (d) Prokopchuk, E. M.; Puddephatt, R. J. *Can. J. Chem.*, **2003**, 81, 476.

15. Appleton, T. G.; D'Alton, C. J.; Hall, J. R.; Mathieson, M. T.; Williams, M. A. *Can. J. Chem.*, **1996**, 74, 2008.

16. (a) Hall, J. R.; Swile, G. A. *J. Organomet. Chem.*, **1976**, 122, C19. (b) Hall, J. R.; Hirons, D. A.; Swile, G. A.; *Inorg. Synth.*, **1980**, 20, 185. (c) Hall, J. R.; Swile, G. A. *J. Organomet. Chem.*, **1977**, 139, 403.

17. Pope, W. J.; Peachey, S. J. *Proc. Chem. Soc.*, *London,* **1907**, 23, 868.

18. (a) Rundle. R. E.; Sturdivant, J. H. *J. Am. Chem. Soc.*, **1947**, 69, 1561. (b) Preston, H. S.; Mills, J. C.; Kennard, C. H. L. *J. Organomet. Chem.*, **1968**, 14, 447. (c) Spiro, T. G.; Templeton, D. H.; Zalkin, A. *Inorg. Chem.*, **1968**, 7, 2165. (d) Ebert, K. H.; Massa, W.; Donath, H.; Lorberth, J.; Seo, B. S.; Herdtweck, E. *J. Organomet. Chem.*, **1998**, 559, 203. (e) Cross, R. J.; Haupt, M.; Rycroft, D. S.; Winfield, J. M. *J. Organomet. Chem.*, **1999**, 587, 195.

19. (a) Hall, J. R.; Swile, G. A. *Aust. J. Chem.*, **1971**, 24, 423. (b) Hall, J. R.; Swile, G. A. *J. Organomet. Chem.*, **1973**, 56, 419.

20. (a) Godbole, M. D.; Roubeau, O.; Mills, A. M.; Kooijman, H.; Spek, A. L.; Bouwman, E. *Inorg. Chem.*, **2006**, 45, 6713. (b) Mandal, D.; Ray, D. *Inorg. Chem. Commun.*, **2007**, 10, 1202.

21. (a) Sivaramakrishna, A.; Su, H.; Moss, J. R. *Acta Crystallogr., Sect. E*, **2007**, E63, m3097. (b) Scholz, S.; Lerner, H. W.; Bolte, M. *Acta Crystallogr., Sect. E*, **2006**, E62, m312.

22. (a) Ravera, M.; Bagni, G.; Mascini, M.; Dabrowiak, J. C.; Osella, D. *J. Inorg. Biochem.*, **2007**, 101, 1023. (b) Todd, R. C.; Lovejoy, K. S.; Lippard, S. J. *J. Am. Chem. Soc.*, **2007**, 129, 6370. (c) Di Pasqua, A. J.; Goodisman, J.; Kerwood, D. J.; Toms, B. B.; Dabrowiak, J. C. *J. Inorg. Biochem.*, **2007**, 101, 1438. (d) Mahtani, H. K.; Chang, S. C.; Ruble, J. R.; Black, I. N. L.; Steib, P. B. *Inorg. Chem.*, **1993**, 32, 4976.

23. (a) Lee, Y. A.; Jung, S. M.; Kang, S. W.; Jung, O. S. *Transition Met. Chem.*, **2004**, 29, 710. (b) Battle, A. R.; Choi, R.; Hibbs, D. E.; Hambley, T. W. *Inorg. Chem.*, **2006**, 45, 6317. (c) Khusnutdinova, J. R.; Zavalij, P. Y.; 'vedernikov, A. N. *Organometallics*, **2007**, 26, 3466.

24. Binns, S. E.; Cragg, R. H.; Gillard, R. D.; Heaton, B. T.; Pilbrow, M. F. *J. Chem Soc. A*, **1969**, 1227.

CHAPTER 3

The Chemistry of Platinum Complexes Containing

Bis(2-pyridyl)dimethylsilane Ligands

3.1 Introduction

The organoplatinum complexes containing nitrogen donor chelating ligands have been studied extensively during the past several decades.[1,2] Some of these complexes have been used effectively in catalytic reactions.[3] The ligand bis(2-pyridyl)dimethylsilane (bps) can easily coordinate to palladium, platinum, and nickel.[4] Organoplatinum(II) complexes containing nitrogen donor ligands are very reactive toward oxidative addition reactions, and this reactivity is essential in the activation of normally inert chemical bonds.[5] Palladium complexes containing bps ligands were studied, characterized, and used previously in organostannane cross-coupling reactions.[6] Also bis(2-pyridyl)dimethylsilane ligands were reacted with $NiBr_2$ to give the complex $[NiBr_2\{Me_2Si(2-C_5H_4N)_2\}]$ in excellent yield, which was found to be an efficient catalyst for the cross-coupling of Grignard reagents with aryl and vinyl halides.[7]

The oxidative activation of organosilanes has been studied intensively in recent years. It has been found the reaction can be initiated both thermally and photochemically.[8] The activation of silicon-carbon bonds by transition metal complexes has not been studied in detail, but it could be important in providing a route to new transformations of organosilicon complexes.[9] Several reactions for cleaving methyl and phenyl groups from silicon in some compounds were achieved using platinum and palladium complexes.[10] The silicon-carbon bond is thermodynamically nearly as strong as a single carbon-carbon bond. The silicon-carbon bond is always polarized with the partial positive charge on the silicon atom.[11] The intermolecular insertion of platinum(0) to the silicon bond of distorted silacyclobutanes, and the activation of tetramethylsilane by *cis*-[PtH(CH₂-*t*-Bu)(bis{di-*tert*-butylphosphino} methane)], were reported in recent years.[12] Many of these reactions that involve the activation of a silicon-carbon bond occur under harsh conditions, such as the one reported lately by the Sasamori group.[13] They used heat and excess of sodium

metal to reduce a dichloroplatinum(II) complex, which then caused an intramolecular carbon-hydrogen insertion, followed by a silicon-carbon bond activation that finally gave the (methyl)(silyl)platinum complex (Scheme 3.1).[13]

Bbt = 2,6-bis[bis(trimethylsilyl)methyl]-4-[tris(trimethylsilyl)methyl]phenyl
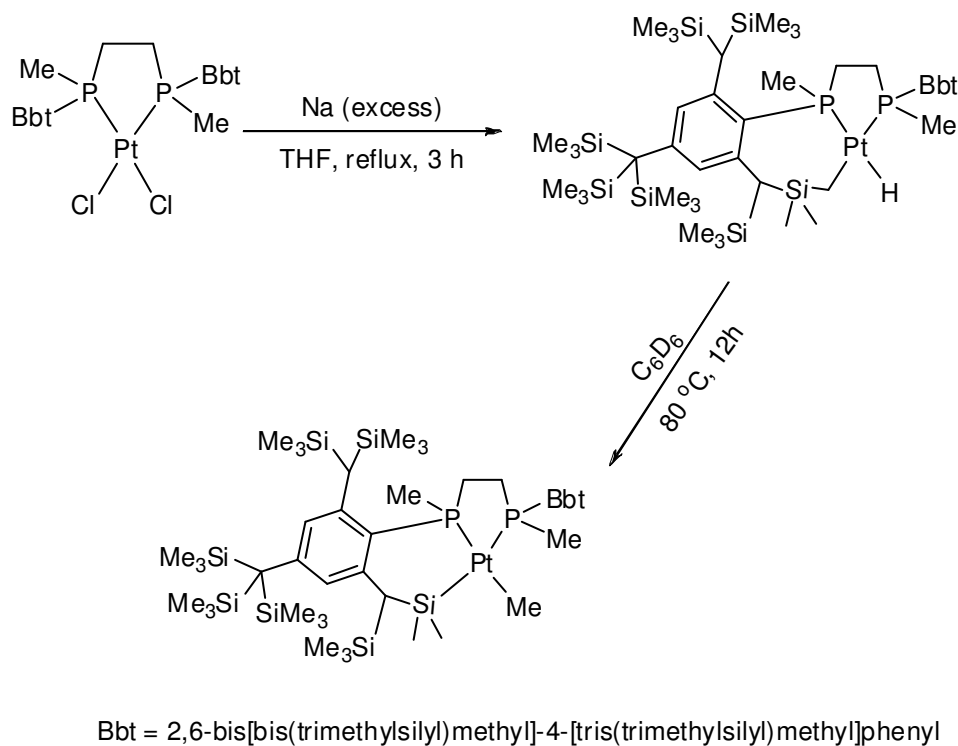
Scheme 3.1

There is intense current interest in the development organosilicon based cross-coupling reactions (Hiyama coupling reaction), and there is an associated need to understand the mechanism of transfer of organic groups from silicon to transition metals and the factors that control the reactivity.[14] The activation of non-polar bonds by electrophilic platinum(II)

compounds and the subsequent functionalization of organic groups on platinum by oxygen or equivalent reagents are also important areas, and typically involve platinum(IV) intermediates.[15,16] Most previous studies of Si-C activation by nickel group complexes have focused on compounds in low oxidation states.[17] The Si-C bond activation part of this chapter was shown to be triggered by an oxidation step.

3.2 Results and Discussion

3.2.1 The Preparation of Complex [PtMe$_2$(bps)]

It was shown earlier that the complex [PtMe$_2$(bpm)], bpm = CH$_2$(2-C$_5$H$_4$N)$_2$, is a useful precursor for C-H bond activation when activated by reaction in CF$_3$CH$_2$OH with B(C$_6$F$_5$)$_3$.[18] This led to an investigation of the related complex [PtMe$_2$(bps)], **3.2**, bps = Me$_2$Si(2-C$_5$H$_4$N)$_2$, with the expectation that the larger bridging silicon atom in bps might enhance reactivity. The compound 1,2-bis(2-pyridyl)dimethylsilane, **3.1**, is easily prepared in a one pot, two step procedure using a modified method of Wright *et al.*[4] and isolated as on oily product. The ligand is stable to air at room temperature. It is soluble in many organic solvents such as chloroform, acetone, and dichloromethane. The complex [PtMe$_2$(bps)], **3.2**, was prepared via the reaction of the known precursor [Pt$_2$Me$_4$(μ-SMe$_2$)$_2$][19] with compound **3.1**, in ether as shown Equation 3.1. The product precipitated as a brown solid which was stable in air at room temperature. The ^{1}H-NMR spectrum of complex **3.2**, showed a proton resonance at δ = 0.71, with coupling constant $^2J_{Pt-H}$ = 80 Hz due to the methyl platinum groups. Two single proton resonances were observed at δ = 0.77 and 1.11, due to the methyl silicon groups. The obtained crystal structure for complex **3.2** is shown in Figure 3.1, which shows that one of the methyl groups on silicon is pointing away from the platinum atom, and other is pointing in the opposite direction. Only one set of

pyridyl resonances was observed for complex **3.2** in its ^{1}H-NMR spectrum. The proton resonance of the *ortho* pyridyl protons was observed at $\delta = 8.97$, with coupling constant $^3J_{Pt-H} = 25$ Hz, which is in the range found for similar platinum(II) complexes.[5]

(3.1)
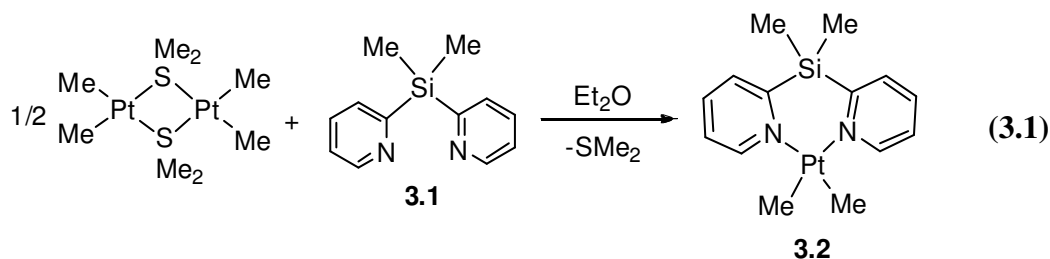
The molecular structure of complex **3.2** (Figure 3.1), shows that the chelate ring is in the boat conformation. Also the angle at the atom coupling both pyridyl rings C16-Si17-C20 is 104.7(4)^o which is close to the ideal 109° tetrahedral angle, while the pyridyl rings are twisted out of the coordination plane of the platinum atom by 74° which aids in minimizing the steric effects between the *ortho* hydrogen atom of each pyridyl and the neighboring methylplatinum group.[20] Table 3.1 shows selected bond lengths and angles for complex **3.2**. The most significant feature of the structure of **3.2** (Figure 3.1) is the bowing of the bps ligand which leads to one methylsilicon group being *anti* and the other *syn* to the platinum atom.
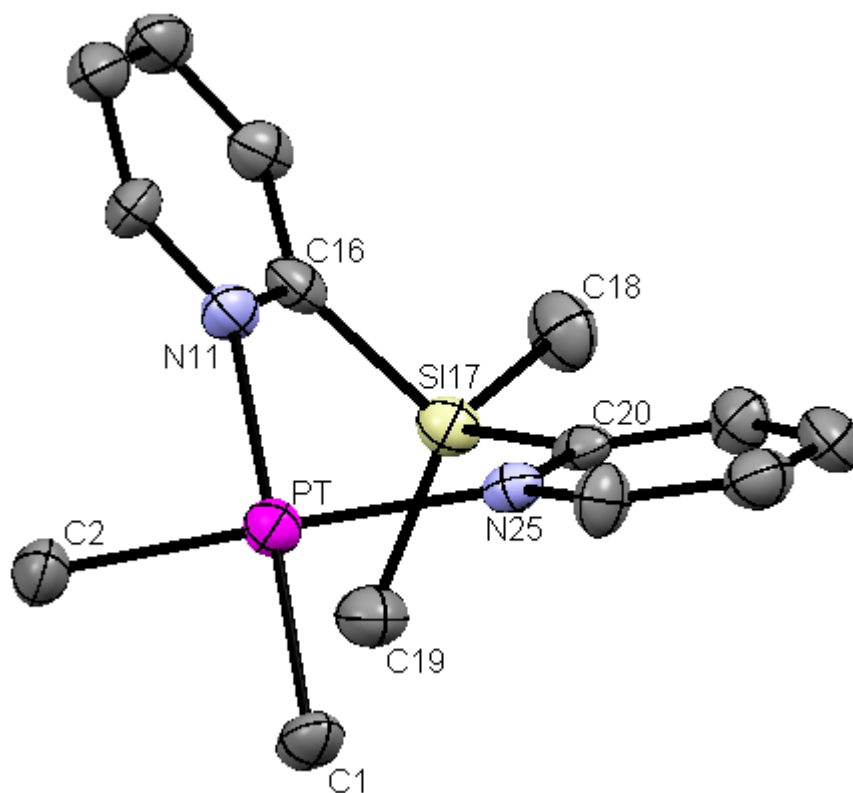
Figure 3.1. The structure of complex **3.2**, [PtMe$_2$(bps)].

Table 3.1. Selected bond lengths [Å] and angles [°] for [PtMe$_2$(bps)], **3.2**.

Pt-C(2)	2.043(8)	Pt-C(1)	2.048(8)
Pt-N(25)	2.108(7)	Pt-N(11)	2.121(7)
Si(17)-C(18)	1.878(9)	Si(17)-C(19)	1.874(9)
C(2)-Pt-C(1)	88.3(4)	C(2)-Pt-N(25)	178.4(3)
C(1)-Pt-N(11)	176.6(3)	N(25)-Pt-N(11)	90.7(2)
C(19)-Si(17)-C(18)	109.7(4)	C(19)-Si(17)-C(16)	114.6(4)
C(18)-Si(17)-C(16)	107.7(4)	C(19)-Si(17)-C(20)	112.7(4)
C(18)-Si(17)-C(20)	107.1(4)	C(16)-Si(17)-C(20)	104.7(4)
N(25)-C(20)-Si(17)	115.4(6)	N(11)-C(16)-Si(17)	116.6(6)

3.2.2 Easy Oxidatively Induced Silicon-Carbon Bond Activation

3.2.2.1 The Reaction of [PtMe$_2$(bps)] with B(C$_6$F$_5$)$_3$

$$2 \quad \text{3.2} \quad \xrightarrow[\text{- CH}_4]{\substack{\text{1. CF}_3\text{CH}_2\text{OH/ 1/2 O}_2 \\ \text{2. B(C}_6\text{F}_5)_3}} \quad [\text{Me(bps)Pt-OSiMe(2-C}_5\text{H}_4\text{N)}_2\text{PtMe}_3]^{\oplus} [\text{CF}_3\text{CH}_2\text{OB(C}_6\text{F}_5)_3]^{\ominus} \quad (3.2)$$

3.3
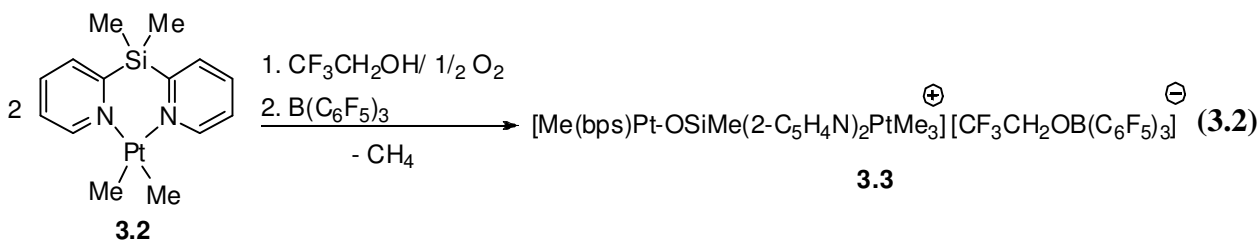
The complex **3.2**, [PtMe$_2$(bps)] was reacted with B(C$_6$F$_5$)$_3$/H$_2$O in CF$_3$CH$_2$OH at room temperature according to Equation 3.2, which yielded the novel and very interesting dimer **3.3** that was characterized by ^{1}H and ^{19}F NMR (Figure 3.2), including gCOSY and NOESY spectra, X-ray structure determination (Figure 3.3), and elemental analysis. The dimer, **3.3**, contained a platinum(II) d^8 metal center and a platinum(IV) d^6 octahedral metal center. The metal centers are linked via an oxygen atom as shown in Figure 3.3. The platinum(II) center has one methyl group, while the platinum(IV) center contains three methyl groups. One of these three methyl groups was transferred from the silicon center. The silicon-carbon bond activation evidently occurred under milder conditions compared to many other silicon-carbon bond activation reactions.[12, 13]
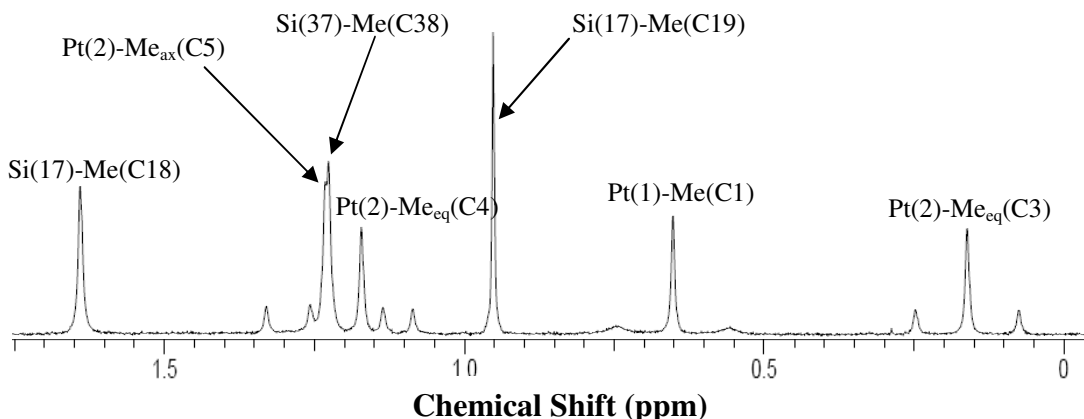
Figure 3.2: ^{1}H-NMR spectrum (400 MHz, acetone-d$_6$) of complex **3.3** in the methyl region.
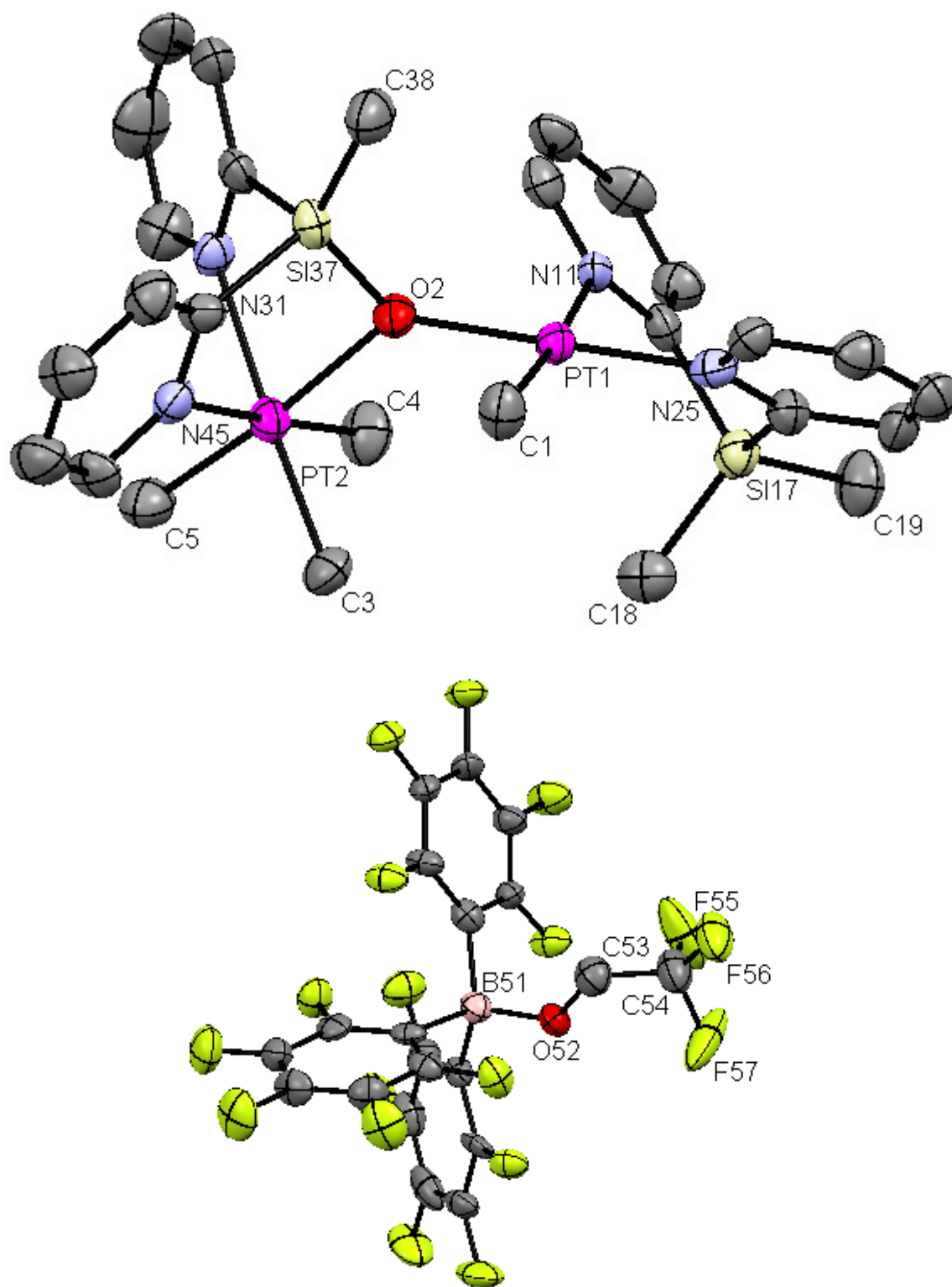
Figure 3.3. The structure of complex **3.3**.

The NMR data for the complex support the structure and show the proton resonances of the $[CF_3CH_2OB(C_6F_5)_3]^-$ anion in the acetone-d_6 solution. The ^{1}H-NMR spectrum (Figure 3.2) shows four different methyl platinum groups in total because the complex has no symmetry. The platinum(IV) metal center has three methylplatinum proton resonances at δ = 0.15 (C3), 1.17 (C4), and 1.23 (C5), with coupling constants $^2J_{Pt-H}$ = 69, 68, and 78 Hz respectively. The two methyl groups (C3 and C4) are neighbors, and they both occupy equatorial positions (*trans* to N). This was proven by the NOESY NMR spectrum that showed a coupling through space between both methyl groups. Also, they have similar coupling constants since the two methyl groups are *trans* to nitrogen, and they have similar Pt-C bond distances, with Pt(2)-C(3) = 2.043(8) Å, and Pt(2)-C(4) = 2.047(8) Å. The methyl (C5) group *trans* to the oxygen has a shorter bond distance Pt(2)-C(5) = 2.028(8) Å due to the lower *trans* influence of the oxygen, and it gives a higher coupling constant value $^2J_{Pt-H}$ = 78 Hz. The platinum(II) metal center has one methyl proton resonance at δ = 0.64, with coupling constant $^2J_{Pt-H}$ = 75 Hz. The bond distance Pt(1)-C(1) = 2.039(5) Å (*trans* to nitrogen) is shorter than the distances Pt(2)-C(3) and Pt(2)-C(4). It also has a higher coupling constant ^2J(Pt-H). There were three methyl silicon proton resonances observed in the ^{1}H-NMR spectrum. The two proton resonances at δ = 0.95, and 1.63 are on silicon (Si17) in the platinum(II) portion, which was proven via the NOESY NMR that showed a cross peak between these resonances. The proton resonance at δ = 1.22 is the one connected to silicon (Si37) in the platinum(IV) section of the dimer.

The CH$_2$ group in the counter anion has a proton resonance at $\delta = 3.57$ and the peak is a quartet because the protons are coupled to the three neighboring fluorine atoms. In the pyridyl region at $\delta = 7.01$-8.15 there are proton resonances that account for 12 *para* and *meta* protons of the nitrogen donor ligand. There are four *ortho* protons at $\delta = 8.49$, 8.60, 8.72, 8.96, with coupling constants $^3J_{Pt-H} = 23$, 20, 21 and 65 Hz respectively. The *ortho* proton resonances at $\delta = 8.60$, and 8.72 arise from the platinum(IV) pyridyl groups. The pyridyl groups are both *trans* to a methyl group and so there is little difference in the platinum-nitrogen bond distances Pt(2)-N(31) $= 2.195(6)$Å, and Pt(2)-N(45) $= 2.190(6)$Å or in the coupling constant values. The other two *ortho* proton resonances at $\delta = 8.49$, and 8.96 arise from the platinum(II) pyridyl groups, and the *ortho* proton on the pyridyl group *trans* to oxygen has a higher coupling constant value due to the low *trans* influence of oxygen compared to methyl group. There is a very short bond distance (Pt(1)-N(25) $= 2.001(6)$Å) to the pyridyl group *trans* to oxygen. On the other hand, the other *ortho* proton (Pt(1)-N(11) $= 2.134(6)$Å) has a coupling constant $^3J_{Pt-H} = 23$ Hz, which is similar to the observed coupling constants of the *ortho* protons in the pyridyl groups coordinated to the platinum(IV) side of the molecule. The bridging oxygen (O2) atom is bonded to both platinum metal centers and to the silicon atom on the platinum(IV) side of the molecule. The oxygen to platinum(II) bond distance (Pt(1)-O(2) $= 2.028(5)$Å) is shorter than the oxygen to platinum(IV) bond distance (Pt(2)-O(2) $= 2.244(5)$Å). Table 3.2 shows selected bond lengths and angles for complex **3.3**.

The formation of the platinum(IV) unit in complex **3.3** was considered likely to involve oxidation of complex **3.2** by air, accompanied by transfer of a methyl group from silicon to platinum. A study of this reaction was therefore made, and complex **3.2** was reacted with

alcohols, and peroxides to explore the mechanistic pathway of the carbon-silicon bond activation.

Table 3.2. Selected bond lengths [Å] and angles [°] for complex **3.3**.

Pt(1)-N(25)	2.001(6)	Pt(1)-O(2)	2.028(5)
Pt(1)-C(1)	2.039(8)	Pt(1)-N(11)	2.134(6)
O(2)-Si(37)	1.632(5)	O(2)-Pt(2)	2.244(5)
C(3)-Pt(2)	2.043(8)	C(4)-Pt(2)	2.047(8)
Si(17)-C(18)	1.837(8)	Si(17)-C(19)	1.866(8)
Pt(2)-N(45)	2.190(6)	Pt(2)-N(31)	2.195(6)
Si(37)-C(38)	1.816(9)	B(51)-O(52)	1.467(1)
N(25)-Pt(1)-O(2)	179.0(2)	N(25)-Pt(1)-C(1)	91.1(3)
O(2)-Pt(1)-C(1)	88.5(3)	N(25)-Pt(1)-N(11)	94.3(2)
O(2)-Pt(1)-N(11)	86.0(2)	C(1)-Pt(1)-N(11)	174.5(3)
Si(37)-O(2)-Pt(1)	126.3(3)	Si(37)-O(2)-Pt(2)	99.8(2)
Pt(1)-O(2)-Pt(2)	132.0(2)	C(18)-Si(17)-C(19)	111.3(4)
C(5)-Pt(2)-C(3)	87.4(4)	C(5)-Pt(2)-C(4)	88.9(4)
C(3)-Pt(2)-C(4)	89.0(4)	C(5)-Pt(2)-N(45)	94.2(3)
C(3)-Pt(2)-N(45)	90.8(3)	C(4)-Pt(2)-N(45)	176.9(3)
C(5)-Pt(2)-N(31)	95.3(3)	C(3)-Pt(2)-N(31)	177.2(3)
C(4)-Pt(2)-N(31)	90.9(3)	N(45)-Pt(2)-N(31)	89.1(2)
C(5)-Pt(2)-O(2)	175.1(3)	C(3)-Pt(2)-O(2)	96.8(3)
C(4)-Pt(2)-O(2)	93.6(3)	N(45)-Pt(2)-O(2)	83.3(2)
N(31)-Pt(2)-O(2)	80.4(2)	O(2)-Si(37)-C(38)	119.2(3)

3.2.2.2 The reaction of [PtMe₂(bps)] with H₂O₂ and Alcohols

Platinum(II) complexes containing nitrogen-donor ligands are typically highly reactive toward peroxides and alcohols.[1,21] These complexes [PtMe₂(LL)], LL = diimine ligand, usually react with hydrogen peroxide to give the corresponding platinum(IV) complexes [PtMe₂(OH)₂(LL)] by oxidative addition.[5,22] In an NMR experiment, a sample of complex **3.2**, [PtMe₂(bps)], was dissolved in CD₃OD. The NMR tube was placed in the NMR probe, and then monitored over a long period of time. Complex **3.2** reacts slowly with the solvent and O₂ to produce complex **3.4a** (Equation 3.3), which was characterized as follows. The ^{1}H-NMR spectrum of complex **3.4a** in CD₃OD showed two different methylplatinum proton resonances at $\delta = 0.98$ (6H), and 1.15 (3H), with coupling constant $^2J_{Pt-H} = 69$ (*trans* to nitrogen), and 75 (*trans* to oxygen) Hz respectively. There is only one methyl silicon proton resonance at $\delta = 0.94$ (3H). The methyl group (*trans* to oxygen) was produced via the methyl transfer from the silicon atom to the axial position at the platinum metal center. The other axial position of the octahedral platinum(IV) complex is occupied by an oxygen atom that is also bonded to the silicon atom. The reaction is very slow and takes several days to occur, but when the experiment is repeated and hydrogen peroxide is added the reaction becomes fast and takes minutes to proceed to produce complex **3.4b**.

(3.3)

3.4a: X = CD₃O
3.4b: X = OH
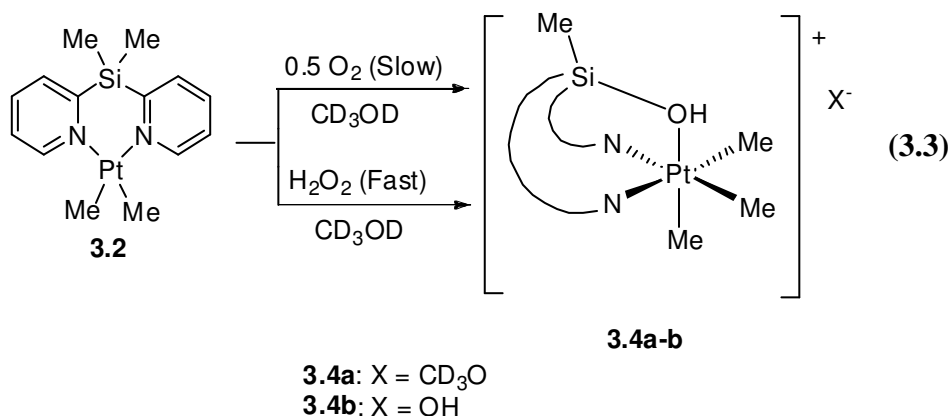
Over a period of one day, a solution of complex **3.2** in acetone-d_6 did not react with air but, on the other hand, it reacted with air in CD_3OD to give complex **3.4a**, and with H_2O_2 in CD_3OD to give complex **3.4b**, whose ^{1}H-NMR properties were consistent with those expected for the platinum(IV) fragment in complex **3.3**. The ^{1}H-NMR spectra for both complexs **3.4a** and **3.4b** in the low field region of the spectrum have only one set of pyridyl resonances, which means that the pyridyl groups are equivalent. The *ortho* pyridyl proton resonance was observed at $\delta = 8.61$, with coupling $^3J_{Pt-H} = 20$ Hz. A mass spectrometry experiment was run. Complex **3.2** was dissolved in methanol and H_2O_2 was added, then within minutes the mass spectrum was obtained which showed peaks at m/z = 456, 848, and 911 corresponding to the cation in complexes **3.4a-b**, $[PtMe_3(HOSiMe(2-C_5H_4N)_2)]^+$, complex **3.3** with one less methyl group, and the binuclear cation $[H\{PtMe_3(HOSiMe(2-C_5H_4N)_2)\}_2]^+$, respectively.

The precursor $[Pt_2(CD_3)_4(\mu-SMe_2)_2]$, **3.5**, was synthesized according to the literature[19] by using methyl-d_3-lithium instead of the MeLi (1.4 M in diethyl ether) as shown in Equation 3.4. Complex **3.5** was reacted with the ligand bis(2-pyridyl)dimethylsilane, **3.1**, in diethyl ether to produce complex **3.6**, $[Pt(CD_3)_2(bps)]$, as a brown precipitate.

$$(3.4)$$
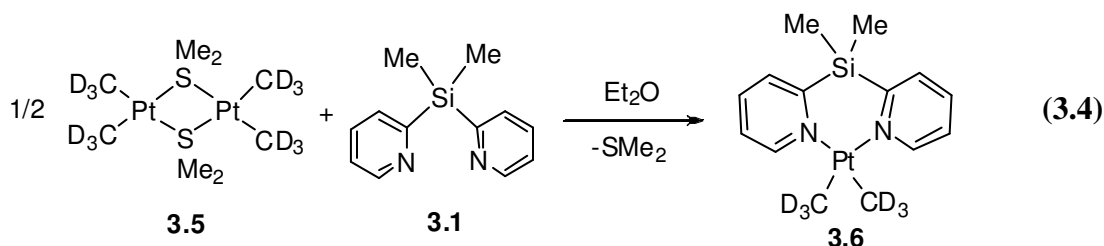
The ^{1}H-NMR spectrum of complex **3.6**, was analyzed by comparing it to the ^{1}H-NMR spectrum of complex **3.2**. They have very similar spectra, except that complex **3.6** did not contain any methyl platinum proton resonances. A solution of [Pt(CD$_3$)$_2$(bps)], **3.6**, in CD$_3$OD reacted slowly to produce compound **3.7a** (Equation 3.5), which was characterized using ^{1}H-NMR and mass spectrometry analysis. The ^{1}H-NMR spectrum of complex **3.7a** was comparable to the ^{1}H-NMR spectra of complexes **3.4a**. Complex **3.7a** was identified via the absence of the equatorial methyl platinum proton resonance. The reaction is very slow and takes several days to occur, but when the experiment is repeated and hydrogen peroxide is added the reaction becomes fast and takes minutes to proceed to produce complex **3.7b**. Also the mass spectrometry experiment for the mixture of methanol, complex **3.6**, and hydrogen peroxide showed peaks at m/z = 462, and 923 corresponding to complex **3.7a-b** cation, [Pt(CD$_3$)$_2$Me(HOSiMe(2-C$_5$H$_4$N)$_2$)]$^+$, and the binuclear cation of complex **3.7a-b**, respectively. Figure 3.4 shows the ^{1}H-NMR spectra in the methyl region for complexes **3.4b** (i) and **3.7b** (ii). Complexes **3.4a-b** and **3.7a-b** decompose slowly, and both of them decompose upon attempted isolation under high vacuum.

3.7a: X = CD$_3$O
3.7b: X = OH

(3.5)
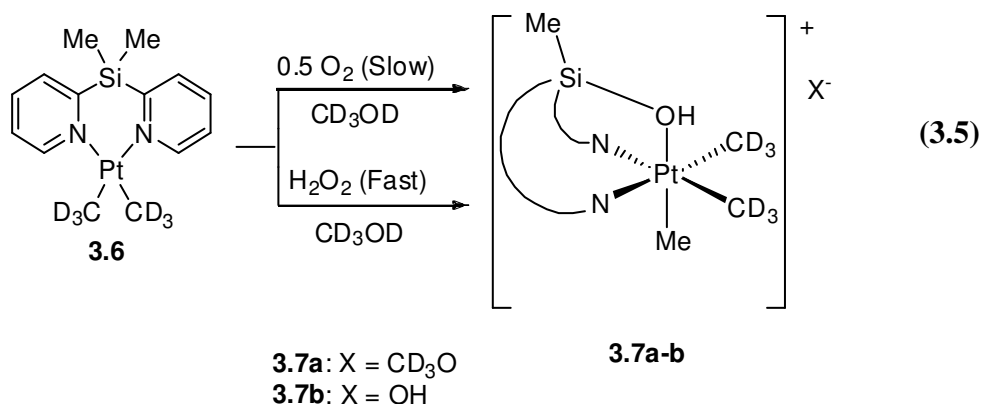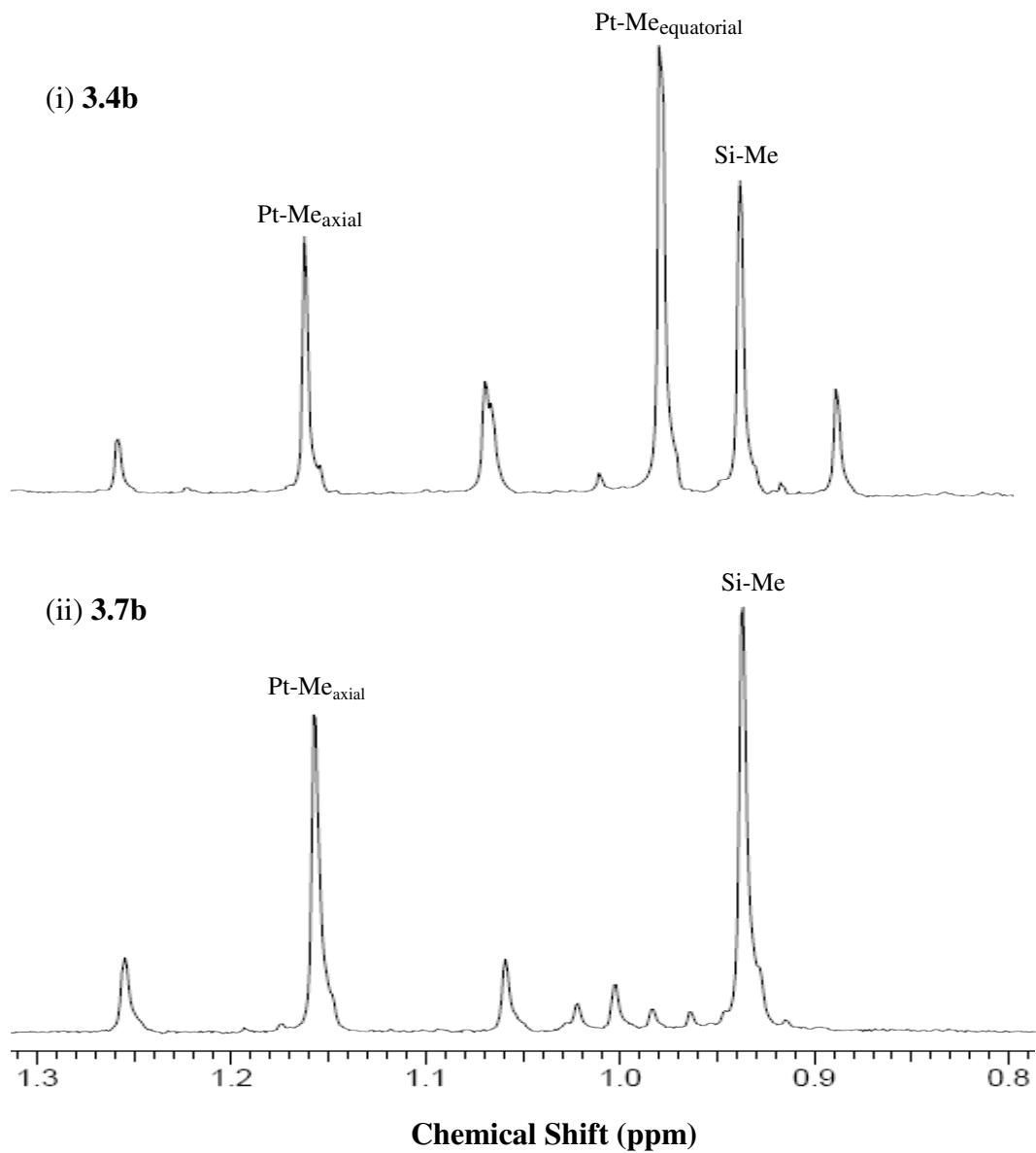
Figure 3.4. The ^{1}H-NMR spectra (400 MHz, CD$_3$OD) in the methyl region

for complexes **3.4b** (i) and **3.7b** (ii).

3.2.2.3 The reaction of [PtMe₂(bps)] with Dibenzoyl Peroxide

The complex **3.2**, [PtMe₂(bps)] reacted rapidly at room temperature with dibenzoyl peroxide in acetone to give complex **3.8** (Equation 3.6), which was isolated as a white solid. The product is stable at room temperature and soluble in several solvents such as acetone, chloroform, and methylene chloride, so it was characterized using ^{1}H-NMR, gCOSY, ^{13}C, and X-ray crystallography.
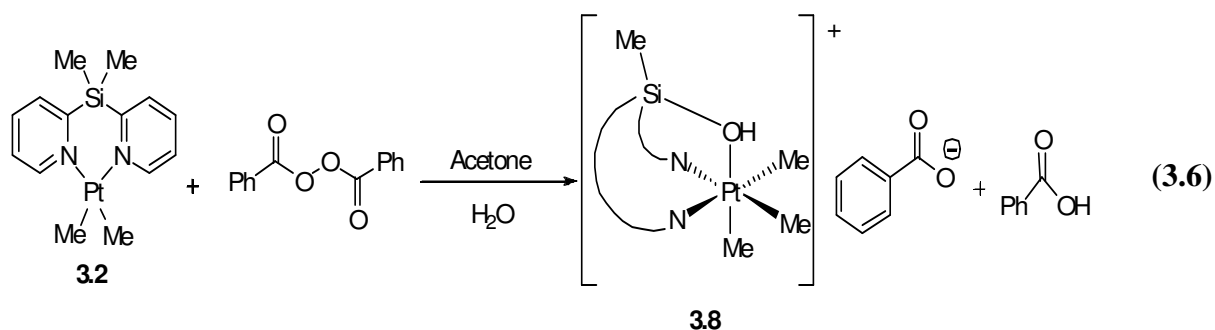
The ^{1}H-NMR spectrum (Figure 3.5) of complex **3.8** showed two different methyl platinum proton resonances at δ = 1.05 (6H), and 1.14 (3H), with coupling constant $^2J_{\text{Pt-H}}$ = 70 (*trans* to nitrogen), and 75 (*trans* to oxygen) Hz respectively, which are very similar to the spectra found for complexes **3.4a-b** and **3.7a-b**. Only one methylsilicon resonance was observed at δ = 1.04 (3H). The reaction in the presence of a good oxidizer such as dibenzoyl peroxide caused a similar methyl transfer from silicon to the axial position of the platinum metal center as observed before upon the reaction with hydrogen peroxide and methanol. The molecular structure of complex **3.8** was proven by the X-ray crystallography (Figure 3.6). The oxygen atom is bonded to the silicon and the platinum(IV) octahedral center. The structure of the cation unit in complex **3.8**, [Me₃Pt(HOSiMe(2-C₅H₄N)₂)]⁺ is similar to that of the [Me₃Pt(OSiMe(2-

$C_5H_4N)_2)]^+$ unit in complex **3.3**, and the presence of the rare coordinated silanol group in **3.8** (in place of the siloxide group in **3.3**) is indicated by the presence of a strong hydrogen bonding interaction with the benzoate anion [O(3)---O(1A) = 2.463(1) Å].[23] An interesting feature of the structure of **3.8** is that the benzoate anion is oriented so as to give a very weak interaction with the silicon atom [Si(1)---O(2A) = 3.07(1) Å], as expected for the onset of a nucleophilic substitution reaction.[24]

The ^{1}H-NMR spectrum for complex **3.8**, in the aromatic region showed one set of pyridyl proton resonances for both pyridyl groups. The proton resonance of the *ortho* hydrogen was observed at δ = 8.58, with coupling constant $^3J_{Pt-H}$ = 20 Hz. The obtained crystal structure showed a [PhCOO]⁻ counter anion, and the benzoate group gave three proton resonances in the ^{1}H-NMR spectrum that accounted for five hydrogen atoms.
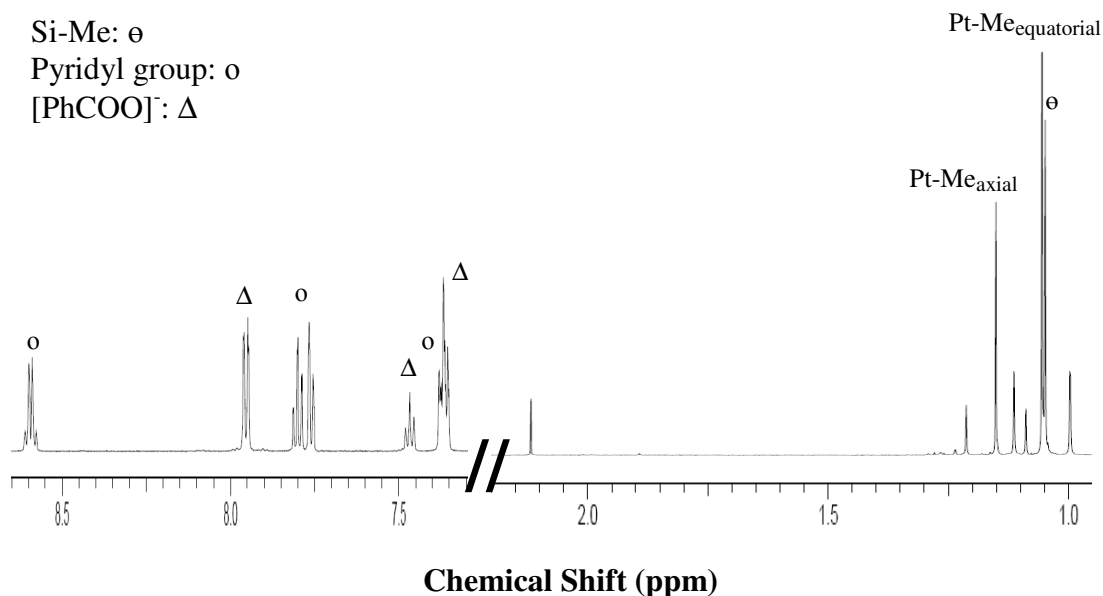
Figure 3.5. The ^{1}H-NMR spectrum (600 MHz, CD$_2$Cl$_2$) of complex **3.8,** [PtMe$_3$(OH){(NC$_5$H$_4$)-(μ-SiMe)-(C$_5$H$_4$N)}]$^+$ [PhCOO]⁻.
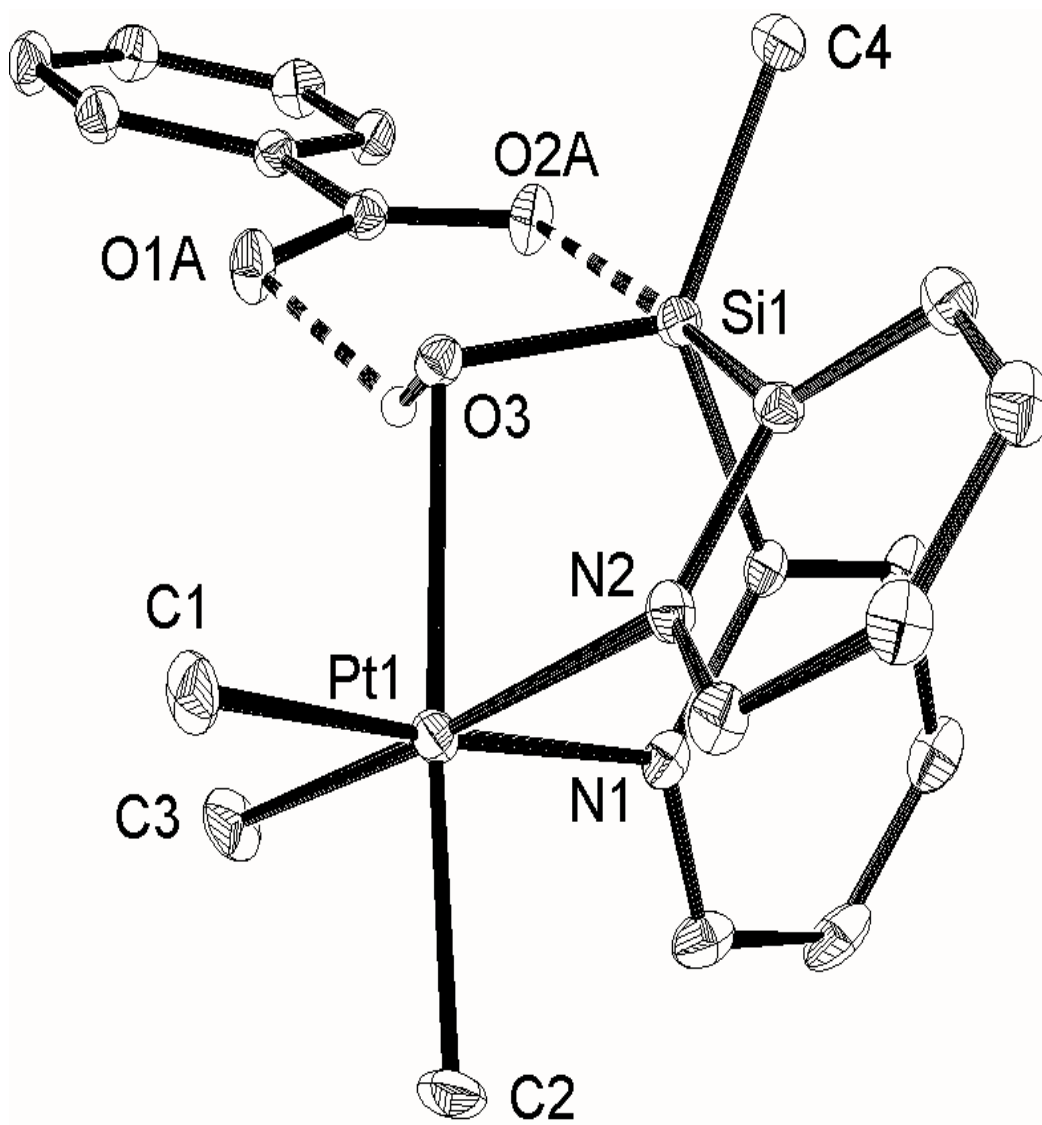
Figure 3.6. The crystal structure of complex **3.8**, [PtMe$_3$(OH){(NC$_5$H$_4$)-(μ-SiMe)-(C$_5$H$_4$N)}]$^+$ [PhCOO]$^-$.

Table 3.3. Selected bond lengths [Å] and angles [°] for complex **3.8**

Pt(1)-C(2)	2.045(4)	Pt(1)-C(1)	2.050(5)
Pt(1)-C(3)	2.051(5)	Pt(1)-N(2)	2.168(4)
Pt(1)-N(1)	2.181(4)	Pt(1)-O(3)	2.237(3)
Pt(1)-Si(1)	2.964(1)	Si(1)-O(3)	1.623(3)
C(2)-Pt(1)-C(1)	88.2(2)	C(2)-Pt(1)-C(3)	88.6(2)
C(1)-Pt(1)-C(3)	89.8(2)	C(2)-Pt(1)-N(2)	94.6 (2)
C(1)-Pt(1)-N(2)	90.3(2)	C(3)-Pt(1)-N(2)	176.8(2)
C(2)-Pt(1)-N(1)	94.8 (2)	C(1)-Pt(1)-N(1)	177.0 (2)
C(3)-Pt(1)-N(1)	90.2 (2)	N(2)-Pt(1)-N(1)	89.6(1)
C(2)-Pt(1)-O(3)	176.3(2)	C(1)-Pt(1)-O(3)	93.9(2)
O(3)-Pt(1)-Si(1)	32.7 (8)	O(3)-Si(1)-C(4)	120.8(2)

Complex **3.6**, $[Pt(CD_3)_2(bps)]$ was reacted with dibenzoyl peroxide under the same conditions of the reaction that produced complex **3.8** previously (Equation 3.7). The reaction proceeded to form complex **3.9**, $[PtMe(CD_3)_2(OH)\{(NC_5H_4)-(\mu-SiMe)-(C_5H_4N)\}]^+$ $[PhCOO]^-$. Complex **3.9** showed two different isomers **3.9a** and **3.9b** in 1:2 ratio, which were observed by analyzing the methyl region of the ^{1}H-NMR that showed two methyl platinum proton resonances at δ = 1.04, and 1.14, with coupling constant $^2J_{Pt-H}$ = 70 (*trans* to nitrogen), and 75 (*trans* to oxygen) Hz, respectively. A day later, intensity of the proton resonance for the methyl *trans* to oxygen (axial) decreased, while the one *trans* to nitrogen (equatorial) increased (**3.9a** and **3.9b** in 2:1 ratio). There are two possible equatorial positions on the octahedral platinum(IV) metal center, and only one possible axial position, so the two isomers **3.9a** and **3.9b** are produced in a 2:1 ratio. There was only one methylsilicon resonance observed at δ = 1.05. The ^{1}H-NMR

spectrum for complex **3.9** in CD_2Cl_2 in the aromatic low field region was exactly similar to the

aromatic region for complex **3.8**. Figure 3.7 shows the ^{1}H-NMR spectra for complex **3.9** on day

one and a day after.

(3.7)
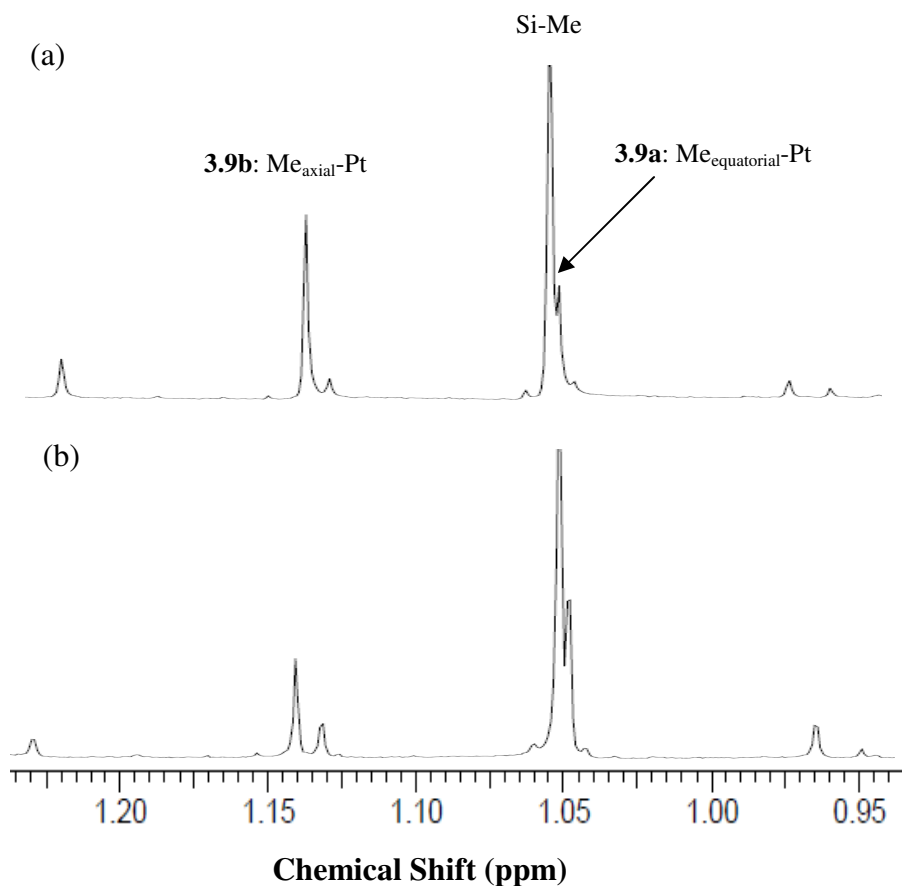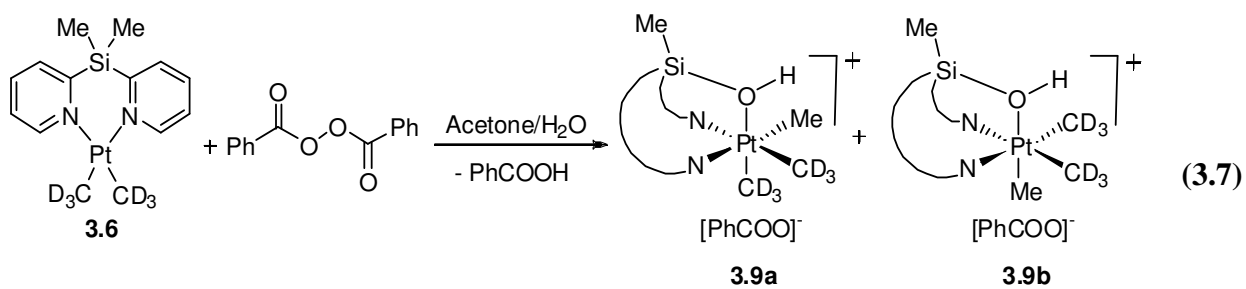
Figure 3.7. The ^{1}H-NMR spectrum (400 MHz, CD_2Cl_2) of complex **3.9**,

[PtMe(CD$_3$)$_2$(OH){(NC$_5$H$_4$)-(μ-SiMe)-(C$_5$H$_4$N)}]; (a) day one. (b) a day after.

103

As shown by the ^{1}H-NMR spectrum for the more stable complex **3.9** in CD_2Cl_2 solution, a slow scrambling of the MePt and CD_3Pt groups occurred over a period of two days to give a 2:1 mixture of **3.9a** and **3.9b**. There was no CD_3/CH_3 exchange with the MeSi group, indicating that the methyl group transfer to give **3.9** is irreversible.

The ease of the methyl group transfer to form complexes **3.4a-b**, **3.7a-b**, and **3.9** without forming a Pt-Si bond and the mutually *trans* positions of the methyl and silanol units are unusual.[14, 16] Some mechanistic insight was obtained by carrying out **DFT** calculations for the reaction of **3.2** with H_2O_2 and results are shown in Figure 3.8. The initial reaction of **A** (**3.2** + H_2O_2) occurs easily and the O-O bond is essentially broken in the first intermediate **B**, followed by hydrogen bonding between the forming PtOH and the $^-$OH groups to give **C**. In **C**, there is a weak SiCH---Pt interaction but complete methyl transfer to give **F** is unfavorable because the Si-Me bond is stronger than the Pt-Me bond.[25] The hydroxide group in **C** might attack at platinum to give **E**, the product of simple oxidative addition, but this is not observed. Instead, a more favorable reaction is attack by hydroxide at silicon with simultaneous methyl group transfer to platinum to give **D**. Inversion of the chelate ring, with formation of a 5-coordinate silicon centre, then occurs to give **G**, from which loss of hydroxide occurs to give **H**, which is likely structure of **3.4b**. The calculation suggests that **H** is best considered as the siloxide complex hydrogen bonded to water, rather than the silanol complex hydrogen bonded to hydroxide [PtO---H = 1.44, H---OH = 1.00 Å]. It is also shown that the methyl group transfer is driven by the nucleophilic attack at silicon, with formation of a Si-OH bond.[16]
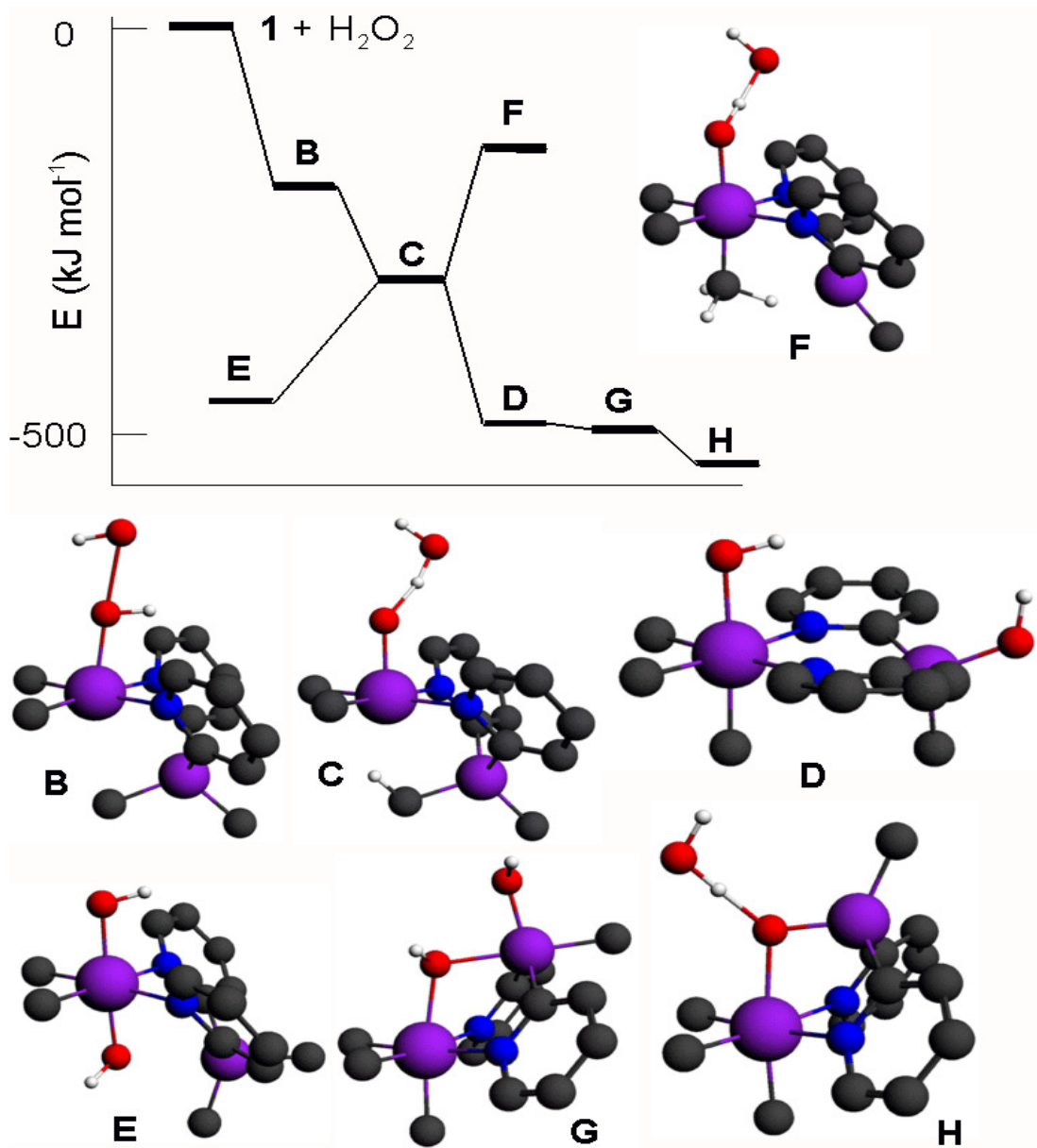
Figure 3.8. Calculated relative energies and structures of platinum complexes and potential reaction intermediates.

3.2.2.4 The Reaction of [PtMe$_2$(bps)] with I$_2$

The reaction of complex **3.2**, [PtMe$_2$(bps)], with iodine proceeded rapidly at room temperature to give the complex [PtMe$_2$I$_2$(bps)], **3.10**, according to Equation 3.8. The complex was characterized spectroscopically, and the structure of complex **3.10** was confirmed crystallographically (Figure 3.9). The ^{1}H-NMR spectrum of complex **3.10** gave single resonances for the two methylplatinum groups at δ = 2.31, with coupling constant $^2J_{\text{Pt-H}}$ = 71 Hz, and for the two methylsilicon groups at δ = 0.76. The ^{1}H-NMR spectrum in the aromatic region showed one set of pyridyl resonances due to symmetry. The doublet resonance of the ortho hydrogen atoms of the pyridine ring also show a coupling to platinum with $^3J_{\text{Pt-H}}$ = 22 Hz (Py-H$_{ortho}$). In addition, the ESI-MS of **3.10** in CH$_2$Cl$_2$ gave a peak at m/z = 678.1, for the cation [MeI$_2$Pt(bps)]$^+$.

(3.8)
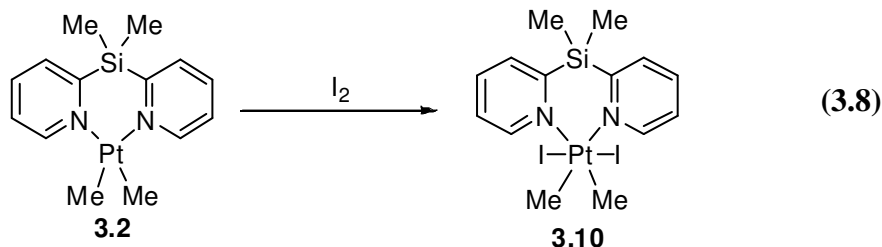
In the structure of **3.10** (Figure 3.9) the two Me-Si groups are nonequivalent, so variable temperature ^{1}H-NMR study was carried out to determine if the exchange between the methylsilicon groups could be frozen out at low temperature. The NMR spectra were recorded at 20 °C intervals between -80 and +20 °C. The methylsilicon resonance becomes broad on cooling to -80 °C but does not split, indicating very much easier inversion of the chelate ring than in the square planar complex **3.2**. The mean twist of the pyridine rings with respect to the PtC2N2 square plane is 54° in **3.2** and 40° in **3.10**, while the distance Pt---

C(19) = 3.52 Å in **3.2** but 4.80 Å in **3.10**. Clearly, the chelate ring is less distorted from planarity and the close methylsilicon group in **3.2** moves to open up the coordination site at platinum(IV) for iodide coordination in forming complex **3.10**. Thus, it can be expected that the chelate ring inversion needed to convert **D** to **G** (Figure 3.8) should also be easy. The unexpected formation of complex **3.3** (Figure 3.3) is finally explained by competitive methylplatinum group cleavage from **3.1** by the acid H[B(OCH$_2$CF$_3$)(C$_6$F$_5$)$_3$] to give the platinum(II) fragment and oxidation by air to give the platinum(IV) fragment. Combination of the two units then gives the binuclear complex **3.3** (Figure 3.3).
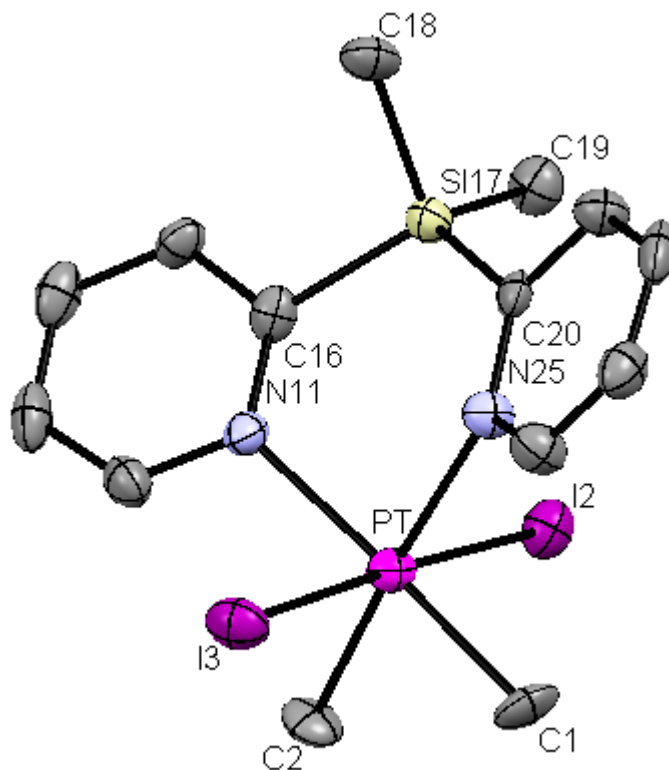
Figure 3.9. The structure of complex **3.10**, [PtMe$_2$I$_2$(bps)].

Table 3.4. Selected bond lengths [Å] and angles [°] for complex **3.10**

Pt-C(2)	2.077(8)	Pt-C(1)	2.079(8)
Pt-N(11)	2.210(6)	Pt-N(25)	2.217(6)
Pt-I(2)	2.628 (6)	Pt-I(3)	2.652 (6)
Si(17)-C(18)	1.877(8)	Si(17)-C(20)	1.908(8)
C(2)-Pt-C(1)	85.7(4)	C(2)-Pt-N(11)	90.8(3)
C(1)-Pt-N(11)	176.2(3)	C(2)-Pt-N(25)	176.3(3)
C(1)-Pt-N(25)	90.9(3)	N(11)-Pt-N(25)	92.6(2)
C(2)-Pt-I(2)	87.3(2)	C(1)-Pt-I(2)	87.3(3)
I(2)-Pt-I(3)	177.2(2)	N(11)-Pt-I(2)	91.2(2)
N(25)-Pt-I(2)	91.2 (2)	C(2)-Pt-I(3)	90.9(2)
C(19)-Si(17)-C(18)	106.8(4)	C(19)-Si(17)-C(20)	115.3(4)

3.2.3 Oxidative Addition Reaction of MeI to Complex 3.2

Complex **3.11**, [PtMe$_3$I(bps)], was produced via the *trans* oxidative addition reaction of complex **3.2**, [PtMe$_2$(bps)], with MeI in ether (Equation 3.9). The reaction was complete within 10 minutes, as determined from the change in color of **3.2** (yellow) to **3.11** (white). The product was isolated as an air stable solid, and is soluble in several comman organic solvents such as actone, methylene chloride, and chloroform. Complex **3.11** has been characterized by NMR spectroscopy, and mass spectrometry.

The ^{1}H-NMR spectrum (Figure 3.10) of **3.11** contained two methylplatinum proton resonances at $\delta = 0.94$, with coupling constant $^2J_{Pt-H} = 72$ Hz (3H, *trans* to I), and at $\delta = 1.32$, with coupling constant $^2J_{Pt-H} = 68$ Hz (6H, *trans* to N). There were two singlet resonances at $\delta =$

0.65 and 0.81 for two methylsilicon groups. The ^{1}H-NMR spectrum had only one set of pyridyl resonances. The proton resonance of the *ortho* pyridyl protons was observed at δ = 9.63, $^3J_{\text{Pt-H}}$ = 20 Hz. The ESI-MS of **3.11** in CH$_2$Cl$_2$ gave a peak at *m/z* = 454, for the cation [Me$_3$Pt(bps)]$^+$.

$$(3.9)$$
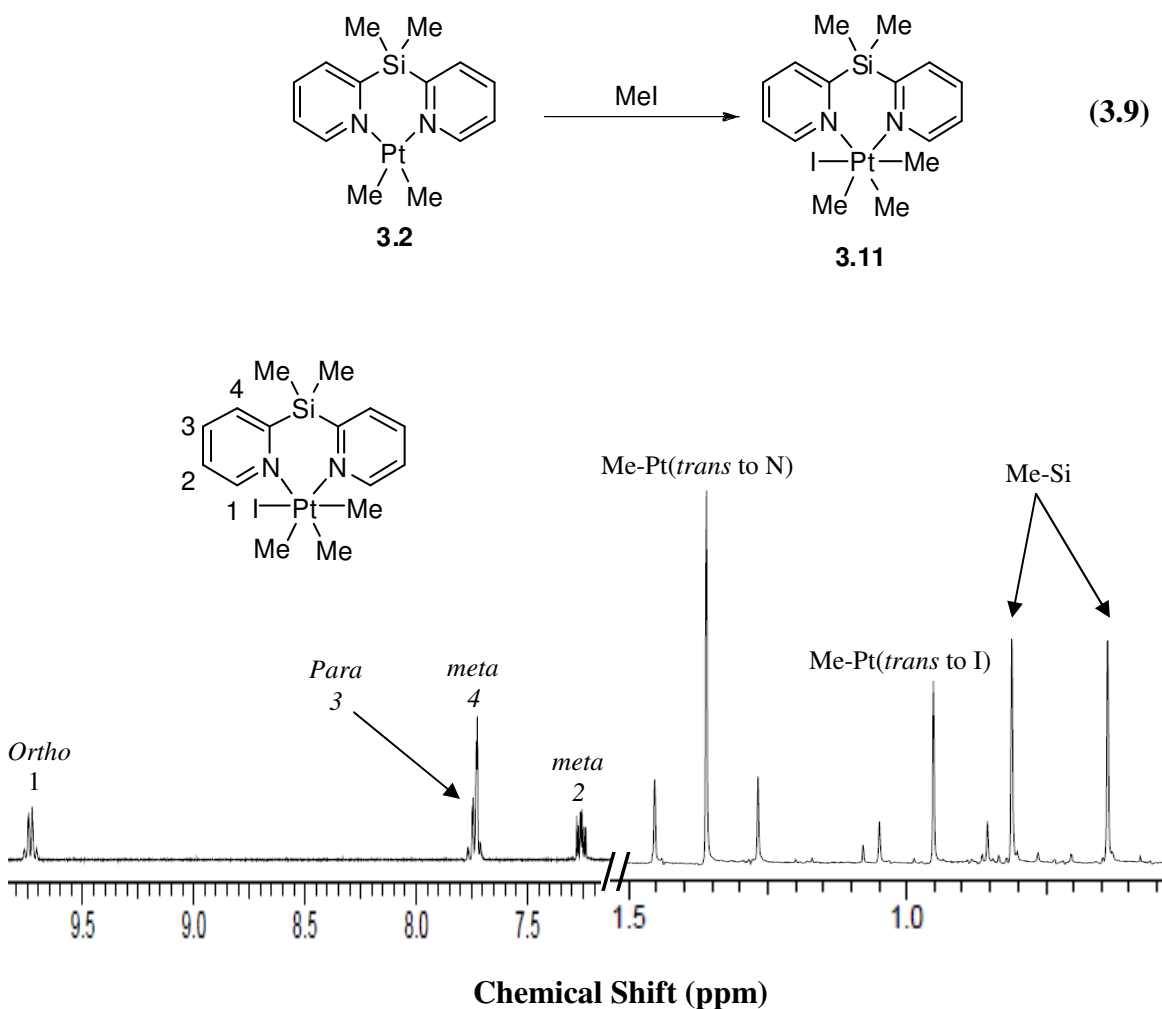
Figure 3.10. The ^{1}H NMR spectrum (400 MHz, CD$_2$Cl$_2$) for complex **3.11**, [PtMe$_3$I(bps)].

109

Complex **3.11** was dissolved in methylene chloride and layered with pentane to obtain a crystal for X-ray analysis. The structure determination showed that the complex had decomposed by hydrolysis to give complex **3.12** (Figure 3.11, Equation 3.10). The methylene chloride and pentane solvent mixture was decanted, and the crystals were dried under high vacuum. Then the crystals were dissolved in CD_2Cl_2, and a ^{1}H-NMR experiment was run. The ^{1}H-NMR spectrum (Figure 3.12) showed a mixture of complex **3.11** and **3.12** (2:1 ratio) in addition to a single proton resonance at $\delta = 0.1$ which is due to the methyl groups of the polymer dimethylsilicone. The spectrum contained two single methyl platinum proton resonances at $\delta = 0.97$, $^2J_{Pt-H} = 72$ Hz (3H, *trans* to I), and at $\delta = 1.44$, with coupling constant $^2J_{Pt-H} = 70$ Hz (6H, *trans* to N) which were assigned for complex **3.12**. In the aromatic region for complex **3.12** only one set of pyridyl group resonances was observed. The *ortho* pyridyl proton had a single resonance at $\delta = 8.78$, $^3J_{Pt-H} = 19$ Hz. Several ^{1}H-NMR experiments were taken over a period of two weeks, and the intensity of the proton resonances of complex **3.11** decreased with time, while the ones of complex **3.12** increased. The sample was dissolved in methylene chloride, and ESI-MS of the solution was recorded. The mass spectrum showed peaks that are multiples of the polymer $(Me_2SiO)_n$-.
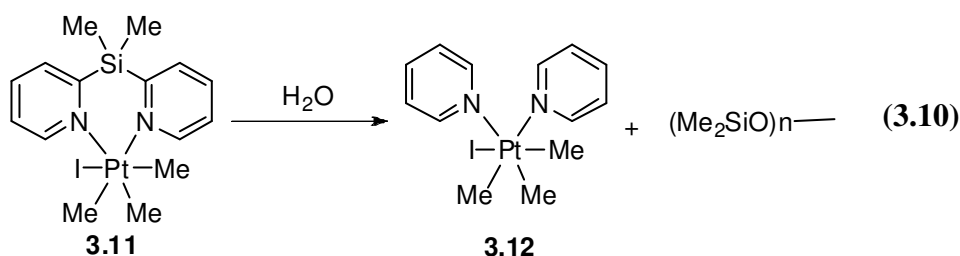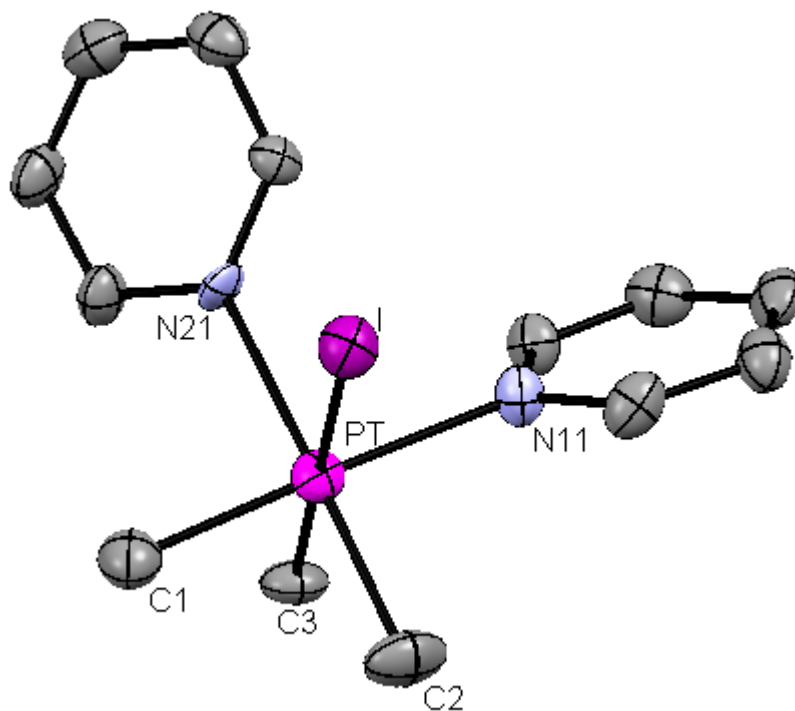
Figure 3.11. The structure of complex **3.12**, [PtMe$_3$I(pyridine)$_2$].
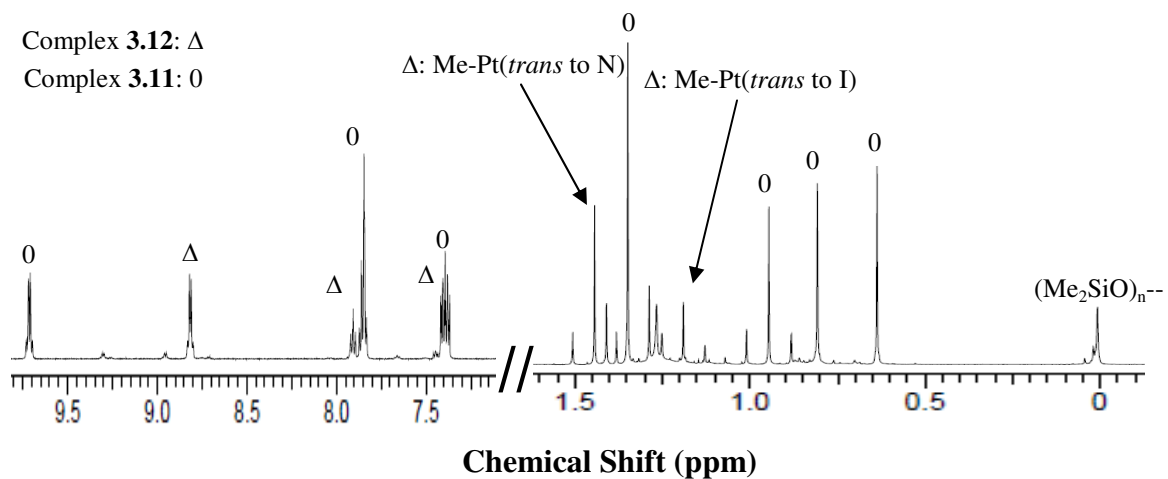
Figure 3.12. The ^{1}H NMR spectrum (400 MHz, CD$_2$Cl$_2$) for complex **3.12**, [PtMe$_3$I(pyridine)$_2$].

A VT-NMR experiment for the reaction of complex **3.2**, [PtMe$_2$(bps)] with CD$_3$I was performed to check the reactivity and the mechanistic pathway of the reaction. Complex **3.2** was dissolved in acetone-d$_6$, placed in an NMR tube, and then the NMR probe was cooled down to -50 $^{\circ}$C. After recording the ^{1}H-NMR for the starting material, chilled CD$_3$I was added and then the reaction was monitored. The reaction proceeded rapidly via the *trans* oxidative addition to form complex **3.13**, [PtMe$_2$(CD$_3$)I(bps)].

Complex **3.13** was identified by 3 different methyl proton resonances. The two methyl-silicon proton resonances were seen at δ = 0.74 and 0.86. One methyl platinum proton resonance existed at δ = 1.25, $^2J_{Pt-H}$ = 69 Hz (*trans* to N). The ^{1}H-NMR spectrum at -50 $^{\circ}$C showed no traces of the starting material. Then the NMR probe was warmed up slowly, and a ^{1}H-NMR spectrum was taken every 10 $^{\circ}$C. Nothing happened during the warm up of the probe, until a methyl platinum(IV) proton resonances started appearing at 0 $^{\circ}$C which happened to be a methyl platinum proton resonance at the axial position. That axial position proton resonance existed via CD$_3$/CH$_3$ exchange and was seen at δ = 0.91, $^2J_{Pt-H}$ = 71 Hz (*trans* to I). The ^{1}H-NMR spectra for the solution of complex **3.13** were recorded over a period of three days, and the intensity of the axial position didn't change after the first day. It was observed from the ^{1}H-NMR spectra that the CD$_3$I reacted with **3.2** via oxidative addition to give a mixture of **3.13a** and **3.13b** in ~1:2 ratio. Figure 3.13 shows selected spectra for the reaction of complex **3.2** with CD$_3$I. A ^{2}H-NMR was recorded to prove that the CD$_3$/CH$_3$ is occurring (Figure 3.14). The ^{2}H-NMR showed the presence of two different CD$_3$-platinum(IV) resonances. The two ^{2}H resonances appeared at δ = 0.90 ($^2J_{Pt-D}$ = 10 Hz, *trans* to I), and 1.28 ($^2J_{Pt-D}$ = 10 Hz, *trans* to N) in a 1:2 ratio. Scheme 3.2 shows the reaction process for complex **3.2** with CD$_3$I in acetone-d$_6$.
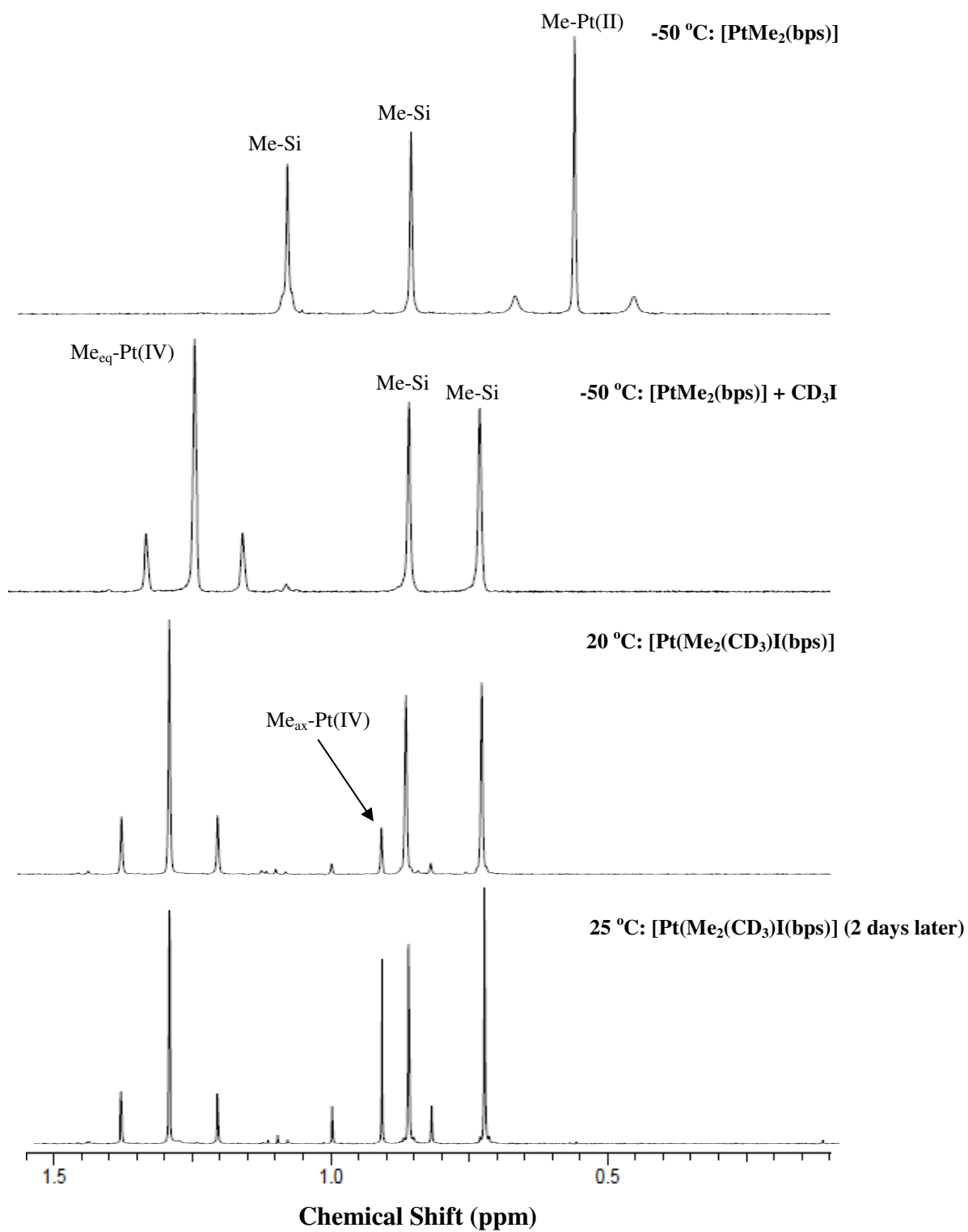
Figure 3.13. Chosen spectra of VT-NMR (400 MHz, acetone-d$_6$) experiment for the reaction of CD$_3$I with **3.2.**
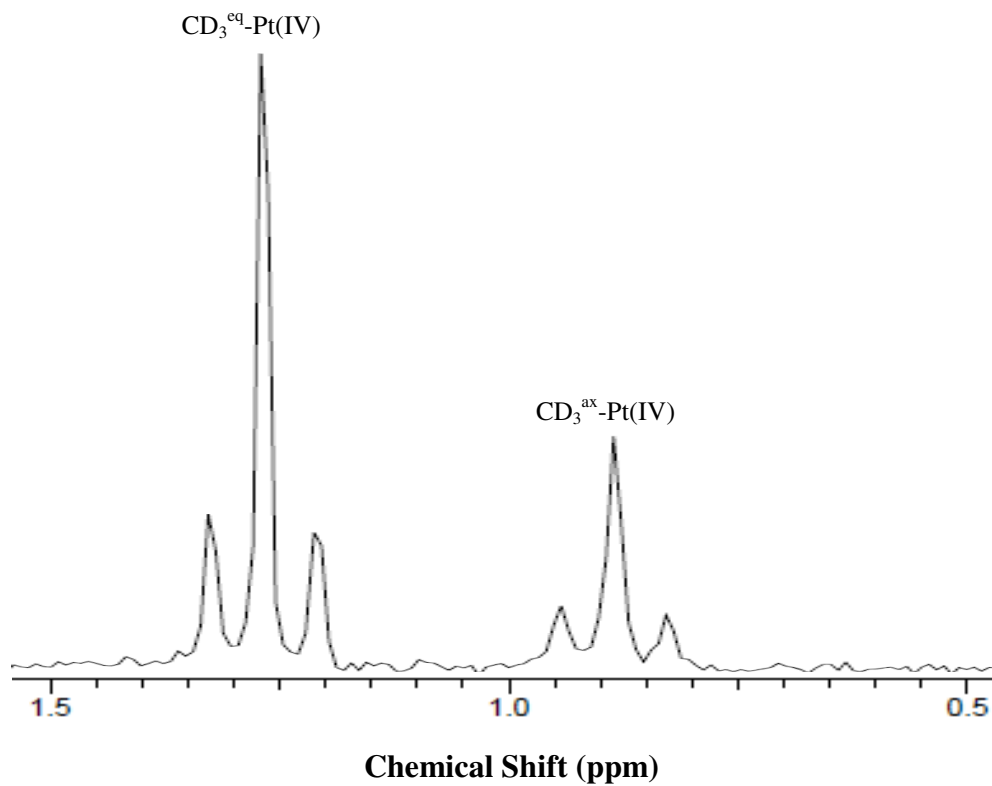
Figure 3.14. The ^{2}H-NMR spectrum (600 MHz, acetone-d$_6$) of complex **3.13** at room

temperature.
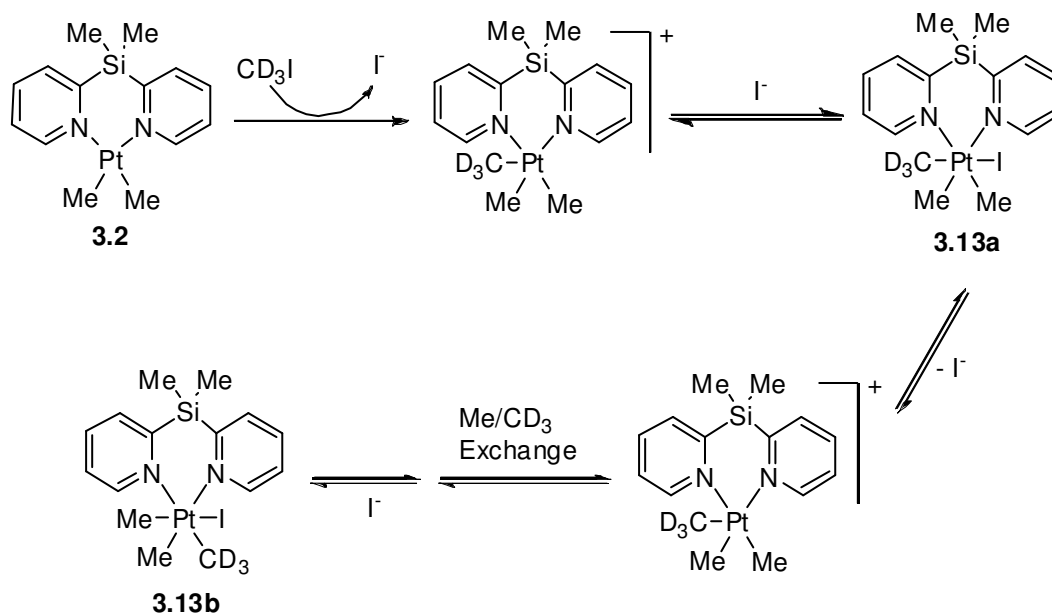
Scheme 3.2

3.2.4 Protonolysis Reactions of Complex 3.2 Using HCl

The chemistry of alkyl(hydrido)platinum(IV) complexes has given important details about the mechanism of C-H bond activation by electrophilic methylplatinum(II) complexes.[18,19,21,26] Most of the methyl(hydrido)platinum(IV) complexes have been prepared via the protonation of the corresponding methylplatinum(II) complexes.[27] The reaction of complex **3.2** with HCl at room and low temperature proceeded very rapidly to produce complex **3.15** (Figure 3.15), according to scheme 3.3. The reaction was initiated in an NMR tube and then monitored at different temperatures.
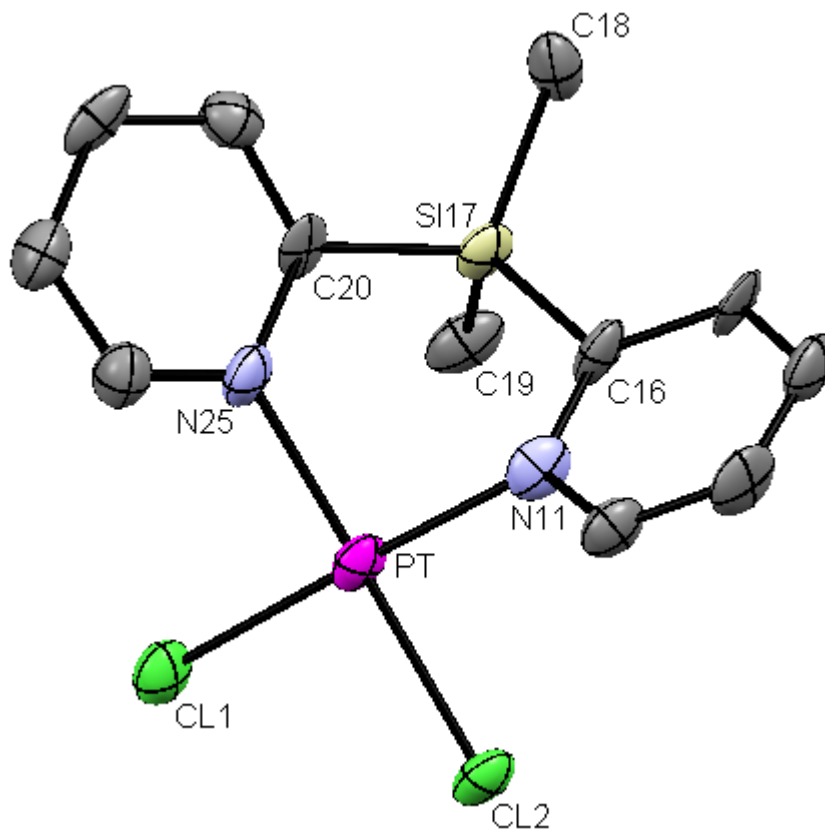
Figure 3.15. The molecular structure of complex **3.15**, [PtCl$_2$(bps)].

Complex **3.15** was characterized using ^{1}H-NMR spectroscopy, and X-ray crystallography. The ^{1}H-NMR spectrum (Figure 3.16) of complex **3.15** showed no methyl platinum resonances, since those were reductively eliminated to produce methane which was identified via a single proton resonance at $\delta = 0.2$. The two methyl silicon proton resonances existed as singlets at $\delta = 0.9$, and 1.45. In the aromatic region, there were 4 different proton resonances for both pyridyl groups. The *ortho* proton was seen at $\delta = 9.15$, with $^3J_{Pt-H} = 42$ Hz (*trans* to Cl).
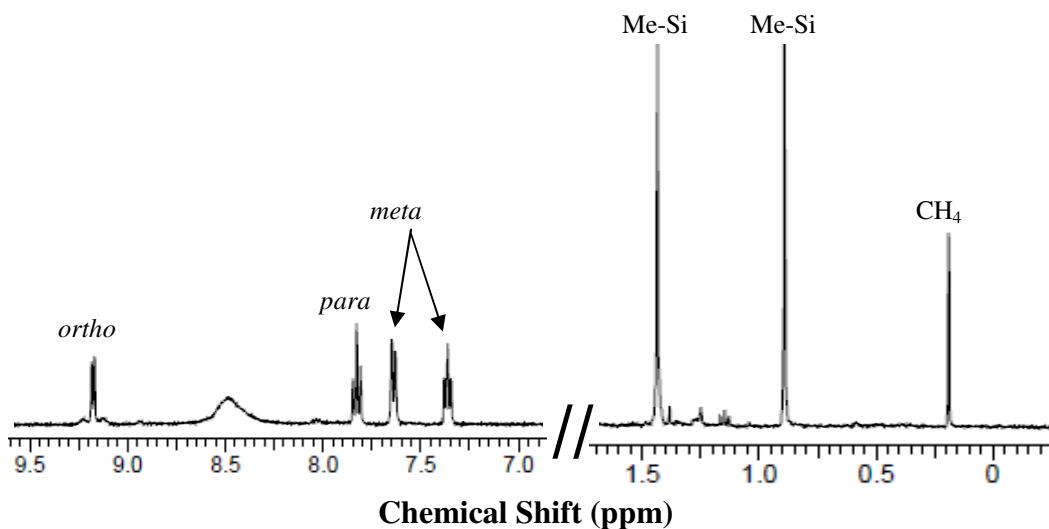
Figure 3.16. The ^{1}H-NMR spectrum (400 MHz, CD$_2$Cl$_2$) of complex **3.15**, [PtCl$_2$(bps)].

The reaction of complex **3.2** with HCl proceeded via an oxidative addition at -80 °C to produce compound **3.14**, [PtMe$_2$(H)Cl(bps)], which was not stable and started decomposing by producing methane via the reductive elimination reaction. Complex **3.14** was identified via the hydride platinum single proton resonance, which was seen at $\delta = -20.64$, with $^1J_{Pt-H} = 1593$ Hz (*trans* to Cl), a methylplatinum resonance at $\delta = 1.11$, with $^2J_{Pt-H} = 65$ Hz, and one set of pyridyl proton resonances. The platinum(IV) hydride complex was not stable upon warming up the NMR probe, and the hydride platinum completely disappeared at 0 °C. Figure 3.17 shows the ^{1}H-NMR spectra in the hydride-platinum region at -80 °C and 0 °C.

116
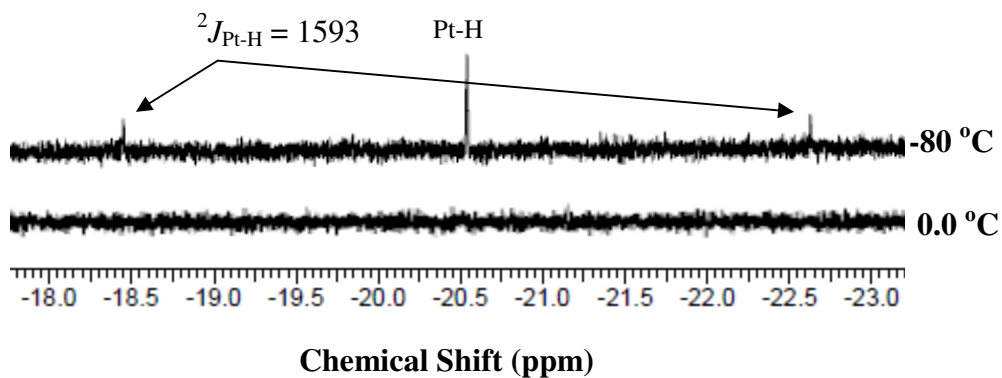
Figure 3.17. The hydride-platinum region ^{1}H-NMR spectra (400 MHz, CD$_2$Cl$_2$) at -80 ^{o}C and 0.0 ^{o}C.
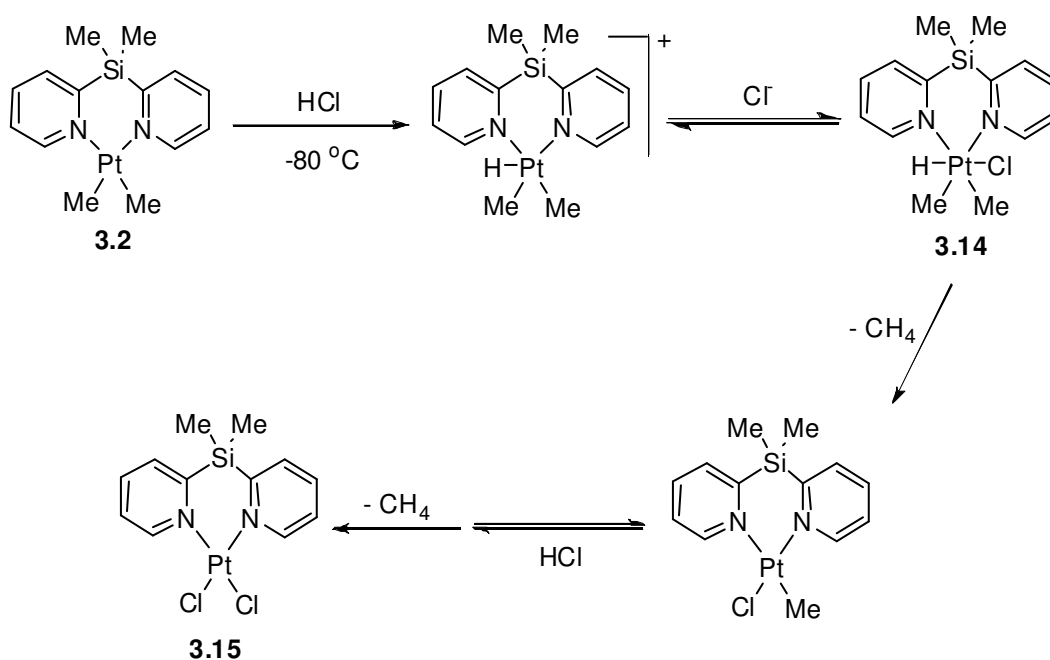
Scheme 3.3

Table 3.5. Selected bond lengths [Å] and angles [°] for complex **3.15**

Pt-N(25)	2.022(11)	Pt-N(11)	2.026(11)
Pt-Cl(1)	2.294(4)	Pt-Cl(2)	2.296(3)
N(25)-Pt-N(11)	91.2(5)	N(25)-Pt-Cl(1)	90.3(3)
N(11)-Pt-Cl(1)	177.0(3)	N(25)-Pt-Cl(2)	177.2(3)
N(11)-Pt-Cl(2)	88.4(3)	Cl(1)-Pt-Cl(2)	90.3(1)

3.2.5 The Oxidative Addition Reaction of Methyl Triflate to Complex 3.2

The reactions of methyl triflate with methylplatinum(II) complexes usually proceeds via oxidative addition. The reaction of methyl triflate with complex **3.2**, [PtMe$_2$(bps)] in acetone proceeds rapidly via oxidative addition to produce complex **3.16**, [PtMe$_3$(OH$_2$)(bps)]$^+$ [CF$_3$SO$_3$]$^-$. The ^{1}H-NMR of complex **3.16** in acetone-d$_6$ was obtained (Figure 3.18). Complex **3.16** was identified using ^{1}H-NMR due to the presence of a single proton resonance at $\delta = 0.85$, which was assigned to the two methyl silicon groups. The three methylplatinum groups gave a single proton resonance at $\delta = 1.21$, with $^2J_{Pt\text{-}H} = 71$ Hz. One set of pyridyl groups proton resonances was seen, and the *ortho* proton was seen at $\delta = 9.05$, with $^3J_{Pt\text{-}H} = 18$ Hz (*trans* to Me).
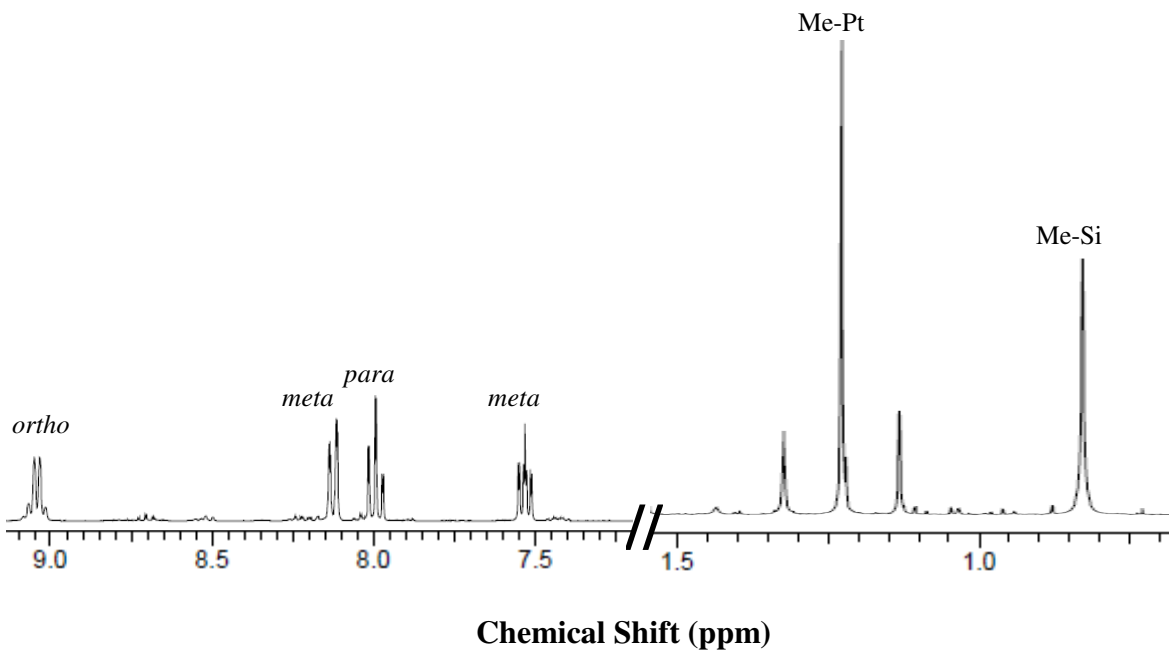
Figure 3.18. The ^{1}H-NMR spectrum (400 MHz, acetone-d$_6$) of complex **3.16**, [PtMe$_3$(OH$_2$)(bps)]$^+$ [CF$_3$SO3]$^-$.
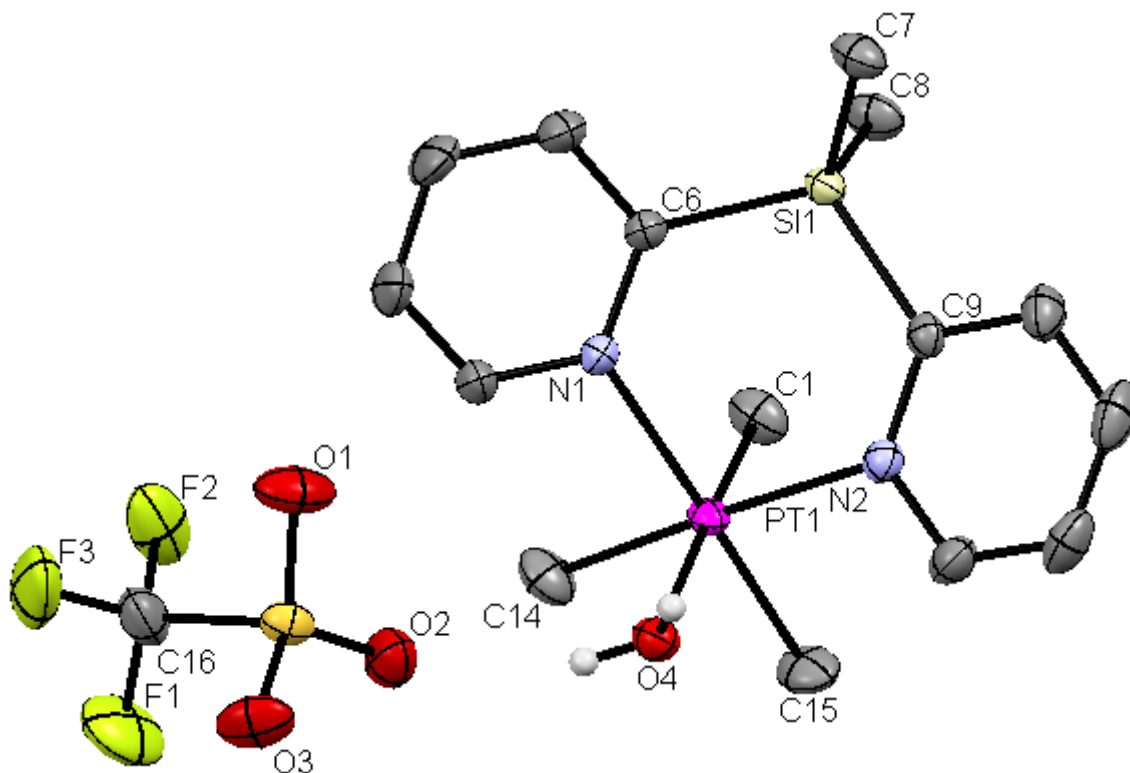
Figure 3.19. A view of the structure of complex **3.16**, [PtMe$_3$(OH$_2$)(bps)]$^+$ [CF$_3$SO3]$^-$.

Table 3.6. Selected bond lengths [Å] and angles [°] for complex **3.16**

Pt(1)-C(1)	2.027(2)	Pt(1)-C(15)	2.039(2)
Pt(1)-C(14)	2.048(2)	Pt(1)-N(1)	2.179(2)
Pt(1)-N(2)	2.189(2)	Pt(1)-O(4)	2.371(2)
C(1)-Pt-C(15)	85.8 (1)	C(1)-Pt-N(1)	94.8(9)
C(15)-Pt-N(1)	178.9 (9)	N(1)-Pt-N(2)	90.5(6)
C(1)-Pt-O(4)	176.2(9)	C(15)-Pt-O(4)	90.7(9)

Triflate anion is a weakly bound ligand, and upon obtaining a single crystal of complex **3.16**, the X-ray analysis showed the coordination of an aqua ligand to the Pt(IV) metal center. The obtained molecular structure via X-ray (Figure 3.19) also showed the presence of a *fac-*trimethylplatinum(IV) center. In addition, the triflate anion hydrogen bonds to the aqua ligand.

A VT-NMR experiment was set to study the reaction of methyl triflate with complex **3.2**. In an NMR tube to a solution of complex **3.2**, [PtMe$_2$(bps)] in acetone-d$_6$ was added methyl triflate. The reaction was monitored at variable temperatures using ^{1}H-NMR (Figure 3.20). As the NMR probe was cooled down, the single resonance of the two methyl silicon groups started splitting into two resonances. The resonance for the Me-Si protons is broad at room temperature due to the fast exchange, and two resonances started appearing at -10 ^{o}C. The coalescence temperature T$_c$= -10°C, which is used to calculate the free activation energy using the Eyring equation. The calculated value for the free activation energy $\Delta G^{\ddagger}$ is 56 kJ.mol^{-1}. Also the single proton resonance for the three methyl platinum groups started splitting into two different resonances *axial* and *equatorial* (1:2 ratio) at low temperatures. The exchange is likely to occur within a 5-coordinate platinum(IV) intermediate formed by reversible dissociation of the weakly bound aqua ligand. The same VT-NMR experiment was repeated using acetonitrile-d$_3$ instead which produced complex **3.17**. The acetonitrile solvent is known to be a good ligand to platinum(IV) complexes.[5] The presence of a good coordinating solvent stopped the fast exchange even at room temperature. The ^{1}H-NMR spectrum for **3.17** at room temperature (Figure 3.21), showed the presence of two proton single proton resonances for the two methyl silicon groups at δ = 0.69 and 0.79. Also two different methyl platinum single proton resonances were seen at δ = 0.93 and 1.04, with $^2J_{\text{Pt-H}}$ = 76 (3H), and 66 (6H) Hz. Scheme 3.4 shows the reactions of complex **3.2** with MeOTf using two different solvents acetone and acetonitrile.

Me-Pt

Me-Si

20 °C

Me$_{equatorial}$-Pt

Me$_{axial}$-Pt

0.0 °C

i) Coalescence temperature

-10 °C

-20 °C

Me$_{axial}$-Pt: $^2J_{Pt-H}$ = 53

Me$_{equatorial}$-Pt: $^2J_{Pt-H}$ = 65

-30 °C

Me-Si: δ = 0.89

Me-Si: δ = 0.83

-40 °C

1.5   1.0   0.5

Chemical Shift (ppm)
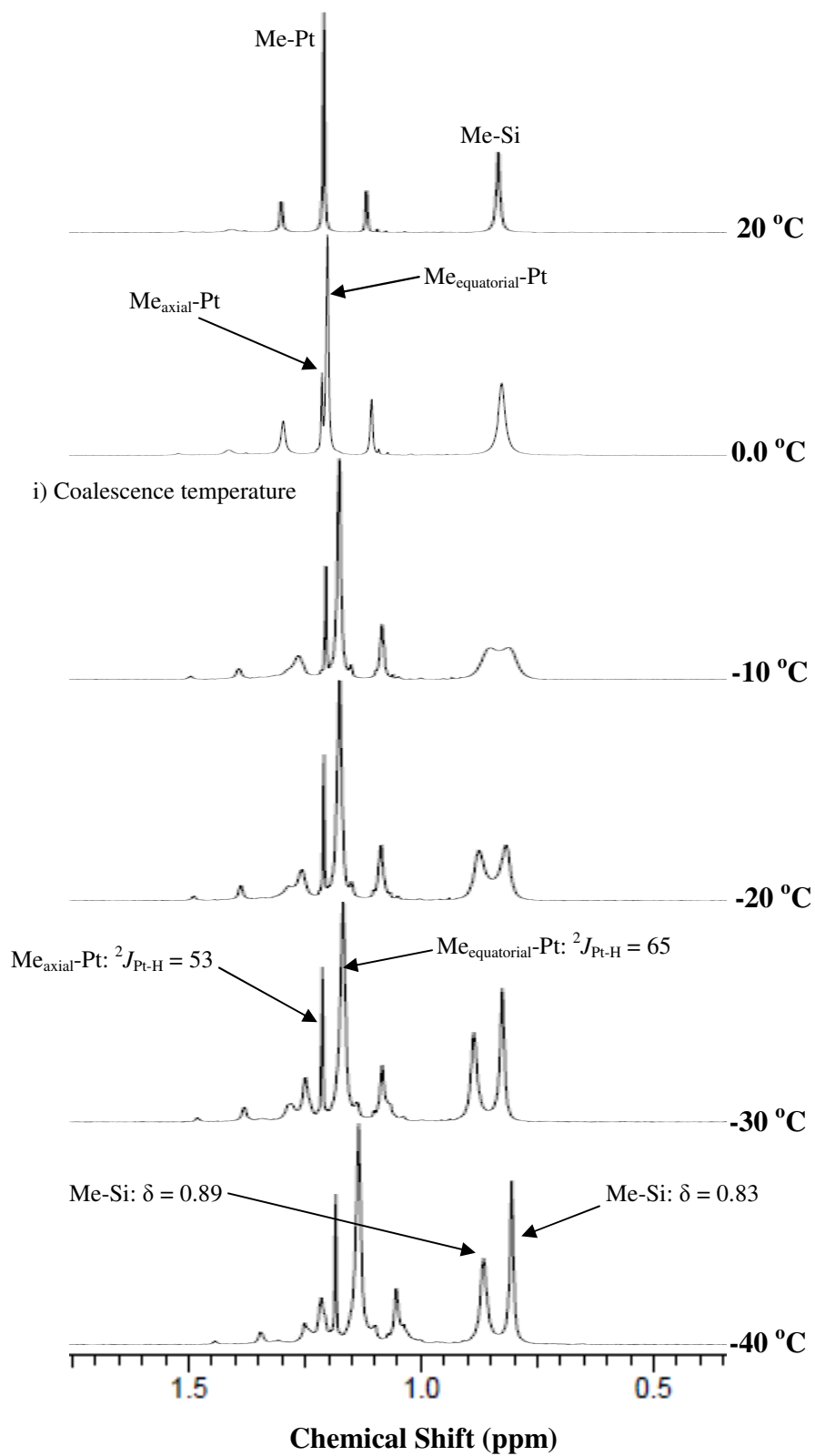
Figure 3.20. The VT-NMR spectra (400 MHz, acetone-d$_6$) for the reaction of complex **3.2** with methyl triflate.

3.17: [PtMe$_3$(NCCD$_3$)(bps)]$^+$ [CF$_3$SO$_3$]$^-$
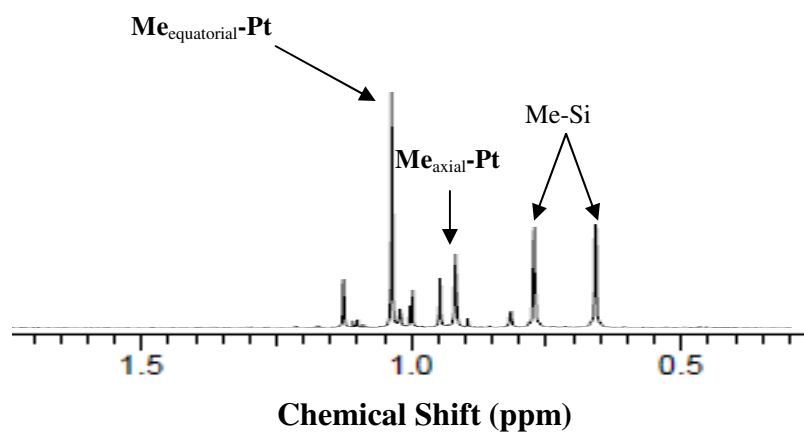
Figure 3.21. The ^{1}H-NMR spectrum (400 MHz, acetonitrile-d$_3$) for complex **3.17**; the reaction of complex **3.2** with methyl triflate at 25 ^{0}C.
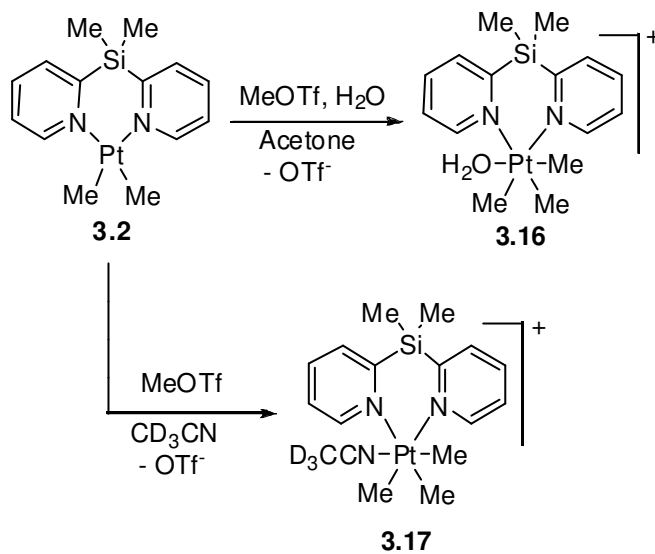
Scheme 3.4

3.3 Conclusions

Complex **3.2**, [PtMe$_2$(bps)] is an air stable solid and was easily prepared via the reaction of the ligand bps {bis(2-pyridyl)dimethylsilane} with [Pt$_2$Me$_4$(μ-SMe$_2$)$_2$]. It undergoes easy oxidative addition to produce platinum(IV) complexes.

The reaction of complex **3.2** with B(C$_6$F$_5$)$_3$ in trifluoroethanol in air occurred to give the unexpected complex **3.3**, [Me(bps)Pt-OSiMe(2-C$_5$H$_4$N)$_2$PtMe$_3$]$^+$ [B(OCH$_2$CF$_3$)(C$_6$F$_5$)$_3$]$^-$. A study for the reactions of complex **3.2** with alcohols, peroxides, and iodine was made to investigate the formation of complex **3.3** via the Si-C bond activation. Finally the formation of complex **3.3** could be explained via the competitive methyl platinum group cleavage from **3.2** by the acid H[B(OCH$_2$CF$_3$)(C$_6$F$_5$)$_3$] to give the platinum(II) fragment and oxidation by air to give the platinum(IV) fragment. Combination of the two units then gives the binuclear complex **3.3** which involves a very easy methylsilicon group cleavage reaction.

Complex **3.2** reacts with MeI and CD$_3$I via oxidative addition reactions to give the platinum(IV) complexes. Upon using CD$_3$I a Me/CD$_3$ exchange is observed that occurs probably via a 5-coordinate platinum(IV) intermediate. The attempts at recrystallizing complex **3.11**, [PtMe$_3$I(bps)] resulted in the formation of complex **3.12**, [PtMe$_3$I(pyridine)$_2$] and the polymer (Me$_2$SiO)$_n$ via the reaction with H$_2$O.

The reactions of complex **3.2** with HCl proceed via oxidative addition and reductive elimination processes. The hydridoplatinum(IV) intermediate is identified at low temperature through the ^{1}H-NMR spectra.

The reaction of complex **3.2** with MeOTf proceeds in acetone to produce **3.16**, [PtMe$_3$(OH$_2$)(bps)]$^+$[CF$_3$SO$_3$]$^-$ via oxidative addition. The two methylsilicon groups undergo fast exchange at room temperature, and also the three methyl-platinum groups, and such fast exchange probably occurs via a 5-coordinate platinum(IV) intermediate. The exchange can be stopped at lower temperatures. The use of a solvent that can coordinate very well to platinum(IV) complexes such as acetonitrile resulted in the formation of complex **3.17**, [PtMe$_3$(NCCD$_3$)(bps)]$^+$ [CF$_3$SO$_3$]$^-$ which shows no fast methyl exchange at elevated temperatures.

3.4 Experimental

All reactions were carried out under nitrogen, either using Schlenk techniques or in a dry box, unless otherwise specified. NMR spectra were recorded on Inova 400 MHz, Inova 600 MHz, and Mercury 400 MHz spectrometers. Chemical shifts are reported relative to TMS. Elemental analyses were performed by Guelph Chemical Laboratories. Mass spectrometry studies were carried out using an electrospray PE-Sciex Mass Spectrometer (ESI MS), and a high resolution Finnigan MAT 8200 instrument. The complexes *cis/trans*-[$PtCl_2(SMe_2)_2$] and [$Pt_2Me_4(\mu\text{-}SMe_2)_2$] were prepared from $K_2[PtCl_4]$ according to the literature.[19] DFT calculations were performed by Dr. Richard Puddephatt using the Amsterdam Density Functional program based on the Becke-Perdew functional, with first-order scalar relativistic corrections.
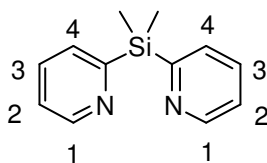
[bis(2-pyridyl)dimethylsilane], (bps), 3.1. A modified procedure of *Wright et al.*[4] was followed. Using a two-necked round bottom flask equipped with N_2 gas in a dry ice-acetone bath, a 1.6 M solution of butyllithium in hexane (31.25 mL, 0.05 mol) and anhydrous ethyl ether (40 mL) were added. Then at -78 °C 2-bromo-pyridine (4.76 mL, 0.05 mol) was added dropwise, under stirring, giving an orange solution. The mixture was stirred for 4 hours at -78 °C. Then dichlorodimethylsilane (3.02 mL, 0.025 mol) was added in one portion. The mixture was

warmed to room temperature, and then washed with NH_4Cl (10 mL) and H_2O (10 mL). The organic layer was extracted using ether (3x50 mL), and then dried (Na_2SO_4). The removal of the solvent under reduced pressure gave an oily product, which was distilled under high vacuum to afford pure compound. Yield 72%. ^{1}H NMR in $CDCl_3$: $\delta = 0.60$ (s, 6H, $2CH_3$), 7.12 (t, 2H, $^3J_{H-H}$ = 5 Hz, Py{H^2}), 7.48 (t, 2H, $^3J_{H-H}$ = 2 Hz, Py{H^3}), 7.49 (d, 2H, $^3J_{H-H}$ = 2 Hz, Py{H^4}), 8.72 (td, 2H, $^3J_{H-H}$ = 2 Hz, $^3J_{H-H}$ = 5 Hz, Py{H^1}).

[PtMe$_2$(bps)], 3.2. [Pt$_2$Me$_4$(μ-SMe$_2$)$_2$] (1.0 g, 1.74 mmol) was added to a stirring solution of [bis(2-pyridyl)dimethylsilane], (0.75 g, 3.48 mmol) in ether (10 mL). Within 20 minutes of stirring, the complex precipitated out of solution as a brown solid. The product was first separated from the solution by decanting most of the solvent. It was then washed with ether (3x2 mL) and pentane (3x2 mL), and then dried under high vacuum. Yield 88%. ^{1}H NMR in $CDCl_3$: δ = 0.71 (s, 6H, $^2J_{Pt-H}$ = 80 Hz, Pt-CH$_3$), 0.77 (s, 3H, Si-CH$_3$), 1.11 (s, 3H, Si-CH$_3$), 7.21 (t, 2H, $^3J_{H-H}$ = 5 Hz, Py{H^2}), 7.55 (d, 2H, $^3J_{H-H}$ = 7 Hz, Py{H^4}), 7.67 (t, 2H, $^3J_{H-H}$ = 7 Hz, Py{H^3}), 8.97 (dd, 2H, $^3J_{H-H}$ = 5 Hz, $^3J_{Pt-H}$ = 25 Hz, Py{H^1}). ^{13}C NMR ($CDCl_3$): δ = - 20.0 (s, Pt-C), - 3.91 (s, Si-C$_{syn}$), - 1.74 (s, Si-C$_{anti}$), 125.4, 130.4, 133.7, 152.4, 163.1 (pyridyl C). Anal. Calcd. for $C_{14}H_{20}N_2PtSi$ (%): C 38.26, H 4.59, N 6.37. Found: C 38.53, H 4.85, N 6.33.

{[Me(bps)Pt-OSiMe(2-C$_5$H$_4$N)$_2$PtMe$_3$]$^+$[CF$_3$CH$_2$OB(C$_6$F$_5$)]$^-$}, 3.3. To a solution of [PtMe$_2$(bps)], **3.2**, (0.09 g, 0.45 mmol) in CF_3CH_2OH (5 mL) was added a solution of $B(C_6F_5)_3$ (0.11 g, 0.45 mmol) in CF_3CH_2OH (5 mL). The mixture was stirred for 2 days. Then the volume of the solution was reduced to 2 mL. The mixture was placed in the fridge and 2 days later the product crystallized out. The solution was decanted, and the crystals were dried under high vacuum. Yield 37 %. ^{1}H NMR in acetone-d$_6$: δ = 0.15 (s, 3H, $^2J_{Pt-H}$ = 69 Hz, Pt-CH$_3$), 0.64 (s, 3H, $^2J_{Pt-H}$ = 75 Hz, Pt-CH$_3$), 0.95 (s, 3H, Si-CH$_3$), 64 (s, 3H, $^2J_{Pt-H}$ = 75 Hz, Pt-CH$_3$), 1.17 (s, 3H,

$^2J_{Pt-H}$ = 68 Hz, Pt-CH$_3$), 1.22 (s, 3H, Si-CH$_3$), 1.23 (s, 3H, $^2J_{Pt-H}$ = 78 Hz, Pt-CH$_3$), 1.63 (s, 3H, Si-CH$_3$), 3.57 (q, 2H, CH$_2$), 7.01 8.15 (12H, Py), 8.49 (dd, 1H, $^3J_{H-H}$ = 5 Hz, $^3J_{Pt-H}$ = 20 Hz, Py{H^1}), 8.60 (dd, 1H, $^3J_{H-H}$ = 5 Hz, $^3J_{Pt-H}$ = 20 Hz, Py{H^1}), 8.72 (dd, 1H, $^3J_{H-H}$ = 5 Hz, $^3J_{Pt-H}$ = 21 Hz, Py{H^1}), 8.96 (dd, 1H, $^3J_{H-H}$ = 6 Hz, $^3J_{Pt-H}$ = 65 Hz, Py{H^1}). ^{19}F (Acetone-d$_6$) δ = -75 (br, 3F, CF$_3$), -133 (br m, 6F, Ar-F$_{ortho}$), = -164 (t, 3F, Ar-F$_{para}$), -168 (br, 6F, Ar-F$_{meta}$); Anal. Cald. for C$_{47}$H$_{39}$BF$_{18}$N$_4$O$_2$Pt$_2$Si$_2$ (%): C 37.82, H 2.63, N 3.75. Found: C 36.77, H 2.32, N 3.62.

[PtMe$_3$(O){(NC$_5$H$_4$)-(μ-SiMe)-(C$_5$H$_4$N)}], 3.4b. The reaction of CD$_3$OD with complex **3.2** was performed in an NMR tube. Complex **3.2**, [PtMe$_2$(bps)], (0.001 g, 0.002 mmol) was dissolved in CD$_3$OD (1 mL), and then excess hydrogen peroxide (0.01 mL) was added to the solution. The mixture transferred to an NMR tube, which was then placed in the NMR probe (Inova 400 MHz). ^{1}H-NMR CD$_3$OD δ = 0.94 (s, 3H, Si-Me), 0.98 (s, 6H, $^2J_{Pt-H}$ = 69 Hz, Pt-Me), 1.15 (s, 3H, $^2J_{Pt-H}$ = 75 Hz, Pt-Me), 7.43 (t, 2H, $^3J_{H-H}$ = 5 Hz, Py{H^2}), 7.80 (d, 2H, $^3J_{H-H}$ = 7 Hz, Py{H^4}), 7.86 (t, 2H, $^3J_{H-H}$ = 7 Hz, Py{H^3}), 8.97 (dd, 2H, $^3J_{H-H}$ = 5 Hz, $^3J_{Pt-H}$ = 20 Hz, Py{H^1}).

[Pt$_2$(CD$_3$)$_4$(μ-SMe$_2$)$_2$], 3.5. The procedure was followed according to the literature.[19] Using a three-necked round bottom flask equipped with N$_2$ gas in ice bath, a 0.5 M solution of methyl-d$_3$-lithium, as complex with lithium iodide solution in ether (12 mL, 0.006 mol) was used instead. The product was isolated as a white product, which should be stored under N$_2$ and in the fridge. ^{1}H-NMR in CDCl$_3$ δ = 2.76 (s, 12H, $^3J_{Pt-H}$= 20 Hz, Pt-SMe).

[Pt(CD$_3$)$_2$(bps)], 3.6. This was prepared in a similar way to complex **3.2**. Yield 85%. ^{1}H NMR in CDCl$_3$: δ = 0.79 (s, 3H, Si-CH$_3$), 1.12 (s, 3H, Si-CH$_3$), 7.24 (t, 2H, $^3J_{H-H}$ = 5 Hz, Py{H^2}), 7.58 (d, 2H, $^3J_{H-H}$ = 7 Hz, Py{H^4}), 7.70 (t, 2H, $^3J_{H-H}$ = 7 Hz, Py{H^3}), 8.99 (dd, 2H, $^3J_{H-H}$ = 5 Hz, $^3J_{Pt-H}$ = 25 Hz, Py{H^1}).

[PtMe(CD₃)₂(O){(NC₅H₄)-(μ-SiMe)-(C₅H₄N)}], 3.7b. This was prepared in a similar way to complexes **3.4a-b**. The reaction was monitored for several days. ^{1}H-NMR CD₃OD δ = 0.94 (s, 3H, Si-Me), 1.15 (s, 3H, $^2J_{Pt-H}$ = 75 Hz, Pt-Me) , 7.43 (t, 2H, $^3J_{H-H}$ = 5 Hz, Py{H^2}), 7.80 (d, 2H, $^3J_{H-H}$ = 7 Hz, Py{H^4}), 7.86 (t, 2H, $^3J_{H-H}$ = 7 Hz, Py{H^3}), 8.97 (dd, 2H, $^3J_{H-H}$ = 5 Hz, $^3J_{Pt-H}$ = 20 Hz Py{H^1}).

{[PtMe₃(OH){(NC₅H₄)-(μ-SiMe)-(C₅H₄N)}]⁺[PhCOO]⁻}, 3.8. To a solution of complex **3.2** (0.05 g, 0.113 mmol) in acetone (10 mL) was added dibenzoyl peroxide (0.03 g, 0.113 mmol). The mixture was stirred for 2 hours. The color of the solution changed from yellow to off white color. The volume was reduced to 1 mL, and pentane (5 mL) was added to precipitate the product as a white solid. The solution was decanted, and the product was then washed with ether (3x2mL) and pentane (3x2mL). Finally the white solid was dried under high vacuum. ^{1}H-NMR CD₂Cl₂ δ = 1.04 (s, 3H, Si-Me), 1.05 (s, 6H, $^2J_{Pt-H}$ = 70 Hz, Pt-Me), 1.14 (s, 3H, $^2J_{Pt-H}$ = 75 Hz, Pt-Me), 2.12 (s, 1H, O-H), 7.37-7.95 (11H, Aromatic), 8.58 (dd, 2H, $^3J_{H-H}$ = 5 Hz, $^3J_{Pt-H}$ = 20 Hz, Py{H^1}). Anal. Calcd. for C₂₁H₂₆N₂O₃PtSi (%): C 43.67, H 4.54, N 4.85. Found: C 43.95, H 4.42, N 5.06.

{[PtMe(CD₃)₂(O){(NC₅H₄)-(μ-SiMe)-(C₅H₄N)}]⁺[PhCOO]⁻}, 3.9. This was prepared similarly to complex **3.8** from complex **3.6**, and isolated as a white solid. ^{1}H-NMR in CD₂Cl₂ δ = 1.04 (s, (9a), $^2J_{Pt-H}$ = 70 Hz, Pt-Me$_{equatorial}$), 1.05 (s, 3H, Si-Me), 1.14 (s, (9b), $^2J_{Pt-H}$ = 75 Hz, Pt-Me$_{axial}$), 2.12 (s, 1H, O-H), 7.37-7.95 (11H, Aromatic), 8.58 (dd, 2H, $^3J_{H-H}$ = 5 Hz, $^3J_{Pt-H}$ = 20 Hz, Py{H^1}).

[PtMe₂I₂(bps)], 3.10. To a stirred solution of [PtMe₂(bps)] (0.2 g, 0.455 mmol) in CH₂Cl₂ (5 mL) was added excess iodine (0.012 g). The solution color turned from yellow to red. The reaction was kept stirring for 2 hours. The solvent was then pumped off using a high vacuum. A

red precipitate remained in the bottom of the flask, which was washed with pentane (3x3 mL) and ether (3x3 mL) and then dried under high vacuum. Yield 84%. ^{1}H NMR in CD_2Cl_2: δ = 0.81 (s, 6H, Si-Me), 2.39 (s, 6H, $^2J_{Pt-H}$ = 71 Hz, Pt-Me), 7.42 (t, 2H, $^3J_{H-H}$ = 5 Hz, Py{H^2}), 7.78 (d, 2H, $^3J_{H-H}$ = 7 Hz, Py{H^4}), 7.86 (t, 2H, $^3J_{H-H}$ = 7 Hz, Py{H^3}), 9.36 (dd, 2H, $^3J_{H-H}$ = 5 Hz, $^3J_{Pt-H}$ = 22 Hz, Py{H^1}). Anal. Calcd. for $C_{14}H_{20}I_2N_2PtSi$ (%): C 24.25, H 2.91, N 4.04. Found: C 23.88, H 2.77, N 4.32.

[PtMe$_3$I(bps)], 3.11. To a solution of [PtMe$_2$(bps)], **3.2** (0.1 g, 0.277 mmol) in ether (10 mL) was added MeI (0.032 g, 0.277 mmol). There was an intermediate color change from yellow to white. The reaction mixture was stirred for 30 mintues. The product precipitated out, and was collected using a buchner funnel. The collected product was washed with pentane (3x5 mL). Yield 82%. ^{1}H NMR in CD_2Cl_2: δ = 0.65 (s, 3H, Si-Me), 0.81 (s, 3H, Si-Me), 0.94 (s, 3H, $^2J_{Pt-H}$ = 72 Hz, Pt-Me), 1.32 (s, 6H, $^2J_{Pt-H}$ = 68 Hz, Pt-Me), 7.35 (t, 2H, $^3J_{H-H}$ = 4 Hz, Py{H^2}), 7.79 (d, 2H, $^3J_{H-H}$ = 7 Hz, Py{H^4}), 7.81 (t, 2H, $^3J_{H-H}$ = 7 Hz, Py{H^3}), 9.63 (dd, 2H, $^3J_{H-H}$ = 4 Hz, $^3J_{Pt-H}$ = 20 Hz, Py{H^1}). Anal. Calcd. for $C_{15}H_{23}IN_2PtSi$ (%): C 30.99, H 3.99, N 4.82. Found: C 31.24, H 3.72, N 4.57.

[PtMe$_3$I(pyridine)$_2$], 3.12. This complex was produced in solution via the decomposition of complex **3.11** during recrystallization. The solution contained a mixture of both complexes **3.11** and **3.12**. ^{1}H NMR of **3.12** in CD_2Cl_2: δ = 1.20 (s, 3H, $^2J_{Pt-H}$ = 69 Hz, Pt-Me), 1.44 (s, 6H, $^2J_{Pt-H}$ = 70 Hz, Pt-Me), 7.44 (m, 4H, Ar-H$_{meta}$), 7.88 (t, 2H, $^3J_{H-H}$ = 7 Hz, Ar-H$_{para}$), 9.63 (dd, 2H, $^3J_{H-H}$ = 6 Hz, $^3J_{Pt-H}$ = 19 Hz, Ar-H$_{ortho}$).

[Pt(CD$_3$)Me$_2$I(bps)], 3.13. The reaction of CD$_3$I with complex 3.2. Complex **3.2**, [PtMe$_2$(bps)], (0.01 g, 0.022 mmol) was dissolved in acetone-d$_6$ (1 mL). Then the solution was placed in an NMR tube. The NMR tube was then placed in the NMR machine (Inova 400 MHz),

and the temperature of the probe was brought down to -50 °C. Then an excess chilled solution of CD$_3$I (0.06 mL) was added to the NMR, and the reaction was monitored via ^{1}H-NMR spectroscopy. The oxidative addition reaction proceeded very quickly to produce the *trans* product **3.13a**, then upon warming the NMR probe a new methyl platinum resonance started appearing due to the presence of the *cis* product **3.13b**. ^{1}H NMR in Acetone-d$_6$: δ = 0.73 (s, 3H, Si-Me), 0.87 (s, 3H, Si-Me), 1.29 (s, 6H, $^2J_{Pt-H}$ = 69 Hz, Pt-Me), 7.52 (t, 2H, $^3J_{H-H}$ = 6 Hz, Py{H^4}), 7.99 (t, 2H, $^3J_{H-H}$ = 7 Hz, Py{H^3}), 8.07 (d, 2H, $^3J_{H-H}$ = 7 Hz, Py{H^4}), 9.62 (dd, 2H, $^3J_{H-H}$ = 6 Hz, $^3J_{Pt-H}$ = 19 Hz, Py{H^1}), *cis* (**3.13b**) at δ = 0.91 (s, 3H, $^2J_{Pt-H}$ = 71 Hz, Pt-Me).

[Pt(H)ClMe$_2$(bps)] (3.14) and [PtCl$_2$(bps)] (3.15). Complex **3.2**, [PtMe$_2$(bps)], (0.01 g, 0.022 mmol) was dissolved in CD$_2$Cl$_2$ and placed in an NMR tube. The NMR tube containing complex **3.2** was placed in the NMR machine (400 MHz), and the temperature of the probe was brought down to -80 °C. Then the chilled solution of HCl was added to the NMR tube, and the reaction was monitored by ^{1}H-NMR spectroscopy. Complex **3.14** was observed at low temperatures, but as reductive elimination of methane progressed, the peaks for [PtCl$_2$(bps)] (**3.15**) started appearing upon warming up the NMR probe. ^{1}H NMR: (**3.14**) δ = -20.64 (s, 1H, $^1J_{Pt-H}$ = 1593 Hz, Pt-H), 0.71 (s, 3H, Si-Me), 0.81 (s, 3H, Si-Me), 1.11 (s, 6H, $^2J_{Pt-H}$ = 65 Hz, Pt-Me), 7.46 (t, 2H, $^3J_{H-H}$ = 5 Hz, Py{H^2}), 7.69 (d, 2H, $^3J_{H-H}$ = 8 Hz, Py{H^4}), 7.96 (t, 2H, $^3J_{H-H}$ = 8 Hz, Py{H^3}), 9.31 (dd, 2H, $^3J_{H-H}$ = 5 Hz, $^3J_{Pt-H}$ = 18 Hz, Py{H^1}); (**3.15**) δ = 0.90 (s, 3H, Si-Me), 1.45 (s, 3H, Si-Me), 7.39 (t, 2H, $^3J_{H-H}$ = 4 Hz, Py{H^2}), 7.61 (d, 2H, $^3J_{H-H}$ = 7 Hz, Py{H^4}), 7.80 (t, 2H, $^3J_{H-H}$ = 7 Hz, Py{H^3}), 9.15 (dd, 2H, $^3J_{H-H}$ = 4 Hz, $^3J_{Pt-H}$ = 42 Hz, Py{H^1}).

{[PtMe$_3$(OH$_2$)(bps)]$^+$[CF$_3$SO$_3$]$^-$}, 3.16. To a solution of complex **3.2** (0.01 g, 0.022 mmol) in acetone-d$_6$ (1 mL) was added methyl triflate (2.57 µL). The NMR tube containing the mixture was placed in the NMR machine (400 MHz), and the temperature of the probe was brought down

to -50 $^{\circ}$C. ^{1}H NMR: δ = 0.85 (s, 6H, Si-Me), 1.21 (s, 6H, $^2J_{Pt-H}$ = 71 Hz, Pt-Me), 7.73 (t, 2H, $^3J_{H-H}$ = 6 Hz, Py{H^2}), 8.12 (t, 2H, $^3J_{H-H}$ = 8 Hz, Py{H^3}), 8.23 (d, 2H, $^3J_{H-H}$ = 8 Hz, Py{H^4}), 9.05 (dd, 2H, $^3J_{H-H}$ = 6 Hz, $^3J_{Pt-H}$ = 18 Hz, Py{H^1}).

[PtMe$_3$(CD$_3$CN)(bps)]$^+$[CF$_3$SO$_3$]$^-$, 3.17. This was prepared in a similar way to complex **3.16**, but acetonitrile-d$_3$ (1 mL) was used instead of acetone-d$_6$. The temperature of the NMR probe was brought down to -30 $^{\circ}$C. ^{1}H NMR: δ = 0.69 (s, 3H, Si-Me), 0.79 (s, 3H, Si-Me), 0.93 (s, 3H, $^2J_{Pt-H}$ = 76 Hz, Pt-Me), 1.04 (s, 4H, $^2J_{Pt-H}$ = 66 Hz, Pt-Me), 7.58 (t, 2H, $^3J_{H-H}$ = 6 Hz, Py{H^2}), 8.00-8.09 (m, 4H, Py{H^3, H^4}), 8.93 (dd, 2H, $^3J_{H-H}$ = 6 Hz, $^3J_{Pt-H}$ = 20 Hz, Py{H^1}).

X-ray Structure Determinations: X-ray data were obtained and solutions were determined by Dr. M. Jennings in this chapter. Suitable crystals were mounted on a glass fiber, and data were collected at low temperature (-123 °C) on a Nonius Kappa-CCD area detector diffractometer with COLLECT (Nonius B.V., 1997-2002). The unit cell parameters were calculated and refined from the full data set. The crystal data and refinement parameters for all complexes are listed in the following tables.

Table 3.7. Crystallographic data for **3.2**.

_____

[PtMe$_2$(bps)]

_____

Empirical formula	C$_{14}$ H$_{20}$ N$_2$ Pt Si
Formula weight	439.50
Wavelength	0.71073 Å
Crystal system	Monoclinic
Space group	C 2/c
Unit cell dimensions	a = 15.298(7) Å α = 90°
	b = 12.860(6) Å β = 102.19(3)°
	c = 15.837(8) Å γ = 90°
Volume	3045.1(3) Å^3
Z	8
Density (calculated)	1.917 Mg/m^3
Absorption coefficient	9.280 mm^{-1}
Crystal size	0.28 x 0.22 x 0.10 mm^3
Refinement method	Full-matrix least-squares on F^2
Goodness-of-fit on F^2	1.003
Final R indices [I>2sigma(I)]	R1 = 0.0469, wR2 = 0.1124
R indices (all data)	R1 = 0.0657, wR2 = 0.1230

Table 3.8. Crystallographic data for **3.3**.

_____

$\{[Me(bps)Pt\text{-}OSiMe(2\text{-}C_5H_4)_2PtMe_3]^+[CF_3CH_2OB(C_6F_5)]^-\}$

_____

Empirical formula	C47 H39 B F18 N4 O2 Pt2 Si2
Formula weight	1490.99
Wavelength	0.71073 Å
Crystal system	Triclinic
Space group	P -1
Unit cell dimensions	a = 11.812(2) Å $\quad$ α= 79.94(3)°
	b = 13.535(3) Å $\quad$ β= 80.78(3)°
	c = 16.700(3) Å $\quad$ γ = 79.76(3)°
Volume	2564.0(9) Å^3
Z	2
Density (calculated)	1.931 Mg/m^3
Absorption coefficient	5.605 mm^{-1}
Crystal size	0.30 x 0.09 x 0.06 mm^3
Refinement method	Full-matrix least-squares on F^2
Goodness-of-fit on F^2	1.050
Final R indices [I>2sigma(I)]	R1 = 0.0437, wR2 = 0.0972
R indices (all data)	R1 = 0.0673, wR2 = 0.1062

Table 3.9. Crystallographic data for **3.8**.

_____

$\{[PtMe_3(O)\{(NC_5H_4)-(\mu-SiMe)-(C_5H_4N)\}]^+[PhCOO]^-\}$

_____

Empirical formula	C21 H26 N2 O3 Pt Si
Formula weight	577.62
Wavelength	0.71073 A
Crystal system	Monoclinic
Space group	P 2_1/n
Unit cell dimensions	a = 14.305(3) Å $\alpha = 90°$
	b = 10.130(2) Å $\beta = 99.04(3)°$
	c = 14.985(3) Å $\gamma = 90°$
Volume	2144.6(7) Å^3
Z	4
Density (calculated)	1.789 Mg/m^3
Absorption coefficient	6.622 mm^{-1}
Crystal size	0.32 x 0.25 x 0.22 mm
Refinement method	Full-matrix least-squares on F^2
Goodness-of-fit on F^2	1.071
Final R indices [I>2sigma(I)]	R1 = 0.0298, wR2 = 0.0732
R indices (all data)	R1 = 0.0366, wR2 = 0.0824

Table 3.10. Crystallographic data for **3.10**.

[PtMe$_2$I$_2$(bps)]

Empirical formula	C14 H20 I2 N2 Pt Si
Formula weight	693.30
Wavelength	0.71073 Å
Crystal system	Monoclinic
Space group	P 2$_1$/n
Unit cell dimensions	a = 9.369(3) Å$\qquad\qquad$ α = 90°
	b = 13.796(5) Å$\qquad\quad$ β = 100.96(2)°
	c = 14.472(5) Å$\qquad\quad$ γ = 90°
Volume	1836.52(11) Å^3
Z	4
Density (calculated)	2.507 Mg/m^3
Absorption coefficient	11.061 mm^{-1}
Crystal size	0.22 x 0.20 x 0.05 mm^3
Refinement method	Full-matrix least-squares on F^2
Goodness-of-fit on F^2	1.065
Final R indices [I>2sigma(I)]	R1 = 0.0507, wR2 = 0.1369
R indices (all data)	R1 = 0.0594, wR2 = 0.1429

Table 3.11. Crystallographic data for **3.12**.

	[PtMe$_3$I(pyridine)$_2$]	
Empirical formula	C13 H19 I N2 Pt	
Formula weight	525.29	
Wavelength	0.71073 Å	
Crystal system	Triclinic	
Space group	P -1	
Unit cell dimensions	a = 8.184(2) Å	α= 79.72(3)°
	b = 8.309(2) Å	β= 89.37(3)°
	c = 13.131(3) Å	γ = 60.64(3)°
Volume	762.7(3) Å^3	
Z	2	
Density (calculated)	2.287 Mg/m^3	
Absorption coefficient	11.205 mm^{-1}	
Crystal size	0.05 x 0.05 x 0.03 mm^3	
Refinement method	Full-matrix least-squares on F^2	
Goodness-of-fit on F^2	1.089	
Final R indices [I>2sigma(I)]	R1 = 0.0502, wR2 = 0.1047	
R indices (all data)	R1 = 0.0774, wR2 = 0.1164	

Table 3.12. Crystallographic data for **3.15**.

	[PtCl$_2$(bps)]	
Empirical formula	C12 H14 Cl2 N2 Pt Si	
Formula weight	480.33	
Wavelength	0.71073 Å	
Crystal system	Orthorhombic	
Space group	P b c a	
Unit cell dimensions	a = 13.855(3) Å	$\alpha = 90°$
	b = 14.006(3) Å	$\beta = 90°$
	c = 15.074(3) Å	$\gamma = 90°$
Volume	2925.2(10) Å^3	
Z	8	
Density (calculated)	2.181 Mg/m^3	
Absorption coefficient	10.024 mm^{-1}	
Crystal size	0.20 x 0.18 x 0.13 mm^3	
Refinement method	Full-matrix least-squares on F^2	
Goodness-of-fit on F^2	1.079	
Final R indices [I>2sigma(I)]	R1 = 0.0631, wR2 = 0.1583	
R indices (all data)	R1 = 0.0994, wR2 = 0.1823	

Table 3.13. Crystallographic data for **3.16**.

_____

$\{[PtMe_3(OH_2)(bps)]^+[CF_3SO_3]^-\}$

_____

Empirical formula	$C_{16}H_{25}F_3N_2O_4PtSSi$
Formula weight	621.62
Wavelength	0.71073 Å
Crystal system	triclinic
Space group	P -1
Unit cell dimensions	a = 9.458(3) Å $\quad$ α= 80.14(2)°
	b = 11.201 (4) Å $\quad$ β= 70.69(2)°
	c = 11.294(4) Å $\quad$ γ= 82.77(2)°
Volume	1109.35(7) Å^3
Z	2
Density (calculated)	1.861 Mg/cm^3
Absorption coefficient	6.520 mm^{-1}
Crystal size	0.03 x 0.04 x 0.08 mm
Refinement method	Full-matrix least-squares on F^2
Data / restraints / parameters	7061 / 0 / 266
Goodness-of-fit on F^2	1.042
Final R indices [I>2sigma(I)]	R1 = 0.0195, wR2 = 0.0344
R indices (all data)	R1 = 0.0271, wR2 = 0.0360

3.5 References

1. Rendina, L. M.; Puddephatt, R. J. *Chem. Rev.*, **1997**, 97, 1735.

2. Nabavizadeh, S. M; Hoseini, S. J.; Momeni, B. Z.; Shahabadi, N.; Rashidi, M.; Pakiari, A. H.; Eskandari, K. *Dalton Trans.*, **2008**, 2414.

3. Crabtree, R. H. *Organometallic Chemistry of the Transition Metals*, 3rd ed., John Wiley & Sons, New York, **2001**.

4. Wright, M. E. *Tet. Lett.*, **1987**. Vol. 28, pp 3233.

5. Zhang, F.; Broczkowski, M. E.; Jennings, M. C.; Puddephatt, R. J. *Can. J. Chem.*, **2005**, 83, 595.

6. Lowe-Ma, C. K.; Wright, M. E. *Organometallics.*, **1990**, 9, 347.

7. Wright, M. E.; Jin, M. J. *Organometallics*. **1990**, 387, 373.

8. Budyka, M. F.; Zyubina, T. S.; Zarkadis, A. K. *J. Mol. Struct.*, **2004**, 668, 1.

9. Akhrem, I. S.; Vartanyan, R. S.; Topuzyan, V. O.; Vol'pin, M. E. *Izv. Akad. Nauk SSSR, Ser. Khim.*, **1975**, 1387.

10. Akhrem, I. S.; Chistovalova, N. M.; Vol'pin, M. E. *Izv. Akad. Nauk SSSR, Ser. Khim.*, **1972**, 2130.

11. Pawlenko, S. *Organosilicon Chemistry*; Walter de Gruyter: Berlin, **1986**, 12.

12. a) Yamashita, H.; Tanaka, M.; Honda, K. *J. Am. Chem. Soc.*, **1995**, 117, 8873. **b)** Hofmann, P.; Heiss, H.; Neiteler, P.; Muller, G.; Lachmann, J. *Angew. Chem. Int. Ed. Engl.*, **1990**, 29, 880.

13. Tokitoh, N.; Kawai, M.; Takeda, N.; Sasamori, T. *Heterocycles*, **2009**, 79, 311.

14. a) Hiyama, T. *J. Organomet. Chem.*, **2002**, 653, 58; **b)** Denmark, S. E. *J. Org. Chem.*, **2009**, 74, 2915.

15. a) Boisvert, L.; Denney, M. C.; Hanson, S. K.; Goldberg, K. I. *J. Am. Chem. Soc.*; **2009**, 131, 15802; **b)** Ahlquist, M.; Nielsen, R. J.; Periana, R. A.; Goddard III, W. A. *J. Am. Chem. Soc.*; **2009**, 131, 17110.

16. Vedernikov, A. *Chem. Commun.*, **2009**, 4781.

17. a) Mitton, S. J.; McDonald, R.; Turculet, L. *Angew. Chem. Int. Ed.*, **2009**, 48, 8568; **b)** Takaya, J.; Iwasawa, N. *Organometallics*, **2009**, 28, 6636.

18. Zhang, F.; Kirby, C. W.; Hairsine, D. W.; Jennings, M. C.; Puddephatt, R. J. *J. Am. Chem. Soc.*, **2005**, 127, 14196.

19. Hill, G.; Irwin, M. J.; Levy, C. J.; Rendina, L. M.; Puddephatt, R. J. *Inorg. Synth.*, **1998**, 32 149.

20. Crowder, K. N.; Garcia, S. J.; Burr, R. L.; North, J. M.; Wilson, M. H.; Conley, B. L.; Fanwick, P. E.; White, P. S.; Sienerth, K. D.; Granger II, R. M. *Inorg. Chem.*, **2004**, 43, 72.

21. (a) Shilov, A. E.; Shul'pin, G. B. *Chem. Rev.*, **1997**, 97, 2879. (b) He, Z.; Wong, W.; Yu, X.; Kwok, H.; Lin, Z. *Inorg. Chem.*, **2006**, 45, 10922. (c) Song, D.; Sliwowski, K.; Pang, J.; Wang, S. *Organometallics*, **2002**, 21, 4978.

22. (a) Aye. K. T.; Vittal, J. J.; Puddephatt, R. J. *J. Chem. Soc., Dalton Trans.*, **1993**, 1835. (b) Thorshaug, K.; Fjeldahl, I.; Romming, C.; Tilset, M. *Dalton Trans.*, **2003**, 4051. (c) Prokopchuk, E. M.; Puddephatt, R. J. *Can. J. Chem.*, **2003**, 81, 476.

23. Maddock, S. M.; Rickard, C. E. F.; Roper, W. R.; Wright, L. J. *Organometallics*, **1996**, 15, 1793.

24. Bassindale, A. R.; Parker, D. J.; Taylor, P. G.; Auner, N.; Herrchaft, B. *J. Organomet. Chem.*, **2003**, 667, 66.

25. a) Ong, C. M.; Burchell, T. J.; Puddephatt, R. J. *Organometallics*, **2004**, 23, 1493. **b)** Messaoudi, A.; Deglmann, P.; Braunstein, P.; Hofmann, P. *Inorg. Chem.*, **2007**, 46, 7899.

26. Labinger, J. A.; Bercaw, J. E. *Nature*, **2002**, 507.

27. Puddephatt, R. J. *Coord. Chem. Rev*. **2001**, 219, 221.

CHAPTER 4

The Chemistry of Dimethylplatinum(II) Complexes

Containing Imidazole Nitrogen Donor Ligands

4.1 Introduction

Oxidative addition to a square planar d^8 late transition metal center is considered to be one of the most fundamental processes in transition metal chemistry,[1] and it is a key step in a variety of catalytic reactions.[2] Organoplatinum(II) complexes containing nitrogen-donor ligands are known to be particularly reactive in oxidative addition reactions, so a different class of bidentate ligands containing imidazole rings was picked for this project.[3] Imidazole and its derivatives have been widely used in chemistry and biology.[4] Several platinum(II) complexes with mono-dentate imidazole (Him) derivatives have been reported.[5] These include *cis/trans*-[Pt(Him)$_2$X$_2$] and [Pt(1Me-im)$_2$X$_2$], where X = halide and 1Me-im = 1-methylimidazole; *cis*-[Pt(1Me-im)$_2$(C$_2$O$_4$)], and the tetrakis complex [Pt(Him)$_4$]$^{2+}$.[5a] The use of imidazole ligands in platinum(II) and palladium(II) chemistry gained a lot of attention when it was found by Reedijk *et al.* that the complex *cis*-[Pt(Him)$_2$Cl$_2$] shows cytostatic activity in mice bearing tumor.[5a,6]

Organoplatinum(II) chemistry gained significant attention when Periana *et. al.* reported the usage of platinum catalysts for low temperature, oxidative conversion of methane to methanol through a C-H bond activation using the complex [PtCl$_2$(bpym)], bpym = 2,2'-bipyrimidyl, as a catalyst.[7] The platinum(II) catalysts were found to be stable, active, and selective for the oxidation addition of the C-H bond in methane. Also, the mechanistic studies showed that platinum(II) is the most active oxidation state of platinum for reaction with methane.

These five-membered heterocyclic imidazole ligands (Chart 4.1) were chosen to vary the donor ability of the rings (imidazole > pyridyl).[8] The chosen imidazole ligands have potential in coordination chemistry as relatives of the planar 2,2'-bipyridyl, except that they form N-M-N angles closer to 90°, where the complex [Cu(SO$_4$)(H$_2$O)$_2${(mim)$_2$C=O}] has been shown to have N-Cu-N = 90.25 (5)$^{\circ}$.[9] The common occurrence of two histidine binding sites for metal centers at

bioactive sites of proteins has played a major role in the development of a variety of imidazole containing ligands.[10] These ligands have been used in the synthesis of a wide series of organometallic complexes, and they have provided a convenient and widely applicable route in the synthesis of the complexes [PdMeX(L$_2$)], and [PdMe$_2$(L$_2$)].[11]
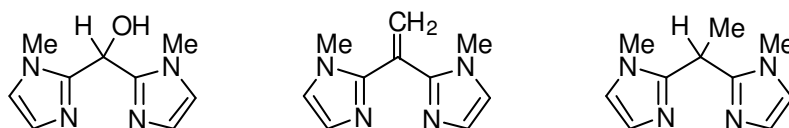
Chart 4.1

In this chapter, a series of dimethylplatinum(II) and dimethylplatinum(IV) complexes containing imidazole nitrogen donor ligands is presented. The reactivity of the dimethylplatinum(II) complexes with alkyl halides is studied, and the stereoselectivity of oxidative addition is determined. Also a series of substituted benzyl bromides has been used to demonstrate the substituent effect on stereoselectivity and reactivity.

4.2 Results and Discussion

4.2.1 The Preparation of [PtMe$_2${(mim)$_2$C=CH$_2$}]

The ligand 1,1-bis(1-methylimidazole-2-yl)ethene, **4.1**, was prepared using a procedure by Byers *et al.*[11] and isolated as on oily product (Scheme 4.1). The ligand is stable to air at room temperature. It is soluble in organic solvents such as chloroform, acetone, and dichloromethane. The platinum(II) complex [PtMe$_2$(bps)], **4.2**, was prepared by the reaction of [Pt$_2$Me$_4$(μ-SMe$_2$)$_2$][12] with compound **4.1**, in ether as shown in Equation 4.1. The dimethylplatinum(II) complex precipitated as a light yellow solid, which is not stable in air at room temperature. In the ^{1}H-NMR spectrum of complex **4.2** in acetone-d$_6$ (Figure 4.1), the methylplatinum proton resonance occurred at δ = 0.53, with coupling constant $^2J_{Pt-H}$ = 86 Hz, while the imidazole protons showed two set of doublets due to symmetry. One doublet was observed at δ = 7.19 with coupling constant $^3J_{Pt-H}$ = 13 Hz, which is lower than the range found for organoplatinum(II) complexes containing dipyridyl ligands.[3] Also the mass spectrum for complex **4.2** showed a peak at m/z = 412 corresponding to the cationic complex, [PtMe$_2${(mim)$_2$C=CH$_2$} - H]$^+$.

Scheme 4.1

(4.1)

145
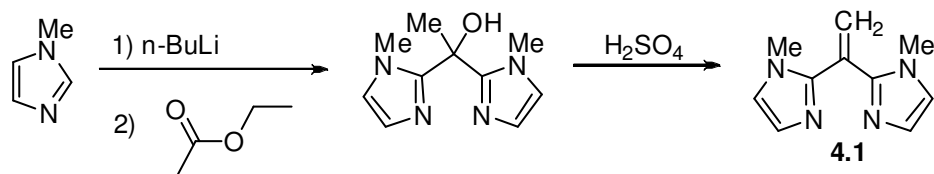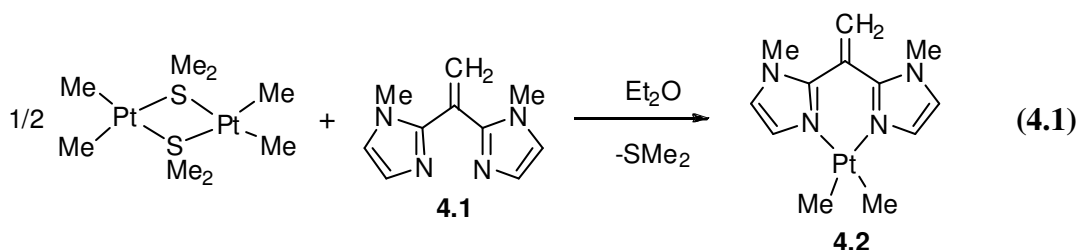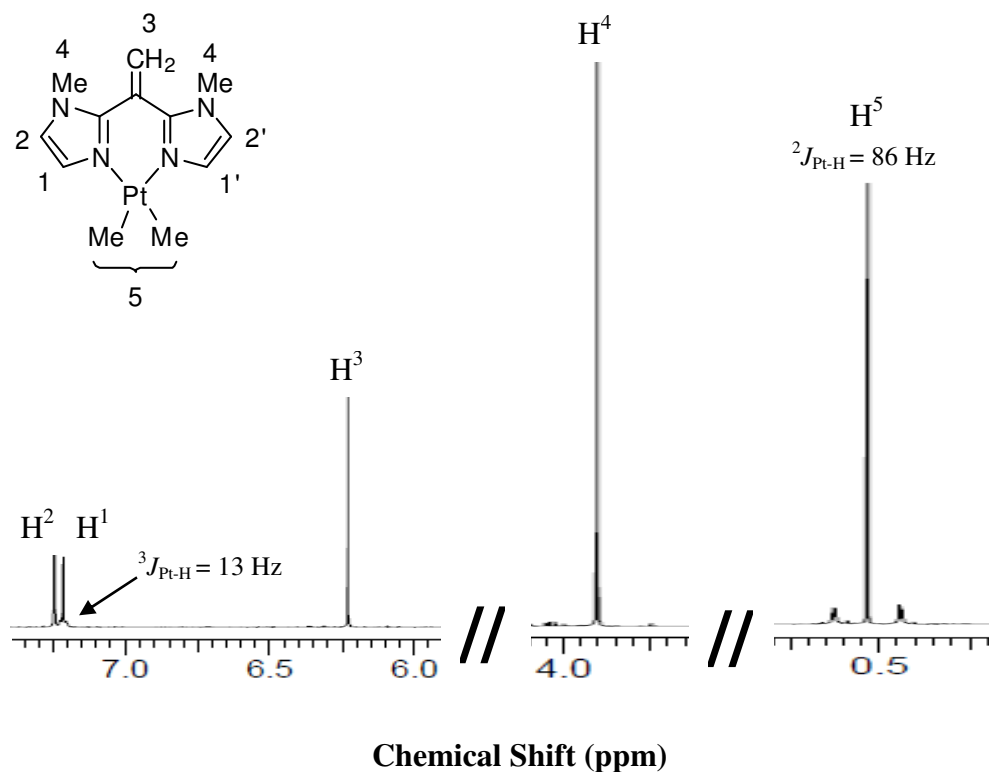
Figure 4.1. The ^{1}H-NMR spectrum (600 MHz, acetone-d$_6$) of complex **4.2**,

[PtMe$_2${(mim)$_2$C=CH$_2$}].

4.2.2 The Reactions of [PtMe$_2${(mim)$_2$C=CH$_2$}] with Alkyl Halides

4.2.2.1 Reactivity Towards Methyl Iodide

Complex **4.2** reacted with methyl iodide in ether according to Equation 4.2 to give the

complex **4.3**, [PtIMe$_3${(mim)$_2$C=CH$_2$}]. The complex was characterized spectroscopically

(Figure 4.2), and its structure was confirmed crystallographically (Figure 4.3). The ^{1}H-NMR

spectrum of complex **4.3** contained two methylplatinum resonances in 1:2 ratio for the methyl

groups *trans* to iodine and nitrogen at δ = 0.89 ($^2J_{Pt-H}$ = 74 Hz) and 1.30 ($^2J_{Pt-H}$ = 71 Hz)

respectively. This is consistent with previous work involving platinum(IV) complexes containing bidentate nitrogen donor ligands, in which it was shown that methylplatinum resonances *trans* to N donor have rather lower value of $^2J_{\text{Pt-H}}$ due to the higher *trans* influence of nitrogen compared to halide.[13] The ^{1}H-NMR spectrum of **4.3** showed two set of doublets in the aromatic region due to symmetry, while one of the doublet occurred at $\delta = 7.41$ with coupling constant $^3J_{\text{Pt-H}} = 9$ Hz, with a lower $^2J_{\text{Pt-H}}$ value as expected for platinum(IV) complexes.[14] One singlet proton resonance was observed at $\delta = 3.83$ due to the two methyl-nitrogen groups.

(4.2)

4.2   4.3
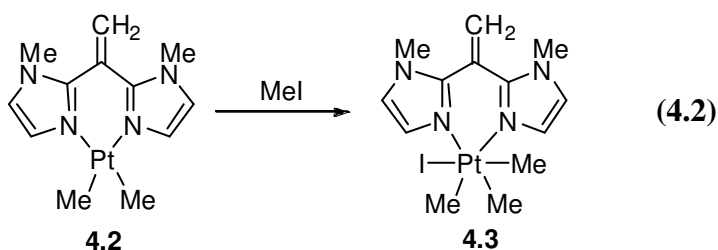
The structure of complex **4.3** is shown in Figure 4.2. The imidazole aromatic rings in complex **4.3** are in the boat conformation as seen in platinum(II) and platinum(IV) complexes containing dipyridyl ligands with a 6-membered chelate ring.[3] The imidazole rings are twisted out of the coordination plane of the platinum atom, which helps in minimizing the steric effects between the *ortho* hydrogen atom of each imidazole and the neighboring methylplatinum group. The platinum-nitrogen distances (Pt(1)-N(1) = 2.155(7) Å) are slightly shorter than Pt-N distances in dimethylplatinum(IV) complexes containing dipyridyl ligands, as observed in the complex [PtIMe$_3$(DPK)] (DPK = di-2-pyridyl ketone) with Pt-N distances = 2.175 Å.[3] Selected bond lengths and angles are shown in table 4.1.
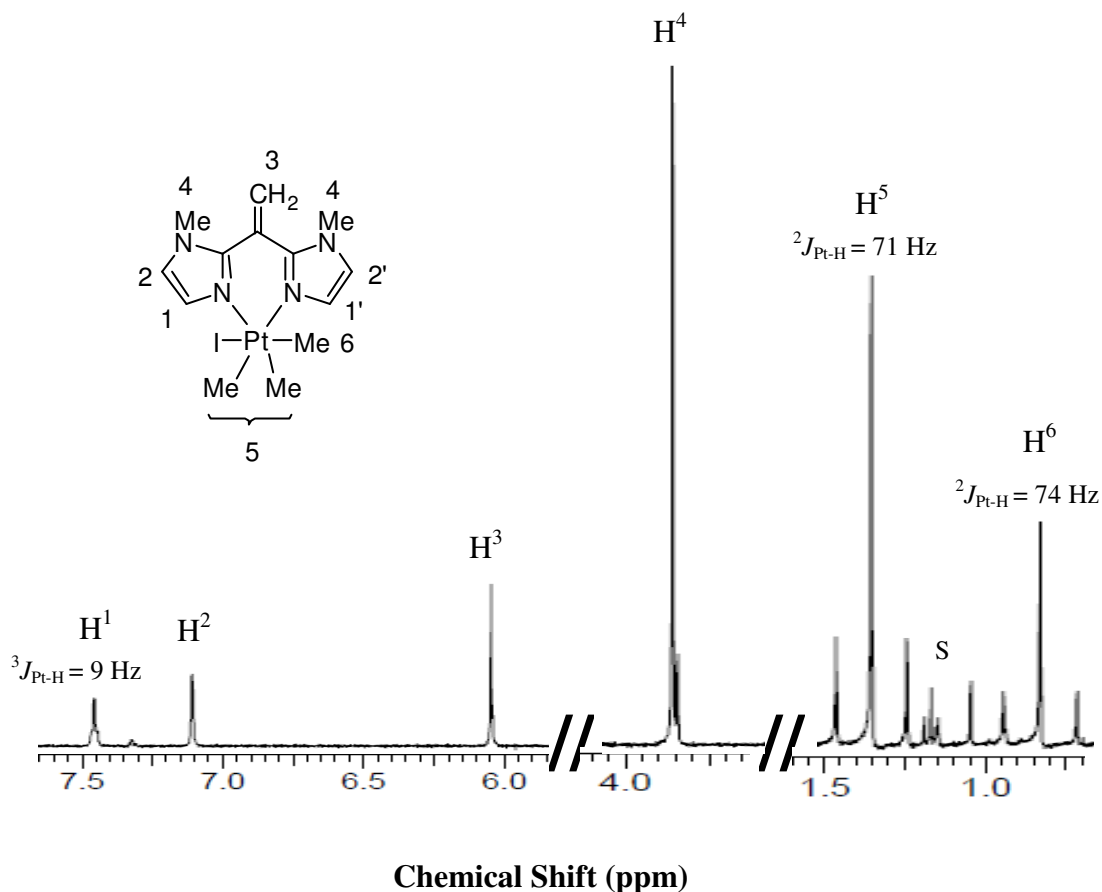
Figure 4.2. The ^{1}H-NMR spectrum (400 MHz, CD$_2$Cl$_2$) of complex **4.3**,

[PtIMe$_3$\{(mim)$_2$C=CH$_2$\}].

Table 4.1. Selected bond lengths [Å] and angles [°] for [PtIMe$_3$\{(mim)$_2$C=CH$_2$\}], **4.3**.

Pt(1)-C(7)	2.062(9)	Pt(1)-C(8)	2.046(1)
Pt(1)-N(1)	2.155(7)	Pt(1)-I(1)	2.804(9)
N(2)-C(3)	1.449(1)	C(5)-C(6)	1.333(2)
C(8)-Pt(1)-C(7)	88.7(4)	C(7)-Pt(1)-C(7)	87.0(6)
C(8)-Pt(1)-N(1)	89.7(3)	C(7)-Pt(1)-N(1)	178.2(3)
C(7)-Pt(1)-N(1)	93.6(3)	N(1)-Pt(1)-N(1)	85.7(4)
C(8)-Pt(1)-I(1)	179.5(4)	C(7)-Pt(1)-I(1)	91.6(3)
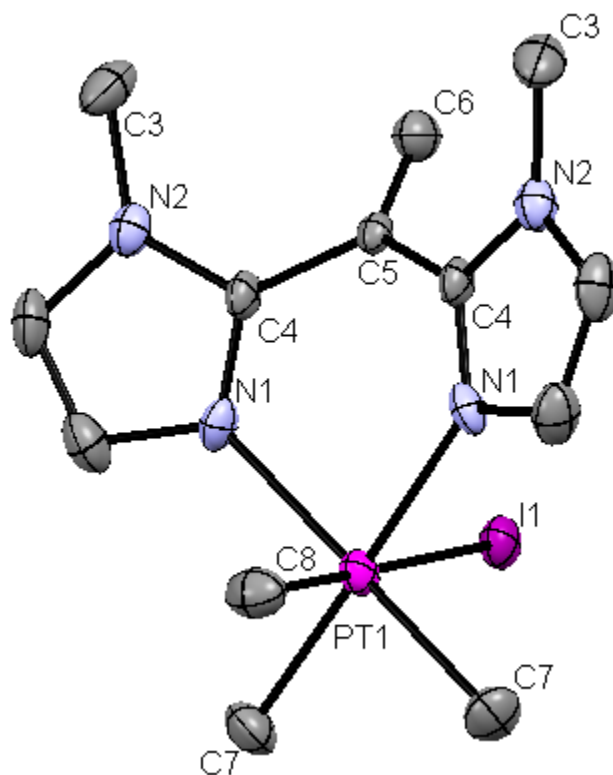
Figure 4.3. A view of the structure of complex **4.3**, [PtIMe$_3${(mim)$_2$C=CH$_2$}].

4.2.2.2 Reactivity and Stereoselectivity Towards Benzyl Halides

The reaction of benzyl bromide with complex **2**, [PtMe$_2${(mim)$_2$C=CH$_2$}], gave the dimethylplatinum(IV) complex [PtBr(CH$_2$-C$_6$H$_5$)Me$_2${(mim)$_2$C=CH$_2$}] (**4.4**), according to Equation 4.3. Complex **4.4** was isolated as a white solid that was soluble in acetone or dichloromethane. The reaction proceeded via the oxidative addition of the Br-CH$_2$ bond to give the *trans*(**4.4a**) and the *cis*(**4.4b**) isomers in a 2:1 ratio according to the ^{1}H-NMR spectra (Figure

4.4). Complex **4.4a** gave a single methylplatinum resonance in the ^{1}H-NMR spectrum at $\delta =$ 1.19, with coupling constant $^2J_{\text{Pt-H}} = 71$ Hz. Only one set of imidazole and methyl-nitrogen resonances was observed, indicating the presence of a plane of symmetry between these groups. The Pt-CH$_2$ resonance of the *trans* isomer was observed at $\delta = 2.99$, with coupling constant $^2J_{\text{Pt-H}}$ $= 99$ Hz, which is in the range for the $^2J(\text{Pt-CH}_2)$ found for organoplatinum(II) complexes containing dipyridyl ligands.[15] The CH$_2(sp^2)$ protons were observed as a singlet at $\delta = 5.98$. Complex **4.4b** gave two methylplatinum resonances in 1:1 ratio at $\delta = 0.79$ (*trans* to I) and 1.05 (*trans* to N), with coupling constants $^2J_{\text{Pt-H}} = 76$ and 71 Hz respectively. Two singlets were observed at $\delta = 6.05$ and 6.06 in the ^{1}H-NMR spectrum due to the CH$_2(sp^2)$ protons. The ^{1}H-NMR spectrum showed a broad peak for the Pt-CH$_2$ protons at $\delta = 3.61$, with coupling constant $^2J_{\text{Pt-H}} = 104$ Hz. This resonance was expected to be two resonances because the Pt-CH$_2$ protons are diastereotopic, so variable temperature NMR study was needed to study the possible fluxionality.

$$(4.3)$$
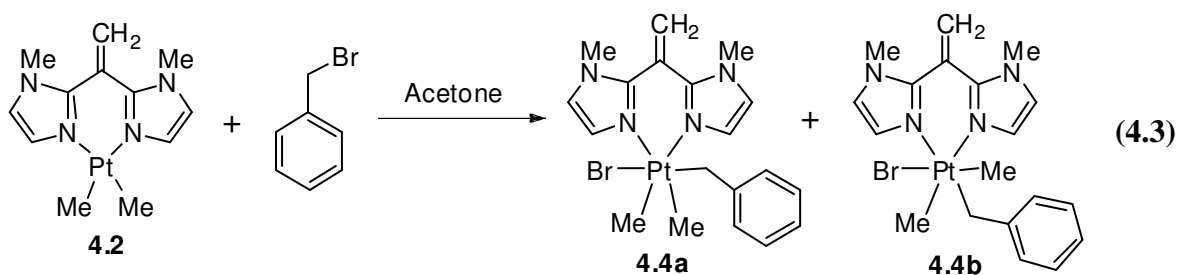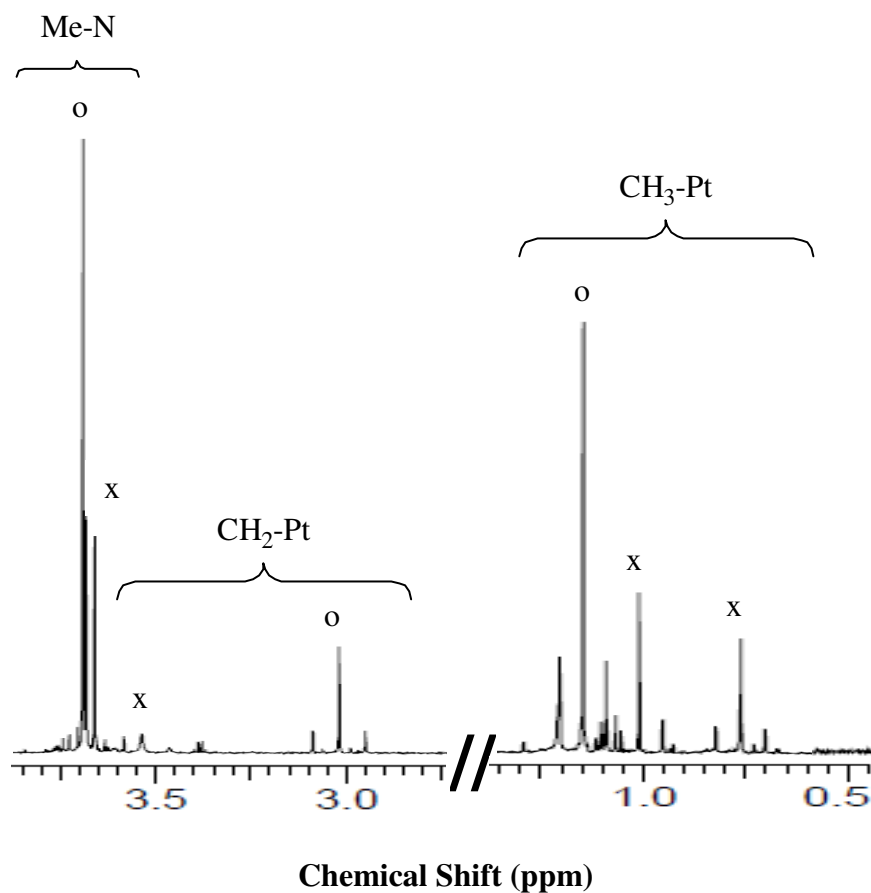
Figure 4.4. The ^{1}H-NMR spectrum (600 MHz, CD$_2$Cl$_2$) of complex **4.4** in

the high field region, [PtBr(CH$_2$-C$_6$H$_5$)Me$_2${(mim)$_2$C=CH$_2$}].

The broad singlet resonance observed at δ = 3.61 for the benzylic CH$_2$ group of the *cis*

isomer **4.4b** in the ^{1}H-NMR spectrum split at lower temperatures into two broad resonances.

Figure 4.5 shows the variable temperature ^{1}H-NMR spectra of **4.4** in the CH$_2$-Pt region.

The structure of the complex **4.4a** was confirmed by an X-ray structure determination, and a view of the structure is shown in Figure 4.6. The platinum(IV) adopts the octahedral geometry. Some selected bond lengths and angles are displayed in Table 4.2.
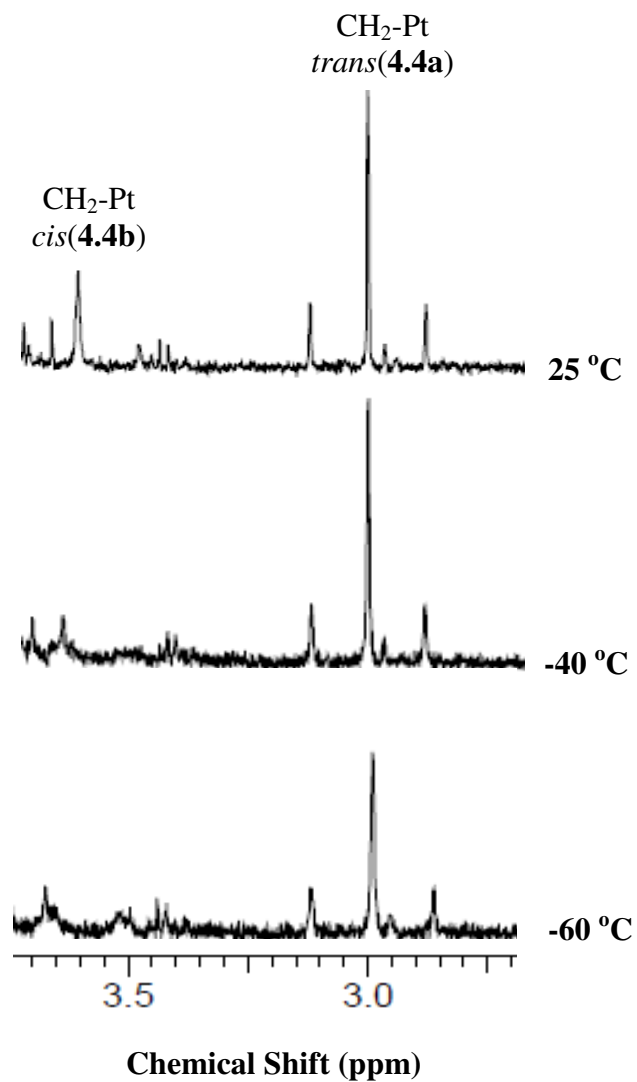
Figure 4.5. The VT-NMR spectra (400 MHz, CD$_2$Cl$_2$) of complex **4.4** in CH$_2$-Pt region at selected temperatures.
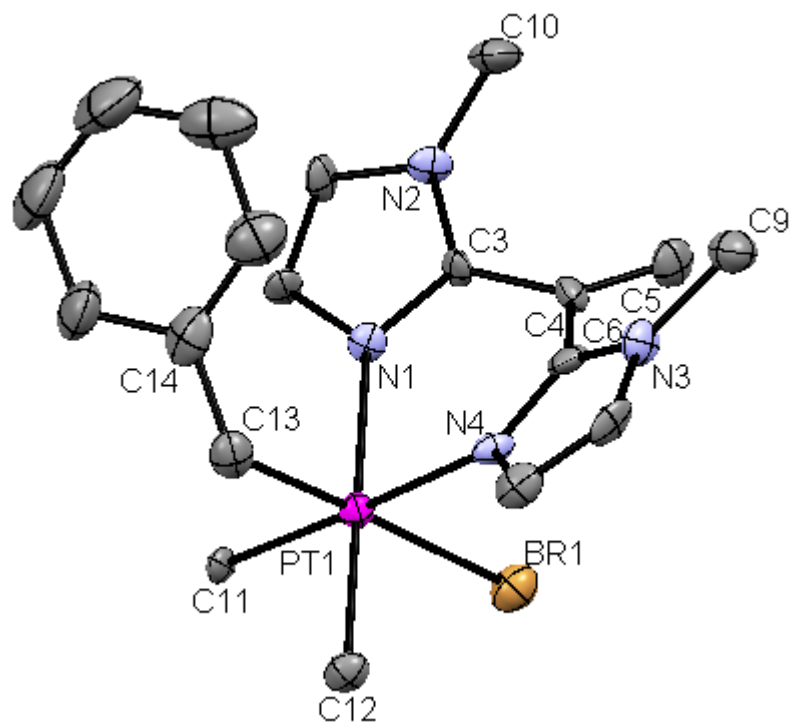
Figure 4.6. A view of the structure of complex **4.4a**, *trans*-[PtBr(CH$_2$-

C$_6$H$_5$)Me$_2${(mim)$_2$C=CH$_2$}].

Table 4.2. Selected bond lengths [Å] and angles [°] for *trans*-[PtBr(CH$_2$-
C$_6$H$_5$)Me$_2${(mim)$_2$C=CH$_2$}], **4.4a**.

Pt(1)-C(11)	2.071(8)	Pt(1)-C(12)	2.071(9)
Pt(1)-C(13)	2.095(1)	Pt(1)-Br(1)	2.617(1)
Pt(1)-N(1)	2.153(7)	Pt(1)-N(4)	2.150(7)
C(11)-Pt(1)-C(12)	87.8(4)	C(3)-C(4)-C(6)	116.3(8)
C(11)-Pt(1)-N(1)	92.3(3)	C(12)-Pt(1)-N(1)	94.1(3)
N(1)-Pt(1)-N(4)	87.0(3)	N(1)-Pt(1)-Br(1)	88.2(2)
C(11)-Pt(1)-Br(1)	91.8(3)	C(13)-Pt(1)-Br(1)	177.7(3)

The complex [PtMe$_2${(mim)$_2$C=CH$_2$}], **4.2**, reacted with Br-CH$_2$-4-C$_6$H$_4$-CF$_3$ in acetone at room temperature to give the mixture of the isomers *trans*(**4.5a**) and *cis*(**4.5b**) of [PtBr(CH$_2$-4-C$_6$H$_4$-CF$_3$Me$_2${(mim)$_2$C=CH$_2$}], **4.5**, in 2:1 ratio (Equation 4.4). Complex **4.5** is stable upon isolation, and both isomers were characterized spectroscopically. The complex **4.5a** gave one methylplatinum resonance in the ^{1}H-NMR spectrum at δ = 1.22, with coupling $^2J_{Pt-H}$ = 70 Hz, and one CH$_2$-Pt resonance at δ = 3.03, with coupling $^2J_{Pt-H}$ = 100 Hz. One proton resonance occurred for each of methyl-nitrogen and CH$_2$(sp^2) protons at δ = 3.80 and 5.99 respectively. The *cis* isomer **4.5b** was characterized by two methylplatinum resonances at δ = 0.79 and 1.00, with coupling $^2J_{Pt-H}$ = 74 and 70 Hz respectively, where the methylplatinum with the higher coupling constant is the one *trans* to the bromide ligand. Two different doublets resonances were observed for the Pt-CH$_2$ group, due to the low symmetry, at δ = 3.59 and 3.86, with coupling $^2J_{Pt-H}$ = 100 and 84 Hz respectively. The ^{1}H-NMR spectrum of the asymmetric *cis* isomer contained two singlets for each of the methyl nitrogen and the olefin protons.

(4.4)
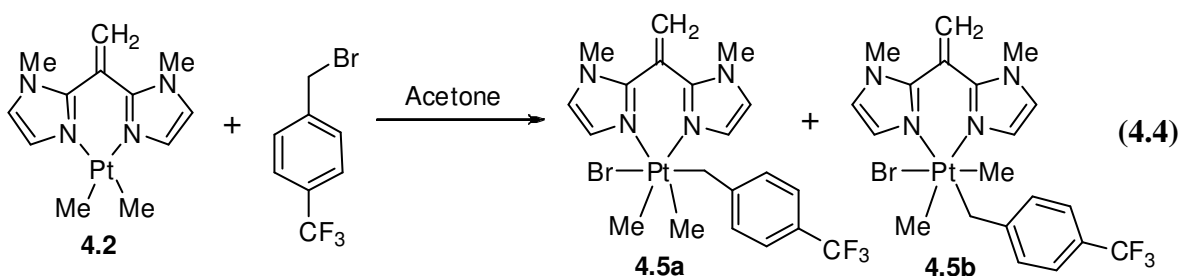
The reaction of complex **4.2**, [PtMe$_2$\{(mim)$_2$C=CH$_2$\}], with Br-CH$_2$-2-C$_6$H$_4$-CF$_3$ gave the complex [PtBr(CH$_2$-2-C$_6$H$_4$-CF$_3$Me$_2$)\{(mim)$_2$C=CH$_2$\}], **4.6**, via oxidative addition according to Equation 4.5. Complex **4.6** existed largely as the *trans* isomer **4.6a** with the benzyl group on the axial position *trans* to the bromide ligand, but a minor amount of the *cis* isomer **4.6b** with the benzyl group *trans* to nitrogen was also present. The *trans*(**4.6a**) to *cis*(**4.6b**) ratio is 3:1 according to the ^{1}H-NMR spectrum. The higher *trans* percentage for **4.6** compared to both complexes **4.4** and **4.5**, arises because the *ortho* substituent causes more steric hindrance. Complex **4.6a** gave a single methylplatinum resonance at δ = 1.28, $^2J_{Pt-H}$ = 70 Hz, and a single set of imidazole resonances, whereas the less symmetrical *cis* complex **4.6b** gave two equal intensity methylplatinum resonances at δ = 0.76 and 1.15, with $^2J_{Pt-H}$ = 74 and 70 Hz respectively, and two sets of imidazole resonances.
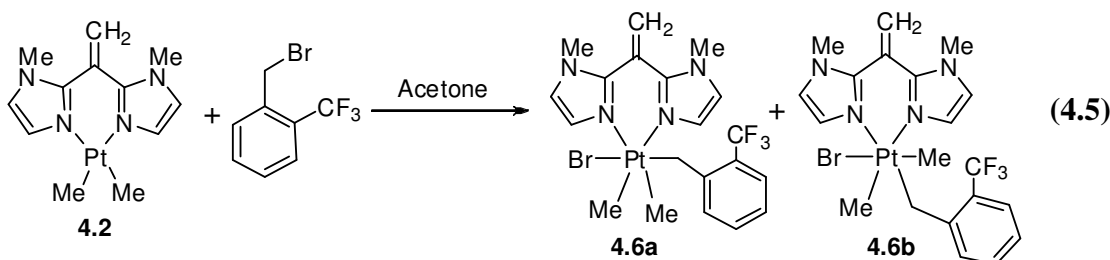
The structure of complex **4.6a** is shown in Figure 4.7. The chelate ring again adopts the boat conformation, and the C(5) atom (sp^2) is syn to the bromo ligand and anti to the benzyl group. The Pt-N distances (Pt(1)-N(1) = 2.149(4) Å, Pt(1)-N(4) = 2.156(4) Å) are similar to the distances found in complex **4.3**. Table 4.3 shows selected bond distances and angles of complex **4.6a**.
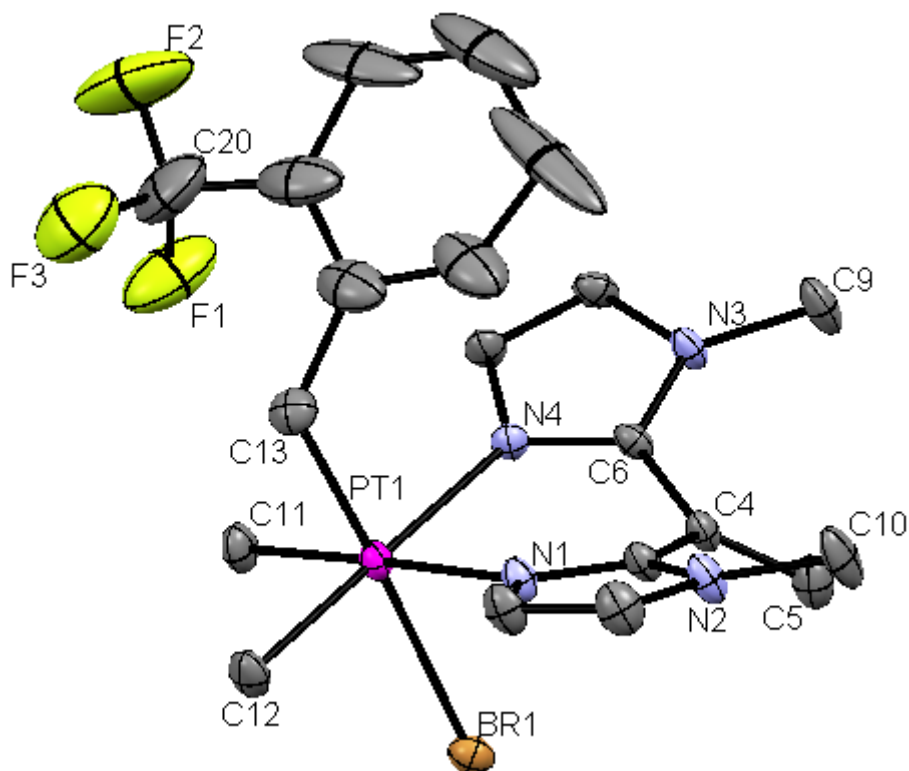
Figure 4.7. The structure of complex **4.6a**, *trans*-[PtBr(CH$_2$-2-C$_6$H$_4$-CF$_3$)Me$_2${(mim)$_2$C=CH$_2$}].

Table 4.3. Selected bond lengths [Å] and angles [°] for *trans*-[PtBr(CH$_2$-2-C$_6$H$_4$-CF$_3$ Me$_2${(mim)$_2$C=CH$_2$}], **4.6a**.

Pt(1)-C(11)	2.050(5)	Pt(1)-C(12)	2.050(5)
Pt(1)-C(13)	2.078(6)	Pt(1)-Br(1)	2.599(6)
Pt(1)-N(1)	2.149(4)	Pt(1)-N(4)	2.156(4)
C(11)-Pt(1)-C(12)	85.9(2)	C(11)-Pt(1)-C(13)	91.0(3)
C(11)-Pt(1)-N(1)	178.1(2)	C(13)-Pt(1)-N(1)	90.8(2)
N(1)-Pt(1)-N(4)	86.1(2)	N(1)-Pt(1)-Br(1)	89.3(1)
C(11)-Pt(1)-Br(1)	88.9(2)	C(13)-Pt(1)-Br(1)	176.8(2)

Reaction of complex **4.2** with Br-CH$_2$-3,5-C$_6$H$_4$-t-Bu$_2$ in acetone proceeded rapidly at room temperature to produce the platinum(IV) complex [PtBr(CH$_2$-3,5-C$_6$H$_3$-t-Bu$_2$)Me$_2${(mim)$_2$C=CH$_2$], **4.7**, via oxidative addition according to Equation 4.6. The complex was fully characterized by ^{1}H-NMR spectroscopy, elemental analysis, and X-ray crystallography. In the ^{1}H-NMR spectrum of **4.7**, two isomers *trans*(**4.7a**) and *cis*(**4.7b**) were formed in a 3:1 ratio. The addition of the bulky t-butyl groups on both *meta* positions of the benzyl ring yielded a high *trans*:*cis* ratio, showing high *trans* stereoselectivity. The ^{1}H-NMR spectrum showed that the *trans* isomer **4.7a** contained a methylplatinum resonance at δ = 1.26, with $^2J_{Pt-H}$ = 71 Hz, and one set of imidazole resonances. While the *cis* isomer **4.7b** was characterized by two equal intensity methylplatinum resonances at δ = 0.80 and 1.14, with $^2J_{Pt-H}$ = 76 and 71 Hz respectively. The ^{1}H-NMR spectrum contained two singlets for the methyl-nitrogen and the CH$_2$(sp^2) protons at δ = 3.75 and 6.01 respectively. On the other hand, the asymmetric *cis* product had four proton resonances, two for each of the methyl-nitrogen and the CH$_2$(sp^2) protons.

$$R = 3,5\text{-}C_6H_3\text{-}(t\text{-Bu})_2$$
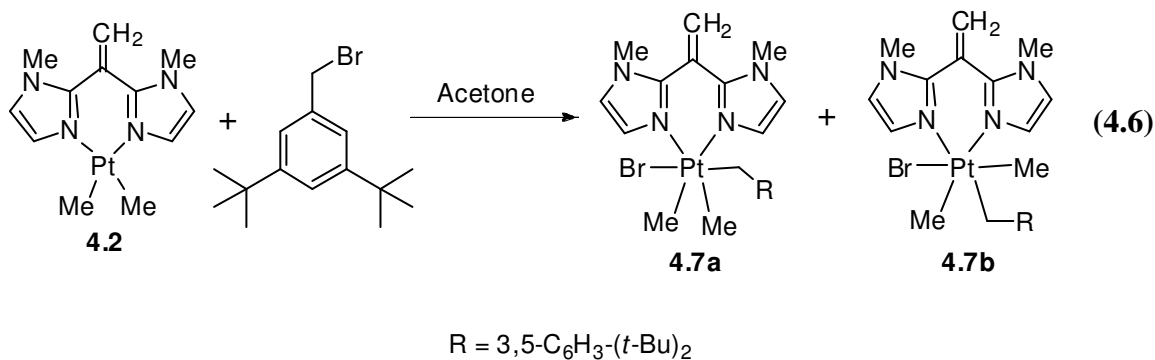
The structure of complex **4.7a** is shown in Figure 4.8. The platinum(IV) atom displays octahedral geometry. The bidentate imidazole ligand adopts a boat conformation with the bridging atom C(10) pointing away from the benzyl group. Table 4.4 shows selected bond lengths and distances of the *trans* complex **4.7a**.
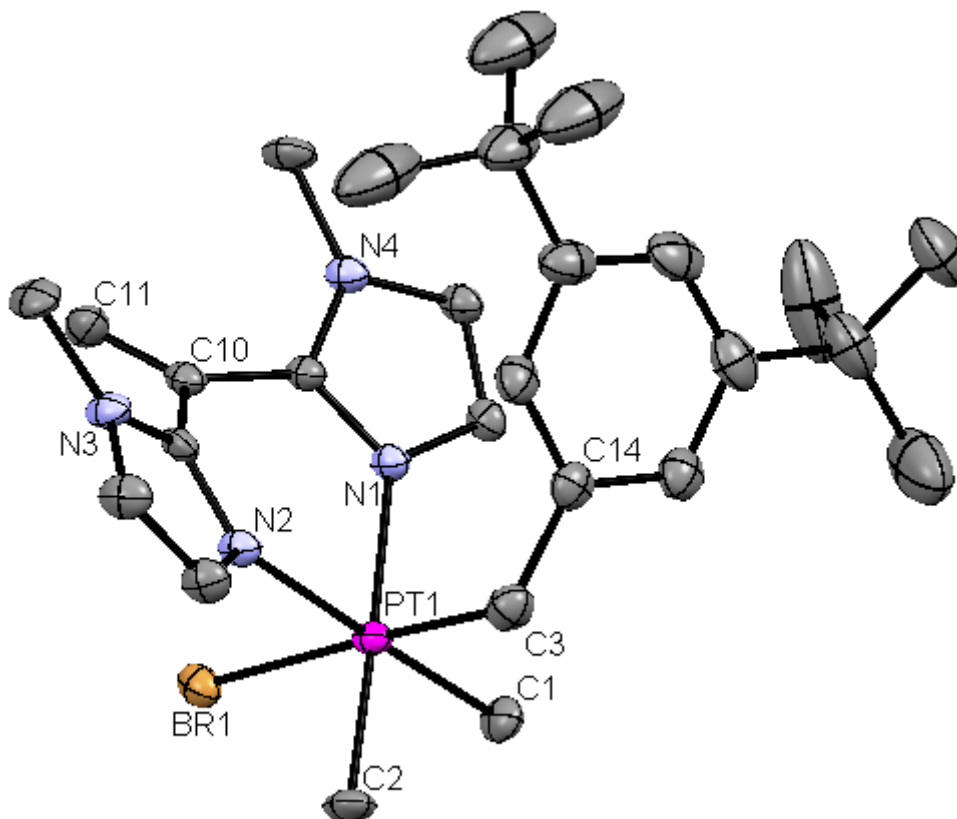
Figure 4.8. The structure of complex **4.7a**, *trans*-[PtBr(CH$_2$-3,5-C$_6$H$_3$-*t*-Bu$_2$)Me$_2${(mim)$_2$C=CH$_2$}].

Table 4.4. Selected bond lengths [Å] and angles [°] for *trans*-[PtBr(CH$_2$-3,5-C$_6$H$_3$-*t*-Bu$_2$)Me$_2${(mim)$_2$C=CH$_2$}], **4.7a**.

Pt(1)-C(1)	2.049(5)	Pt(1)-C(2)	2.049(5)
Pt(1)-C(3)	2.084(6)	Pt(1)-Br(1)	2.636(6)
Pt(1)-N(1)	2.152(4)	Pt(1)-N(2)	2.160(4)
C(10)-C(11)	1.324(8)	C(3)-C(1)	1.494(8)
C(1)-Pt(1)-C(2)	87.6(2)	C(2)-Pt(1)-C(3)	86.0(2)
C(2)-Pt(1)-N(1)	178.1(2)	C(1)-Pt(1)-N(1)	93.2(2)
N(1)-Pt(1)-N(2)	85.7(2)	N(1)-Pt(1)-Br(1)	86.2(1)
C(2)-Pt(1)-Br(1)	91.0(2)	C(3)-Pt(1)-Br(1)	177.8(2)
C(3)-Pt(1)-N(1)	95.8(2)	C(6)-C(10)-C(9)	116.7(5)

4.2.2.3 Oxidative Addition with Dichloromethane

Halogen containing solvents are capable of reacting with metal complexes to form metal halides.[16,17] Dichloromethane is usually reactive to electron rich metal centers such as platinum(II) complexes via oxidative addition of one or both of the C-Cl bonds.[1a] The reaction of complex 4.**2** with methylene chloride at room temperature yielded the platinum(IV) complex [PtCl(CH$_2$Cl)Me$_2${(mim)$_2$C=CH$_2$}], **4.8**, which resulted in a *trans* and *cis* mixture in 1:2 ratio according to Equation 4.7. Dimethylplatinum(II) complexes containing the 2,2'-bipyridine ligand have been shown in recent years to be reactive with dichloromethane by oxidative addition of a C-Cl bond.[17] The kinetic product **4.8b** was shown to be formed via *cis* oxidative addition, but it then isomerizes in solution to give a mixture of the *trans* and *cis* isomers in 5:2 ratio. In the ^{1}H-NMR spectrum, the *trans* isomer **4.8a** gave a single methylplatinum resonance at δ = 1.12, with

$^2J_{Pt-H}$ = 70 Hz, and a single PtCH$_2$Cl resonance at δ = 3.72, with $^2J_{Pt-H}$ = 56 Hz. On the other

hand, the *cis* isomer was identified in the ^{1}H-NMR spectrum via its two equal intensity

methylplatinum resonances at δ = 0.89 and 1.13, with $^2J_{Pt-H}$ = 74 and 69 Hz respectively. There

were two resonances for the PtCH^{a}H^{b}Cl protons of complex **4.8b** at δ = 4.13 and 4.60, with $^2J_{Pt-H}$

= 45 and 88 Hz respectively.

$$\text{(4.7)}$$
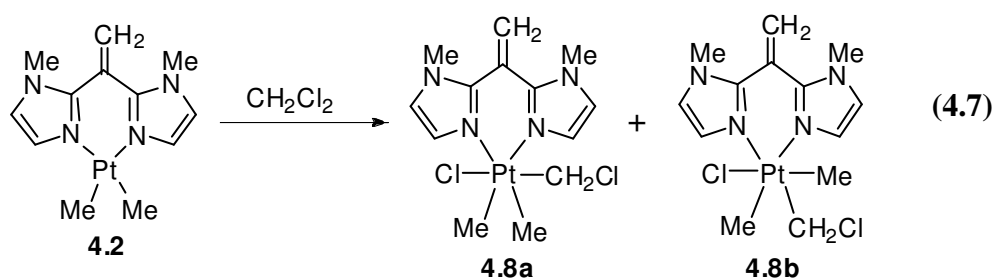
A ^{1}H-NMR experiment was needed to study the mechanistic pathway of the reaction. The

reaction was monitored over a period of several days. The ^{1}H-NMR spectrum showed the

presence of the *cis* isomer **4.8b** and the starting material **4.2** after 10 minutes of mixing. After

one hour, there was no trace of the starting material in the ^{1}H-NMR spectrum, and only complex

4.8b was observed. The ^{1}H-NMR spectrum of the solution after one day showed the presence of

a mixture of the *trans*(**4.8a**) and *cis*(**4.8b**) isomers in 1:2 ratio. The ^{1}H-NMR spectra of the

product of reaction of **4.2** with CH$_2$Cl$_2$ and CD$_2$Cl$_2$ are identical, except in the methylene region.

So a deuterium ^{2}H-NMR was run to identify the PtCD$_2$Cl resonances. The ^{2}H-NMR for the

reaction of CD$_2$Cl$_2$ with **4.2** showed 3 resonances at δ = 3.74, with $^2J_{Pt-D}$ = 9 Hz for the *trans*

isomer, and at δ = 4.14 and 4.60, with $^2J_{Pt-D}$ = 6 and 12 Hz for the *cis* isomer. So complex **4.2**

was proven to be reactive toward dichloromethane by the oxidative addition of a C-Cl bond.

4.2.2.4 The Reactions of [PtMe$_2${(mim)$_2$C=CH$_2$}] with Peroxides

Platinum(II) complexes containing bidentate nitrogen-donor ligands are typically highly reactive towards peroxides.[18] These complexes [PtMe$_2$(LL)], LL = diimine ligand, usually react with peroxides (RO-OR) to give the corresponding platinum(IV) complexes [PtMe$_2$(OR)$_2$(LL)] by oxidative addition.[19] A sample of complex **4.2**, [PtMe$_2${(mim)$_2$C=CH$_2$}], was dissolved in acetone-d$_6$ and the course of the reaction with H$_2$O$_2$ was then monitored over time by ^{1}H-NMR spectroscopy. Hydrogen peroxide reacted rapidly with **4.2** to give [Pt(OH)$_2$Me$_2${(mim)$_2$C=CH$_2$}], **4.9** according to Equation 4.8. The reaction proceeded by *trans* oxidative addition of the HO-OH to the platinum(II) complex forming a platinum(IV)-dihydroxide. The ^{1}H-NMR spectrum of complex **4.9** in acetone-d$_6$ showed one methylplatinum proton resonance at δ = 1.36, with coupling constant $^2J_{Pt-H}$ = 73 Hz. The presence of one proton resonance for each of methylplatinum, methyl-nitrogen, and olefin protons indicates that complex **4.9** possesses a plane of symmetry as expected for a product of *trans* addition. Also the mass spectrum for **4.9** showed a peak at m/z = 430 corresponding to [Pt(OH)Me$_2${(mim)$_2$C=CH$_2$}]$^+$.

(4.8)
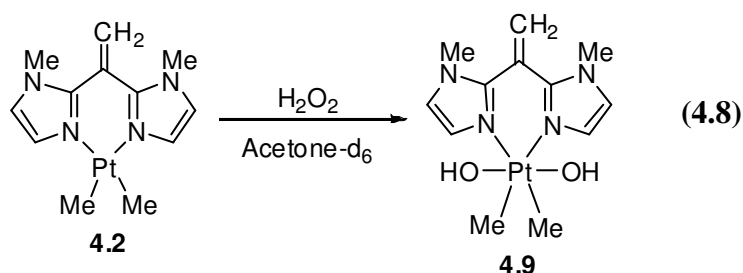
In an NMR tube, complex **4.2** was reacted with dibenzoyl peroxide to give [Pt(OOCPh)$_2$Me$_2${(mim)$_2$C=CH$_2$}] **4.10**, which was characterized via ^{1}H-NMR spectroscopy and mass spectrometry. The ^{1}H-NMR spectrum of this complex, obtained after 30 minutes of dissolving complex **4.2** and dibenzoyl peroxide in acetone-d$_6$ contained two equal intensity methylplatinum resonances at δ = 1.68 (*trans* to O) and 2.10 (*trans* to N), with coupling constants $^2J_{Pt-H}$ = 73 and 67 Hz respectively, which were assigned to the asymmetric *cis* isomer (Equation 4.9). The absence of a plane of symmetry resulted in the presence of two methyl-nitrogen resonances at δ = 4.01 and 4.05, and two singlets for the CH$_2$(sp^2) protons at δ = 6.33 and 6.37 in the ^{1}H-NMR spectrum. There were only traces of the *trans* isomer. The *cis*-addition is unusual since previous mechanistic studies have proved that a concerted three-centre mechanism is not an option for the oxidative addition of E-E bonds (E = O, S, or Se) to platinum(II) complexes.[19] The mass spectrum for **4.10** showed a peak at m/z = 535 corresponding to [Pt(OOCPh)Me$_2${(mim)$_2$C=CH$_2$}]$^+$. The reaction of dibenzoyl peroxide with **4.2**, as monitored by ^{1}H-NMR at low temperature, proceeded to form the *cis* and *trans* isomers in 6:1 ratio. The *trans* isomer was identified in the ^{1}H-NMR spectrum via a singlet methylplatinum resonance at δ = 1.26, with $^2J_{Pt-H}$ = 70 Hz. One singlet resonance was observed for the methyl-nitrogen protons at δ = 3.99, and another singlet resonance was observed at δ = 6.17 for the CH$_2$(sp^2) protons. The ratio slowly changed in two days thus forming eventually the *cis* isomer with traces of the *trans* isomer.

(4.9)
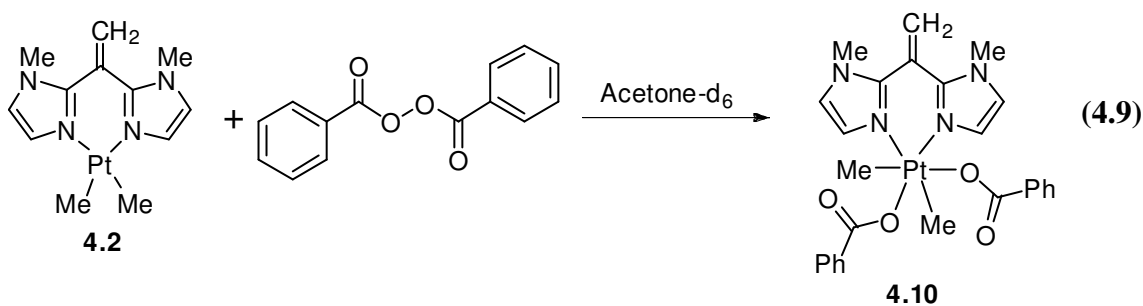
4.2.3 The Synthesis of [PtMe₂{(mim)₂CHMe}]

The ligand 1,1-bis(1-methylimidazole-2-yl)ethane, **4.11**, was prepared using a procedure by Byers *et al*,[11] (Equation 4.10),   and isolated as white crystals. The complex [PtMe₂{(mim)₂CHMe}] **(4.12)** was easily prepared by the reaction of the platinum dimer $[Pt_2Me_4(\mu\text{-}SMe_2)_2]$[12] with complex **4.11** in ether according to Equation 4.11. The reaction proceeded very rapidly, and the platinum(II) complex **(4.12)** was isolated as a yellow solid that is not stable at room temperature for a long period of time. In the ¹H-NMR spectrum (Figure 4.9), the methylplatinum resonance occurred at $\delta = 0.49$, with coupling $^2J_{Pt\text{-}H} = 88$ Hz. Only one set of imidazole and methyl-nitrogen resonances were observed in the ¹H-NMR spectrum due to symmetry.

$$
\text{4.1} \quad \xrightarrow[\text{Ethanol}]{\text{H}_2/\text{Pd}} \quad \text{4.11} \tag{4.10}
$$

$$
\tfrac{1}{2}\,[\text{Pt dimer}] + \text{4.11} \quad \xrightarrow[-\text{SMe}_2]{\text{Et}_2\text{O}} \quad \text{4.12} \tag{4.11}
$$
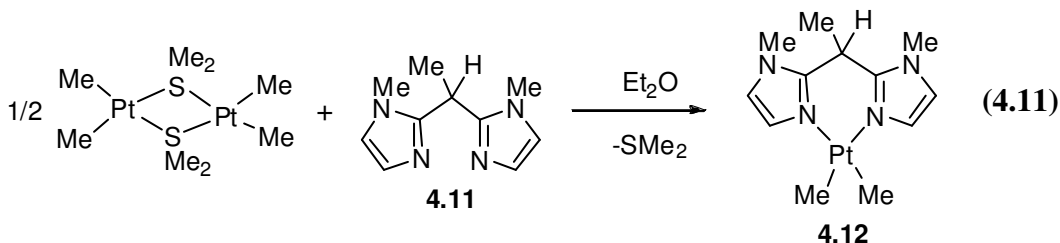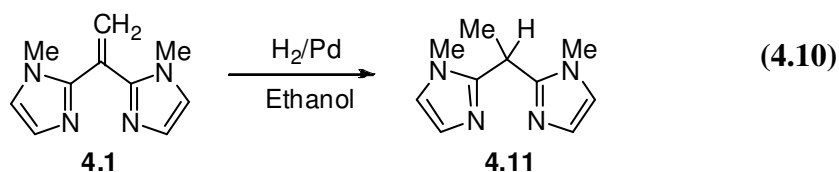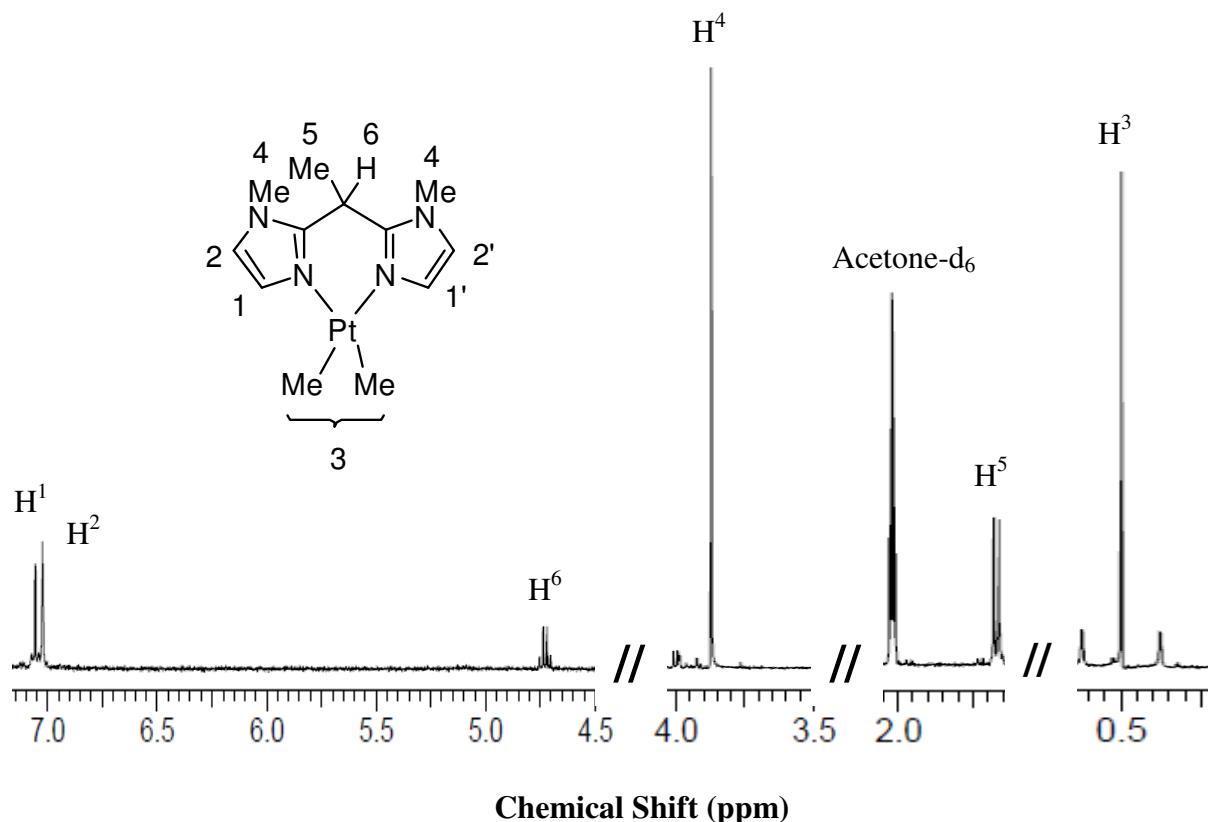
Figure 4.9. The ^{1}H-NMR spectrum (400 MHz, acetone-d$_6$) of complex **4.12**,

[PtMe$_2${(mim)$_2$CHMe}].

4.2.3.1 The Reactivity and Stereoselectivity of Oxidative Addition to [PtMe$_2${(mim)$_2$CHMe}]

An oxidative addition of methyl iodide to complex **4.12** was carried out in acetone at room temperature to produce a pure and stable trimethylplatinum(IV) complex **4.13**. NMR spectroscopy characterizations of complex **4.13** showed the presence of two different isomers, **4.13a** and **4.13b** as shown in Equation 4.12. The complex [PtIMe$_3${(mim)$_2$CHMe}] was isolated as a white product, which was stable at room temperature and soluble in various organic

solvents. The oxidative addition reaction proceeded rapidly to form the isomers **4.13a** and **4.13b** in a 5:4 ratio. The ^{1}H-NMR spectrum of **4.13a** contained two methylplatinum proton resonances at δ = 0.93 ($^2J_{\text{Pt-H}}$ = 75 Hz, *trans* to I), and 1.32 ($^2J_{\text{Pt-H}}$ = 70 Hz, *trans* to N). On the other hand, the minor isomer **4.13b** was characterized via two methylplatinum proton resonances at δ = 0.70 ($^2J_{\text{Pt-H}}$ = 74 Hz, *trans* to I), and 1.37 ($^2J_{\text{Pt-H}}$ = 70 Hz, *trans* to N) in the ^{1}H-NMR spectrum. Each of the complexes **4.13a** and **4.13b** contained one set of methyl-nitrogen and imidazole proton resonances due to symmetry. The orientation of the hydrogen and methyl on the bridging carbon with respect to the *axial* ligand on the platinum(IV) complex was proved via 2D-NOESY NMR, where a coupling between the Me-Pt and CH$_3$-C protons was observed for complex **4.13a** only.
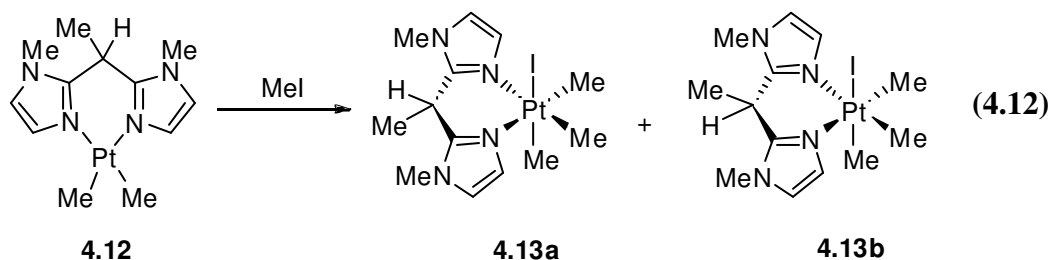
$$(4.12)$$

4.12   **4.13a**   **4.13b**

A variable temperature ^{1}H-NMR study was needed to study the mechanistic pathway of the reaction of CD$_3$I with **4.12**. The NMR spectra were recorded at 20 $^\circ$C intervals between -60 and +20 $^\circ$C. The oxidative addition of CD$_3$I proceeds rapidly, but at lower temperatures both isomers **4.13b** and **4.13a** were observed in a 3:2 ratio. The concentration of the isomer **4.13b** decreased upon increasing the temperature of the probe. The kinetic product **4.13b** became minor upon heating the probe up to room temperature, while thermodynamic product **4.13a** became the major isomer. Figure 4.10 shows the ^{1}H-NMR spectra in the methyl region for the reaction of MeI with **4.12** at room temperature, and the reaction of CD$_3$I with **4.12** at -60 $^\circ$C, which shows

that the kinetic product **4.13b** is favored at low temperatures, while the thermodynamic product

4.13a is favored at room temperature. Note that axial-equatorial exchange of PtMe/PtCD$_3$ groups

occurred even at -60 $^{\circ}$C.
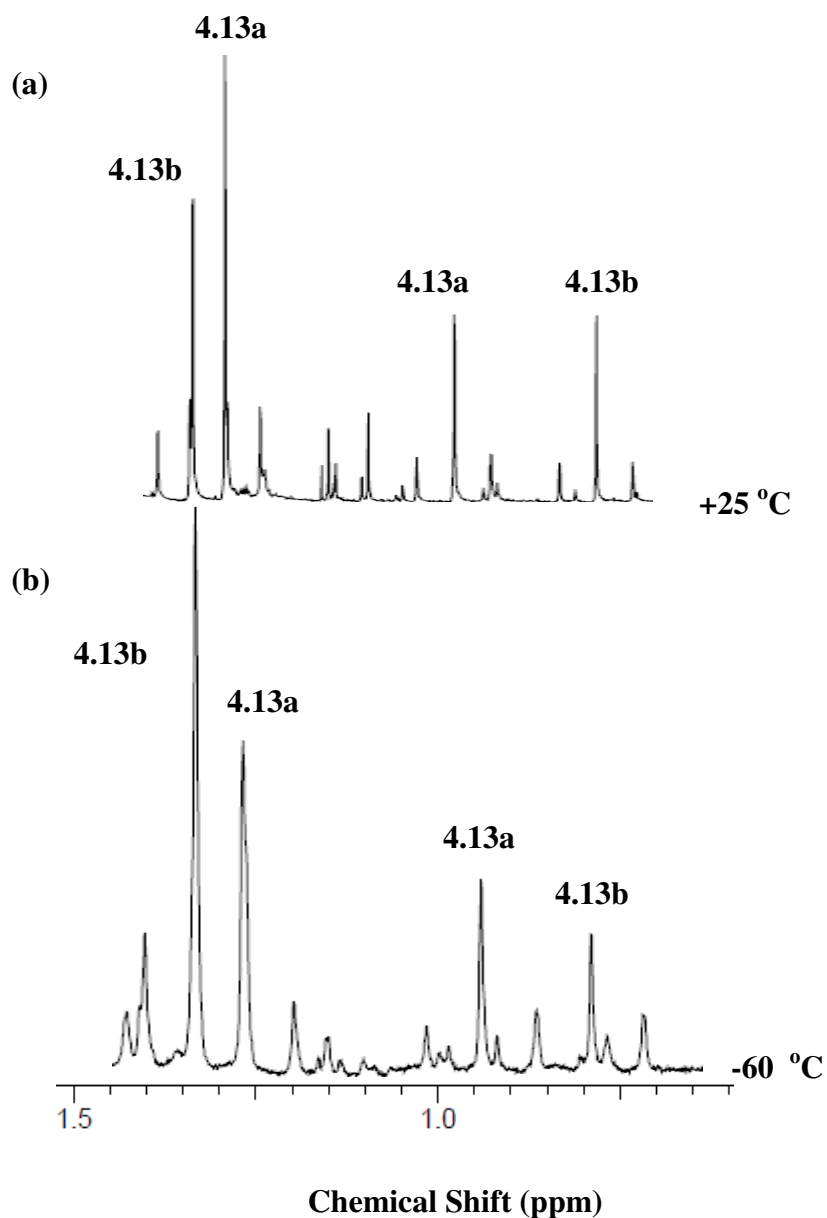
Figure 4.10. The ^{1}H-NMR spectra (400 MHz, acetone-d$_6$) of the methylplatinum region for the

reaction of complex **4.12** with: a) MeI at room temperature. b) CD$_3$I at -60 $^{\circ}$C.

Complex **4.14** [PtI$_2$Me$_2${(mim)$_2$CHMe}] was prepared by the reaction of complex **4.12** with iodine in a methylene chloride solution in an NMR tube, which proceeded rapidly at room temperature to produce the platinum(IV) complex. In this reaction, *trans* oxidative addition of the I-I bond occurred at the platinum center. The solution color changed rapidly to orange upon addition of iodine. The ^{1}H-NMR spectrum of **4.14** contained one single methylplatinum resonance at δ = 2.32 ($^2J_{Pt-H}$ = 71 Hz, *trans* to N), and one set of imidazole and methyl-nitrogen resonances, indicating *trans* oxidative addition.

(4.13)
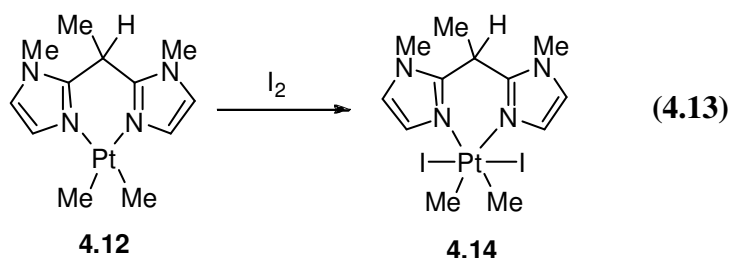
4.2.3.2 The Reactions of [PtMe$_2${(mim)$_2$CHMe}] with Benzyl Halides

The reaction of Br-CH$_2$-2-C$_6$H$_4$-CF$_3$ with complex **4.12** [PtMe$_2${(mim)$_2$CHMe}] produced the platinum(IV) complex [PtBr(CH$_2$-2-C$_6$H$_4$-CF$_3$)Me$_2${(mim)$_2$CHMe}], **4.15**, according to Equation 4.14. Complex **4.15** was isolated as a stable white solid that was soluble in various organic solvents such acetone, and methylene chloride. The reaction proceeded via the oxidative addition of the Br-CH$_2$ bond to produce the *trans* isomer. The ^{1}H-NMR spectrum of complex **4.15** contained only one methylplatinum resonance at δ = 1.34 with $^2J_{Pt-H}$ = 69 Hz

(*trans* to N), and PtCH$_2$ resonances at δ = 3.11 with $^2J_{\text{Pt-H}}$ = 104 Hz (*trans* to Br). The complex is symmetrical, so the ^{1}H-NMR spectrum contained one set of imidazole and methyl-nitrogen resonances. The structure of complex **4.15** was determined via X-ray crystallography, and it confirmed the *trans* oxidative addition with an octahedral geometry (Figure 4.11). Table 4.5 shows selected bond lengths and angles of complex **4.15**.

(4.14)

4.12

4.15
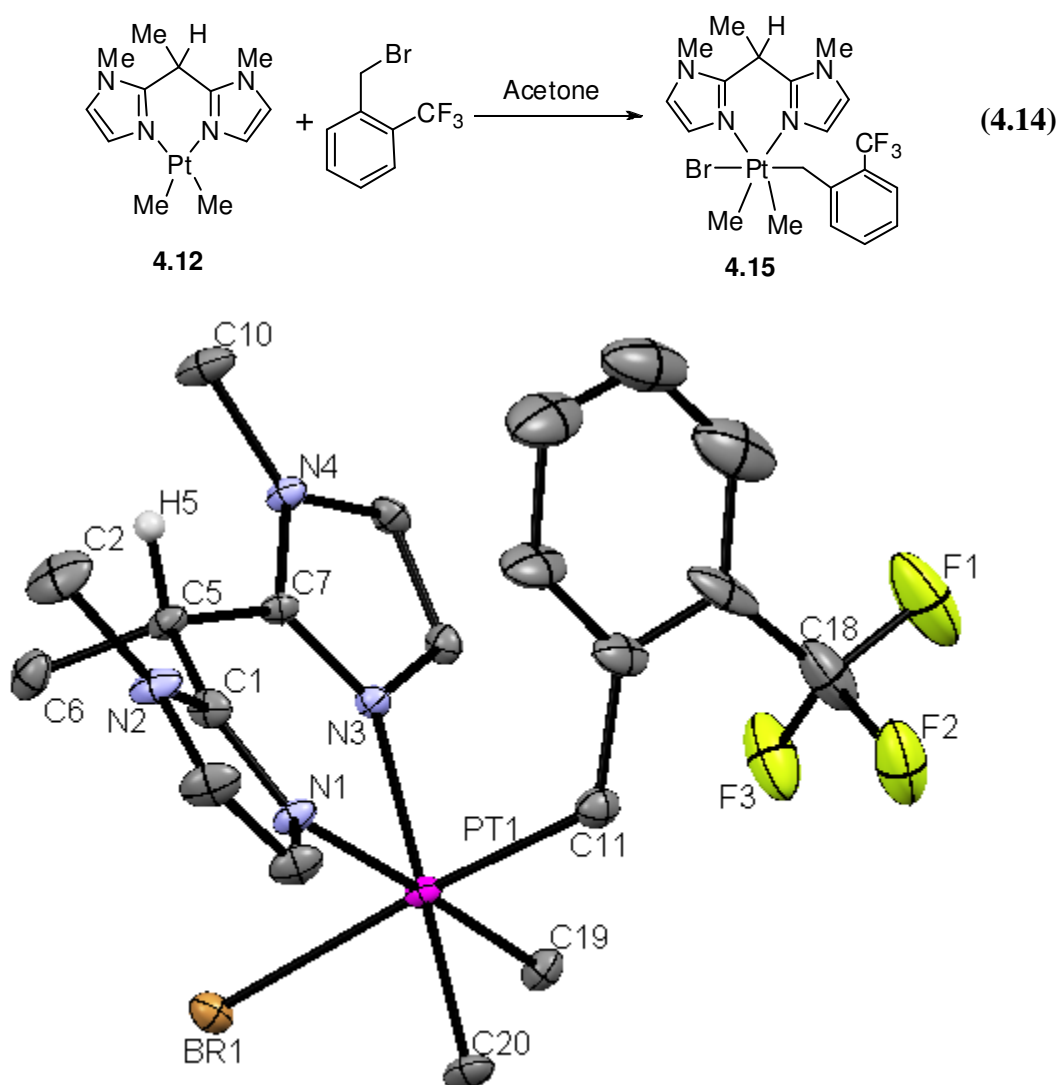
Figure 4.11: The structure of complex **4.15**, *trans*-[PtBr(CH$_2$-2-C$_6$H$_4$-CF$_3$)Me$_2${(mim)$_2$CHMe}].

Table 4.5. Selected bond lengths [Å] and angles [°] for *trans*-[PtBr(CH$_2$-2-C$_6$H$_4$-CF$_3$)Me$_2${(mim)$_2$CHMe], **4.15**.

Pt(1)-C(11)	2.086(5)	Pt(1)-C(19)	2.044(4)
Pt(1)-C(20)	2.051(4)	Pt(1)-Br(1)	2.595(6)
Pt(1)-N(1)	2.152(4)	Pt(1)-N(3)	2.152(4)
C(19)-Pt(1)-C(20)	86.4(2)	C(19)-Pt(1)-N(1)	178.2(2)
C(19)-Pt(1)-N(3)	94.7(2)	N(1)-Pt(1)-N(3)	86.6(1)
C(19)-Pt(1)-Br(1)	87.9(1)	N(1)-Pt(1)-Br(1)	90.8(1)
C(6)-C(5)-H(5)	106.7(4)	C(12)-C(11)-Pt(1)	117.1(3)

The oxidative addition of Br-CH$_2$-4-C$_6$H$_4$-CF$_3$ to **4.12**, [PtMe$_2${(mim)$_2$CHMe}], gave the *trans* isomer of the platinum(IV) complex [PtBr(CH$_2$-4-C$_6$H$_4$-CF$_3$)Me$_2${(mim)$_2$CHMe}], **4.16**, according to Equation 4.15. Only a singlet Pt-CH$_2$ resonance was observed, along with a singlet methylplatinum resonance, a singlet methyl-nitrogen resonance, and a single set of imidazole resonances. The methyplatinum resonance was seen at δ = 1.34 with $^2J_{Pt-H}$ = 69 Hz *trans* to N, while the Pt-CH$_2$ was observed at δ = 2.87 with $^2J_{Pt-H}$ = 97 Hz *trans* Br. Figure 4.12 shows the ^{1}H-NMR spectrum of **4.16**. Complex **4.12** showed only *trans* stereoselectivity upon the oxidative addition of the compounds Br-CH$_2$-*para*/*ortho*-C$_6$H$_4$-CF$_3$. Only one *trans* isomer was observed in each reaction in comparison to the reaction of **4.12** with methyl iodide where two *trans* isomers were observed. The presence of the sterically hindered benzyl group on the axial position resulted in the production of that only *trans* isomer where both the hydrogen and the benzyl groups are *syn* to each other, as seen in the molecular structure of **4.15**, which was confirmed by X-ray crystallography. The complex [PtIMe$_3${(mim)$_2$CHMe}] (**4.13**) had two different *trans* isomers, due to the presence of the less sterically hindered methyl group.
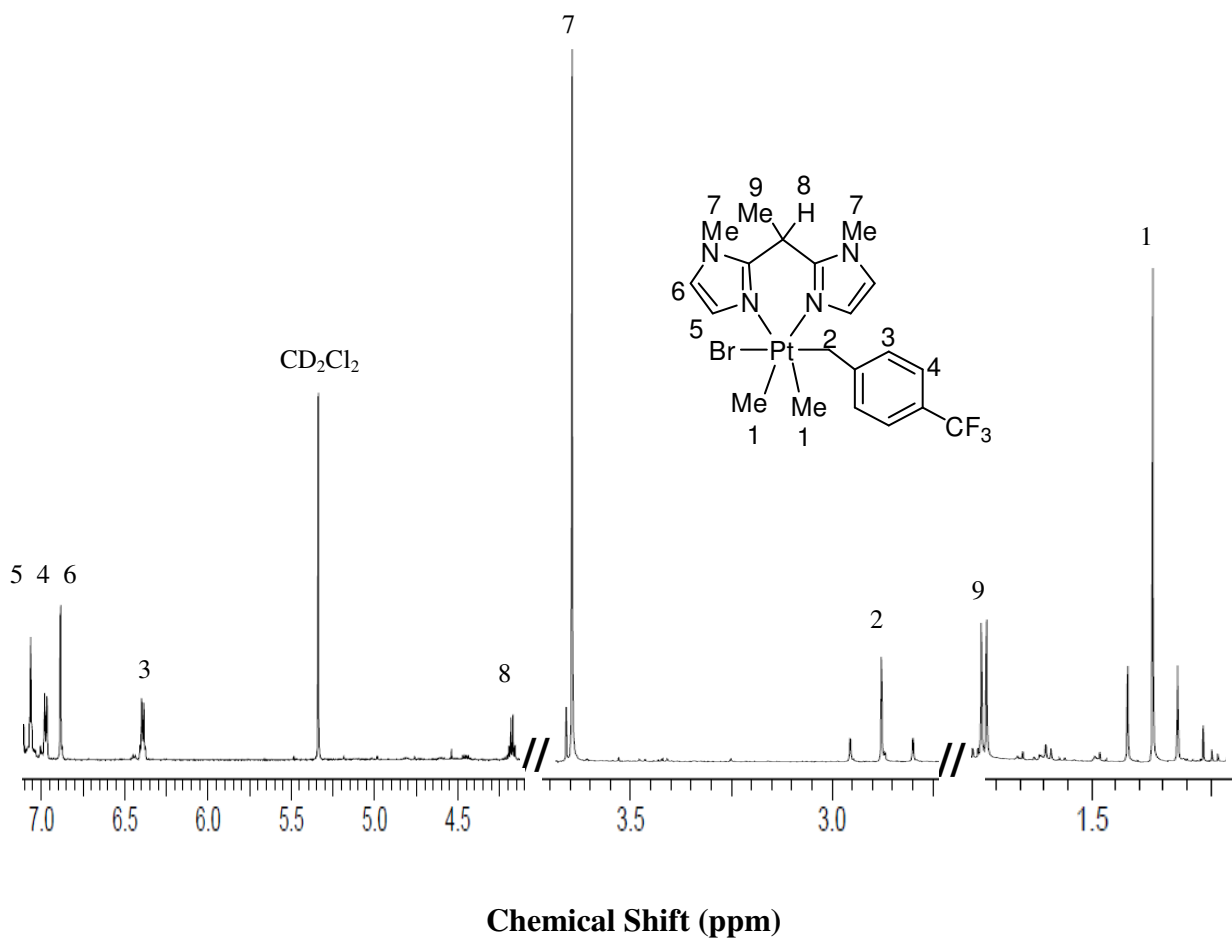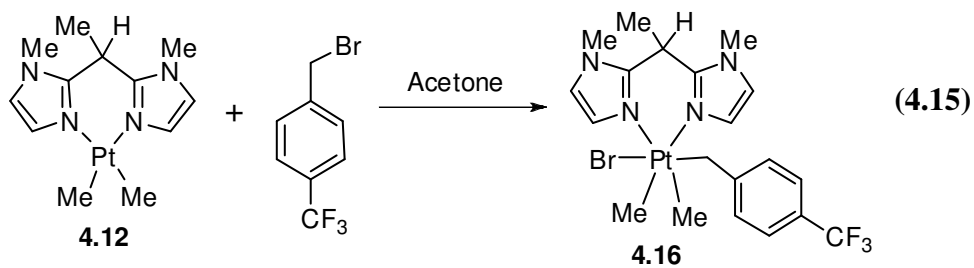
Figure 4.12. The ^{1}H-NMR spectrum of complex **4.16**, *trans*-[PtBr(CH$_2$-4-C$_6$H$_4$-CF$_3$)Me$_2${(mim)$_2$CHMe}].

4.2.3.3 The Reactions of [PtMe$_2$\{(mim)$_2$CHMe\}] with Hydrogen Peroxide

The reaction of hydrogen peroxide with **4.12** [PtMe$_2$\{(mim)$_2$CHMe\}] was monitored through ^{1}H-NMR spectroscopy. The reaction proceeded rapidly at room temperature to produce the complex [Pt(OH)$_2$Me$_2$\{(mim)$_2$CHMe\}] (**4.17**) via oxidative addition of the O-O bond (Equation 4.16). After 10 minutes of mixing the reactants in the NMR tube, there were no traces of the platinum(II) complex (**4.12**) in the ^{1}H-NMR spectra, which shows the high reactivity of **4.12**. Complex **4.17** was characterized via the presence of one methylplatinum proton resonance in the ^{1}H-NMR spectrum at $\delta = 1.37$, with $^2J_{\text{Pt-H}} = 73$ Hz. The ^{1}H-NMR spectrum of complex **4.17** contained one set of imidazole resonances, and a singlet for the methyl-nitrogen protons due to symmetry. The reaction of **4.12** with hydrogen peroxide gave similar results to the reaction with iodine in terms of stereoselectivity.

$$(4.16)$$

4.12   **4.17**
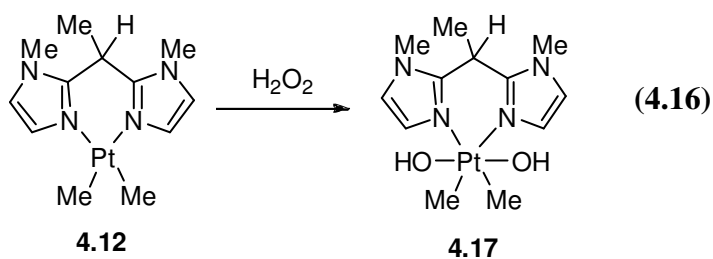
4.3 Conclusions

The dimethylplatinum(II) complex $[PtMe_2\{(mim)_2C=CH_2\}]$ (N-N = 1,1-bis(1-methylimidazole-2-yl)ethene), and $[PtMe_2\{(mim)_2CHMe\}]$ (N-N = 1,1-bis(1-methylimidazole-2-yl)ethane) undergoes easy oxidative addition to give platinum(IV) complexes.

The reaction of $[PtMe_2\{(mim)_2C=CH_2\}]$ with methyl iodide resulted in the formation in the trimethylplatinum(IV) complex, while the reactions with benzyl bromide and trifluoromethyl substituted benzyl bromides resulted in the formation of *cis* and *trans* isomers of the respective platinum(IV) complexes in various ratios. The platinum(II) complex showed high reactivity towards halogenated solvents, since it reacted with methylene chloride via oxidative addition forming the *cis* and *trans* isomers of the platinum(IV) complex. The platinum(II) complex showed high reactivity to hydrogen peroxide where a *trans* oxidative addition was observed, and to dibenzoyl peroxide where it was *cis* stereoselective.

The complex $[PtMe_2\{(mim)_2CHMe\}]$ showed high reactivity towards alkyl halides, halogens, and peroxides. The reaction of the platinum(II) complex with methyl iodide showed unique results in the formation of two isomers, where the major isomer was concluded to be where the iodide and the methyl group on the bridging carbon are *anti* to each other due to steric reasons. Iodine is bigger so should be near the smaller H substituent. While the platinum(IV) complexes formed via the oxidative addition of iodine and hydrogen peroxide were *trans* stereoselective, and only one *trans* isomer was observed. The platinum(IV) complexes formed via the oxidative addition of benzyl halides showed *trans* stereoselectivity.

4.4 Experimental

All reactions were carried out under nitrogen, either using Schlenk techniques or in a dry box, unless otherwise specified. NMR spectra were recorded on Inova 400 MHz, Inova 600 MHz, and Mercury 400 MHz spectrometers. Chemical shifts are reported relative to TMS. Elemental analyses were performed by Guelph Chemical Laboratories. Mass spectrometry studies were carried out using an electrospray PE-Sciex Mass Spectrometer (ESI MS), and a high resolution Finnigan MAT 8200 instrument. The complexes *cis/trans*-[PtCl$_2$(SMe$_2$)$_2$] and [Pt$_2$Me$_4$(μ-SMe$_2$)$_2$] were prepared from K$_2$[PtCl$_4$] according to the literature.[12]

[(mim)$_2$C=CH$_2$], 4.1. The procedure was followed according to the literature.[11] The product was isolated as an oil. Yield 57 %. ^{1}H NMR in acetone-d$_6$: δ = 3.34 (s, 6H, N-CH$_3$), 5.85 (s, 2H, CH$_2$), 6.92 (d, 2H, $^3J_{\text{H-H}}$ = 1 Hz, Im{H^1 and H$^{1'}$}), 7.07 (d, 2H, $^3J_{\text{H-H}}$ = 1 Hz, Im{H^2 and H$^{2'}$}).

[PtMe$_2${(mim)$_2$C=CH$_2$}]·0.5CH$_2$Cl$_2$, 4.2. [Pt$_2$Me$_4$(μ-SMe$_2$)$_2$] (0.4 g, 0.70 mmol) was added to a stirring solution of [(mim)$_2$C=CH$_2$], (0.262 g, 1.40 mmol) in ether (15 mL). The complex precipitated out of the solution as a light yellow solid. The suspension was placed in the fridge overnight, and the next day it was filtered. The yellow solid was washed with ether (6 mL) and pentane (6 mL), dissolved in CH$_2$Cl$_2$ precipitated in pentane, and then dried under high vacuum.

Yield 81%. ^{1}H NMR in Acetone-d$_6$: $\delta = 0.53$ (s, 6H, $^2J_{\text{Pt-H}} = 86$ Hz, Pt-CH$_3$), 3.91 (s, 6H, N-CH$_3$), 6.18 (s, 2H, CH$_2$), 7.19 (d, 2H, $^3J_{\text{H-H}} = 1$ Hz, $^3J_{\text{Pt-H}} = 13$ Hz, Im{H^1 and H$^{1'}$}), 7.23 (d, 2H, $^3J_{\text{H-H}} = 1$ Hz, Im{H^2 and H$^{2'}$}). Anal. Calcd. for C$_{12.5}$H$_{19}$ClN$_4$Pt (%): C 32.94, H 4.20, N 12.29; Found: C 32.80, H 4.82, N 11.72.

[PtIMe$_3$\{(mim)$_2$C=CH$_2$\}], 4.3. To a solution of [PtMe$_2$\{(mim)$_2$C=CH$_2$\}], **4.2**, (0.1 g, 0.24 mmol) in ether (10 mL) was added MeI (0.015 mL, 0.24 mmol). There was an immediate color change from yellow to white. The mixture was stirred for 4 hours. A white solid precipitated out. The solvent was decanted, and then the solid was washed with pentane (3 x 1 mL) and ether (3 x 1 mL). Finally the white product was dried under high vacuum. Yield 65 %. ^{1}H NMR in CD$_2$Cl$_2$: $\delta = 0.89$ (s, 3H, $^2J_{\text{Pt-H}} = 74$ Hz, Pt-CH$_3$), 1.30 (s, 6H, $^2J_{\text{Pt-H}} = 71$ Hz, Pt-CH$_3$), 3.83 (s, 6H, N-CH$_3$), 6.08 (s, 2H, CH$_2$), 7.09 (d, 2H, $^3J_{\text{H-H}} = 1$ Hz, Im{H^2 and H$^{2'}$}), 7.41 (d, 2H, $^3J_{\text{H-H}} = 1$ Hz, $^3J_{\text{Pt-H}} = 9$ Hz, Im{H^1 and H$^{1'}$}). Anal. Calcd. for C$_{13}$H$_{21}$IN$_4$Pt (%): C 28.12, H 3.81, N 10.09; Found: C 28.19, H 4.15, N 9.44.

[PtBr(CH$_2$-C$_6$H$_5$)Me$_2$\{(mim)$_2$C=CH$_2$\}]·0.1\{acetone\}, 4.4. To a solution of complex **4.2** (0.1 g, 0.24 mmol) in acetone (15 mL) was added benzyl bromide (0.04 g, 0.24 mmol). The mixture was stirred for 3 hours. The color of the solution changed from yellow to off white color. The volume was reduced to 1 mL, and pentane (5 mL) was added to precipitate the product as a white solid. The solution was decanted, and the product was then washed with ether and pentane (1 x 2 mL). Finally the white solid was dried under high vacuum. Yield 82 %. ^{1}H-NMR CD$_2$Cl$_2$: *trans*(**4.4a**) $\delta = 1.19$ (s, 6H, $^2J_{\text{Pt-H}} = 71$ Hz, Pt-CH$_3$), 2.99 (s, 2H, $^2J_{\text{Pt-H}} = 99$ Hz, Pt-CH$_2$), 3.79 (s, 6H, N-CH$_3$), 5.98 (s, 2H, CH$_2$), 6.56 (d, 2H, $^3J_{\text{H-H}} = 7$ Hz, $^4J_{\text{Pt-H}} = 11$ Hz, Bn-H$_{ortho}$), 6.81 (t, 2H, $^3J_{\text{H-H}} = 7$ Hz, Bn-H$_{meta}$), 6.92 (d, 1H, $^3J_{\text{H-H}} = 7$ Hz, Bn-H$_{para}$), 6.94 (d, 2H, $^3J_{\text{H-H}} = 2$ Hz, Im{H^2 and H$^{2'}$}), 7.04 (d, 2H, $^3J_{\text{H-H}} = 2$ Hz, $^3J_{\text{Pt-H}} = 9$ Hz, Im{H^1 and H$^{1'}$}); *cis*(**4.4b**) $\delta = 0.79$ (s, 3H, $^2J_{\text{Pt-H}} = 76$

Hz, Pt-CH$_3$), 1.05 (s, 3H, $^2J_{\text{Pt-H}}$ = 71 Hz, Pt-CH$_3$), 3.61 (br, 2H, $^2J_{\text{Pt-H}}$ = 104 Hz, Pt-CH$_2$), 3.76 (s, 3H, N-CH$_3$), 3.78 (s, 3H, N-CH$_3$), 6.05 (s, 1H, CH$_2$), 6.06 (s, 1H, CH$_2$), 6.90-6.92 (m, 2H, Im{H^2 and H$^{2'}$}), 7.06-7.07 (m, 2H, Im{H^1 and H$^{1'}$}), 7.08 (d, 2H, $^3J_{\text{H-H}}$ = 8 Hz, $^4J_{\text{Pt-H}}$ = 11 Hz, Bn-H$_{ortho}$), 7.30 (m, 3H, $^3J_{\text{H-H}}$ = 8 Hz, Bn-H$_{para/meta}$). Anal. Calcd. for C$_{19.3}$H$_{25.6}$BrN$_4$O$_{0.1}$Pt (%): C 39.05, H 4.31, N 9.59; Found: C 39.27, H 4.37, N 9.49.

[PtBr(CH$_2$-4-C$_6$H$_4$-CF$_3$)Me$_2${(mim)$_2$C=CH$_2$}], 4.5. This was prepared similarly to complex **4.4** from complex **2**, and isolated as a white solid. Yield 80 %. ^{1}H-NMR in CD$_2$Cl$_2$: *trans*(**4.5a**) δ = 1.22 (s, 6H, $^2J_{\text{Pt-H}}$ = 70 Hz, Pt-CH$_3$), 3.03 (s, 2H, $^2J_{\text{Pt-H}}$ = 100 Hz, Pt-CH$_2$), 3.80 (s, 6H, N-CH$_3$), 5.99 (s, 2H, CH$_2$), 6.62 (d, 2H, $^3J_{\text{H-H}}$ = 8 Hz, $^4J_{\text{Pt-H}}$ = 11 Hz, Bn-H$_{ortho}$), 6.95 (d, 2H, $^3J_{\text{H-H}}$ = 1 Hz, Im{H^2 and H$^{2'}$}), 7.02 (d, 2H, $^3J_{\text{H-H}}$ = 1 Hz, $^3J_{\text{Pt-H}}$ = 8 Hz, Im{H^1 and H$^{1'}$}),7.07 (d, 2H, $^3J_{\text{H-H}}$ = 8 Hz, Bn-H$_{meta}$); *cis*(**4.5b**) δ = 0.79 (s, 3H, $^2J_{\text{Pt-H}}$ = 74 Hz, Pt-CH$_3$), 1.00 (s, 3H, $^2J_{\text{Pt-H}}$ = 70 Hz, Pt-CH$_3$), 3.59 (d, 1H, $^2J_{\text{H-H}}$ = 9 Hz, $^2J_{\text{Pt-H}}$ = 100 Hz, Pt-CH$_2$), 3.86 (d, 1H, $^2J_{\text{H-H}}$ = 9 Hz, $^2J_{\text{Pt-H}}$ = 84 Hz, Pt-CH$_2$), 3.78 (s, 3H, N-CH$_3$), 3.82 (s, 3H, N-CH$_3$), 6.08 (s, 1H, CH$_2$), 6.09 (s, 1H, CH$_2$), 6.94-6.98 (m, 2H, Im{H^2 and H$^{2'}$}), 7.04-7.07 (m, 2H, Im{H^1 and H$^{1'}$}), 7.34 (d, 2H, $^3J_{\text{H-H}}$ = 8 Hz, Bn-H$_{meta}$), 7.43 (m, 2H, $^3J_{\text{H-H}}$ = 8 Hz, $^4J_{\text{Pt-H}}$ = 11 Hz, Bn-H$_{ortho}$). Anal. Calcd. for C$_{20}$H$_{24}$BrF$_3$N$_4$Pt (%): C 36.82, H 3.71, N 8.59; Found: C 36.59, H 3.60, N 8.78.

[PtBr(CH$_2$-2-C$_6$H$_4$-CF$_3$)Me$_2${(mim)$_2$C=CH$_2$}]·0.05{acetone}, 4.6. This was prepared similarly to complex **4.4** from complex **4.2**, and isolated as a white solid. Yield 81 %. ^{1}H-NMR in CD$_2$Cl$_2$: *trans*(**4.6a**) δ = 1.28 (s, 6H, $^2J_{\text{Pt-H}}$ = 70 Hz, Pt-CH$_3$), 3.25 (s, 2H, $^2J_{\text{Pt-H}}$ = 108 Hz, Pt-CH$_2$), 3.77 (s, 6H, N-CH$_3$), 5.79 (s, 2H, CH$_2$), 6.96 (d, 1H, $^3J_{\text{H-H}}$ = 6 Hz, $^4J_{\text{Pt-H}}$ = 13 Hz, Bn-H$_{ortho}$), 6.99 (d, 2H, $^3J_{\text{H-H}}$ = 1 Hz, Im{H^2 and H$^{2'}$}), 7.11 (d, 1H, $^3J_{\text{H-H}}$ = 1 Hz, $^3J_{\text{Pt-H}}$ = 8 Hz, Im{H^1 and H$^{1'}$}),7.15-7.18 (m, 2H, Bn-H$_{meta/para}$), 7.18 (d, 1H, $^3J_{\text{H-H}}$ = 8 Hz, Bn-H$_{meta}$); *cis*(**4.6b**) δ = 0.76 (s, 3H, $^2J_{\text{Pt-H}}$ = 74 Hz, Pt-CH$_3$), 1.15 (s, 3H, $^2J_{\text{Pt-H}}$ = 70 Hz, Pt-CH$_3$), 3.69 (m, 2H, Pt-CH$_2$), 3.78 (s, 3H, N-

CH$_3$), 3.80 (s, 3H, N-CH$_3$), 6.08 (s, 1H, CH$_2$), 6.10 (s, 1H, CH$_2$), 7.05-7.08 (m, 4H, Im{H^1, H$^{1'}$, H^2 and H$^{2'}$}), 7.19-7.21 (d, 1H, Bn-H$_{meta}$), 7.28 (t, 1H, $^3J_{\text{H-H}}$ = 8 Hz, Bn-H$_{para}$), 7.32 (d, 1H, $^3J_{\text{H-H}}$ = 5 Hz, $^4J_{\text{Pt-H}}$ = 9 Hz, Bn-H$_{ortho}$), 7.43 (d, 1H, $^3J_{\text{H-H}}$ = 8 Hz, Bn-H$_{meta}$). Anal. Calcd. for C$_{20.1}$H$_{24.3}$BrF$_3$N$_4$O$_{0.05}$Pt (%): C 36.82, H 3.71, N 8.59; Found: C 36.93, H 3.74, N 8.55.

[PtBr(CH$_2$-3,5-C$_6$H$_3$-{*t*-Bu}$_2$)Me$_2${(mim)$_2$C=CH$_2$}], 4.7. This was prepared similarly to complex **4.4** from complex **4.2**, and isolated as a white solid. Yield 83 %. ^{1}H-NMR in CD$_2$Cl$_2$: *trans*(**4.7a**) δ = 1.07 (s, 18H, *t*-Bu), 1.26 (s, 6H, $^2J_{\text{Pt-H}}$ = 71 Hz, Pt-CH$_3$), 2.99 (s, 2H, $^2J_{\text{Pt-H}}$ = 93 Hz, Pt-CH$_2$), 3.75 (s, 6H, N-CH$_3$), 6.01 (s, 2H, CH$_2$), 6.26 (d, 2H, $^4J_{\text{H-H}}$ = 2 Hz, $^4J_{\text{Pt-H}}$ = 10 Hz, Bn-H$_{ortho}$), 6.87 (d, 2H, $^3J_{\text{H-H}}$ = 2 Hz, Im{H^2 and H$^{2'}$}), 6.90 (t, 2H, $^3J_{\text{H-H}}$ = 2 Hz, Bn-H$_{para}$), 6.95 (d, 2H, $^3J_{\text{H-H}}$ = 2 Hz, $^3J_{\text{Pt-H}}$ = 7 Hz, Im{H^1 and H$^{1'}$}); *cis*(**4.7b**) δ = 0.80 (s, 3H, $^2J_{\text{Pt-H}}$ = 76 Hz, Pt-CH$_3$), 1.06 (s, 18H, *t*-Bu), 1.14 (s, 3H, $^2J_{\text{Pt-H}}$ = 71 Hz, Pt-CH$_3$), 3.67 (b, 2H, Pt-CH$_2$), 3.74 (s, 3H, N-CH$_3$), 3.79 (s, 3H, N-CH$_3$), 6.03 (s, 1H, CH$_2$), 6.05 (s, 1H, CH$_2$), 7.04-7.11 (m, 4H, Im{H^1, H$^{1'}$, H^2, and H$^{2'}$}), 7.18 (s, 2H, $^4J_{\text{Pt-H}}$ = 11 Hz, Bn-H$_{ortho}$), 7.29 (m, 1H, Bn-H$_{para}$). Anal. Calcd. for C$_{27}$H$_{41}$BrN$_4$Pt (%): C 46.55, H 5.93, N 8.04; Found: C 46.79, H 5.71, N 7.85.

[PtCl(CH$_2$Cl)Me$_2${(mim)$_2$C=CH$_2$}], 4.8. [PtMe$_2${(mim)$_2$C=CH$_2$}], **4.2**, (0.05 g, 0.12 mmol) was dissolved in CH$_2$Cl$_2$ (2 mL). The colorless mixture was stirred for 2 days. The solvent was pumped off, and a white precipitate was produced. The solid was washed with pentane (3 x 1 mL) and ether (3 x 1 mL). Finally the white product was dried under high vacuum. Yield 78 %. ^{1}H-NMR in CD$_2$Cl$_2$: *trans*(**4.8a**) δ = 1.12 (s, 6H, $^2J_{\text{Pt-H}}$ = 70 Hz, Pt-CH$_3$), 3.72 (s, 2H, $^2J_{\text{Pt-H}}$ = 56 Hz, Pt-CH$_2$), 3.84 (s, 6H, N-CH$_3$), 6.11 (s, 2H, CH$_2$), 7.15 (d, 2H, $^3J_{\text{H-H}}$ = 2 Hz, $^3J_{\text{Pt-H}}$ = 9 Hz, Im{H^1 and H$^{1'}$}), 7.20 (d, 2H, $^3J_{\text{H-H}}$ = 2 Hz, Im{H^2 and H$^{2'}$}); *cis*(**4.8b**) δ = 0.89 (s, 3H, $^2J_{\text{Pt-H}}$ = 74 Hz, Pt-CH$_3$), 1.13 (s, 3H, $^2J_{\text{Pt-H}}$ = 69 Hz, Pt-CH$_3$), 3.80 (s, 3H, N-CH$_3$), 3.81 (s, 3H, N-CH$_3$), 4.13 (s, 1H, $^2J_{\text{Pt-H}}$ = 45 Hz, Pt-CH$_2$Cl), 4.60 (s, 1H, $^2J_{\text{Pt-H}}$ = 88 Hz, Pt-CH$_2$Cl), 6.09 (s, 1H, CH$_2$),

6.10 (s, 1H, CH$_2$), 7.07 (br, 2H, Im{ H^2, and H$^{2'}$}), 7.27 (d, 1H, $^3J_{H-H}$ = 2 Hz, $^3J_{Pt-H}$ = 12 Hz, Im{H^1 or H$^{1'}$} *trans* to CH$_2$Cl), 7.50 (d, 1H, $^3J_{H-H}$ = 2 Hz, $^3J_{Pt-H}$ = 6 Hz, Im{H^1 or H$^{1'}$} *trans* to CH$_3$). Anal. Calcd. for C$_{13}$H$_{20}$Cl$_2$N$_4$Pt (%): C 29.25, H 3.90, N 10.25; Found: C 29.24, H 3.86, N 10.23.

[Pt(OH)$_2$Me$_2${(mim)$_2$C=CH$_2$}], 4.9. The reaction of H$_2$O$_2$ with complex **4.2** was performed in an NMR tube. Complex **4.2**, [PtMe$_2${(mim)$_2$C=CH$_2$}], (0.001 g, 0.002 mmol) was dissolved in acetone-d$_6$ (1 mL), and then excess hydrogen peroxide (0.001 mL) was added to the solution. The solution color turned from yellow to white rapidly. The mixture was transferred to an NMR tube, which was then placed in the NMR probe (Inova 400 MHz). ^{1}H-NMR acetone-d$_6$: δ = 1.36 (s, 6H, $^2J_{Pt-H}$ = 73 Hz, Pt-CH$_3$), 2.99 (br, 2H, OH), 3.98 (s, 6H, N-CH$_3$), 6.21 (s, 2H, CH$_2$), 7.25 (d, 2H, $^3J_{H-H}$ = 2 Hz, Im{H^2 and H$^{2'}$}), 7.30 (d, 2H, $^3J_{H-H}$ = 1 Hz, $^3J_{Pt-H}$ = 14 Hz, Im{H^1 and H$^{1'}$}).

[Pt(OOCPh)$_2$Me$_2${(mim)$_2$C=CH$_2$}], 4.10. This was prepared similarly to complex **4.9** from complex **4.2**. ^{1}H-NMR acetone-d$_6$: δ = 1.68 (s, 3H, $^2J_{Pt-H}$ = 73 Hz, Pt-CH$_3$), 2.10 (s, 3H, $^2J_{Pt-H}$ = 67 Hz, Pt-CH$_3$), 4.01 (s, 3H, N-CH$_3$), 4.05 (s, 3H, N-CH$_3$), 6.33 (s, 1H, CH$_2$), 6.37 (s, 1H, CH$_2$), 7.32-7.37 (m, 4H, Im{H^1, H$^{1'}$,H^2 and H$^{2'}$}), 7.65-8.07 (8H, Phenyl).

[(mim)$_2$CHMe], 4.11. The procedure was followed according to the literature.[11] The product was isolated as white crystals. Yield 78 %. ^{1}H NMR in CD$_2$Cl$_2$: δ = 1.75 (d, 3H, $^3J_{H-H}$ = 7 Hz, CCH$_3$), 3.39 (s, 6H, N-CH$_3$), 4.48 (q, 1H, $^3J_{H-H}$ = 7 Hz, C-H), 6.79 (d, 2H, $^3J_{H-H}$ = 1 Hz, Im{H^1 and H$^{1'}$}), 6.87 (d, 2H, $^3J_{H-H}$ = 1 Hz, Im{H^2 and H$^{2'}$}).

[PtMe$_2${(mim)$_2$CHMe}], 4.12, This was prepared similarly to complex **4.2** from complex **4.11**, and isolated as a yellow solid. Yield 83 %. ^{1}H-NMR in acetone-d$_6$: δ = 0.49 (s, 6H, $^2J_{Pt-H}$ = 88 Hz, Pt-CH$_3$), 1.66 (d, 3H, $^3J_{H-H}$ = 7 Hz, CCH$_3$), 3.82 (s, 6H, N-CH$_3$), 4.64 (q, 1H, $^3J_{H-H}$ = 7 Hz, C-H), 7.03 (d, 2H, $^3J_{H-H}$ = 2 Hz, Im{H^2 and H$^{2'}$}), 7.08 (d, 2H, $^3J_{H-H}$ = 2 Hz, $^3J_{Pt-H}$ = 14 Hz, Im{H^1

and H$^{1'}$}). Anal. Calcd. for C$_{12}$H$_{20}$N$_4$Pt (%): C 34.70, H 4.85, N 13.49; Found: C 34.48, H 5.02, N 13.29.

[PtIMe$_3$\{(mim)$_2$CHMe\}], 4.13, This was prepared similarly to complex **4.3** from complex **4.12**, and isolated as a white solid. Yield 79 %. ^{1}H-NMR in CD$_2$Cl$_2$: (**4.13a**) δ = 0.93 (s, 3H, $^2J_{Pt-H}$ = 75 Hz, Pt-CH$_3$), 1.32 (s, 6H, $^2J_{Pt-H}$ = 70 Hz, Pt-CH$_3$), 1.55 (d, 3H, $^3J_{H-H}$ = 8 Hz, CCH$_3$), 3.75 (s, 6H, N-CH$_3$), 4.45 (q, 1H, $^3J_{H-H}$ = 8 Hz, C-H), 7.01 (d, 2H, $^3J_{H-H}$ = 2 Hz, Im\{H^2 and H$^{2'}$\}), 7.38 (d, 2H, $^3J_{H-H}$ = 2 Hz, $^3J_{Pt-H}$ = 10 Hz, Im\{H^1 and H$^{1'}$\}); (**4.13b**) δ = 0.70 (s, 3H, $^2J_{Pt-H}$ = 74 Hz, Pt-CH$_3$), 1.37 (s, 6H, $^2J_{Pt-H}$ = 70 Hz, Pt-CH$_3$), 1.94 (d, 3H, $^3J_{H-H}$ = 7 Hz, CCH$_3$), 3.74 (s, 6H, N-CH$_3$), 4.49 (q, 1H, $^3J_{H-H}$ = 7 Hz, C-H), 6.99 (d, 2H, $^3J_{H-H}$ = 2 Hz, Im\{H^2 and H$^{2'}$\}), 7.20 (d, 2H, $^3J_{H-H}$ = 2 Hz, $^3J_{Pt-H}$ = 11 Hz, Im\{H^1 and H$^{1'}$\}). Anal. Calcd. for C$_{13}$H$_{23}$IN$_4$Pt (%): C 28.02, H 4.16, N 10.05; Found: C 28.29, H 3.97, N 9.77.

[PtI$_2$Me$_2$\{(mim)$_2$CHMe\}], 4.14. The reaction of I$_2$ with complex **4.12** was performed in an NMR tube. Complex **4.12**, [PtMe$_2$\{(mim)$_2$CHMe\}], (0.014 g, 0.33 mmol) was dissolved in acetone-d$_6$ (1 mL), and then iodine (0.085 mL) was added to the solution. The solution color turned from colorless to organge rapidly. ^{1}H-NMR CD$_2$Cl$_2$: δ = 1.89 (d, 3H, $^3J_{H-H}$ = 7 Hz, CCH$_3$), 2.32 (s, 6H, $^2J_{Pt-H}$ = 71 Hz, Pt-CH$_3$), 3.87 (s, 6H, N-CH$_3$), 4.64 (q, 1H, $^3J_{H-H}$ = 7 Hz, C-H), 7.08 (d, 2H, $^3J_{H-H}$ = 2 Hz, $^4J_{Pt-H}$ = 3 Hz Im\{H^2 and H$^{2'}$\}), 7.26 (d, 2H, $^3J_{H-H}$ = 2 Hz, $^3J_{Pt-H}$ = 9 Hz, Im\{H^1 and H$^{1'}$\}).

[PtBr(CH$_2$-2-C$_6$H$_4$-CF$_3$)Me$_2$\{(mim)$_2$CHMe\}], 4.15. This was prepared similarly to complex **4.4** from complex **4.12**, and isolated as a white solid. Yield 81 %. ^{1}H-NMR CD$_2$Cl$_2$: δ = 1.34 (s, 6H, $^2J_{Pt-H}$ = 69 Hz, Pt-CH$_3$), 1.86 (d, 3H, $^3J_{H-H}$ = 7 Hz, CCH$_3$), 3.11 (s, 2H, $^2J_{Pt-H}$ = 104 Hz, Pt-CH$_2$), 3.69 (s, 6H, N-CH$_3$), 4.32 (q, 1H, $^3J_{H-H}$ = 7 Hz, C-H), 6.71 (m, 1H, Bn-H$_{ortho}$), 6.78 (d, 2H, $^3J_{H-H}$ = 1 Hz, Im\{H^2 and H$^{2'}$\}), 6.81 (d, 2H, $^3J_{H-H}$ = 1 Hz, $^3J_{Pt-H}$ = 7 Hz, Im\{H^1 and H$^{1'}$\}), 7.01-7.08 (m,

3H, Bn-H*meta/para*). Anal. Calcd. for $C_{20}H_{26}BrF_3N_4Pt$ (%): C 36.71, H 4.00, N 8.56; Found: C 36.54, H 3.73, N 8.81.

[PtBr(CH$_2$-4-C$_6$H$_4$-CF$_3$)Me$_2${(mim)$_2$CHMe}], 4.16. This was prepared similarly to complex **4.4** from complex **4.12**, and isolated as a white solid. Yield 79 %. ^{1}H-NMR CD$_2$Cl$_2$: δ = 1.34 (s, 6H, $^2J_{Pt-H}$ = 69 Hz, Pt-CH$_3$), 1.73 (d, 3H, $^3J_{H-H}$ = 8 Hz, CCH$_3$), 2.87 (s, 2H, $^2J_{Pt-H}$ = 97 Hz, Pt-CH$_2$), 3.66 (s, 6H, N-CH$_3$), 4.18 (q, 1H, $^3J_{H-H}$ = 8 Hz, C-H), 6.36 (d, 2H, $^3J_{H-H}$ = 8 Hz, $^4J_{Pt-H}$ = 11 Hz, Bn-H*ortho*), 6.84 (d, 2H, $^3J_{H-H}$ = 2 Hz, Im{H^2 and H$^{2'}$}), 6.93 (d, 2H, $^3J_{H-H}$ = 8 Hz, Bn-H*meta*), 7.02 (d, 2H, $^3J_{H-H}$ = 2 Hz, $^3J_{Pt-H}$ = 7 Hz, Im{H^1 and H$^{1'}$}). Anal. Calcd. for $C_{20}H_{26}BrF_3N_4Pt$ (%): C 36.71, H 4.00, N 8.56; Found: C 36.65, H 3.84, N 8.31.

[Pt(OH)$_2$Me$_2${(mim)$_2$CHMe}], 4.17. The reaction of H$_2$O$_2$ with complex **4.12** was performed in an NMR tube in a similar way to the reaction of iodine with **4.12**. Complex **4.12**, [PtMe$_2${(mim)$_2$CHMe}], (0.005 g, 0.012 mmol) was dissolved in acetone-d$_6$ (1 mL), and then H$_2$O$_2$ (0.0004 mL) was added to the solution. The solution color turned from colorless to orange rapidly. ^{1}H-NMR in acetone-d$_6$: δ = 1.37 (s, 6H, $^2J_{Pt-H}$ = 73 Hz, Pt-CH$_3$), 1.80 (d, 3H, $^3J_{H-H}$ = 7 Hz, CCH$_3$), 3.92 (s, 6H, N-CH$_3$), 4.80 (q, 1H, $^3J_{H-H}$ = 7 Hz, C-H), 7.17 (d, 2H, $^3J_{H-H}$ = 2 Hz, $^3J_{Pt-H}$ = 10 Hz, Im{H^1 and H$^{1'}$}), 7.19 (d, 2H, $^3J_{H-H}$ = 2 Hz, Im{H^2 and H$^{2'}$}).

X-ray Structure Determinations: X-ray data were obtained and solutions were determined by Dr. G. Popov and Dr. Benjamin Cooper in this chapter. Suitable crystals were mounted on a glass fiber, and data were collected at low temperature (-123 °C) on a Nonius Kappa-CCD area detector diffractometer with COLLECT (Nonius B.V., 1997-2002). The unit cell parameters were calculated and refined from the full data set. The crystal data and refinement parameters for all complexes are listed in the following tables.

Table 4.6. Crystallographic data for **4.3**.

_____

$[PtIMe_3\{(mim)_2C=CH_2\}]$

_____

Empirical formula	$C_{13} H_{21} I N_4 Pt$
Formula weight	555.32
Wavelength	0.71073 Å
Crystal system	Monoclinic
Space group	$P\,2_1/n$
Unit cell dimensions	$a = 16.424(8)$ Å $\quad\quad \alpha = 90°$
	$b = 13.051(6)$ Å $\quad\quad \beta = 96.09(2)°$
	$c = 16.649(7)$ Å $\quad\quad \gamma = 90°$
Volume	$3548.9(3)$ Å^3
Z	4
Density (calculated)	1.917 Mg/m^3
Absorption coefficient	9.796 mm^{-1}
Crystal size	0.4 x 0.2 x 0.1 mm^3
Refinement method	Full-matrix least-squares on F^2
Goodness-of-fit on F^2	1.033
Final R indices [I>2sigma(I)]	R1 = 0.0504, wR2 = 0.1003
R indices (all data)	R1 = 0.0746, wR2 = 0.1154

Table 4.7. Crystallographic data for **4.4a**.

_____

$[PtIMe_3\{(mim)_2C=CH_2\}]\cdot 0.5CH_2Cl_2$

_____

Empirical formula	$C_{19.5} H_{26} Br Cl N_4 Pt$
Formula weight	626.89
Wavelength	0.71073 Å
Crystal system	Monoclinic
Space group	C 2/c
Unit cell dimensions	a = 21.034(1) Å $\qquad$ α= 90°
	b = 16.738(1) Å $\qquad$ β= 110.30(3)°
	c = 12.754(6) Å $\qquad$ γ = 90°
Volume	4211.2(4) $Å^3$
Z	8
Density (calculated)	1.978 Mg/m^3
Absorption coefficient	8.700 mm^{-1}
Crystal size	0.08 x 0.06 x 0.04 mm^3
Refinement method	Full-matrix least-squares on F^2
Goodness-of-fit on F^2	1.008
Final R indices [I>2sigma(I)]	R1 = 0.0499, wR2 = 0.1078
R indices (all data)	R1 = 0.0864, wR2 = 0.1241

Table 4.8. Crystallographic data for **4.6a**.

———

$trans$-[PtBr(CH_2-2-C_6H_4-CF_3)Me_2{$(mim)_2C=CH_2$}]

———

Empirical formula	$C_{20} H_{24} Br F_3 N_4 Pt$	
Formula weight	652.43	
Wavelength	0.71073 Å	
Crystal system	Monoclinic	
Space group	$P\,2_1/c$	
Unit cell dimensions	a = 10.831 (4) Å	$\alpha = 90°$
	b = 16.855(5) Å	$\beta = 105.87(1)°$
	c = 12.585(7) Å	$\gamma = 90°$
Volume	2209.9(3) Å^3	
Z	4	
Density (calculated)	1.961 Mg/m^3	
Absorption coefficient	8.196 mm^{-1}	
Crystal size	0.4 x 0.2 x 0.2 mm^3	
Refinement method	Full-matrix least-squares on F^2	
Goodness-of-fit on F^2	1.038	
Final R indices [I>2sigma(I)]	R1 = 0.0350, wR2 = 0.0809	
R indices (all data)	R1 = 0.0577, wR2 = 0.0900	

Table 4.9. Crystallographic data for **4.7a**.

_____

trans-[PtBr(CH$_2$-3,5-C$_6$H$_4$-{*t*-Bu}$_2$)Me$_2${(mim)$_2$C=CH$_2$}]

_____

Empirical formula	C$_{27}$ H$_{41}$ Br N$_4$ Pt	
Formula weight	696.62	
Wavelength	0.71073 Å	
Crystal system	Orthorhombic	
Space group	Pbcn	
Unit cell dimensions	a = 30.038(2) Å	α= 90°
	b = 16.554(1) Å	β= 90°
	c = 12.574(9) Å	γ = 90°
Volume	6252.4 (8) Å^3	
Z	8	
Density (calculated)	1.585 Mg/m^3	
Absorption coefficient	5.802 mm^{-1}	
Crystal size	0.4 x 0.2 x 0.2 mm^3	
Refinement method	Full-matrix least-squares on F^2	
Goodness-of-fit on F^2	1.209	
Final R indices [I>2sigma(I)]	R1 = 0.0514, wR2 = 0.0829	
R indices (all data)	R1 = 0.0620, wR2 = 0.0867	

Table 4.10. Crystallographic data for **4.15**.

_____

$trans$-[PtBr(CH$_2$-2-C$_6$H$_4$-CF$_3$)Me$_2${(mim)$_2$CHMe}]

_____

Empirical formula	C$_{20}$ H$_{26}$ Br F$_3$ N$_4$ Pt
Formula weight	654.45
Wavelength	0.71073 Å
Crystal system	Monoclinic
Space group	P2$_1$/c
Unit cell dimensions	a = 10.627(7) Å α= 90°
	b = 16.545(1) Å β= 105.74(2)°
	c = 12.967(9) Å γ = 90°
Volume	2194.4 (3) Å^3
Z	4
Density (calculated)	1.981 Mg/m^3
Absorption coefficient	8.254 mm^{-1}
Crystal size	0.4 x 0.4 x 0.3 mm^3
Refinement method	Full-matrix least-squares on F^2
Goodness-of-fit on F^2	1.013
Final R indices [I>2sigma(I)]	R1 = 0.0310 wR2 = 0.0522
R indices (all data)	R1 = 0.0529, wR2 = 0.0579

4.5 References

1. a) Rendina, L. M.; Puddephatt, R. J. *Chem. Rev.*, **1997**, 97, 1735. b) Yahav, A.; Goldberg, I.; Vigalok, A. *Organometallics*, **2005**, 24, 5654.

2. a) Stille, J. K.; *The Chemistry of the Metal-Carbon Bond*; Hartley, F. R.; Patai, S., Eds.; Wiley: New York, **1985**; vol. 2, Chapter 9.

3. Zhang, F.; Broczkowski, M. E.; Jennings, M. C.; Puddephatt, R. J. *Can. J. Chem.*, **2005**, 83, 595.

4. Frausto da Silva, J. J. R.; Williams, R. J. P. *The Biological Chemistry of the Elements, The Inorganic Chemistry of Life*, Clarendon Press, Oxford, **1991**.

5. a) Van Kralingen, C. G.; Reedijk, J. *Inorg. Chem. Acta*, **1978**, 30, 171. b) Fazakerley, G. V.; Koch, K. R. *Inorg. Chem. Acta*, **1979**, 36, 13.

6. Graves, B. J.; Hodgson, D. J.; Van Kralingen, C. G.; Reedijk, J. *Inorg. Chem.*, **1978**, 17, 3007.

7. Periana, R. A.; Taube, D. J.; Gamble, S.; Taube, H.; Satoh, T.; Fujii, H. *Science*, **1998**, 280, 560.

8. Canty, A. J.; Lee, C. V. *Organometallics*, **1982**, 1, 1063.

9. Byers, P. K.; Canty, A. J.; Engelhardt, L. M.; Patrick, J. M.; White, A. H. *J. Chem. Soc. Dalton Trans.*, **1985**, 981.

10. a) Bulak, E.; Sarper, O.; Dogan, A.; Lissner, F.; Schleid, T.; Kaim, W. *Polyhedron*, **2006**, 25, 2577. b) Messerschmidt, A. *Handbook of Metalloproteins*, Wiley, New York, **2004**.

11. Byers, P. K.; Canty, A. J. *Organometallics*, **1990**, 9, 210.

12. Hill, G.; Irwin, M. J.; Levy, C. J.; Rendina, L. M.; Puddephatt, R. J. *Inorg. Synth.*, **1998**, 32 149.

13. Baar, C. R.; Jenkins, H. A.; Vittal, J. J.; Yap, G. P. A.; Puddephatt, R. J. *Organometallics*, **1998**, 17, 2805.

14. a) Monaghan, P. K.; Puddephatt, R. J. *Organometallics*, **1985**, 4, 1406. b) Scott, J. D.; Puddephatt, R. J. *Organometallics*, **1986**, 5, 1538. c) Achar, S.; Scott, J. D.; Puddephatt, R. J. *Polyhedron*, **1996**, 15, 2363.

15. a) Au. R. H. W.; Fraser, C. S. A.; Eisler, D. J.; Jennings, M. C.; Puddephatt, R. J. *Organometallics*, **2009**, 28, 1719. b) Au. R. H. W.; Jennings, M. C.; Puddephatt, R. J. *Organometallics*, **2009**, 28, 3754. c) Au. R. H. W.; Jennings, M. C.; Puddephatt, R. J. *Organometallics*, **2009**, 28, 5052.

16. Miao, W. S; Chan, T. H. *Acc. Chem. Res.*, **2006**, 39, 897.

17. a) Kuyper, J. *Inorg. Chem.*, **1978**, 17, 77. b) Momeni, B. Z.; Moradi, Z.; Rashidi, M.; Rominger, F.; *Polyhedron*, **2009**, 28, 381.

18. (a) Shilov, A. E.; Shul'pin, G. B. *Chem. Rev.*, **1997**, 97, 2879. (b) He, Z.; Wong, W.; Yu, X.; Kwok, H.; Lin, Z. *Inorg. Chem.*, **2006**, 45, 10922. (c) Song, D.; Sliwowski, K.; Pang, J.; Wang, S. *Organometallics*, **2002**, 21, 4978.

19. (a) Aye. K. T.; Vittal, J. J.; Puddephatt, R. J. *J. Chem. Soc., Dalton Trans.*, **1993**, 1835. (b) Thorshaug, K.; Fjeldahl, I.; Romming, C.; Tilset, M. *Dalton Trans*., **2003**, 4051. (c) Prokopchuk, E. M.; Puddephatt, R. J. *Can. J. Chem.*, **2003**, 81, 476.

CHAPTER 5

Supramolecular Organoplatinum(IV) Chemistry

5.1 Introduction

Hydrogen bonding is a vital phenomenon in the field of supramolecular chemistry, self-assembly, and crystal engineering. It is widely used in supramolecular chemistry to organize macromolecules into functional molecular materials.[1] The hydrogen bond is easily introduced and directional, and it has become vital tool in crystal design strategies for the self-assembly of solid state supramolecular compounds.[2] Also, this type of bonding is weak enough to be reversibly dissociated in solution, thus playing a very significant role in supramolecular processes.[1,2]

The chemistry of platinum is responsible for several important advances in the field of coordination chemistry. The organometallic chemistry of platinum(II) and platinum(IV) has been thoroughly studied, which is a key to the understanding of several catalytic reactions.[3] The crystal engineering in the field of organometallic complexes has developed more gradually than with coordination chemistry, and that is mainly because of the high reactivity of many metal-carbon bonds to the hydrogen bond donor functional groups.[1,4] The use of platinum complexes in self-assembly chemistry has been limited due to the slow ligand substitution on platinum(II) and platinum(IV) complexes compared to the analogues of palladium, but the relative inertness of organoplatinum compounds is an advantage in self-assembly via secondary bonding interactions such as hydrogen bonding.[1] In recent years, there has been great interest in self-assembly of polymers and networks using simple coordination complexes and organometallic complexes as building blocks to give functional molecular materials via the combination of inorganic and organometallic synthetic methods with self-assembly through hydrogen bonding.[5]

There is continuing interest in the usage of dimethylplatinum(II) complexes containing bidentate nitrogen donor ligands in the field of supramolecular chemistry. Some of those recently used ligands contain ester and amide functional groups as hydrogen bond acceptors, and others contained neither hydrogen bond acceptors nor donors, but such acceptors and donors were introduced upon oxidative addition (Chart 5.1).[4,6] The self-assembly usually occurs among platinum(IV) complexs via hydrogen bonding and π-stacking to form molecular materials. The platinum(IV) complexes are produced by the oxidative addition of various alkyl bromide derivatives containing hydrogen bond donors, such as carboxylic acids, and amides. Most of the known supramolecular organoplatinum(IV) chemistry has been based on the oxidative addition of functional alkyl bromide derivatives, RCH_2Br, to the electron rich platinum(II) complexes.[6,7]
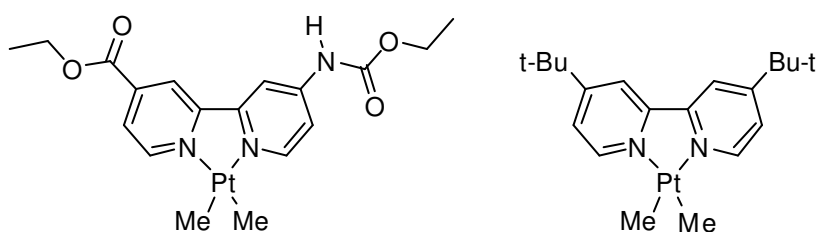
Chart 5.1. Recent platinum(II) complexes used in crystal engineering containing bidentate nitrogen donor ligands.

The oxidative addition of the platinum(II) complex containing both ester and amide functional groups resulted in the corresponding platinum(IV) complexes which formed supramolecular compounds via weak secondary bonding. Several functional groups were introduced upon the oxidative addition, and generally it was challenging to predict the preferred hydrogen-bonding patterns for crystal engineering in the these complexes due to the presence of

several interactions of similar energy.[4,7] However, self-assembly has given several extraordinary

polymer, sheet, and network structures. The most predictable form of self-assembly was through

π-stacking. As known, in order to form polymers by self-assembly, it is necessary to have at

least two hydrogen-bonding donor/acceptor pairs per molecule. Recently organometallic

polymers were produced through hydrogen bonding of diplatinum(IV) complexes containing the

ligand 4,4'-di-*t*-butyl-2,2'-bipyridine.[8] The reaction of RCH$_2$Br with [PtMe$_2$(bu$_2$bipy)] complex

proceeds via a *trans* oxidative addition to give the platinum(IV) complex

[PtBrMe$_2$(CH$_2$R)(bu$_2$bipy)], R = C$_6$H$_4$CO$_2$H (Scheme 5.1). The platinum(IV) complex contain a

hydrogen bond donor/acceptor carboxylic acid, and self-assembly of the platinum(IV)

complexes to form a dimer occurs via hydrogen bonding according to scheme 5.1.
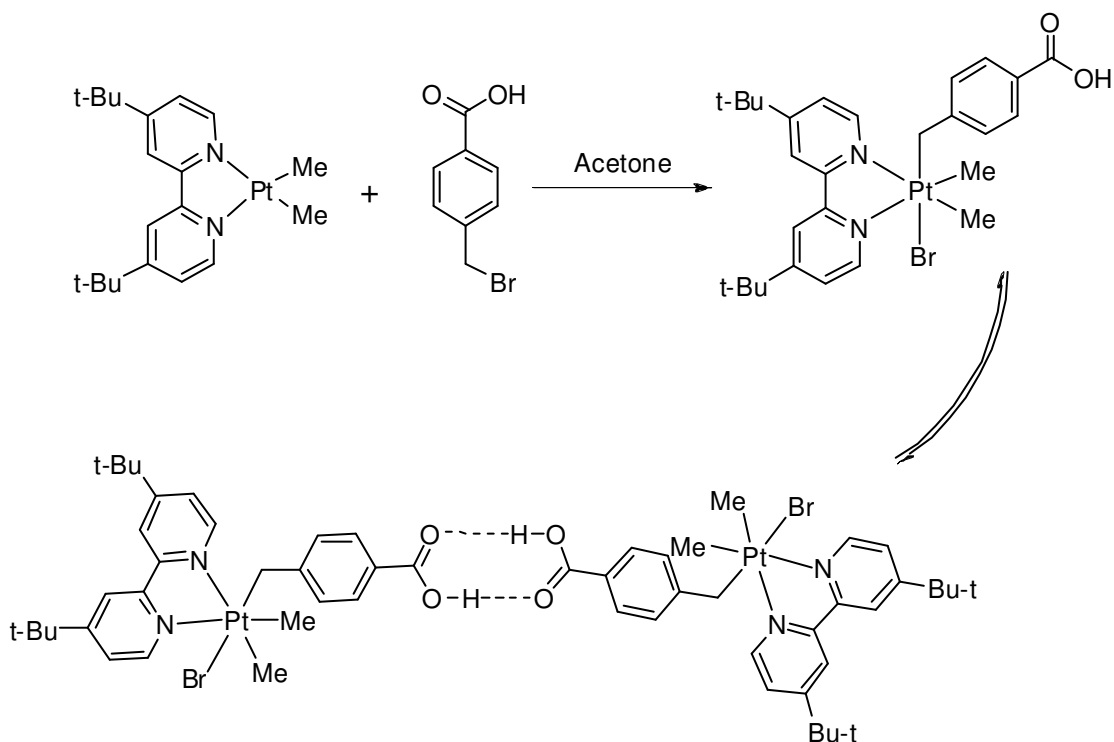
Scheme 5.1

The studies performed in this project expand the work of the crystal engineering using platinum(IV) containing bidentate nitrogen donor ligands. The ligand used in this study contained two ester functional groups and no amide functional group, and it was synthesized from 4,4'-dimethyl-2,2'-bypyridine. Amide groups often form strong intermolecular hydrogen bonds and this typically leads to low solubility in many organic solvents, so such problem is solved by eliminating the amide functional groups from the ligand, and introducing it later via the alkyl bromide reagents with bulky organic groups to increase solubility.[9] Several alkyl bromide groups containing amide, carboxylic acids, and alcohol functional groups are introduced via oxidative addition. The resulted platinum(IV) complexes formed polymers and networks via some predictable self-assembly and other unpredictable ones.

5.2 Results and Discussion

5.2.1 Synthesis and Characterization of [PtMe$_2$(DECBP)]

The ligand 4,4'-diethoxycarbonyl-2-2'-bipyridine (DECBP), **5.1**, was prepared using a modified procedure of Sprintschnik *et al.* (Equation 5.1),[10] and isolated as white crystals. It is very soluble in organic solvents such as acetone, methylene chloride, and chloroform, and it is stable at room temperature.

$$(5.1)$$
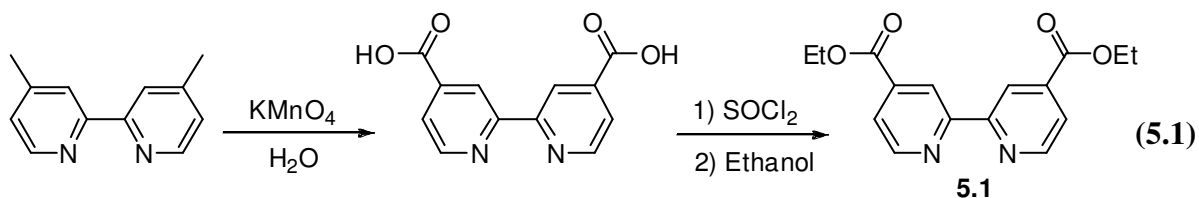
The complex [PtMe$_2$(DECBP)] **(5.2)** was easily prepared by the reaction of the platinum dimer [Pt$_2$Me$_4$(μ-SMe$_2$)$_2$][11] with the ligand DECBP in ether (Equation 5.2). The reaction proceeded very rapidly, and the platinum(II) complex **(5.2)** was isolated as a purple solid that is stable at room temperature, and soluble in various organic solvents. The complex was characterized using its ^{1}H-NMR spectrum, elemental analysis, and X-ray crystallography. In the ^{1}H-NMR spectrum (Figure 5.1), the methylplatinum resonance occurred at δ = 1.14, with coupling $^2J_{Pt-H}$ = 86 Hz, while the *ortho* pyridyl protons occurred at δ = 9.42, with coupling $^3J_{Pt-H}$ = 28 Hz. Only one set of pyridyl resonances was observed due to symmetry.
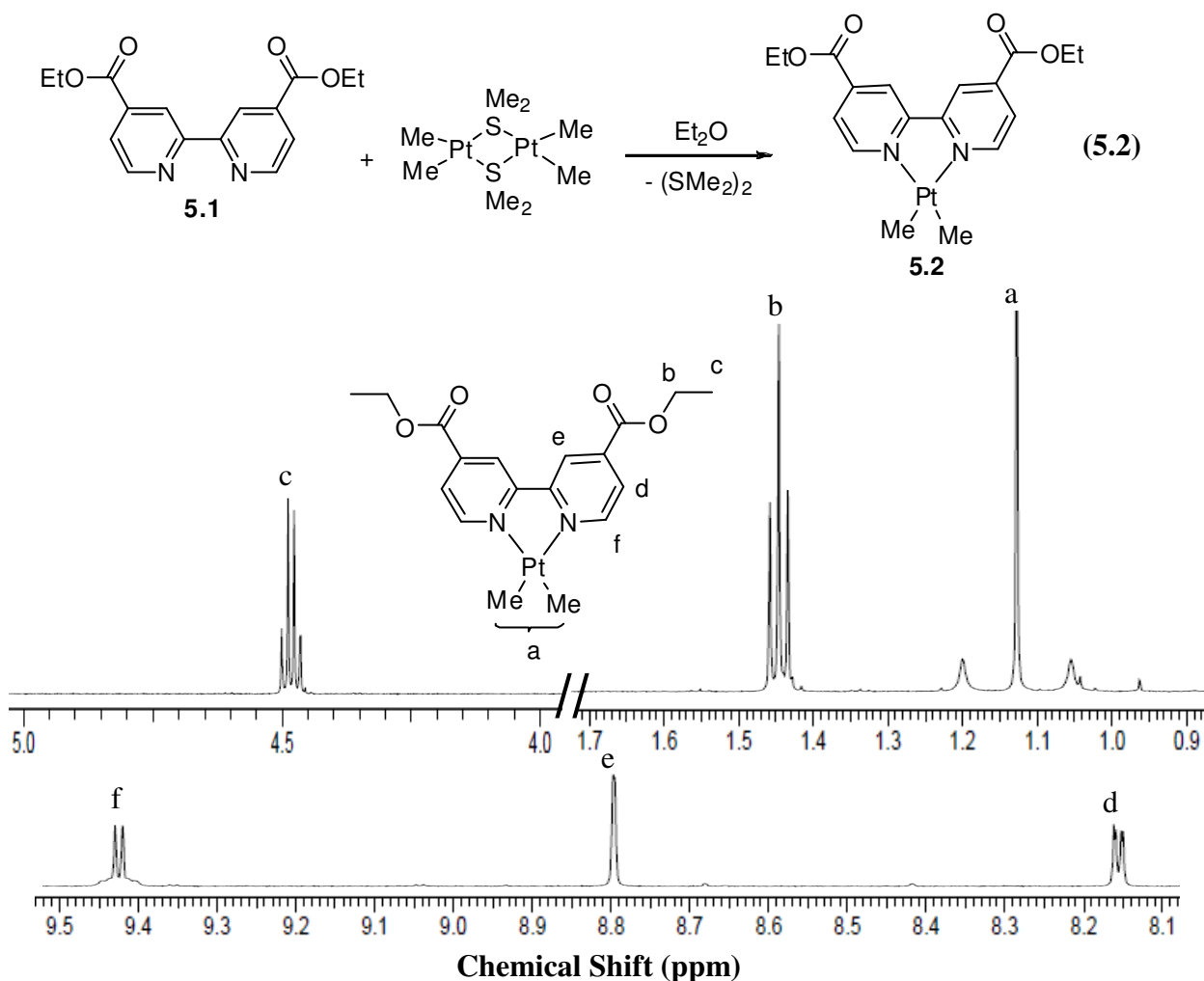
Figure 5.1. ^{1}H-NMR spectrum (400 MHz, acetone-d$_6$) of [PtMe$_2$(DECBP)], **5.2**.

The molecular structure of complex **5.2** was determined using X-ray crystallography, and is shown in Figure 5.2. There is a square planar platinum(II) centre with *cis*-PtC2N2 coordination. The angle N(11)-Pt(1)-N(24) = 78.3(7)^o, which is different from the ideal 90° angle due to the constraints caused by the 5-membered chelate ring. The Pt-N distances (2.075(2) and 2.099(2) Å) are very similar to those in other reported platinum(II) complexes containing dipyridine ligands.[12] Table 5.1 shows selected bond lengths and angles of complex **5.2**.
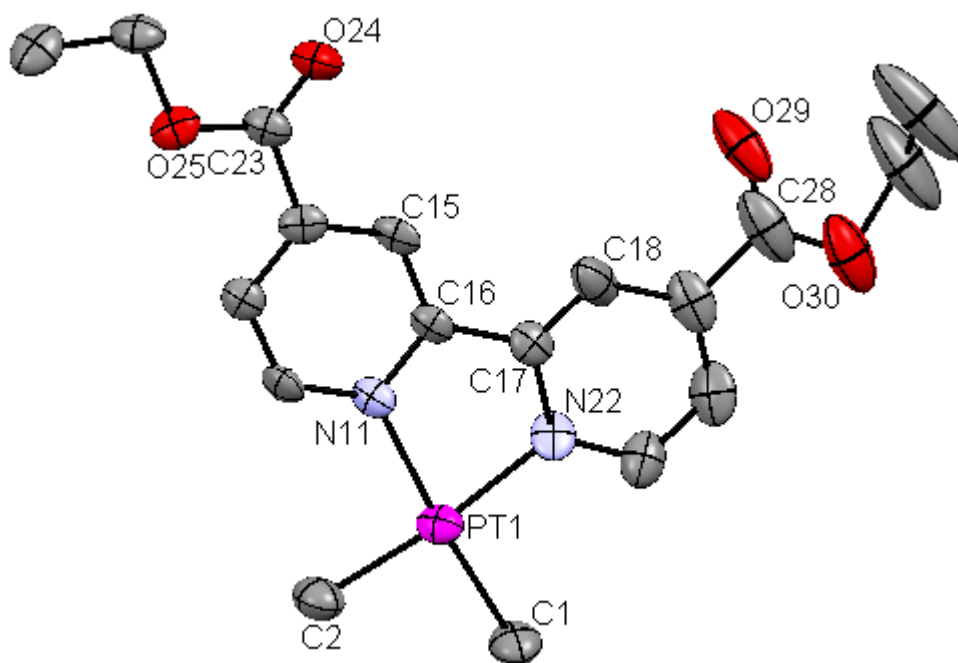
Figure 5.2. A view of the structure of complex **5.2**.

Table 5.1. Selected bond lengths [Å] and angles [°] for **5.2** [PtMe$_2$(DECBP)].

Pt-N(11)	2.099(2)	Pt-N(22)	2.075(2)
Pt-C(1)	2.050(2)	Pt-C(2)	2.070(2)
N(11)-Pt-N(22)	78.3(7)	N(11)-Pt-C(1)	174.5(8)
N(22)-Pt-C(1)	96.7(9)	N(11)-Pt-C(2)	95.3(8)
N(22)-Pt-C(2)	173.4(9)	C(1)-Pt-C(2)	89.7(1)

5.2.2 The Oxidative Addition Chemistry of [PtMe$_2$(DECBP)]

Oxidative addition reaction to the electron-rich metallic center of transition metal complexes is a key step in many catalytically important chemical processes.[13] Several oxidative addition reactions were performed using the complex [PtMe$_2$(DECBP)] **(5.2)** with reagents such as halogens, alkyl halides, peroxides, and hydrochloric acid (Scheme 5.2).
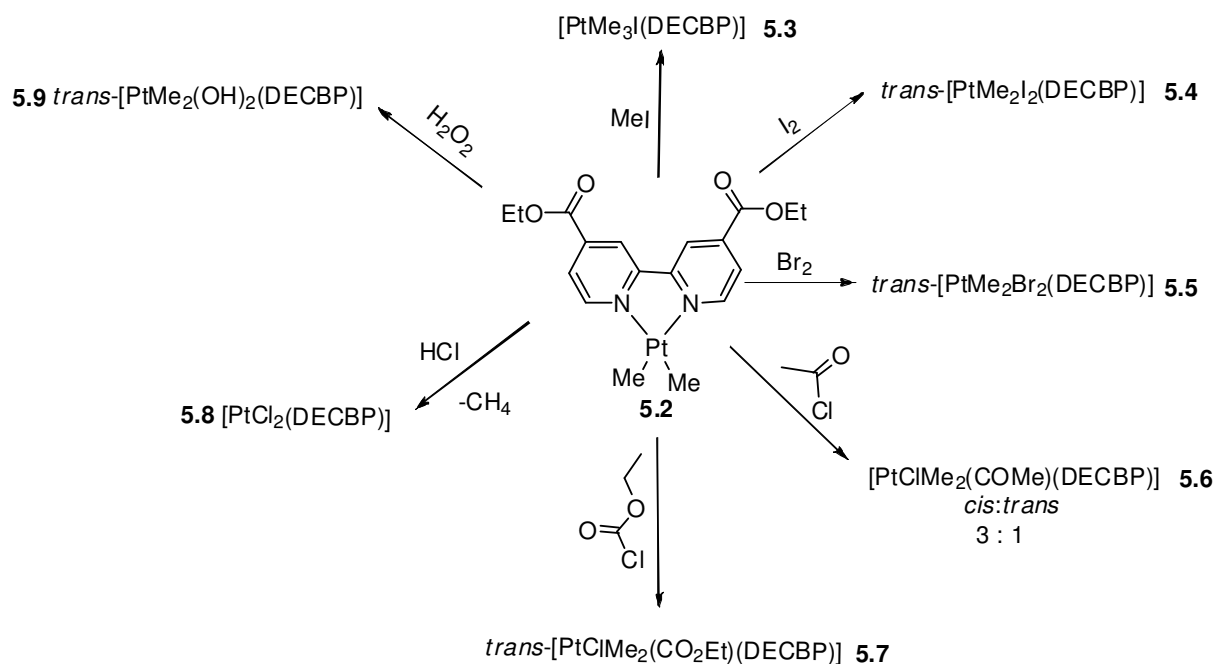
Scheme 5.2

An oxidative addition of methyl iodide to complex **5.2** was carried out in acetone at room temperature to produce a pure and stable trimethylplatinum(IV) complex **5.3** (Scheme 5.2). The complex [PtIMe$_3$(DECBP)] was isolated as a yellow product, and characterized using NMR spectroscopy. The oxidative addition reaction proceeded within five minutes. The ^{1}H-NMR spectrum of **5.3** contained two methyl proton resonances at $\delta = 0.60$ ($^2J_{\text{Pt-H}} = 72$ Hz, *trans* to N), and 1.52 ($^2J_{\text{Pt-H}} = 71$ Hz, *trans* to I). Only one set of pyridyl proton resonances was observed in the ^{1}H-NMR spectrum due to symmetry. The *ortho* proton resonance occurred at $\delta = 9.25$ ($^3J_{\text{Pt-H}} = 20$ Hz, *trans* to C).

Complex **5.4** [PtI$_2$Me$_2$(DECBP)] was prepared by the reaction of complex **5.2** with iodine in a methylene chloride solution (Scheme 5.2). In this reaction, *trans* oxidative addition of the I-I bond occurred at the platinum center. Complex **5.4** was isolated as a stable red solid that is soluble in various organic solvents, which helped in its characterization via NMR spectroscopy. The ^{1}H-NMR spectrum of **5.4** contained one single methylplatinum resonance at $\delta = 2.42$ ($^2J_{\text{Pt-H}} = 73$ Hz, *trans* to N), and one set of pyridyl resonances with *ortho* proton resonance at $\delta = 9.07$ ($^3J_{\text{Pt-H}} = 21$ Hz, *trans* to C), indicating *trans* oxidative addition. The magnitude of ^2J(PtMe) decreased from 86 Hz in the starting platinum(II) complex **5.2** to 73 Hz in the product platinum(IV) complex **5.4**.

The structure of complex **5.4** was determined crystallography, and a view of the structure is shown in Figure 5.3, with selected bond distances and angles listed in the Table 5.2. The structure of complex confirmed that two iodide ligands added *trans* to the platinum center. The platinum(IV) center displays octahedral geometry, with both iodide ligands occupying the axial positions. A primary supramolecular structure, which is a dimer, was formed through secondary bonding between an iodine molecule and two iodide ligands of two platinum(IV) complexes,

with I(1A)••••I(5A) and I(1)••••I(5) = 3.407 Å (Figure 5.4). Part of the supramolecular polymer

structure self-assembled through π-stacking. The I(5A)-I(5) bond distance = 2.748 Å, which is

slightly longer than the usual I-I bond distance in free iodine molecules (2.67 Å).[14]
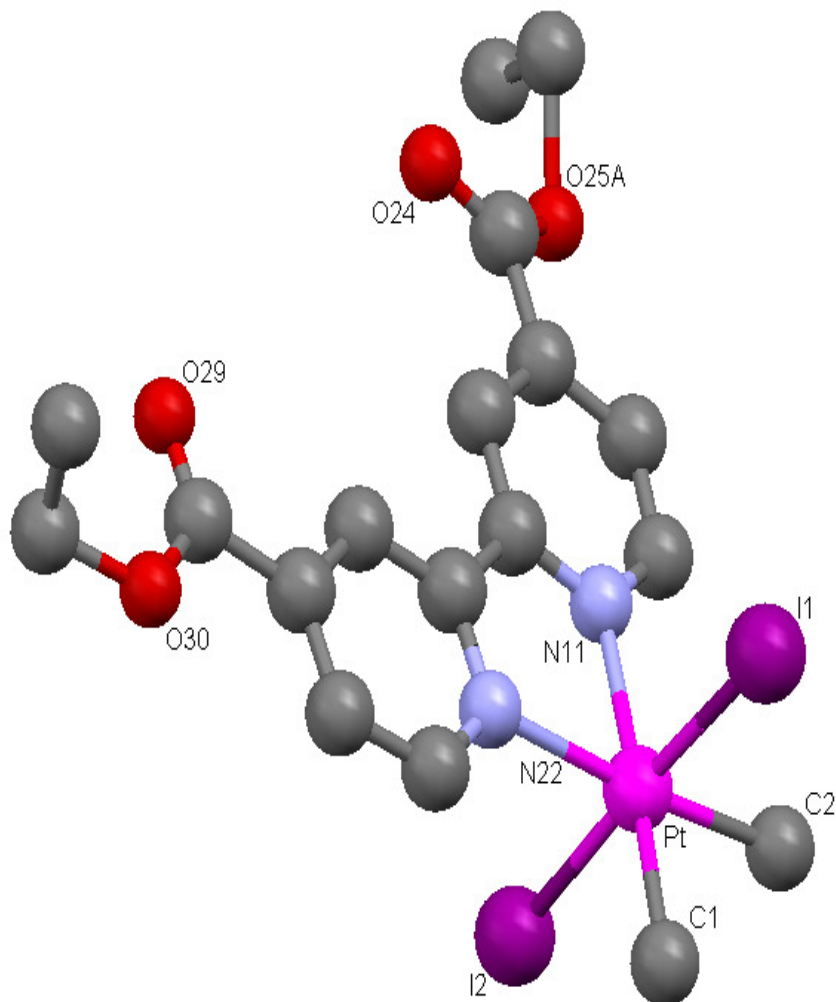
Figure 5.3. A view of the structure of complex **5.4**.

Table 5.2. Selected bond lengths [Å] and angles [°] for **5.4** [PtI$_2$Me$_2$(DECBP)].

Pt-N(11)	2.179(5)	Pt-N(22)	2.171(5)
Pt-C(1)	2.119(6)	Pt-C(2)	2.104(7)
Pt-I(1)	2.638(5)	Pt-I(2)	2.642(5)
I(3)-I(4)	2.733(7)	I(5)-I(5A)	2.748(1)
N(11)-Pt-N(22)	76.7(2)	N(11)-Pt-I(1)	91.9(1)
N(22)-Pt-C(1)	98.8(2)	I(1)-Pt-C(2)	89.2(2)
N(22)-Pt-C(2)	174.1(2)	C(1)-Pt-C(2)	87.1(3)
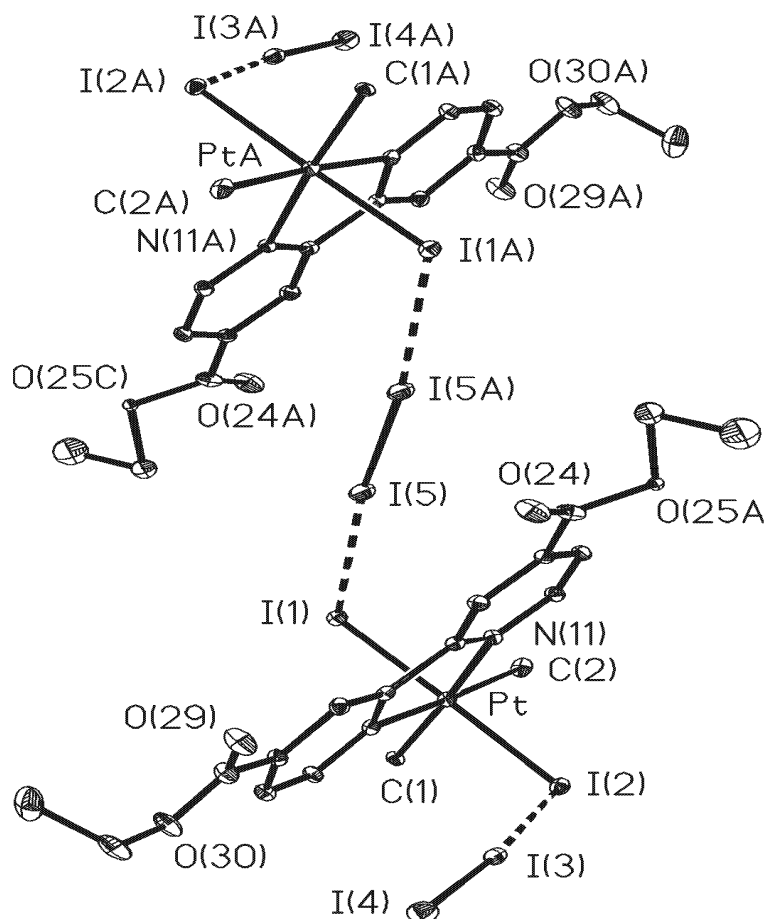
Figure 5.4. Supramolecular dimer structure of **5.4** and iodine.

The reaction of **5.2** [PtMe$_2$(DECBP)] with bromine in a solution of methylene chloride occurred to produce complex **5.5** as a result of *trans* oxidative addition at the platinum center (Scheme 5.2). The reaction is very fast, and compound **5.5** was isolated as a stable orange solid. Characterization of **5.5** [PtBr$_2$Me$_2$(DECBP)] was done using NMR spectroscopy. The ^{1}H-NMR spectrum of **5.5** contained only one methylplatinum proton resonance at δ = 2.07 ($^2J_{\text{Pt-H}}$ =71 Hz, *trans* to N), and one set of pyridyl resonances with *ortho* proton peak at δ = 9.07 ($^3J_{\text{Pt-H}}$ = 18 Hz, *trans* to C), which indicated the presence of only the *trans* isomer.

A variable temperature ^{1}H-NMR study was needed to study the mechanistic pathway of the reaction of bromine with **5.2**. The NMR spectra were recorded at 20 ^{o}C intervals between -80 and +20 ^{o}C. In an NMR tube was placed a solution of complex in CD$_2$Cl$_2$, the temperature of the NMR probe was lowered to -80 ^{o}C, and then Br$_2$ was added. The temperature was increased then to investigate the reaction pathway. The oxidative addition of bromine proceeds rapidly, but at lower temperatures the *cis* isomer of [PtBr$_2$Me$_2$(DECBP)] was observed in the ^{1}H-NMR spectra along with the *trans* isomer. The concentration of the *cis* isomer **5.5b** decreased upon increasing the temperature of the probe. The *cis* product **5.5b** is proposed to result via the exchange through a 5-coordinate intermediate which is shown in Scheme 5.3. The octahedral system is rigid, so when a bromide ligand is dissociated, then fast exchange would happen followed by the association of the bromide ligand. Complex **5.5b** was characterized by the presence of two methylplatinum proton resonances that occurred at δ = 1.97 ($^2J_{\text{Pt-H}}$ =70 Hz, *trans* to N), and 1.66 (broad, 3H, *trans* to Br). The methylplatinum proton resonance of **5.5b** at δ = 1.66 exchanged very fast at lower temperatures, and the *J* coupling value (Pt-Me) could not be obtained due to the broadness of the peak.
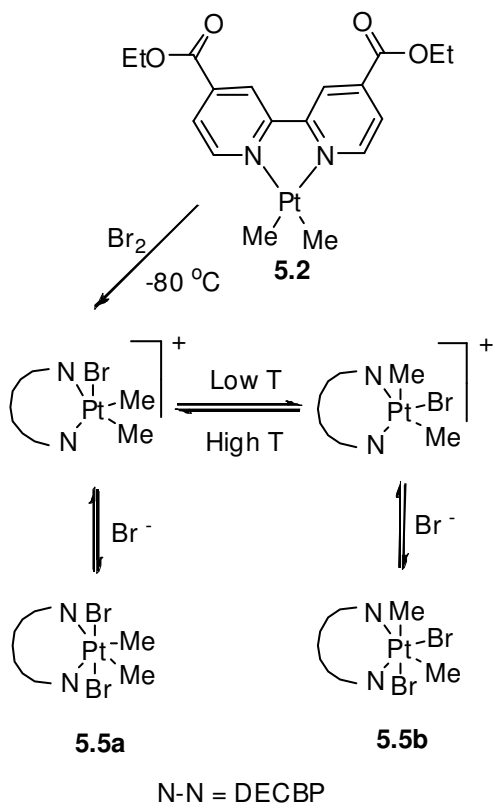
Scheme 5.3

The solid state structure of complex **5.5a** is shown Figure 5.5 and selected bond distances and angles are listed in Table 5.3. The observed molecular structure **5.5a** confirms the *trans* oxidative addition of bromine at the platinum(II) center to form the octahedral platinum(IV) structure.
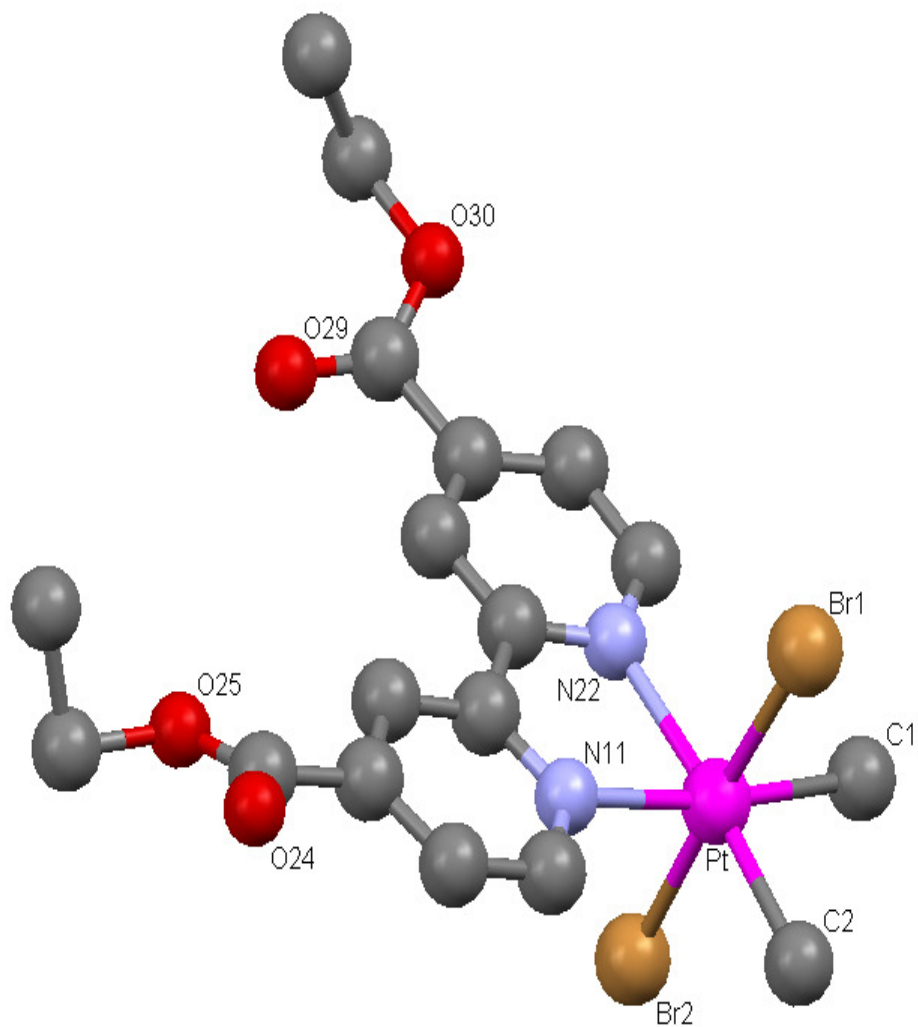
Figure 5.5. A view of the molecular structure of complex **5.5a**.

Table 5.3. Selected bond lengths [Å] and angles [°] for **5.5a** *trans*-[PtBr$_2$Me$_2$(DECBP)].

Pt-N(11)	2.174(1)	Pt-N(22)	2.172(1)
Pt-C(1)	2.173(1)	Pt-C(2)	2.105(2)
Pt-Br(1)	2.405 (2)	Pt-Br(2)	2.437(2)
N(11)-Pt-N(22)	75.6(4)	N(11)-Pt-Br(1)	94.3(3)
N(22)-Pt-C(1)	97.8(4)	Br(1)-Pt-C(2)	87.4(4)
N(22)-Pt-C(2)	174.2(5)	C(1)-Pt-C(2)	87.8(5)

Complex **5.2** reacted with acetyl chloride in methylene chloride according to Scheme 5.2, to produce **5.6** [Pt(CH$_3$CO)ClMe$_2$(DECBP)], which was isolated as a green solid. The reaction proceeded via oxidative addition to produce two different isomers *cis* and *trans* in 3:1 ratio according to analysis by ^{1}H-NMR (Chart 5.2). The *cis* isomer **5.6a** was characterized by the presence of two methylplatinum proton resonances at δ = 0.75 ($^2J_{Pt-H}$ = 74 Hz, *trans* to N), and 1.57 ($^2J_{Pt-H}$ = 72 Hz, *trans* to C), and two sets of pyridyl resonances with *ortho* proton peaks at δ = 8.97 ($^3J_{Pt-H}$ = 20 Hz), and 9.33 ($^3J_{Pt-H}$ = 19 Hz). The methyl group of the acetyl ligand occurred for **5.6a** at δ = 2.58 with $^3J_{Pt-H}$ = 10 Hz. On the other hand, the *trans* isomer **5.6b** was identified by the presence of only one methylplatinum resonance in the ^{1}H-NMR spectrum at δ = 1.59 with $^2J_{Pt-H}$ = 72 Hz *trans* to N, and one methyl group of the acetyl ligand at δ = 2.00 with $^3J_{Pt-H}$ = 14 Hz *trans* to chloride ligand. The methyl group of the acetyl ligand for complex **5.6b** has a higher coupling constant than **5.6a** due to the presence of a lower *trans* influence chloride ligand in **5.6b**. Only one set of pyridyl resonances occurred for the *trans* isomer **5.6b**, and its *ortho* proton resonance in the ^{1}H-NMR spectrum was observed at δ = 9.13 with $^3J_{Pt-H}$ = 20 Hz. Both isomers are stable at room temperature, and the ratio of concentrations of the complexes did not change with time.
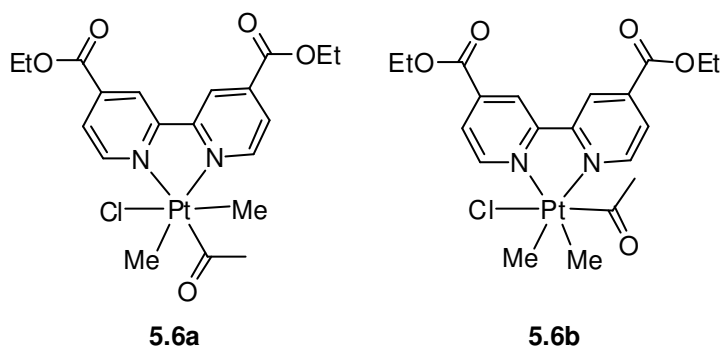
Chart 5.2. The structures of both complexes **5.6a** and **5.6b**.

A previous study on the oxidative addition of acetyl chloride to the dimethylplatinum(II) complex [PtMe$_2$(DPK)] (DPK = di-2-pyridyl ketone) showed the *trans* addition of the reagent to the metal center as the major product.[12] In our case, the *cis* product **5.6a** is the major product, so an ^{1}H-NMR study was needed to investigate the mechanistic pathway of the reaction. To an NMR tube containing complex **5.2** in CD$_2$Cl$_2$ was added one equivalent of acetyl chloride. ^{1}H-NMR spectra were then recorded over a period of 2 days. The reaction proceeded rapidly at room temperature to produce both isomers *trans* (major) and *cis* (minor). The kinetic *trans* product isomerized with time to produce the thermodynamic *cis* product. Figure 5.6 shows the ^{1}H-NMR spectra for the reaction of complex **5.2** with acetyl chloride after 30 minutes, and after 24 hours. The spectra proved that the acetyl chloride adds in *trans* fashion, but then isomerized to the stable *cis* product with time. The solid state structure of the *cis* isomer **5.6a** is shown in Figure 5.7. Table 5.4 shows selected bond distances and angles of **5.6a**.

Table 5.4. Selected bond lengths [Å] and angles [°] for **5.6a** *cis*-[Pt(CH$_3$CO)ClMe$_2$(DECBP)].

Pt-N(11)	2.177(5)	Pt-N(22)	2.184(5)
Pt-C(1)	2.068(6)	Pt-C(2)	2.072(6)
Pt-Cl	2.437(1)	Pt-Br(2)	2.026(6)
N(11)-Pt-N(22)	75.8(2)	N(11)-Pt-C(3)	99.6(2)
N(22)-Pt-C(1)	97.2(2)	N(22)-Pt-C(3)	175.3(2)
N(22)-Pt-C(2)	90.7(2)	C(1)-Pt-C(2)	87.4(3)
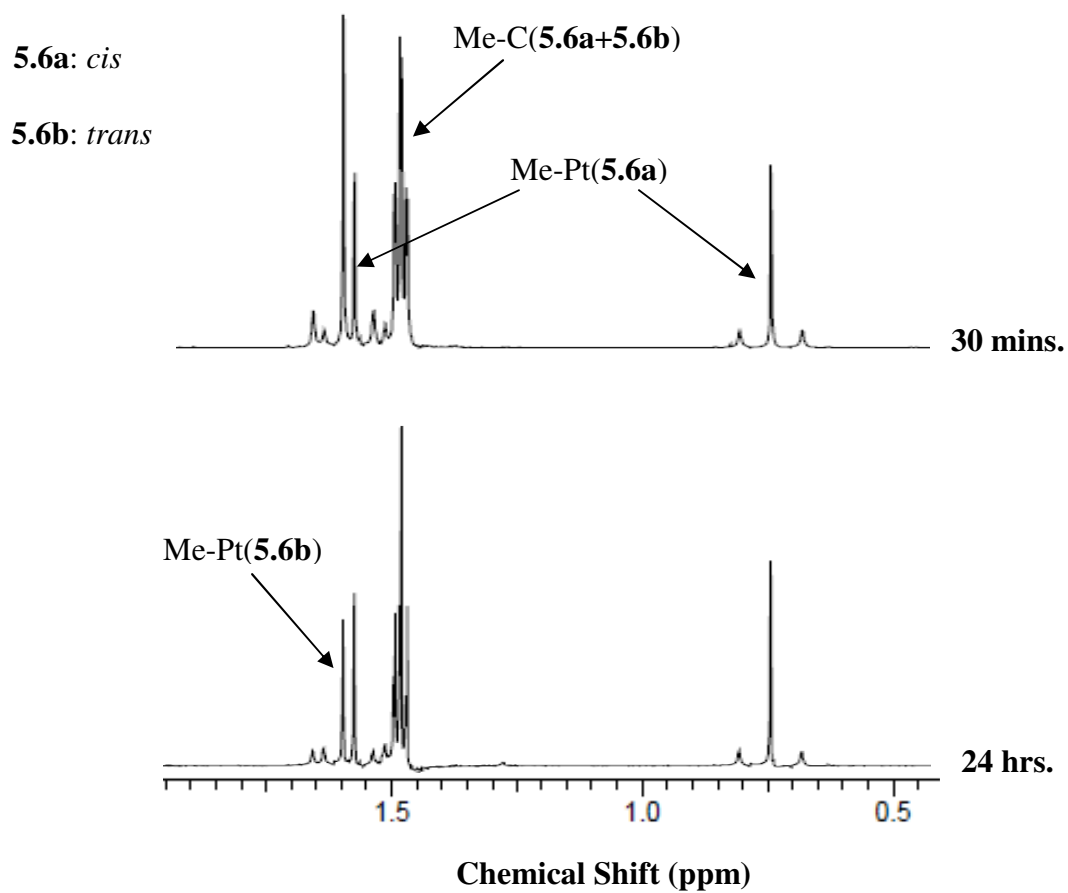
Figure 5.6. ^{1}H-NMR spectra (400 MHz, CD_2Cl_2) for the reaction of complex **5.2** with acetyl chloride after 30 minutes, and after 24 hours.
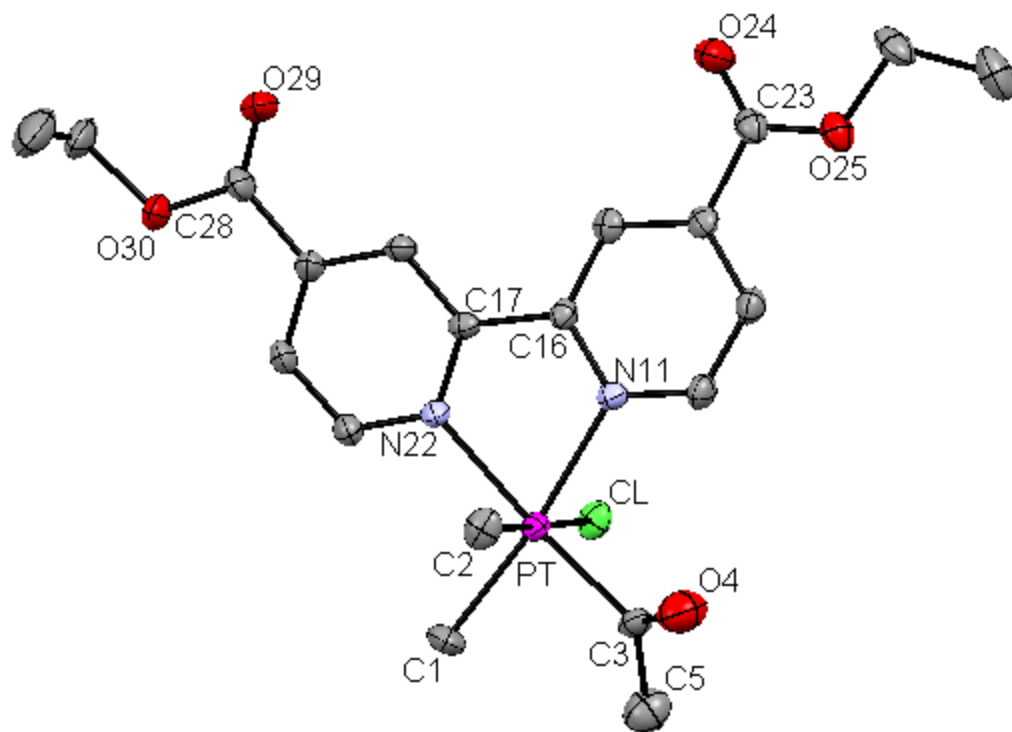
Figure 5.7. A view of the molecular structure of complex **5.6a**.

Complex **5.7** was synthesized from **5.2** and ethyl chloroformate in a solution of methylene chloride according to Scheme 5.2. The reaction produced the *trans* isomer **5.7** by oxidative addition mechanism of the C-Cl bond. The *trans* product was identified by its ^{1}H-NMR spectrum. The ^{1}H-NMR contained a singlet with platinum satellites at $\delta = 1.65$ with $^2J_{Pt-H}$ = 74 Hz, which was clearly assigned to the two methylplatinum groups. The presence of only one signal indicates the symmetrical stereochemistry of the complex. One set of pyridyl resonances was observed in the ^{1}H-NMR spectrum, with an *ortho* proton resonance $\delta = 9.13$ with $^3J_{Pt-H}$ = 17 Hz *trans* to carbon. The recrystallization of complex **5.7** to confirm its molecular structure via x-ray resulted in the production of the platinum(II) complex [PtClMe(DECBP)], which was produced by the decomposition of complex **5.7.** The structure of the complex [PtClMe(DECBP)] was confirmed by an X-ray structure determination, and a view of the structure is shown in Figure 5.8. The platinum(II) complex has square planar geometry. Some selected bond lengths and angles are displayed in Table 5.5.

Table 5.5. Selected bond lengths [Å] and angles [°] for [PtClMe(DECBP)].

Pt(1)-N(11)	1.997(1)	Pt(1)-N(22)	2.086(1)
Pt(1)-C(1A)	2.086(2)	Pt(1)-Cl(1A)	2.276(4)
N(11)-Pt(1)-N(22)	78.5(4)	N(11)-Pt(1)-C(1A)	95.7(6)
N(22)-Pt(1)-C(1A)	170.1(6)	N(11)-Pt(1)-Cl(1A)	173.7(4)
N(22)-Pt(1)-Cl(1A)	90.7(2)	C(1A)-Pt(1)-Cl(1A)	89.7(6)
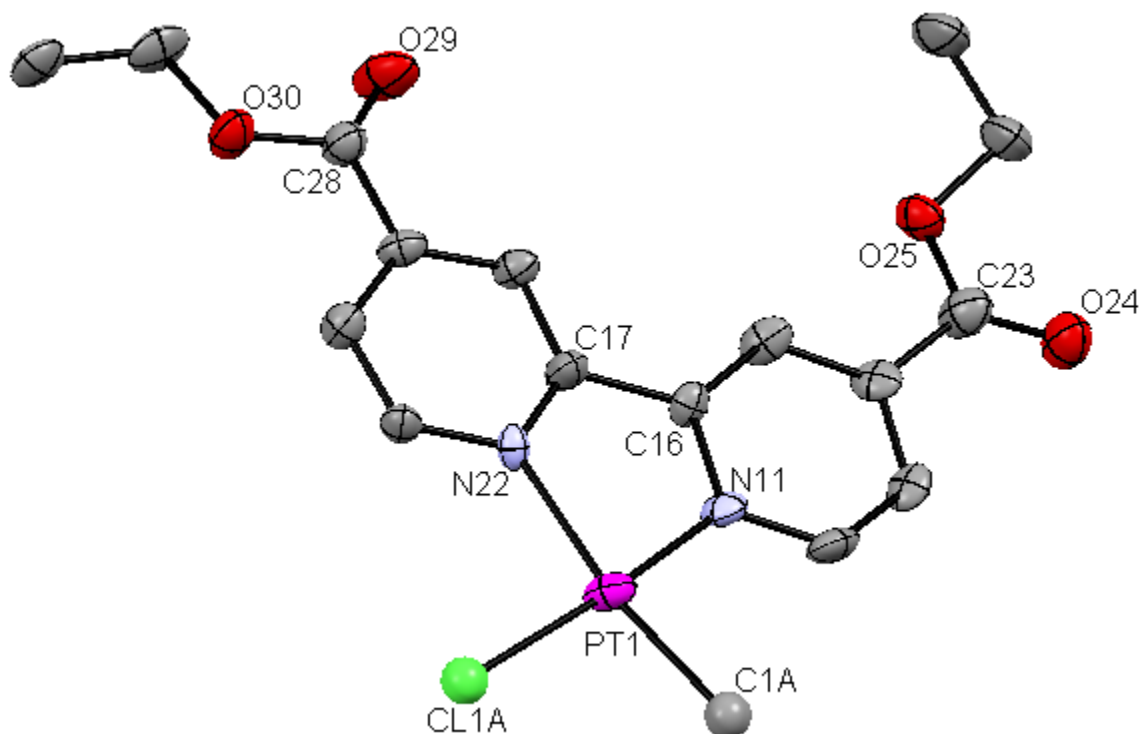
Figure 5.8. A view of the molecular structure of the complex [PtClMe(DECBP)].

The reaction of complex **5.2** with HCl was studied by using NMR spectroscopy. The reaction proceeded rapidly at room temperature in CD_2Cl_2 in an NMR tube to produce complex **5.8** [PtCl$_2$(DECBP)] (Scheme 5.2), which was characterized crystallography and by its NMR spectrum. Complex **5.8** was identified by the absence of any methylplatinum group in the high

field region of the NMR spectrum. One set of pyridyl proton resonances was seen, and the *ortho* proton peak occurred at $\delta = 9.97$ with $^3J_{Pt-H} = 48$ Hz, *trans* to a Cl ligand. Such high coupling is due to the low *trans* influence of a chloride ligand compared to a methyl group. Complex **5.8** is formed probably via the *trans* oxidative addition of HCl followed by the reductive elimination of methane. The molecular structure of **5.8** was proven via X-ray crystallography (Figure 5.9). The complex adopts the expected square planar platinum(II) geometry. Selected bond distances and angles are shown in Table 5.6. The Pt-N(*trans* to Cl) distances in **5.8** = 2.072(1), and 2.016(1) Å are slightly shorter than the Pt-N(*trans* to C) distances in **5.2** [PtMe$_2$(DECBP)]. This is consistent with the Pt-N distances being determined by the *trans* influence of the *trans* ligands which follows the series Me > Cl.[15]

Table 5.6. Selected bond lengths [Å] and angles [°] for **5.8** [PtCl$_2$(DECBP)].

Pt(1)-N(11)	2.072(1)	Pt(1)-N(22)	2.016(1)
Pt(1)-Cl(1)	2.213(7)	Pt(1)-Cl(2)	2.256(6)
N(11)-Pt(1)-N(22)	79.4(5)	N(11)-Pt(1)-Cl(1)	175.7(5)
N(22)-Pt(1)-Cl(1)	96.4(4)	N(11)-Pt(1)-Cl(2)	96.7(4)
N(22)-Pt(1)-Cl(2)	175.7(3)	C(1A)-Pt(1)-Cl(1A)	87.5(3)
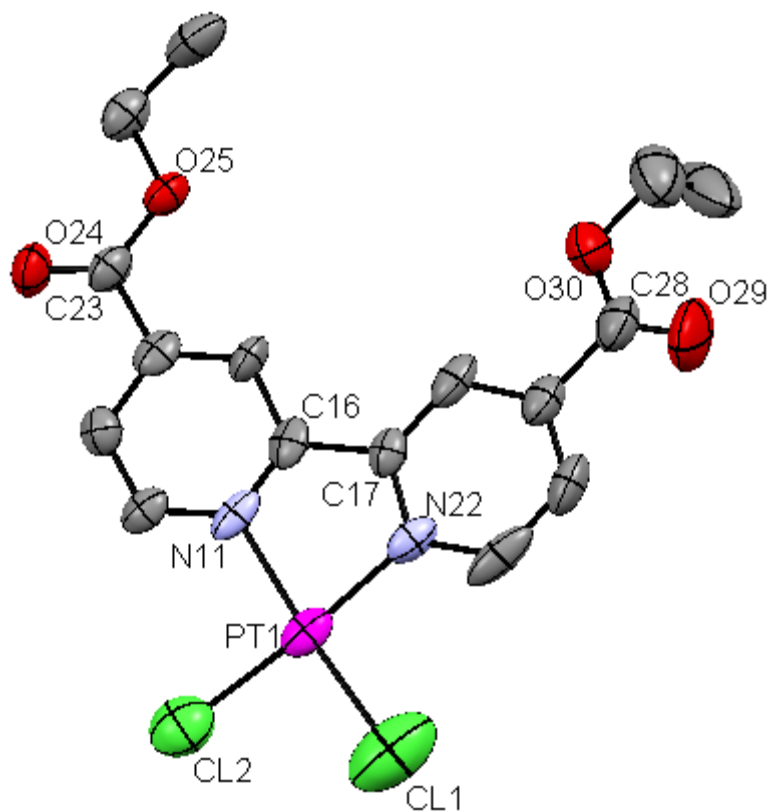
Figure 5.9. A view of the molecular structure of complex **5.8**.

Hydrogen peroxide reacted rapidly with [PtMe$_2$(DECBP)] **5.2** in acetone at room temperature according to Scheme 5.2 to give [PtMe$_2$(OH)$_2$(DECBP)] **5.9**, which was isolated as a white solid. The reaction proceeded via *trans* oxidative addition of the O-O bond to form the octahedral *trans*-dihydroxo platinum(IV) complex.[16] The oxidative addition reaction of H$_2$O$_2$ or related compounds of the type RXXR, where X = O, S, or Se, generally results in the formation of *trans*-L$_n$Pt(XR)$_2$ complexes.[16,17] In the ^{1}H-NMR spectrum of complex **5.9**, there is a single

methylplatinum resonance $\delta = 1.66$ ($^2J_{Pt-H} = 70$ Hz). The presence of only one methyl platinum and one set of pyridyl resonances indicate that the complex has a plane of symmetry as expected for a product of *trans* geometry. The *ortho* proton resonance occurred at $\delta = 9.01$ ($^3J_{Pt-H} = 18$ Hz), and both the chemical shift and coupling constant are typical of a platinum(IV) complex with a methyl group *trans* to a nitrogen of pyridyl group.[9,12]

In the ^{1}H-NMR spectrum of [PtMe$_2$(OH)$_2$(DECBP)] **5.9** additional proton resonances were observed and assigned to compound **5.1** the uncoordinated DECBP ligand. An NMR reaction was carried out to study the reaction of hydrogen peroxide with **5.2**. An NMR tube containing **5.2** and H$_2$O$_2$ in acetone-d$_6$ was prepared and five minutes later the ^{1}H-NMR spectrum was obtained. The reaction proceeded via *trans* oxidative addition, and no *cis* isomer was observed in the spectrum. Free ligand proton resonances were also observed, and so multiple NMR runs were taken during the next two days. The intensity of the free ligand resonances increased with time, while a white insoluble precipitated formed around the walls of the tube which was suspected to be the known complex [PtMe$_2$(OH)$_2$]. Figure 5.10 shows the ^{1}H-NMR spectra in the aromatic region after 5 minutes and 24 hours from adding H$_2$O$_2$ to complex **5.2**. To prove that [PtMe$_2$(OH)$_2$] was formed, a drop of sulfuric acid in D$_2$O was added to the NMR tube, which would form a known soluble complex [PtMe$_2$(OH)$_4$]$^{2+}$ that was characterized via its methylplatinum resonance at $\delta = 2.26$ ($^2J_{Pt-H} = 66$ Hz).[18]

DECBP(Free ligand): *

Complex **5.9**: Δ
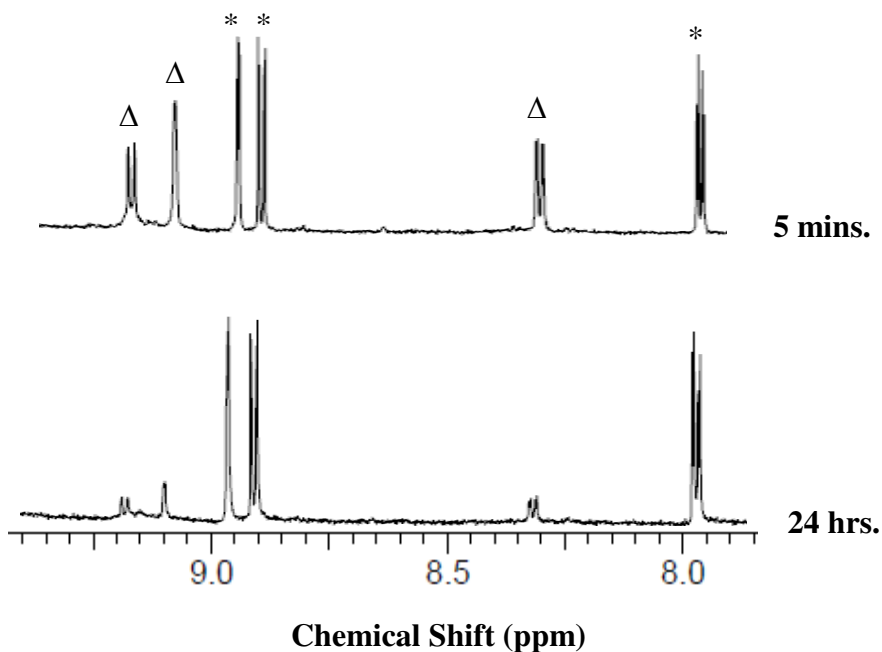
Figure 5.10. The ^{1}H-NMR spectra (400 MHz, acetone-d$_6$) in the aromatic region after 5 minutes and 24 hours from adding H$_2$O$_2$ to complex **5.2**.

Complex **5.2** was very reactive towards oxidative addition of several reagents. The reaction of **5.2** with halogens, alkyl halides, hydrogen peroxide, and acid resulted in the formation of platinum(IV) complexes, and some then undergone reductive elimination to form platinum(II) complexes. The next step in the project was to introduce hydrogen donors/acceptors which could cause self-assembly through hydrogen bonding, and π-stacking that would result in the formation of supramolecular platinum(IV) complexes.

5.2.3 The Self-Assembly of Organoplatinum(IV) Complexes

5.2.3.1 Carboxylic Acids as Hydrogen Bonding Groups

The oxidative addition of the Br-CH_2 bond in α-bromo-4-toluic acid, 4-(bromomethyl)phenylacetic acid, and bromoacetic acid to complex **5.2** in acetone occurred easily at room temperature to produce the corresponding platinum(IV) complexes according to Scheme 5.4, and all compounds were isolated as stable solids. Only *trans* isomers were produced in all three reactions, in contrast to similar reactions with other dimethylplatinum(II) complexes which gave mixtures of *cis* and *trans* isomers.[6] The reaction of **5.2** with α-bromo-4-toluic acid produced complex **5.10**, *trans*-[PtBrMe$_2$(CH$_2$-4-C$_6$H$_4$CO$_2$H)(DECBP)]. The ^{1}H-NMR spectrum of **5.10** contained only one methylplatinum proton resonance at δ = 1.54 with $^2J_{Pt-H}$ = 72 Hz, which proved the formation of only the *trans* isomer. The CH_2 proton resonance was observed at δ = 2.87 with $^2J_{Pt-H}$ = 95 Hz, as expected.[4-6] One set of pyridyl and phenyl resonances was observed, and the *ortho* proton appeared at δ = 8.97(pyridyl) and 6.46(phenyl) with $^3J_{Pt-H}$ = 19 and 18 Hz respectively. The molecular structure of **5.10** is shown in Figure 5.11. The complex contained an octahedral platinum(IV) center. Selected bond distances and angles of complex **5.10** are shown in Table 5.7.

The oxidative addition reaction of **5.2** with 4-(bromomethyl)phenylacetic acid occurred with *trans* stereochemistry to produce complex **5.11** [PtBrMe$_2$(CH$_2$-4-C$_6$H$_4$CH$_2$CO$_2$H)(DECBP)] (Scheme 5.4), which is a stable yellow solid that is soluble in organic solvents. The ^{1}H-NMR spectrum of **5.11** contained one methylplatinum resonance at δ = 1.50 with $^2J_{Pt-H}$ = 70 Hz *trans* to N, and one CH$_2$Pt resonance at δ = 2.77 with $^2J_{Pt-H}$ = 90 Hz *trans* to Br. One set of pyridyl resonances was observed in the ^{1}H-NMR spectrum, which proved the *trans* addition. The resonance for the *ortho* protons of the pyridyl groups was seen at δ = 8.95

with $^3J_{\text{Pt-H}}$ = 19 Hz *trans* to C, while the resonance for the phenyl *ortho* protons occurred at δ = 6.27 with $^4J_{\text{Pt-H}}$ = 18 Hz *trans* to Br.

Complex **5.12** was formed in high yields according to Scheme 5.4 by the reaction of complex **5.2** with bromoacetic acid. The ^{1}H-NMR spectrum of complex **5.12** showed that reaction occurred by *trans* oxidative addition. Thus, there was one methylplatinum resonance at δ = 1.53 with $^2J_{\text{Pt-H}}$ = 70 Hz *trans* to N. The benzylic CH$_2$Pt proton resonance was seen at δ = 2.01 with $^2J_{\text{Pt-H}}$ = 95 Hz *trans* to Br, while the *ortho* proton resonance existed at δ = 9.09 with $^3J_{\text{Pt-H}}$ = 19 Hz *trans* to C.
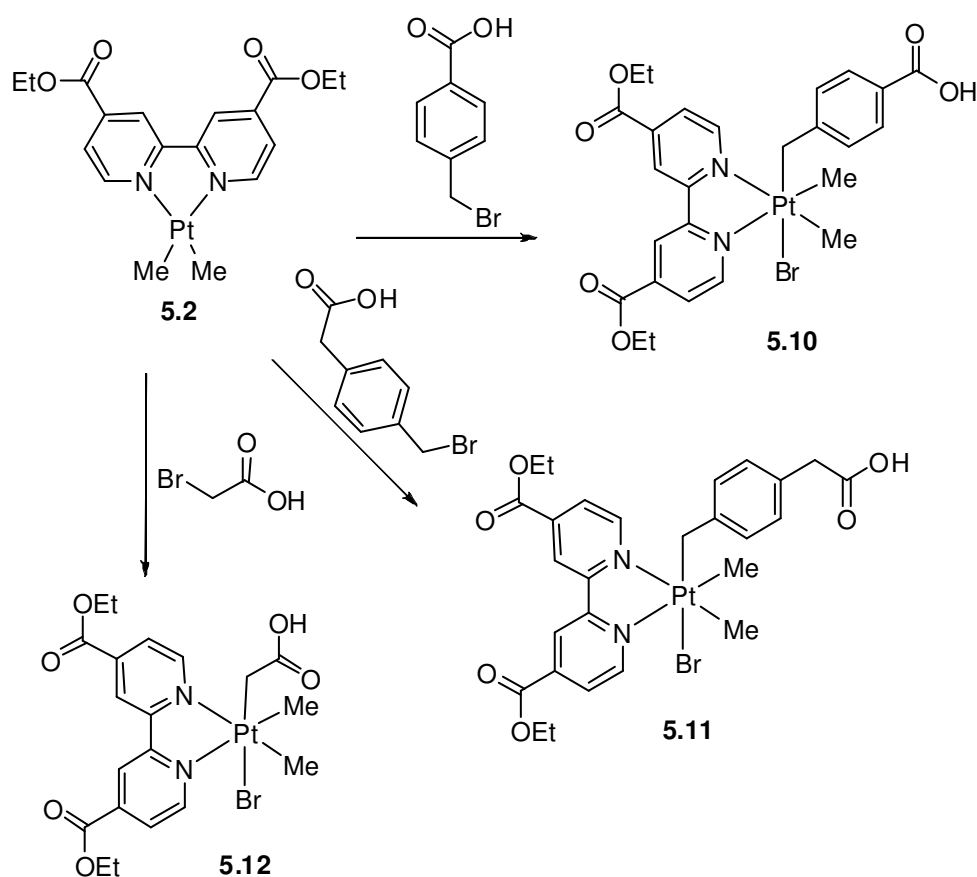
Scheme 5.4

Table 5.7. Selected bond lengths [Å] and angles [°] for **5.10** *trans*-[PtBrMe$_2$(CH$_2$-4-C$_6$H$_4$-CO$_2$H)(DECBP)].

Pt(1)-N(1)	2.160(4)	Pt(1)-N(2)	2.162(4)
Pt(1)-C(17)	2.048(6)	Pt(1)-C(18)	2.063(5)
Pt(1)-C(19)	2.103(5)	Pt(1)-Br(1)	2.596(6)
N(1)-Pt(1)-N(2)	76.9(2)	N(1)-Pt(1)-C(17)	96.9(2)
N(2)-Pt(1)-Br(1)	92.1(1)	N(2)-Pt(1)-C(17)	173.3(2)
Br(1)-Pt(1)-C(18)	90.6(2)	C(17)-Pt(1)-C(18)	88.2(2)
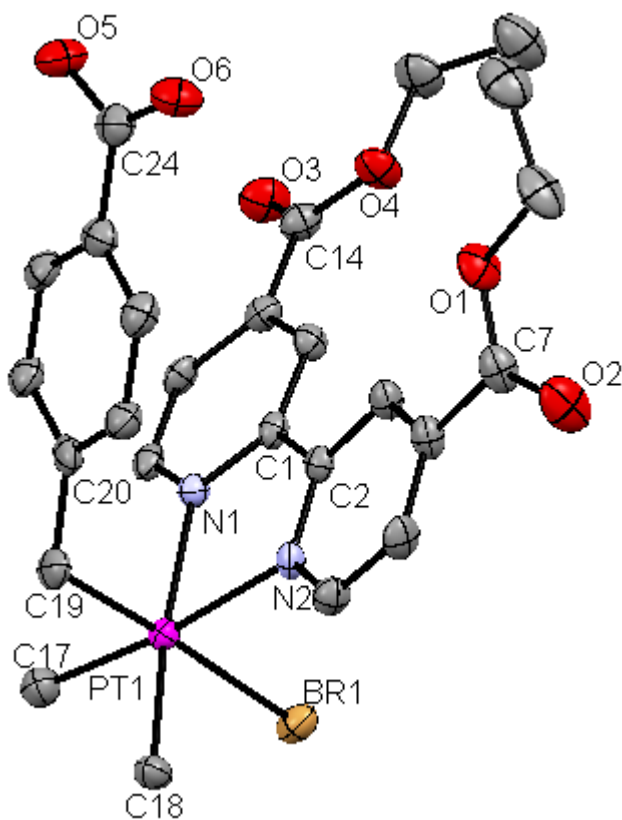
Figure 5.11. A view of the molecular structure of complex **5.10**.

Figure 5.12 shows a view of the primary supramolecular dimer structure of **5.10** which was formed via strong hydrogen bonding between carboxylic acid groups, with O•••O = 2.64 Å. The carboxylic acid groups took part in hydrogen bonding as both an acceptor and a donor, as was expected. Another type of self-assembly was observed through weak C(19)H•••BrPt hydrogen bonding (2.98 Å). Each benzyl group is π-stacked with a pyridyl group of the adjacent DECBP ligand, which probably helped in stabilizing the kinetic product *trans* isomer. The graph set description for the dimer system is $R_2^2(8)$, which is usual for acid groups.[19] The DECBP ligand contained two ester functional groups whose O=C units can act as a hydrogen bond acceptor, but those units were not involved in any of the secondary bonding that formed the supramolecular dimer structure. This could not be due to the steric hindrance caused by the ester substituent, since such hydrogen bonding was observed in similar systems upon replacing the ester groups by amide units,[6] where the amide groups were involved in the formation of several supramolecular complexes via self assembly as a hydrogen bond acceptor and donor as seen in similar recent studies.[20]

Complex **5.12** was confirmed crystallographically to be formed by *trans* oxidative addition (Figure 5.13). The carboxylic acid groups in the acetic acid ligand (**5.12**) take part as expected in hydrogen bonding as an acceptor and as a donor forming the supramolecular dimer structure of **5.12** (Figure 5.14). The carboxylic acid groups are oriented as expected for formation of intermolecular OH•••O=C hydrogen bonds, with very strong hydrogen bonds (O•••O = 2.65 Å). Table 5.8 shows selected bond distances and angles of complex **5.12**.
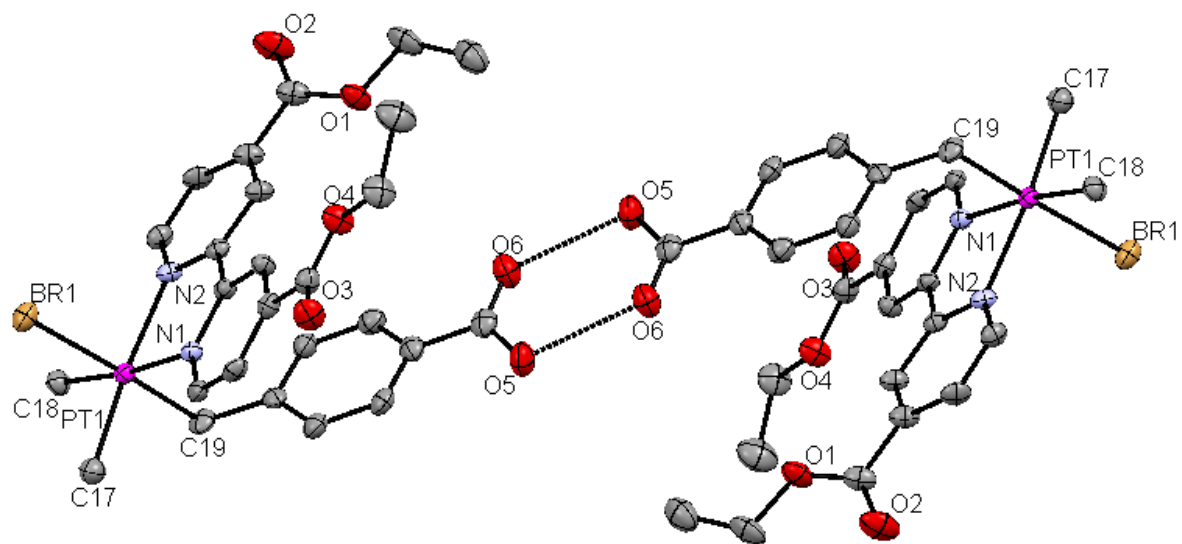
Figure 5.12. A view of supramolecular dimer structure of **5.10**.

Table 5.8. Selected bond lengths [Å] and angles [°] for **5.12** *trans-*
[PtBrMe$_2$(CH$_2$CO$_2$H)(DECBP)].

Pt(1)-N(1)	2.155(6)	Pt(1)-N(2)	2.166(6)
Pt(1)-C(17)	2.085(7)	Pt(1)-C(18)	2.124(6)
Pt(1)-C(19)	2.099(7)	Pt(1)-Br(1)	2.533(8)
N(1)-Pt(1)-N(2)	76.4(2)	N(1)-Pt(1)-C(17)	97.1(2)
N(2)-Pt(1)-Br(1)	88.5(2)	N(2)-Pt(1)-C(17)	173.4(2)
Br(1)-Pt(1)-C(18)	90.8(2)	C(17)-Pt(1)-C(18)	88.8(3)
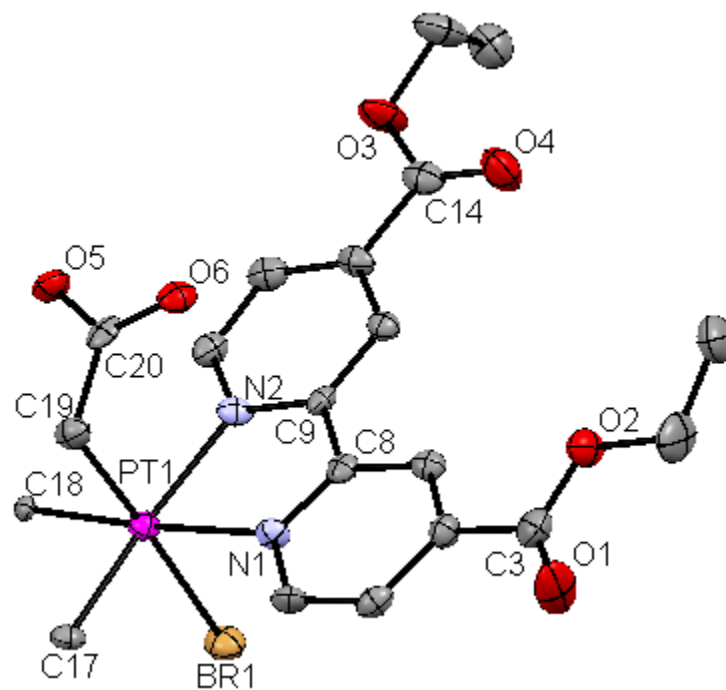
Figure 5.13. A view of the molecular structure of complex **5.12**.
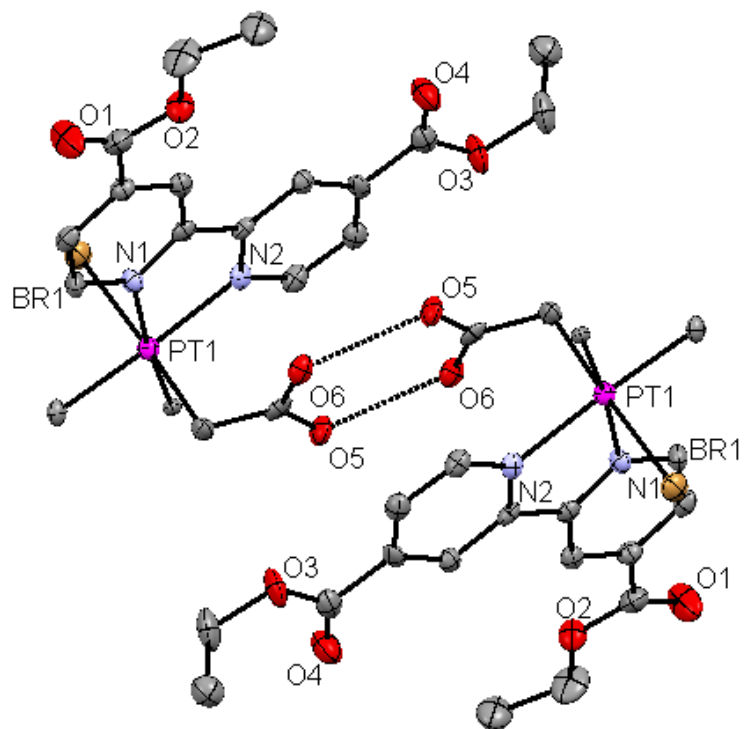
Figure 5.14. A view of supramolecular dimer structure of **5.12**.

5.2.3.2 Introduction of Amide Hydrogen Bonding Groups

The inability to get the ester group to accept a hydrogen bond through the self-assembly of platinum(IV) complexes with carboxylic acid groups was a reason to study the reactions of complex **5.2** with alkyl halides containing amide groups which can act as a hydrogen bond donor, and acceptor. Also the carbonyl of an amide is a better acceptor than the carbonyl of an ester.[20] These studies would help in the understanding of the self-assembly patterns of the organoplatinum DECBP system. Two alkyl bromide ligands containing amide groups were introduced and reacted to complex **5.2** according to Scheme 5.5. The reactions were carried out in an acetone solution.
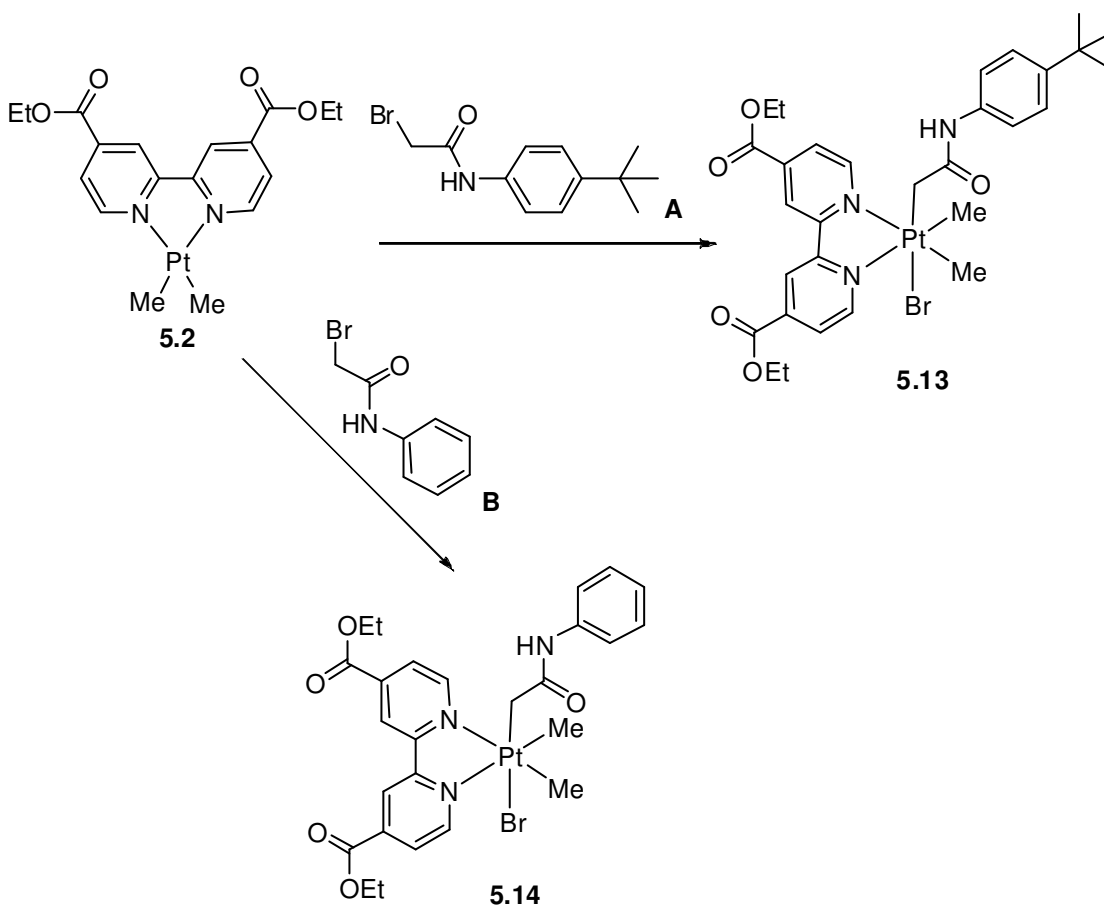
Scheme 5.5

The *trans* oxidative addition of both alkyl bromide compounds **A** and **B** to **2** [PtMe$_2$(DECBP)] is shown in Scheme 5.5, and gave the platinum(IV) products [PtBrMe$_2$(CH$_2$-CONH-4-C$_6$H$_4$-*t*-Bu)(DECBP)], **5.13**, and [PtBrMe$_2$(CH$_2$-CONH-C$_6$H$_5$)(DECBP)], **5.14**, in very good yields. The structure of complex **5.13** was determined by its ^{1}H-NMR spectrum, which contained one methylplatinum resonance at $\delta = 1.56$ with $^2J_{\text{Pt-H}} = 69$ Hz *trans* to N, and a proton resonance at $\delta = 2.10$ with $^2J_{\text{Pt-H}} = 92$ Hz *trans* Br. One set of pyridyl resonances was observed in the ^{1}H-NMR spectrum with $\delta = 8.92$ with $^3J_{\text{Pt-H}} = 19$ Hz *trans* to C.

The oxidative addition of **B** BrCH$_2$-CONH-C$_6$H$_5$ to **5.2** [PtMe$_2$(DECBP)] gave the *trans* isomer of the platinum(IV) complex [PtBrMe$_2$(CH$_2$-CONH-C$_6$H$_5$)(DECBP)], **5.14**, according to Scheme 5.5. Only a singlet Pt-CH$_2$ resonance was observed, along with a single methylplatinum resonance, and a single set of pyridyl resonances. The methyplatinum resonance was seen at $\delta = 1.56$ with $^2J_{\text{Pt-H}} = 69$ Hz *trans* to N, while the Pt-CH$_2$ was observed at $\delta = 2.12$ with $^2J_{\text{Pt-H}} = 92$ Hz trans Br. The structure of **5.14** is shown in Figure 5.15, and the platinum centre adopts an octahedral geometry. Table 5.9 shows selected bond lengths and angles of complex **5.14**. The obtained structure confirmed the *trans* oxidative addition of **5.14**. The amide groups took part in self-assembly via NH•••BrPt hydrogen bonding to give supramolecular polymers, with N(3)•••Br(1) = 3.51 Å. The bond length is considered reasonable for such hydrogen bonding, since the normal range for N-H•••Br hydrogen bonding interactions is N•••Br = 3.12 - 3.69 Å.[21] There was not any self-assembly by NH•••O=C hydrogen bonding. Also π-stacking interactions were observed with interplanar distances of about 3.38 Å. The combination of hydrogen bonding, and π-stacking gave rise to the formation supramolecular polymers, but the common NH•••O=C hydrogen bond interaction was absent. Figure 5.16 shows the supramolecular polymeric structure of complex **5.14**.

Table 5.9. Selected bond lengths [Å] and angles [°] for **5.14** *trans-*[PtBrMe$_2$(CH$_2$-CONH-C$_6$H$_5$)(DECBP)].

Pt(1)-N(1)	2.154(5)	Pt(1)-N(2)	2.163(5)
Pt(1)-C(1)	2.067(7)	Pt(1)-C(2)	2.074(6)
Pt(1)-C(19)	2.103(7)	Pt(1)-Br(1)	2.545(1)
N(1)-Pt(1)-N(2)	76.7(2)	N(1)-Pt(1)-C(2)	175.4(3)
N(1)-Pt(1)-Br(1)	88.7(2)	N(1)-Pt(1)-C(1)	98.2(3)
Br(1)-Pt(1)-C(1)	91.3(3)	C(1)-Pt(1)-C(2)	86.4(3)
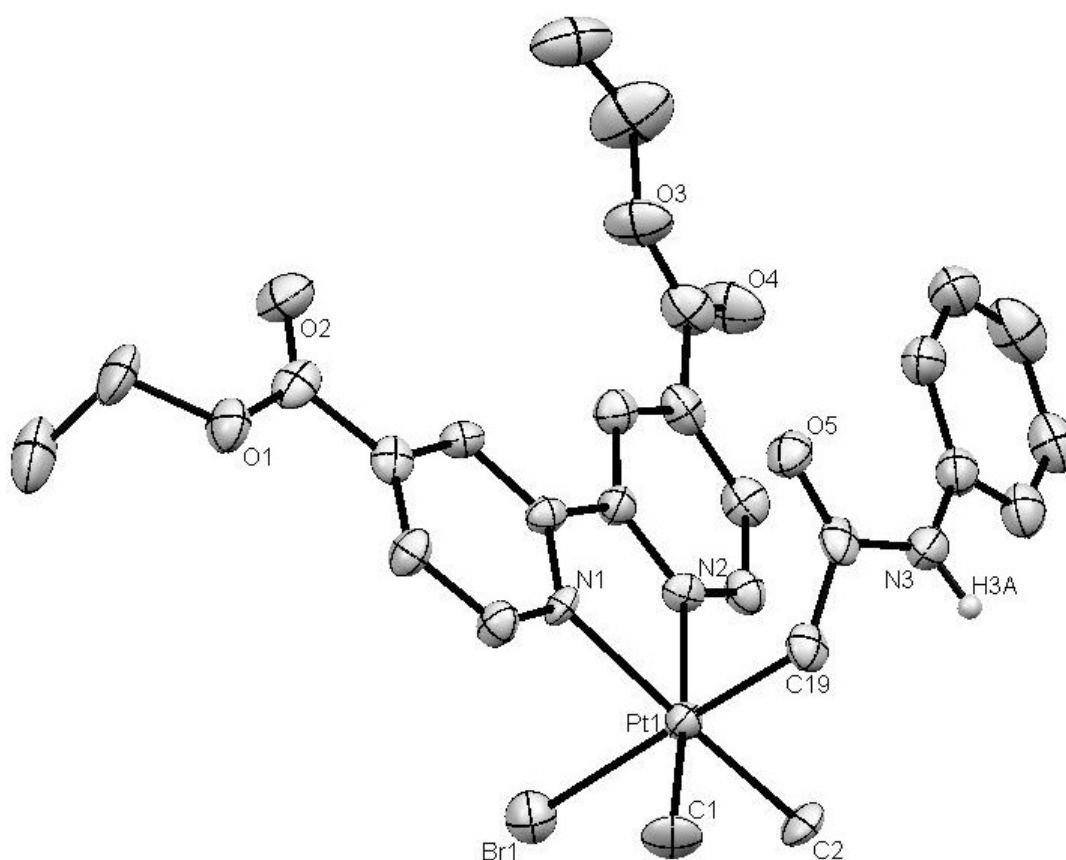
Figure 5.15. A view of the molecular structure of **5.14**.
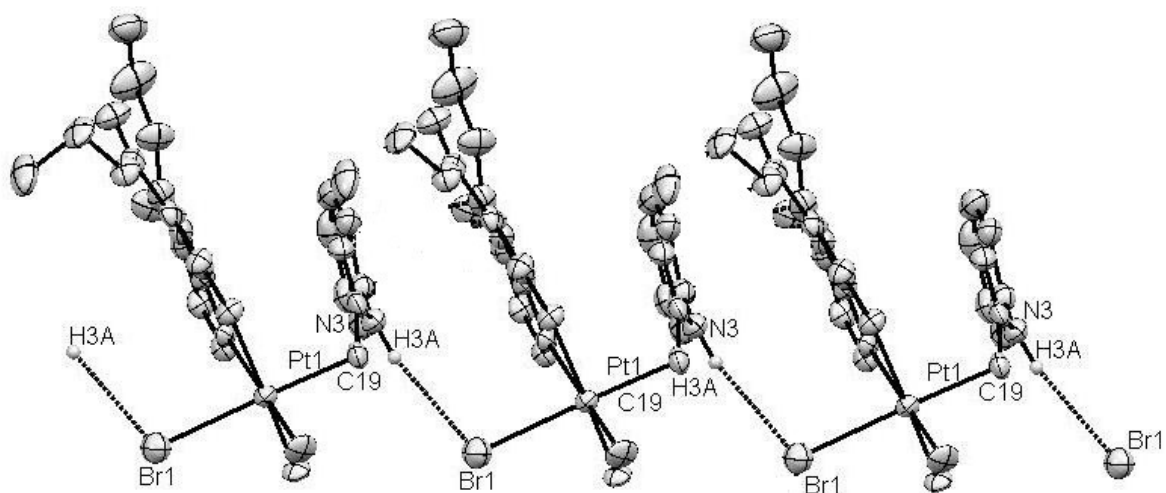
Figure 5.16. A view of the supramolecular polymeric structure of complex **5.14**.

5.2.3.3 Boronic Acid and Alcohol Groups as Hydrogen Bonding Donors

The crystallization of aryl-boronic acids usually produces cyclic hydrogen-bonded dimers, and such secondary interaction has been exploited in supramolecular chemistry.[22] In recent years, boronic acids have been used extensively in molecular recognition,[23] and also in the development of the field of molecular tectonics where the formation of networks takes place under self-assembly conditions (Chart 5.3).[24] So boronic acids, $RB(OH)_2$, have become an object of recent interest due to their new applications in supramolecular chemistry, such high interest is because of the high flexibility of boronic groups.[25] Several phenyl boronic acids and phenyl alcohols where used in this section to design of organoplatinum(IV) supramolecular structures.

Chart 5.3

$$R = \quad C\left(\underset{4}{\overbrace{}}\right)_4 \quad Si\left(\underset{4}{\overbrace{}}\right)_4$$
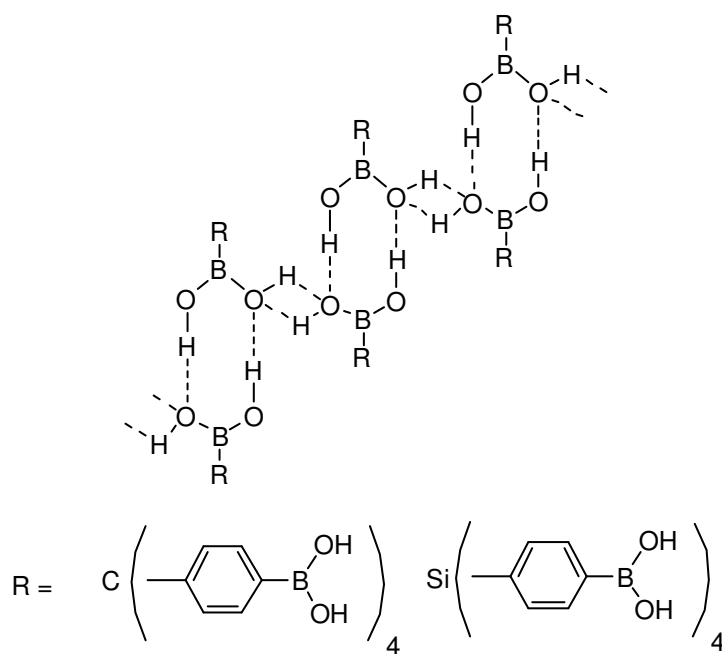
The compound 2-(bromomethyl)benzyl alcohol reacted with complex **5.2** in acetone at room temperature according to Equation 5.3, which produced complex **5.15** [PtBrMe$_2$(CH$_2$-3-C$_6$H$_4$-CH$_2$OH)(DECBP)], in high yield. The NMR characterizations showed the presence of the *trans* isomer only. The ^{1}H-NMR spectrum contained only one methylplatinum resonance at $\delta =$ 1.57 with $^2J_{Pt-H} = 71$ Hz *trans* to N, and one PtCH$_2$ resonance at $\delta = 2.88$ with $^2J_{Pt-H} = 91$ Hz *trans* to Br. Several attempts of growing a single crystal for X-ray analysis failed.

(5.3)
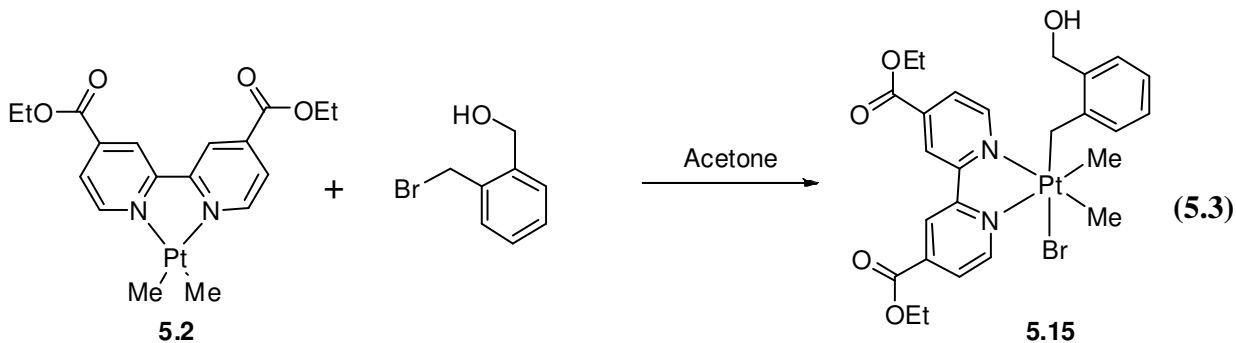
Three different phenyl boronic acids were used in the development of supramolecular structures. The reaction of complex **5.2** with the *ortho*, *meta*, and *para* substituted (bromomethyl)phenyl boronic acids proceeded rapidly at room temperature to produce the respective organoplatinum(IV) complexes. The oxidative addition of the Br-CH_2 bond in *meta*-(bromomethyl)phenyl boronic acid to complex **5.2** [PtMe$_2$(DECBP)] produced complex **5.16** [PtBrMe$_2$(CH$_2$-3-C$_6$H$_4$-B{OH}$_2$)(DECBP)] in good yields, and the product was isolated as a stable yellow solid. The reaction proceeded according to Equation 5.4 to form the *trans* isomer. One set of pyridyl and phenyl resonances were observed in the ^{1}H-NMR spectrum due to symmetry, while the PtCH$_2$ proton resonance was observed at $\delta = 2.80$ with $^2J_{Pt-H} = 90$ Hz trans to Br. Only one methylplatinum resonance occurred in the ^{1}H-NMR spectrum at $\delta = 1.52$ with $^2J_{Pt-H} = 70$ Hz *trans* to N, which proved the formation of *trans* isomer.

(5.4)
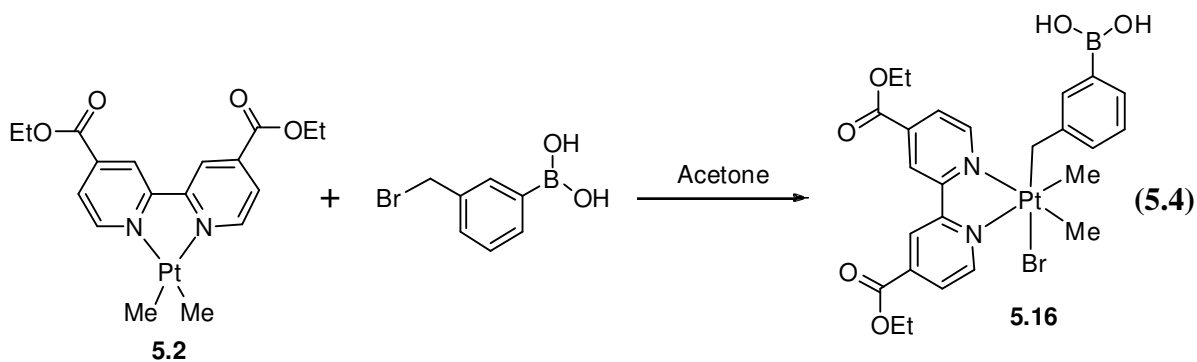
The structure of complex **5.16** is shown in Figure 5.17. Selected bond lengths and angles are shown in Table 5.10. Complex **5.16** self assembled in the solid state to give a supramolecular polymer through two intermolecular O-H•••O=C hydrogen bonding with O(5)•••O(1) = 2.99 Å, and O(3)•••O(2) = 2.83 Å (Figure 5.18). This signifies that the carboxylic acid hydrogen bonds are more covalent than in the boronic acids, these weaker hydrogen bonds formed via the boronic acid groups with respect to the carboxylic analogues could be attributed to the smaller polarization effects.[6, 25] There is additional self-assembly through π-stacking and C(14)H•••BrPt hydrogen bonding, and all these secondary bonding contributed in the formation of the supramolecular dimer. The graph set description for the dimeric structure is $R_2^2(15)$.
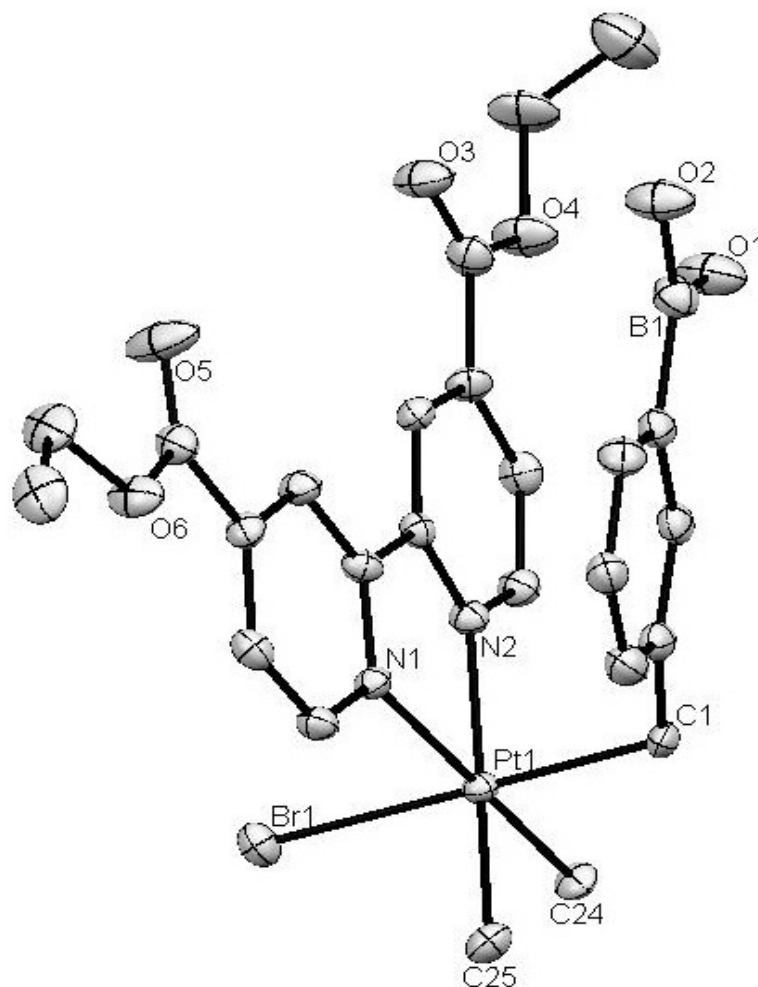
Figure 5.17. A view of the molecular structure of **5.16**.

Table 5.10. Selected bond lengths [Å] and angles [°] for **5.16** *trans-*
[PtBrMe$_2$(CH$_2$-3-C$_6$H$_4$-B{OH}$_2$)(DECBP)].

Pt(1)-N(1)	2.157(3)	Pt(1)-N(2)	2.150(3)
Pt(1)-C(1)	2.100(4)	Pt(1)-C(25)	2.067(4)
Pt(1)-C(24)	2.070(4)	Pt(1)-Br(1)	2.581(5)
O(1)-B(1)	1.370(7)	O(2)-B(1)	1.367(6)
N(1)-Pt(1)-N(2)	76.9(1)	N(2)-Pt(1)-C(24)	99.3(2)
N(1)-Pt(1)-Br(1)	85.6(9)	N(2)-Pt(1)-C(25)	174.5(2)
O(1)-B(1)-O(2)	116.6(4)	C(24)-Pt(1)-C(25)	85.9(2)
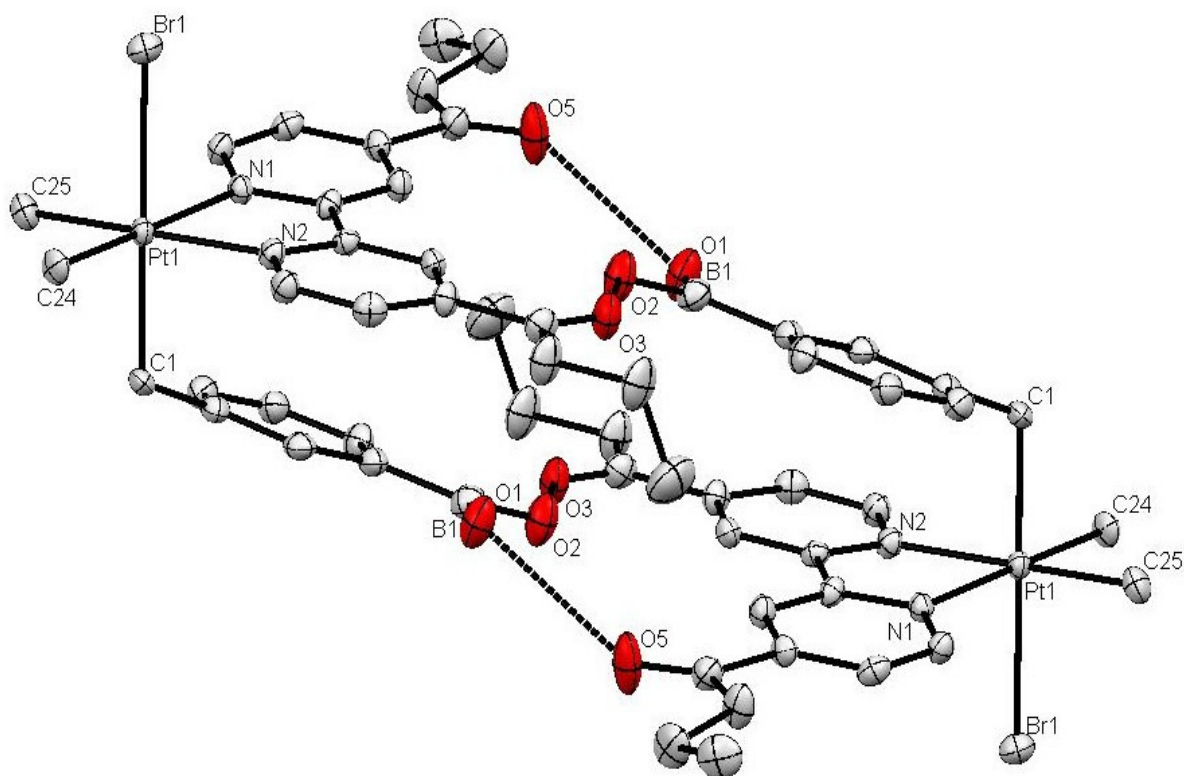
Figure 5.18. A view of the supramolecular dimeric structure of complex **5.16**.

The reaction of *para*-(bromomethyl)phenyl boronic acid with complex **5.2** [PtMe$_2$(DECBP)] produced the platinum(IV) complex [PtBrMe$_2$(CH$_2$-4-C$_6$H$_4$-B{OH}$_2$)(DECBP)], **5.17**, according to Equation 5.5. Complex **5.17** was isolated as a stable yellow solid that was soluble in various organic solvents such acetone, chloroform, and methylene chloride. The reaction proceeded via the oxidative addition of the Br-CH$_2$ bond to produce the *trans* isomer. The ^{1}H-NMR spectrum of complex **5.17** contained only one methylplatinum resonance at $\delta = 1.52$ with $^2J_{Pt-H} = 70$ Hz (*trans* to N), and PtCH$_2$ resonances at $\delta = 2.80$ with $^2J_{Pt-H} = 93$ Hz (*trans* to Br). The complex is symmetrical, so the ^{1}H-NMR spectrum contained one set of pyridyl and phenyl resonances. The *ortho* protons resonance of

the pyridyl groups was observed at $\delta = 8.96$ with $^3J_{\text{Pt-H}} = 19$ Hz (*trans* to C), while the phenyl

ortho resonance was seen at $\delta = 6.31$ with $^3J_{\text{Pt-H}} = 18$ Hz (*trans* to Br). The structure of complex

5.17 was determined via X-ray crystallography, and is shown in Figure 5.19. Table 5.11 shows

selected bond lengths and angles of complex **5.17**.

$$(5.5)$$
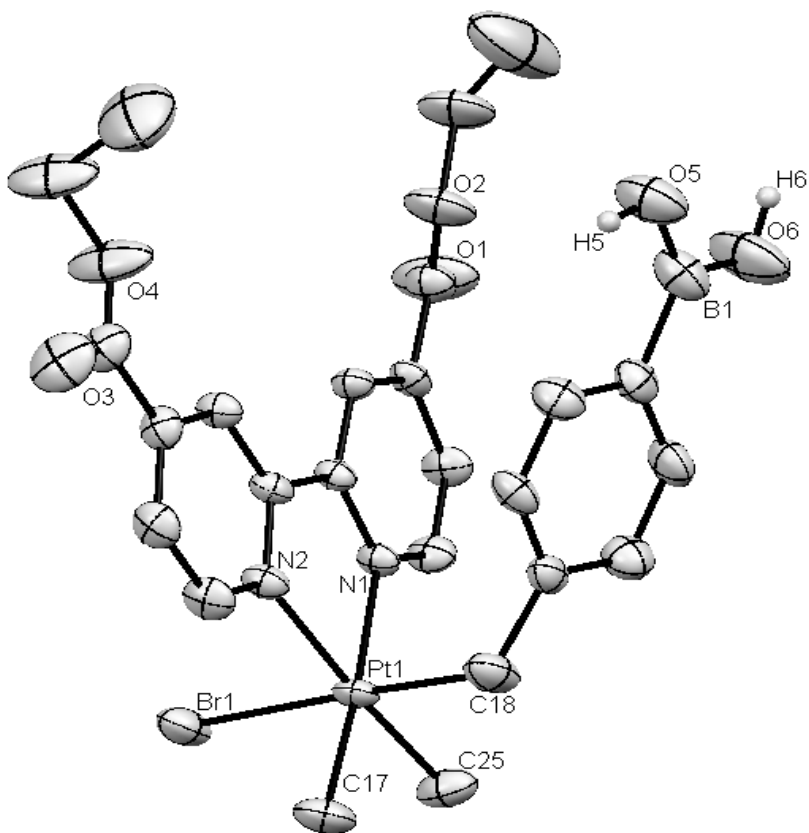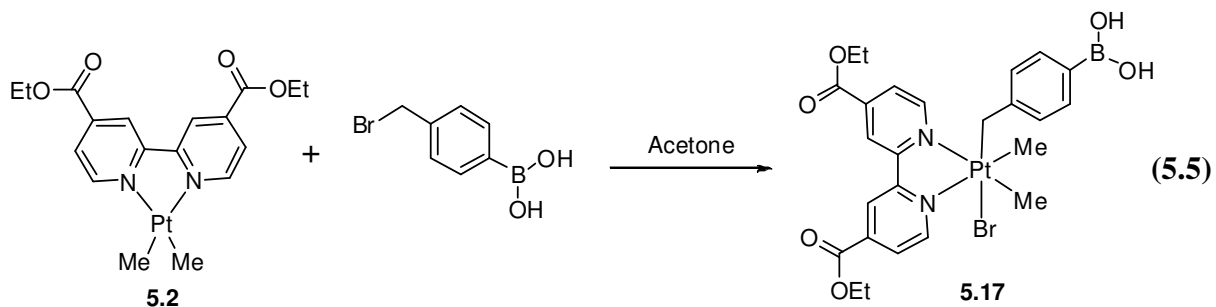
Figure 5.19. A view of the molecular structure of **5.17**.

Table 5.11. Selected bond lengths [Å] and angles [°] for **5.17** *trans*-[PtBrMe$_2$(CH$_2$-4-C$_6$H$_4$-B{OH}$_2$)(DECBP)].

Pt(1)-N(1)	2.158(4)	Pt(1)-N(2)	2.167(5)
Pt(1)-C(17)	2.061(6)	Pt(1)-C(25)	2.050(6)
Pt(1)-C(18)	2.076(6)	Pt(1)-Br(1)	2.598(1)
O(5)-B(1)	1.358(9)	O(6)-B(1)	1.350(9)
N(1)-Pt(1)-N(2)	76.3 (2)	N(2)-Pt(1)-C(25)	174.7(2)
N(1)-Pt(1)-Br(1)	86.5 (1)	N(2)-Pt(1)-C(17)	99.8(2)
O(1)-B(1)-O(2)	120.8(7)	C(17)-Pt(1)-C(18)	85.1(2)

The platinum(IV) complex [PtBrMe$_2$(CH$_2$-4-C$_6$H$_4$-B{OH}$_2$)(DECBP)], **5.17**, self-assembled in the solid state to a give a zigzag polymer as shown in Figure 5.20. The intermolecular PtBr•••HOB hydrogen bond secondary interaction helped in the formation of the supramolecular structure along with π-stacking. The hydrogen bond distance Br(1)•••O(5) = 3.287 Å, which is longer than the hydrogen bond formed in the dimeric structure of complex **5.16**. The ester groups were not involved in any of the self-assembly to form the zigzag polymer, which is probably because the boronic acid group is on the *para* position that is further away from the ester. Another hydrogen bond intermolecular interaction was observed between Br(1) and O(6), with Br(1)•••O(6) = 3.64 Å. Other secondary interactions {C(11)H•••B(1) and C(2)H•••O(3)} helped in linking the sheets formed through hydrogen bonding, which leads to the formation of the supramolecular network structure.
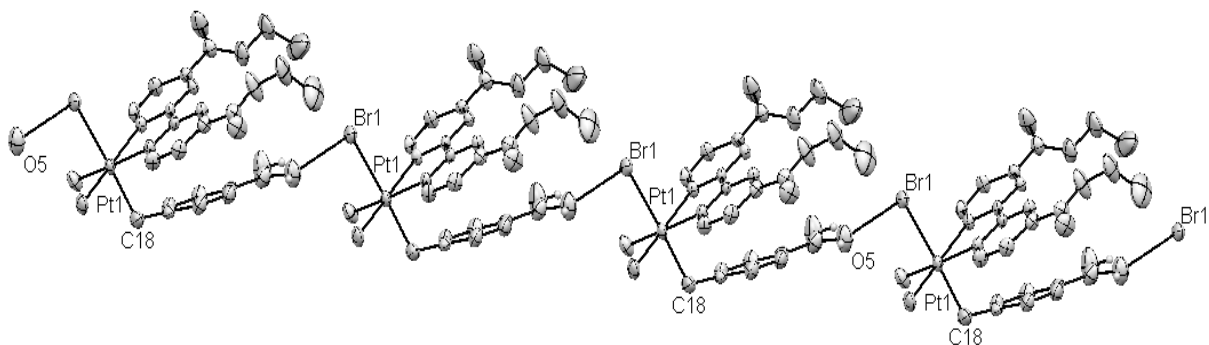
Figure 5.20. A view of the supramolecular polymeric structure of complex **5.17**.

The compound *ortho*-(bromomethyl)phenyl boronic acid was reacted with **5.2** in acetone at room temperature to give the *trans* platinum(IV) complex [PtBrMe$_2$(CH$_2$-2-C$_6$H$_4$-B{OH}$_2$)(DECBP)], **5.18**, according to Equation 5.6. Complex **5.18** was isolated as a stable yellow solid. The ^{1}H-NMR of **5.18** contained one methylplatinum resonance at δ = 1.52 with $^2J_{Pt\text{-}H}$ = 71 Hz (*trans* to N), and another Pt-CH$_2$ resonance at δ = 3.36 with $^2J_{Pt\text{-}H}$ = 94 Hz (*trans* to Br). The structure of **5.18** was determined by X-ray crystallography, and it confirmed the *trans* oxidative addition with an octahedral geometry (Figure 5.21). Table 5.12 shows selected bond lengths and angles of complex **5.18**.

$$(5.6)$$
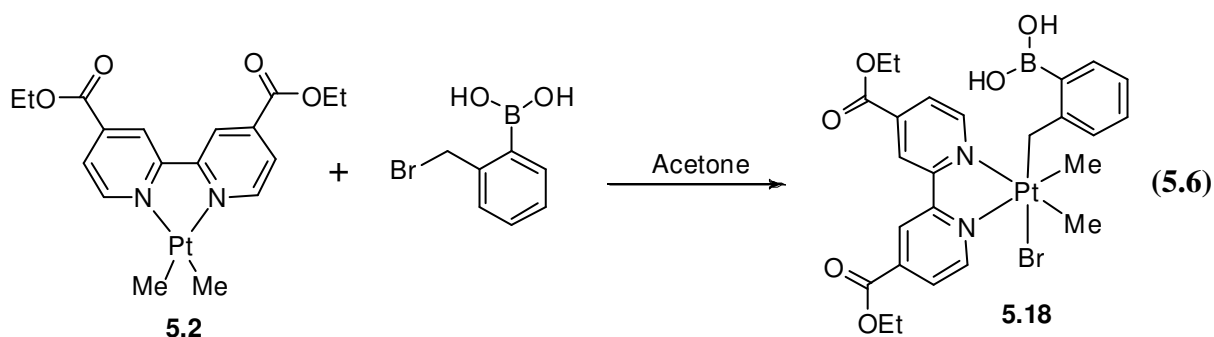
Table 5.12. Selected bond lengths [Å] and angles [°] for **5.18** *trans*-[PtBrMe$_2$(CH$_2$-2-C$_6$H$_4$-B{OH}$_2$)(DECBP)].

Pt(1)-N(1)	2.147(6)	Pt(1)-N(2)	2.059(7)
Pt(1)-C(1)	2.037(7)	Pt(1)-C(21)	2.059(7)
Pt(1)-C(18)	2.080(7)	Pt(1)-Br(1)	2.579(1)
O(5)-B(1)	1.369(1)	O(6)-B(1)	1.371(1)
N(1)-Pt(1)-N(2)	76.9(2)	N(2)-Pt(1)-C(1)	99.3(3)
N(1)-Pt(1)-Br(1)	86.7(2)	N(1)-Pt(1)-C(1)	175.5(3)
O(1)-B(1)-O(2)	116.8(7)	C(1)-Pt(1)-C(21)	87.4(3)
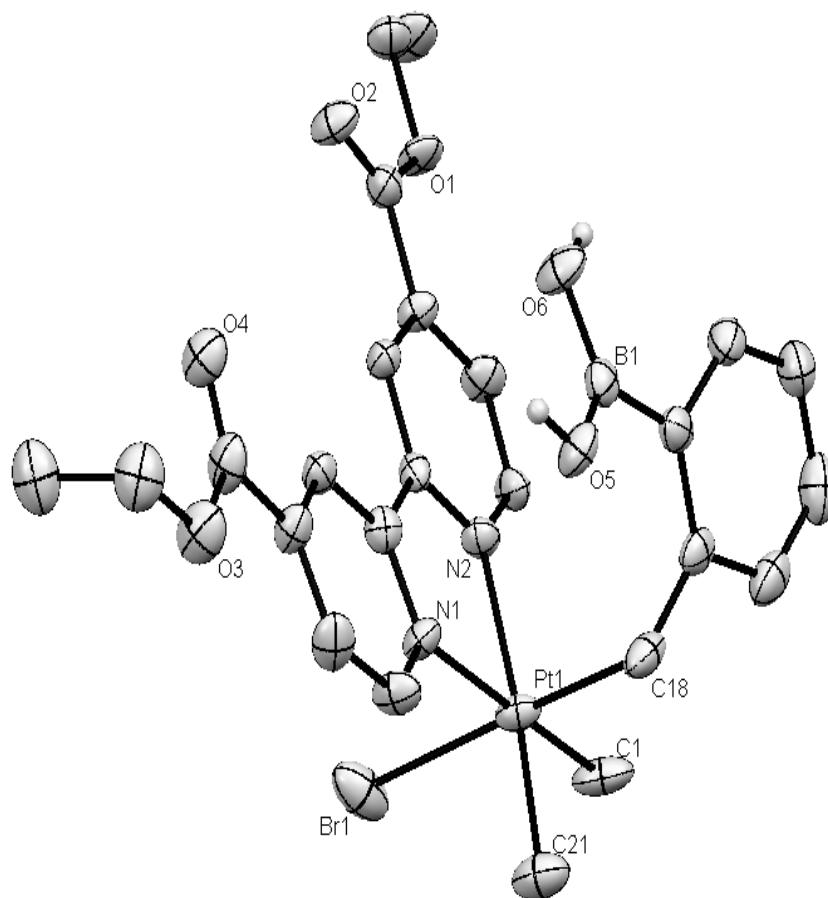
Figure 5.21. A view of the molecular structure of **5.18**.

The B(OH) groups of complex **5.18** formed hydrogen bonds with the carbonyl oxygen atoms of nearby molecule. The ester groups on the DECBP ligand in complex **5.18** were involved in similar hydrogen bonding patterns to the one in complex **5.16**, where a dimer supramolecular structure was formed (Figure 5.22), with graph set description of $R_2^2(15)$. These OH•••O=C hydrogen bond interactions gave rise to the polymer structure along with other self-assembly, C(3)H•••Br(1) = 2.84 Å. The hydrogen bonds O(4)•••O(6) = 2.83 Å and O(5)•••O(2) = 2.94 Å are relatively strong.[6]
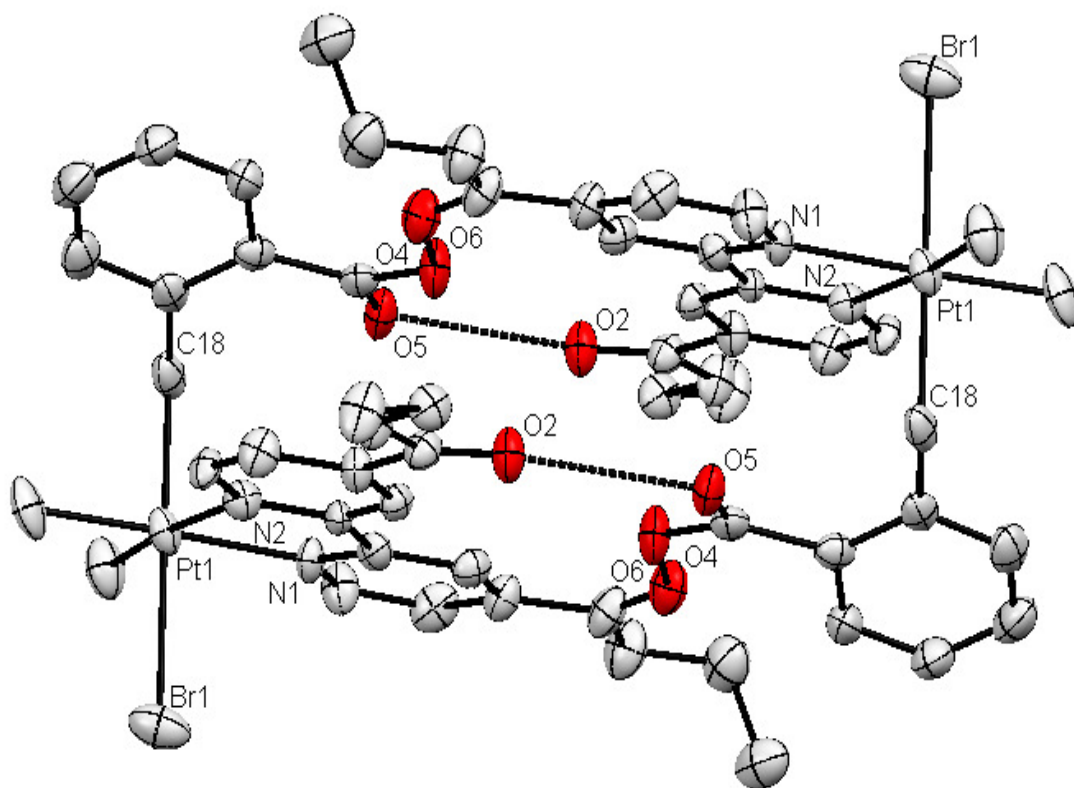
Figure 5.22. A view of the supramolecular dimeric structure of complex **5.18**.

5.3 Conclusions

The dimethylplatinum(II) complex [PtMe$_2$(DECBP)], DECBP = 4,4'-diethoxycarbonyl-2-2'-bipyridine], **5.2**, undergoes easy oxidative addition to the corresponding platinum(IV) complexes. In some cases, as in the addition of HCl, subsequent reductive elimination reaction occurs to produce a new platinum(II) complex.

The DECBP ligand contains two ester units, whose O=C carbonyl oxygen atoms can act as hydrogen bond acceptors. The reaction of the complex [PtMe$_2$(DECBP)], **5.2**, with alkyl bromides RCH$_2$Br, which had a carboxylic acid functional groups in its R groups, resulted in the formation of stable platinum(IV) complexes. Those complexes self-assemble in the solid state to form supramolecular polymers via the intermolecular OH•••O=C interactions, with other predicted interactions such as the π-stacking, and the C(H)•••BrPt secondary weak interactions.

Introduction of amide groups as hydrogen bond donors and acceptors results in self-assembly via NH•••BrPt hydrogen bonding to give supramolecular polymers, with N(3)•••Br(1) = 3.510 Å, which is the normal range for N-H•••Br hydrogen bonding interactions of N•••Br = 3.12 - 3.69 Å.[5a]

Finally, the oxidative addition of *ortho*-, *meta*-, and *para*-(bromomethyl)phenyl boronic acids resulted in forming the trans isomers of the platinum(IV) complexes. The platinum(IV) complexes containing the *ortho* and *meta* substituted boronic acids self-assemble in the solid state to give a supramolecular polymer through two intermolecular O-H•••O=C hydrogen bonding. The ester units in the *para* substituted derivitave is not involved hydrogen bonding, and the complex forms a zigzag polymer through formation of intermolecular OH•••BrPt interactions. Other types of weak secondary interactions are observed in the formation of the polymers, such as π-stacking, and C(H)•••BrPt hydrogen bonds.

5.4 Experimental

All reactions were carried out under nitrogen using standard Schlenk techniques, unless otherwise specified. NMR spectra were recorded on Varian Mercury 400, and Varian Inova 400 and 600 spectrometers. [1]H and ^{13}C chemical shifts are reported relative to tetramethylsilane (TMS). Elemental analyses were carried out by Guelph Chemical Laboratories, Guelph, Canada. The complexes *cis/trans*-[PtCl$_2$(SMe$_2$)$_2$] and [Pt$_2$Me$_4$(μ-SMe$_2$)$_2$] were prepared from K$_2$[PtCl$_4$] according to the literature.[11]

[4,4'-Diethoxycarbonyl-2-2'-bipyridine], 5.1. A modified procedure of Sprintschnik *et al.*[2] was followed. First, 4,4'- dimethyl-2,2'-bipyridine was prepared by refluxing 4-picoline (35 mL) and palladium (1.4 g) for 1 day. Then 12.5 mL of benzene was added to the mixture, and the mixture was refluxed for an hour. After that the mixture was filtered while hot, and then put on high vacuum. The white crystals of the product precipitated. Then 4,4'- dicarboxy-2,2'-bipyridine was prepared by refluxing 10 g of the dimethyl ligand and potassium permanganate (31.3 g) in water (200 mL) for 6 hours. A brown precipitate formed, which was removed by filtration, and the yellowish solution was extracted by ether 3 times. HCl was later added to help the precipitation of white crystals. Compound **5.1** was finally prepared by refluxing 6 g of 4,4'- dicarboxy-2,2'-bipyridine with 60 mL of thionyl chloride. After that excess of ethanol and benzene (100 mL) were added, and the mixture was refluxed for 2 hours. Chloroform was added to the mixture, and it was treated later with cold aqueous sodium bicarbonate. The organic layer was dried and evaporated. White crystals were formed after recrystallization using acetone and chloroform. Yield 82%. ^{1}H NMR in CD$_2$Cl$_2$: δ = 1.43 (t, 6H, $^3J_{H-H}$ = 7 Hz, CH$_3$C), 4.45 (q, 4H, $^3J_{H-H}$ = 7 Hz, CH$_2$C), 7.94 (d, 2H, $^3J_{H-H}$ = 6 Hz, Py-H$_{meta}$), 8.89 (d, 2H, $^3J_{H-H}$ = 6 Hz, Py-H$_{ortho}$),

9.00 (s, 2H, Py-H$_{meta'}$). Anal. Calcd. for C$_{16}$H$_{16}$N$_2$O$_4$ (%): C: 63.99, H: 5.37, N: 9.33; Found: C: 64.15, H: 5.62, N: 9.34.

[PtMe$_2$(DECBP)], 5.2. To a solution of 4,4'-diethoxycarbonyl-2-2'-bipyridine, **5.1**, (0.52 g, 1.73 mmol) in ether (20 mL) was added [Pt$_2$Me$_4$(μ-SMe$_2$)$_2$] (0.5 g, 0.869 mmol). After 5 minutes the solution turned purple, and the product precipitated as a purple solid over 40 minutes. The product was first separated from the solution by decanting. It was washed with (3x3 mL) pentane and then dried under high vacuum. Yield 91%. ^{1}H NMR in acetone-d$_6$: δ = 1.14 (s, 6H, $^2J_{Pt-H}$ = 86 Hz, Pt-CH$_3$), 1.45 (t, 6H, $^3J_{H-H}$ = 7 Hz, CH$_3$C), 4.49 (q, 4H, $^3J_{H-H}$ = 7 Hz, CH$_2$C), 8.14 (d, 2H, $^3J_{H-H}$ = 6 Hz, Py-H$_{meta}$), 8.79 (s, 2H, Py-H$_{meta'}$), 9.42 (d, 2H, $^3J_{H-H}$ = 6 Hz, $^3J_{Pt-H}$ = 28 Hz, Py-H$_{ortho}$). Anal. Calcd. for C$_{18}$H$_{22}$N$_2$O$_4$Pt (%): C: 41.14, H: 4.22, N: 5.33; Found: C: 40.85, H: 4.04, N: 5.45.

[PtIMe$_3$(DECBP)], 5.3. Excess iodomethane (0.025 mL) was added dropwise to a solution of complex **5.2** (0.05 g, 0.095 mmol) in acetone (10 mL). After 3 minutes the color of the solution changed from purple to yellow. 20 minutes later after almost complete precipitation, the volume was reduced to half and then placed overnight in the fridge. The next day solvent was removed by decanting. The precipitate was washed with pentane (3x2 mL) and then dried under high vacuum. Yield 84%. ^{1}H NMR in acetone-d$_6$: δ = 0.60 (s, 3H, $^2J_{Pt-H}$ = 72 Hz, Pt-CH$_3$), 1.45 (t, 6H, $^3J_{H-H}$ = 7 Hz, CH$_3$C), 1.52 (s, 6H, $^2J_{Pt-H}$ = 71 Hz, Pt-CH$_3$), 4.53 (q, 4H, $^3J_{H-H}$ = 7 Hz, CH$_2$C), 8.33 (d, 2H, $^3J_{H-H}$ = 6 Hz, Py-H$_{meta}$), 9.20 (s, 2H, Py-H$_{meta'}$), 9.25 (d, 2H, $^3J_{H-H}$ = 6 Hz, $^3J_{Pt-H}$ = 20 Hz, Py-H$_{ortho}$). Anal. Calcd. for C$_{19}$H$_{25}$IN$_2$O$_4$Pt (%): C: 34.19, H: 3.78, N: 4.20; Found: C: 34.30, H: 3.89, N: 4.16.

[PtI$_2$Me$_2$(DECBP)], 5.4. It was synthesized from complex **5.2** (0.035 g, 0.066 mmol) in dry CH$_2$Cl$_2$ (15 mL), and excess Iodine (0.033 g, 0.129 mmol). The color changed from purple to

dark red in 5 mintues, the solvent was removed by rotavap, leaving behind a dark red powder. The powder was washed with ether (3x2 mL) and pentane (3x2 mL) and then dried under high vacuum. Yield 83%. ^{1}H NMR in CD_2Cl_2: δ = 1.49 (t, 6H, $^3J_{H\text{-}H}$= 7 Hz, CH_3C), 2.42 (s, 6H, $^2J_{Pt\text{-}H}$ =73 Hz, $Pt\text{-}CH_3$), 4.55 (q, 4H, $^3J_{H\text{-}H}$= 7 Hz, CH_2C), 8.30 (d, 2H, $^3J_{H\text{-}H}$ = 5 Hz, Py-H$_{meta}$), 9.02 (s, 2H, Py-H$_{meta'}$), 9.07 (d, 2H, $^3J_{H\text{-}H}$ = 5 Hz, $^3J_{Pt\text{-}H}$ = 21 Hz, Py-H$_{ortho}$). Anal. Calcd. for $C_{18}H_{22}I_2N_2O_4Pt$ (%): C: 27.74, H: 2.85, N: 3.59; Found: C: 28.08, H: 2.86, N: 3.59.

[PtBr$_2$Me$_2$(DECBP)], 5.5. Excess bromine (0.01 mL) was added dropwise to a solution of complex **5.2** (0.03 g, 0.057 mmol) in dry CH_2Cl_2 (20 mL). The color of the solution rapidly changed from purple to orange. After 30 minutes the solvent was reduced to ~1 mL, then pentane (2 mL) was added to precipitate the product as an orange powder. The orange precipitate was washed with pentane (3x2 mL) and ether (3x2 mL) and then dried under high vacuum. Yield 80%. ^{1}H NMR in CD_2Cl_2: δ = 1.48 (t, 6H, $^3J_{H\text{-}H}$ = 7 Hz, CH_3C), 2.07 (s, 6H, $^2J_{Pt\text{-}H}$ = 71 Hz, $Pt\text{-}CH_3$), 4.54 (q, 4H, $^3J_{H\text{-}H}$ = 7 Hz, CH_2C), 8.29 (d, 2H, $^3J_{H\text{-}H}$ = 5 Hz, Py-H$_{meta}$), 8.97 (s, 2H, Py-H$_{meta'}$), 9.07 (d, 2H, $^3J_{H\text{-}H}$ = 5 Hz, $^3J_{Pt\text{-}H}$ = 18 Hz, Py-H$_{ortho}$). Anal. Calcd. for $C_{18}H_{22}Br_2N_2O_4Pt$ (%): C: 31.55, H: 3.24, N: 4.09; Found: C: 31.37, H: 3.13, N: 3.88.

[Pt(CH$_3$CO)ClMe$_2$(DECBP)], 5.6. To a stirred solution of **5.2** [PtMe$_2$(DECBP)] (0.038 g, 0.063 mmol) in dry CH_2Cl_2 (15 mL) was added acetyl chloride (0.004 g, 0.063 mmol). The color of the solution turned to yellow within 5 minutes. Then the color changed to green after 10 minutes. The reaction was kept stirring for an hour. The solvent was pumped off using a rotavap. A green precipitate remained in the bottom of the flask, which was washed pentane (3x3 mL) and ether (3x3 mL) and then dried under high vacuum. Yield 84%. ^{1}H NMR in CD_2Cl_2: **5.6a** *cis* isomer (major), δ = 0.75 (s, 3H, $^2J_{Pt\text{-}H}$ = 74 Hz, $Pt\text{-}CH_3$), 1.47 (t, 6H, $^3J_{H\text{-}H}$ = 7 Hz, CH_3C), 1.57 (s, 3H, $^2J_{Pt\text{-}H}$ = 72 Hz, $Pt\text{-}CH_3$), 2.58 (s, 3H, $^3J_{Pt\text{-}H}$ = 10 Hz, CH_3C), 4.53 (q, 4H, $^3J_{H\text{-}H}$ = 7 Hz,

CH$_2$C), 8.22 (d, 1H, $^3J_{H-H}$ = 5 Hz, Py-H$_{meta}$), 8.23 (d, 1H, $^3J_{H-H}$ = 5 Hz, Py-H$_{meta}$), 8.90 (s, 2H, Py-H$_{meta'}$), 8.97 (d, 1H, $^3J_{H-H}$ = 5 Hz, $^3J_{Pt-H}$ = 20 Hz, Py-H$_{ortho}$), 9.33 (d, 1H, $^3J_{H-H}$ = 5 Hz, $^3J_{Pt-H}$ = 19 Hz, Py-H$_{ortho}$); **5.6b** *trans* isomer (minor), δ = 1.48 (t, 3H, $^3J_{H-H}$ = 7 Hz, CH$_3$C), 1.59 (s, 6H, $^2J_{Pt-H}$ = 72 Hz, Pt-CH$_3$), 2.00 (s, 3H, $^3J_{Pt-H}$ = 14 Hz, CH$_3$C), 4.54 (q, 4H, $^3J_{H-H}$ = 7 Hz, CH$_2$C), 8.27 (d, 2H, $^3J_{H-H}$ = 5 Hz, Py-H$_{meta}$), 8.97 (s, 2H, Py-H$_{meta'}$), 9.13 (d, 2H, $^3J_{H-H}$ = 5 Hz, $^3J_{Pt-H}$ = 20 Hz, Py-H$_{ortho}$). Anal. Calcd. for C$_{20}$H$_{25}$ClN$_2$O$_5$Pt (%): C: 39.77, H: 4.17, N: 4.64; Found: C: 39.51, H: 4.40, N: 4.55.

[Pt(CH$_3$CH$_2$OCO)ClMe$_2$(DECBP)], 5.7. This complex way synthesized in a similar way to complex **5.6**, from complex **5.2**, [PtMe$_2$(DECBP)] (0.035 g, 0.066 mmol) in dry CH$_2$Cl$_2$ (15mL), and the drop wise addition of ethyl chloroformate (0.007 g). The color of the isolated product was yellow. Then the product was washed with pentane (2x2 mL) and ether (2x2 mL) and later dried under high vacuum. Yield 79 %. ^{1}H NMR in CD$_2$Cl$_2$: δ = 0.85 (t, 3H, $^3J_{H-H}$ = 7 Hz, CH$_3$C), 1.48 (t, 6H, $^3J_{H-H}$ = 7 Hz, CH$_3$C), 1.65 (s, 6H, $^2J_{Pt-H}$ = 71 Hz, Pt-CH$_3$), 3.77 (q, 2H, $^3J_{H-H}$ = 7 Hz, $^4J_{Pt-H}$ = 5 Hz, CH$_2$C), 4.54 (q, 4H, $^3J_{H-H}$ = 7 Hz, CH$_2$C), 8.27 (d, 2H, $^3J_{H-H}$ = 5 Hz, Py-H$_{meta}$), 8.93 (s, 2H, Py-H$_{meta'}$), 9.13 (d, 2H, $^3J_{H-H}$ = 5 Hz, $^3J_{Pt-H}$ = 17 Hz, Py-H$_{ortho}$). Anal. Calcd. for C$_{21}$H$_{27}$ClN$_2$O$_6$Pt (%): C: 39.78, H: 4.29, N: 4.42; Found: C: 39.79, H: 4.52, N: 4.37.

[PtCl$_2$(DECBP)], 5.8. Hydrochloric acid (0.0035 mL, 3M) was added to complex **5.2** [PtMe$_2$(DECBP)] (0.0034 g, 0.006 mmol) dissolved in CD$_2$Cl$_2$ (1 g) in an NMR tube. The color of the solution changed from purple to yellow. Then the NMR spectrum was taken using the Inova 400 instrument. ^{1}H NMR in CD$_2$Cl$_2$: δ = 1.48 (t, 6H, $^3J_{H-H}$ = 7 Hz, CH$_3$C), 4.53 (q, 4H, $^3J_{H-H}$ = 7 Hz, CH$_2$C), 8.17 (d, 2H, $^3J_{H-H}$ = 5 Hz, Py-H$_{meta}$), 8.66 (s, 2H, Py-H$_{meta'}$), 9.97 (d, 2H, $^3J_{H-H}$ = 5 Hz, $^3J_{Pt-H}$ = 48 Hz, Py-H$_{ortho}$).

[Pt(OH)$_2$Me$_2$(DECBP)], 5.9. To a solution of complex **5.2**, [PtMe$_2$(DECBP)] (0.03 g, 0.057 mmol) in acetone was added H$_2$O$_2$ (0.001 mL, 0.057 mmol). The mixture was stirred for 30 minutes, and the turned colorless. Then the product was washed with pentane (2x3 mL) and ether (2x3 mL) and later dried under high vacuum. The reaction resulted in a white solid. Yield 80 %. ^{1}H NMR in CD$_2$Cl$_2$: δ = 1.47 (t, 6H, $^3J_{\text{H-H}}$ = 7 Hz, CH$_3$C), 1.66 (s, 6H, $^2J_{\text{Pt-H}}$ = 70 Hz, Pt-CH$_3$), 4.52 (q, 4H, $^3J_{\text{H-H}}$ = 7 Hz, CH$_2$C), 8.21 (d, 2H, $^3J_{\text{H-H}}$ = 5 Hz, Py-H$_{meta}$), 8.91 (s, 2H, Py-H$_{meta'}$), 9.01 (d, 2H, $^3J_{\text{H-H}}$ = 5 Hz, $^3J_{\text{Pt-H}}$ = 18 Hz, Py-H$_{ortho}$); Anal. Calcd. for C$_{21}$H$_{27}$ClN$_2$O$_6$Pt (%): C: 38.64, H: 4.32, N: 5.01.

[PtBrMe$_2$(CH$_2$-4-C$_6$H$_4$-CO$_2$H)(DECBP)]˙4H$_2$O, 5.10. To a solution of complex **5.2**, [PtMe$_2$(DECBP)] (0.05 g, 0.095 mmol) in acetone (15 mL) was added BrCH$_2$-4-C$_6$H$_4$CO$_2$H (0.021 g, 0.095 mmol). The mixture was stirred for 3 hours. The solution turned red after 10 minutes, then yellow after one hour. The solvent was evaporated under vacuum, and then the yellow solid was washed with water (3x3 mL) and pentane (3x3 mL). The product was dried under high vacuum. Yield 86 %. ^{1}H NMR in acetone-d$_6$: δ = 1.44 (t, 6H, $^3J_{\text{H-H}}$ = 7 Hz, CH$_3$C), 1.54 (s, 6H, $^2J_{\text{Pt-H}}$ = 72 Hz, Pt-CH$_3$), 2.87 (s, 2H, $^2J_{\text{Pt-H}}$ = 95 Hz, Pt-CH$_2$), 4.49 (q, 4H, $^3J_{\text{H-H}}$ = 7 Hz, CH$_2$C), 6.46 (d, 2H, $^3J_{\text{H-H}}$ = 8 Hz, $^3J_{\text{Pt-H}}$ = 18 Hz, Ph-H$_{ortho}$), 7.27 (d, 2H, $^3J_{\text{H-H}}$ = 8 Hz, Ph-H$_{meta}$), 8.17 (d, 2H, $^3J_{\text{H-H}}$ = 7 Hz, Py-H$_{meta}$), 8.93 (s, 2H, Py-H$_{meta'}$), 8.97 (d, 2H, $^3J_{\text{H-H}}$ = 7 Hz, $^3J_{\text{Pt-H}}$ = 19 Hz, Py-H$_{ortho}$). Anal. Calcd. for C$_{26}$H$_{37}$BrN$_2$O$_{10}$Pt (%): C: 38.43, H: 4.59, N: 3.45; Found: C: 38.27, H: 4.25, N: 3.32.

[PtBrMe$_2$(CH$_2$-4-C$_6$H$_4$CH$_2$-CO$_2$H)(DECBP)]˙2H$_2$O, 5.11. This was prepared in a similar way to complex **5.11**, from complex **5.2**, [PtMe$_2$(DECBP)] (0.05 g, 0.095 mmol) and BrCH$_2$-4-C$_6$H$_4$CH$_2$CO$_2$H (0.022 g, 0.095 mmol) in acetone (15 mL). The reaction resulted in a yellow solid. Yield 88 %. ^{1}H NMR in acetone-d$_6$: δ = 1.44 (t, 6H, $^3J_{\text{H-H}}$ = 7 Hz, CH$_3$C), 1.50 (s, 6H, $^2J_{\text{Pt-}}$

$_H$ = 70 Hz, Pt-CH$_3$), 2.77 (s, 2H, $^2J_{Pt-H}$ = 90 Hz, Pt-CH$_2$), 3.21 (s, 2H, Ph-CH$_2$CO), 4.50 (q, 4H, $^3J_{H-H}$ = 7 Hz, CH$_2$C), 6.27 (d, 2H, $^3J_{H-H}$ = 8 Hz, $^3J_{Pt-H}$ = 18 Hz, Ph-H$_{ortho}$), 6.51 (d, 2H, $^3J_{H-H}$ = 8 Hz, Ph-H$_{meta}$), 8.15 (d, 2H, $^3J_{H-H}$ = 6 Hz, Py-H$_{meta}$), 8.86 (s, 2H, Py-H$_{meta'}$), 8.95 (d, 2H, $^3J_{H-H}$ = 6 Hz, $^3J_{Pt-H}$ = 19 Hz, Py-H$_{ortho}$). Anal. Calcd. for C$_{27}$H$_{35}$BrN$_2$O$_6$Pt (%): C: 41.02, H: 4.46, N: 3.54; Found: C: 41.01, H: 3.98, N: 3.63.

[PtBrMe$_2$(CH$_2$CO$_2$H)(DECBP)]·3H$_2$O, 5.12. This was prepared in a similar way to complex **5.11**, from complex **5.2**, [PtMe$_2$(DECBP)] (0.05 g, 0.095 mmol) and BrCH$_2$-CO$_2$H (0.013 g, 0.095 mmol) in acetone (20 mL). The reaction resulted in an orange solid. Yield 88 %. ^{1}H NMR in acetone-d$_6$: δ = 1.46 (t, 6H, $^3J_{H-H}$ = 7 Hz, CH$_3$C), 1.53 (s, 6H, $^2J_{Pt-H}$ = 70 Hz, Pt-CH$_3$), 2.01 (s, 2H, $^2J_{Pt-H}$ = 95 Hz, Pt-CH$_2$), 4.53 (q, 4H, $^3J_{H-H}$ = 7 Hz, CH$_2$C), 8.31 (d, 2H, $^3J_{H-H}$ = 6 Hz, Py-H$_{meta}$), 9.09 (d, 2H, $^3J_{H-H}$ = 6 Hz, $^3J_{Pt-H}$ = 19 Hz, Py-H$_{ortho}$), 9.13 (s, 2H, Py-H$_{meta'}$). Anal. Calcd. for C$_{20}$H$_{31}$BrN$_2$O$_9$Pt (%): C: 33.44, H: 4.35, N: 3.90; Found: C: 33.52, H: 3.64, N: 4.09.

[PtBrMe$_2$(CH$_2$-CONH-4-C$_6$H$_4$-t-Bu)(DECBP)], 5.13. A mixture of complex **5.2**, [PtMe$_2$(DECBP)] (0.05 g, 0.095 mmol) and compound **A** BrCH$_2$-CONH-4-C$_6$H$_4$-t-Bu (0.022 g, 0.095 mmol) in acetone (10 mL) was stirred for 5 hours at room temperature. The reaction color changed to orange. The solvent was evaporated under vacuum and the resulting solid was washed with water (3x3 mL) and pentane (3x3 mL). The product was isolated as an orange solid, which was dried under high vacuum. Yield 87 %. ^{1}H NMR in CD$_2$Cl$_2$: δ = 1.24 (s, 9H, t-Bu), 1.45 (t, 6H, $^3J_{H-H}$ = 7 Hz, CH$_3$C), 1.56 (s, 6H, $^2J_{Pt-H}$ = 69 Hz, Pt-CH$_3$), 2.10 (s, 2H, $^2J_{Pt-H}$ = 92 Hz, Pt-CH$_2$), 4.49 (q, 4H, $^3J_{H-H}$ = 7 Hz, CH$_2$C), 6.62 (s, 1H, NH), 6.74 (d, 2H, $^3J_{H-H}$ = 9 Hz, Ph-H$_{ortho}$), 7.06 (d, 2H, $^3J_{H-H}$ = 9 Hz, Ph-H$_{meta}$), 7.99 (d, 2H, $^3J_{H-H}$ = 6 Hz, Py-H$_{meta}$), 8.80 (s, 2H, Py-H$_{meta'}$), 8.92 (d, 2H, $^3J_{H-H}$ = 6 Hz, $^3J_{Pt-H}$ = 19 Hz, Py-H$_{ortho}$).

[PtBrMe$_2$(CH$_2$-CONH-C$_6$H$_5$)(DECBP)], 5.14. This was prepared similarly from complex **5.2**, [PtMe$_2$(DECBP)] (0.05 g, 0.095 mmol) and compound **B** BrCH$_2$-CONH-C$_6$H$_5$ (0.021 g, 0.095 mmol) in acetone (10 mL). Yield 85 %. ^{1}H NMR in CD$_2$Cl$_2$: δ = 1.45 (t, 6H, $^3J_{H-H}$ = 7 Hz, CH$_3$C), 1.56 (s, 6H, $^2J_{Pt-H}$ = 69 Hz, Pt-CH$_3$), 2.12 (s, 2H, $^2J_{Pt-H}$ = 92 Hz, Pt-CH$_2$), 4.47 (q, 4H, $^3J_{H-H}$ = 7 Hz, CH$_2$C), 6.65 (s, 1H, NH), 6.82 (d, 2H, $^3J_{H-H}$ = 8 Hz, Ph-H$_{ortho}$), 6.88 (t, 1H, $^3J_{H-H}$ = 8 Hz, Ph-H$_{para}$), 7.02 (t, 2H, $^3J_{H-H}$ = 8 Hz, Ph-H$_{meta}$), 7.98 (d, 2H, $^3J_{H-H}$ = 6 Hz, Py-H$_{meta}$), 8.75 (s, 2H, Py-H$_{meta'}$), 8.91 (d, 2H, $^3J_{H-H}$ = 6 Hz, $^3J_{Pt-H}$ = 19 Hz, Py-H$_{ortho}$).

[PtBrMe$_2$(CH$_2$-3-C$_6$H$_4$-CH$_2$OH)(DECBP)], 5.15. A solution of BrCH$_2$-3-C$_6$H$_4$CH$_2$OH (0.019 g, 0.095 mmol) in acetone (1 mL) was added to complex **5.2** (0.05 g, 0.095 mmol) in acetone (10 mL) and allowed to stir for 2 hours. The solution color turned to yellow in an hour. The solvent was evaporated under vacuum, and then the yellow solid was washed with pentane (3x3 mL). The product was dried under high vacuum. Yield 84 %. ^{1}H NMR acetone-d$_6$: δ = 1.45 (t, 6H, $^3J_{H-H}$ = 7 Hz, CH$_3$C), 1.57 (s, 6H, $^2J_{Pt-H}$ = 71 Hz, Pt-CH$_3$), 2.88 (s, 2H, $^2J_{Pt-H}$ = 91 Hz, Pt-CH$_2$), 4.03 (s, 2H, Ph-CH$_2$-O), 4.51 (q, 4H, $^3J_{H-H}$ = 7 Hz, CH$_2$C), 6.12 (d, 1H, $^3J_{H-H}$ = 8 Hz, $^3J_{Pt-H}$ = 18 Hz, Ph-H$_{ortho}$), 6.47 (t, 1H, $^3J_{H-H}$ = 8 Hz, Ph-H$_{meta}$), 6.68 (t, 1H, $^3J_{H-H}$ = 8 Hz, Ph-H$_{para}$), 6.78 (d, 1H, $^3J_{H-H}$ = 8 Hz, Ph-H$_{meta'}$), 8.19 (d, 2H, $^3J_{H-H}$ = 6 Hz, Py-H$_{meta}$), 8.81 (s, 2H, Py-H$_{meta'}$), 9.10 (d, 2H, $^3J_{H-H}$ = 6 Hz, $^3J_{Pt-H}$ = 19 Hz, Py-H$_{ortho}$). Anal. Calcd. for C$_{26}$H$_{31}$BrN$_2$O$_5$Pt (%): C: 42.98, H: 4.30, N: 3.86; Found: C: 42.81, H: 4.26, N: 3.79.

[PtBrMe$_2$(CH$_2$-3-C$_6$H$_4$-B{OH}$_2$)(DECBP)]·(Acetone), 5.16. This was prepared similarly to complex **5.15**, from complex **5.2** (0.05 g, 0.095 mmol) in acetone (10 mL), and *m*-BrCH$_2$-4-C$_6$H$_4$B{OH}$_2$ (0.021 g, 0.095 mmol). A yellow product was produced. Yield 86 %. ^{1}H NMR acetone-d$_6$: δ = 1.45 (t, 6H, $^3J_{H-H}$ = 8 Hz, CH$_3$C), 1.52 (s, 6H, $^2J_{Pt-H}$ = 70 Hz, Pt-CH$_3$), 2.80 (s, 2H, $^2J_{Pt-H}$ = 90 Hz, Pt-CH$_2$), 4.50 (q, 4H, $^3J_{H-H}$ = 8 Hz, CH$_2$C), 6.46 (d, 1H, $^3J_{H-H}$ = 8 Hz, $^3J_{Pt-H}$ =

18 Hz, Ph-H$_{ortho}$), 6.60 (t, 1H, $^3J_{\text{H-H}}$ = 8 Hz, Ph-H$_{meta}$), 6.69 (s, 1H, Ph-H$_{para}$), 7.17 (d, 1H, $^3J_{\text{H-H}}$ = 8 Hz, Ph-H$_{ortho'}$), 8.15 (d, 2H, $^3J_{\text{H-H}}$ = 6 Hz, Py-H$_{meta}$), 8.81 (s, 2H, Py-H$_{meta'}$), 8.96 (d, 2H, $^3J_{\text{H-H}}$ = 6 Hz, $^3J_{\text{Pt-H}}$ = 19 Hz, Py-H$_{ortho}$). Anal. Calcd. for C$_{28}$H$_{36}$BrN$_2$BO$_7$Pt (%): C: 42.12, H: 4.54, N: 3.51; Found: C: 41.81, H: 4.07, N: 3.60.

[PtBrMe$_2$(CH$_2$-4-C$_6$H$_4$-B{OH}$_2$)(DECBP)], 5.17. This was prepared similarly to complex **5.15** from complex **5.2** (0.065 g, 0.124 mmol) in acetone (10 mL), and p-BrCH$_2$-4-C$_6$H$_4$B{OH}$_2$ (0.027 g, 0.124 mmol). A yellow product was produced. Yield 85 %. ^{1}H NMR acetone-d$_6$: δ = 1.44 (t, 6H, $^3J_{\text{H-H}}$ = 7 Hz, CH$_3$C), 1.52 (s, 6H, $^2J_{\text{Pt-H}}$ = 70 Hz, Pt-CH$_3$), 2.80 (s, 2H, $^2J_{\text{Pt-H}}$ = 93 Hz, Pt-CH$_2$), 4.50 (q, 4H, $^3J_{\text{H-H}}$ = 7 Hz, CH$_2$C), 6.31 (d, 2H, $^3J_{\text{H-H}}$ = 8 Hz, $^3J_{\text{Pt-H}}$ = 18 Hz, Ph-H$_{ortho}$), 7.10 (d, 2H, $^3J_{\text{H-H}}$ = 8 Hz, Ph-H$_{meta}$), 8.15 (d, 2H, $^3J_{\text{H-H}}$ = 6 Hz, Py-H$_{meta}$), 8.87 (s, 2H, Py-H$_{meta'}$), 8.96 (d, 2H, $^3J_{\text{H-H}}$ = 6 Hz, $^3J_{\text{Pt-H}}$ = 19 Hz, Py-H$_{ortho}$). Anal. Calcd. for C$_{25}$H$_{30}$BrN$_2$BO$_6$Pt (%): C: 40.56, H: 4.08, N: 3.78; Found: C: 40.64, H: 4.05, N: 3.75.

[PtBrMe$_2$(CH$_2$-2-C$_6$H$_4$-B{OH}$_2$)(DECBP)], 5.18. This was prepared similarly to complex **5.15** from complex **5.2** (0.079 g, 0.150 mmol) in acetone (10 mL), and o-BrCH$_2$-4-C$_6$H$_4$B{OH}$_2$ (0.032 g, 0.150 mmol). A yellow product was produced. Yield 88 %. ^{1}H NMR acetone-d$_6$: δ = 1.44 (t, 6H, $^3J_{\text{H-H}}$ = 7 Hz, CH$_3$C), 1.52 (s, 6H, $^2J_{\text{Pt-H}}$ = 71 Hz, Pt-CH$_3$), 3.36 (s, 2H, $^2J_{\text{Pt-H}}$ = 94 Hz, Pt-CH$_2$), 4.50 (q, 4H, $^3J_{\text{H-H}}$ = 7 Hz, CH$_2$C), 6.62 (m, 2H, Ph-H$_{ortho+meta}$), 6.71 (t, 1H, $^3J_{\text{H-H}}$ = 7 Hz, Ph-H$_{para}$), 6.93 (d, 1H, $^3J_{\text{H-H}}$ = 7 Hz, Ph-H$_{meta'}$), 8.09 (d, 2H, $^3J_{\text{H-H}}$ = 5 Hz, Py-H$_{meta}$), 8.82 (s, 2H, Py-H$_{meta'}$), 8.90 (d, 2H, $^3J_{\text{H-H}}$ = 5 Hz, $^3J_{\text{Pt-H}}$ = 19 Hz, Py-H$_{ortho}$). Anal. Calcd. for C$_{25}$H$_{30}$BrN$_2$BO$_6$Pt (%): C: 40.56, H: 4.08, N: 3.78; Found: C: 40.55, H: 3.97, N: 3.72.

X-ray Structure Determinations: X-ray data were obtained and solutions were determined by Dr. G. Popov and Dr. M. Jennings. Suitable crystals were mounted on a glass fiber, and data were collected at low temperature (-123 °C) on a Nonius Kappa-CCD area detector diffractometer with COLLECT (Nonius B.V., 1997-2002). The unit cell parameters were calculated and refined from the full data set. The crystal data and refinement parameters for all complexes are listed in the following tables.

Table 5.13. Crystallographic data for complex **5.2**.

_____

$[PtMe_2(DECBP)]$

_____

Empirical formula	C18 H22 N2 O4 Pt
Wavelength	0.71073 Å
Crystal system	Monoclinic
Space group	P 2_1/c
Unit cell dimensions	a = 8.137(3) Å $\quad$ α= 90°
	b = 31.798(1) Å $\quad$ β= 92.39(2)°
	c = 13.789(5) Å $\quad$ γ = 90°
Volume	3564.4(2) Å^3
Z	8
Density (calculated)	1.958 Mg/m^3
Absorption coefficient (μ)	7.898 mm^{-1}
Crystal size	0.33 x 0.13 x 0.05 mm^3
Refinement method	Full-matrix least-squares on F^2
Goodness-of-fit on F^2	1.163
Final R indices [I>2sigma(I)]	R1 = 0.0961, wR2 = 0.2298
R indices (all data)	R1 = 0.1207, wR2 = 0.2430

Table 5.14. Crystallographic data for complex **5.4**.

	[PtI$_2$Me$_2$(DECBP)]	
Empirical formula	C18 H22 I5 N2 O4 Pt	
Formula weight	1159.97	
Wavelength	0.71073 Å	
Crystal system	Triclinic	
Space group	P -1	
Unit cell dimensions	a = 6.968(3) Å	α= 97.25(3)°
	b = 11.760(7) Å	β= 93.58(3)°
	c = 17.103(8) Å	γ = 96.17(3)°
Volume	1378.16(12) Å^3	
Z	2	
Density (calculated)	2.795 Mg/m^3	
Absorption coefficient(μ)	10.716 mm^{-1}	
Crystal size	0.15 x 0.10 x 0.08 mm^3	
Refinement method	Full-matrix least-squares on F^2	
Goodness-of-fit on F^2	1.061	
Final R indices [I>2sigma(I)]	R1 = 0.0353, wR2 = 0.0856	
R indices (all data)	R1 = 0.0463, wR2 = 0.0909	

Table 5.15. Crystallographic data for complex **5.5**.

	[PtBr$_2$Me$_2$(DECBP)]

Empirical formula	C18 H22 Br2 N2 O4 Pt
Formula weight	685.29
Wavelength	0.71073 Å
Crystal system	Monoclinic
Space group	P 2$_1$/n
Unit cell dimensions	a = 12.068 (1) Å $\quad$ α= 90°
	b = 6.459(7) Å $\quad$ β= 95.308(5)°
	c = 26.273(3) Å $\quad$ γ = 90°
Volume	2039.4(4) Å^3
Z	4
Density (calculated)	2.232 Mg/m^3
Absorption coefficient(μ)	10.825 mm^{-1}
Crystal size	0.28 x 0.22 x 0.05 mm^3
Refinement method	Full-matrix least-squares on F^2
Goodness-of-fit on F^2	1.059
Final R indices [I>2sigma(I)]	R1 = 0.0682, wR2 = 0.1854
R indices (all data)	R1 = 0.0825, wR2 = 0.1986

Table 5.16. Crystallographic data for complex **5.6a**.

[Pt(CH₃CO)ClMe₂(DECBP)]		

Empirical formula	C20 H25 Cl N2 O5 Pt	
Formula weight	603.96	
Wavelength	0.71073 Å	
Crystal system	Monoclinic	
Space group	P 2_1/c	
Unit cell dimensions	a = 9.846(3) Å	α = 90°
	b = 12.273(4) Å	β = 100.873(2)°
	c = 18.078(5) Å	γ = 90°
Volume	2145.33(11) Å^3	
Z	4	
Density (calculated)	1.870 Mg/m^3	
Absorption coefficient(μ)	6.698 mm^{-1}	
Crystal size	0.47 x 0.25 x 0.05 mm^3	
Refinement method	Full-matrix least-squares on F^2	
Goodness-of-fit on F^2	1.057	
Final R indices [I>2sigma(I)]	R1 = 0.0447, wR2 = 0.1181	
R indices (all data)	R1 = 0.0489, wR2 = 0.1221	

Table 5.17. Crystallographic data for complex [PtClMe(DECBP)].

_____

_____

Empirical formula	C17.50 H20 Cl2 N2 O4 Pt
Formula weight	588.34
Wavelength	0.71073 Å
Crystal system	Triclinic
Space group	P -1
Unit cell dimensions	a = 9.798(5) Å $\quad$ α= 95.26(3)°
	b = 13.443(1) Å $\quad$ β= 93.08(4)°
	c = 14.715(1) Å $\quad$ γ = 90.06(4)°
Volume	1927.1(2) Å^3
Z	4
Density (calculated)	2.028 Mg/m^3
Absorption coefficient(μ)	7.584 mm^{-1}
Crystal size	0.35 x 0.07 x 0.03 mm^3
Refinement method	Full-matrix least-squares on F^2
Goodness-of-fit on F^2	0.995
Final R indices [I>2sigma(I)]	R1 = 0.0614, wR2 = 0.1554
R indices (all data)	R1 = 0.0856, wR2 = 0.1707

Table 5.18. Crystallographic data for complex **5.8**.

	[PtCl$_2$(DECBP)]

Empirical formula	C16 H16 Cl2 N2 O4 Pt
Formula weight	566.30
Wavelength	0.71073 Å
Crystal system	Triclinic
Space group	P -1
Unit cell dimensions	a = 9.186(1) Å $\qquad$ α= 61.46(4)°
	b = 14.743(2) Å $\qquad$ β= 84.53(6)°
	c = 15.111(2) Å $\qquad$ γ = 85.25(7)°
Volume	1788.1(4) Å^3
Z	4
Density (calculated)	2.104 Mg/m^3
Absorption coefficient(μ)	8.170 mm^{-1}
Crystal size	0.47 x 0.15 x 0.03 mm^3
Refinement method	Full-matrix least-squares on F^2
Goodness-of-fit on F^2	1.059
Final R indices [I>2sigma(I)]	R1 = 0.0635, wR2 = 0.1835
R indices (all data)	R1 = 0.0796, wR2 = 0.1999

Table 5.19. Crystallographic data for complex **5.10**.

[PtBrMe$_2$(CH$_2$-4-C$_6$H$_4$CO$_2$H)(DECBP)]		
Empirical formula	C$_{29}$H$_{35}$BrN$_2$O$_7$Pt	
Formula weight	798.59	
Wavelength	0.71073 Å	
Crystal system	monoclinic	
Space group	P 2$_1$/n	
Unit cell dimensions	a = 7.434(3) Å	$\alpha = 90°$
	b = 33.108(1) Å	$\beta = 94.14(2)°$
	c = 12.010(5) Å	$\gamma = 90°$
Volume	2948.2(2) Å^3	
Z	4	
Density (calculated)	1.799 Mg/cm^3	
Absorption coefficient(μ)	6.163 mm^{-1}	
Crystal size	0.01 x 0.04 x 0.07 mm	
Refinement method	Full-matrix least-squares on F^2	
Goodness-of-fit on F^2	1.164	
Final R indices [I>2sigma(I)]	R1 = 0.0373, wR2 = 0.0670	
R indices (all data)	R1 = 0.0546, wR2 = 0.0708	

Table 5.20. Crystallographic data for complex **5.12**.

[PtBrMe$_2$(CH$_2$-CO$_2$H)(DECBP)]		
Empirical formula	C$_{20}$H$_{25}$BrN$_2$O$_6$Pt	
Formula weight	664.42	
Wavelength	0.71073 Å	
Crystal system	monoclinic	
Space group	C 2/c	
Unit cell dimensions	a = 23.124(1) Å	$\alpha = 90°$
	b = 6.837(4) Å	$\beta = 92.47(2)°$
	c = 30.223(2) Å	$\gamma = 90°$
Volume	4774.1(5) Å^3	
Z	8	
Density (calculated)	1.849 Mg/cm^3	
Absorption coefficient(μ)	7.588 mm^{-1}	
Crystal size	0.01 x 0.01 x 0.05 mm	
Refinement method	Full-matrix least-squares on F^2	
Goodness-of-fit on F^2	1.130	
Final R indices [I>2sigma(I)]	R1 = 0.0558, wR2 = 0.0957	
R indices (all data)	R1 = 0.0981, wR2 = 0.1067	

Table 5.21. Crystallographic data for complex **5.14**.

[PtBrMe$_2$(CH$_2$-CONH-C$_6$H$_5$)(DECBP)]	

Empirical formula	C$_{26}$H$_{30}$BrN$_3$O$_5$Pt	
Formula weight	739.51	
Wavelength	0.71073 Å	
Crystal system	monoclinic	
Space group	P 2$_1$/c	
Unit cell dimensions	a = 7.269(2) Å	α = 90°
	b = 16.904(3) Å	β = 96.66(3)°
	c = 22.105(4) Å	γ = 90°
Volume	26.98.0(9) Å^3	
Z	4	
Density (calculated)	1.821 Mg/cm^3	
Absorption coefficient(μ)	6.722 mm^{-1}	
Crystal size	0.20 x 0.15 x 0.12 mm^3	
Refinement method	Full-matrix least-squares on F^2	
Goodness-of-fit on F^2	1.005	
Final R indices [I>2sigma(I)]	R1 = 0.0432, wR2 = 0.0809	
R indices (all data)	R1 = 0.0677, wR2 = 0.0867	

Table 5.22. Crystallographic data for complex **5.16**.

$[PtBrMe_2(CH_2\text{-}3\text{-}C_6H_4B\{OH\}_2)(DECBP)]$

Empirical formula	$C_{25}H_{30}BBrN_2O_6Pt$
Formula weight	740.32
Wavelength	0.71073 Å
Crystal system	monoclinic
Space group	$P\,2_1/n$
Unit cell dimensions	a = 7.294(4) Å $\alpha = 90°$
	b = 12.909(7) Å $\beta = 91.64(2)°$
	c = 28.118(15) Å $\gamma = 90°$
Volume	$2646.5(2)\ \text{Å}^3$
Z	4
Density (calculated)	$1.858\ \text{Mg/cm}^3$
Absorption coefficient(μ)	$6.854\ \text{mm}^{-1}$
Crystal size	0.02 x 0.02 x 0.03 mm
Refinement method	Full-matrix least-squares on F^2
Goodness-of-fit on F^2	1.023
Final R indices [I>2sigma(I)]	R1 = 0.0305, wR2 = 0.0493
R indices (all data)	R1 = 0.0536, wR2 = 0.0549

Table 5.23. Crystallographic data for complex **5.17**.

[PtBrMe$_2$(CH$_2$-4-C$_6$H$_4$B{OH}$_2$)(DECBP)]	

Empirical formula	C$_{25}$H$_{30}$BBrN$_2$O$_6$Pt
Formula weight	740.32
Wavelength	0.71073 Å
Crystal system	triclinic
Space group	P -1
Unit cell dimensions	a = 11.451(4) Å α = 92.11(9)°
	b = 12.132(4) Å β = 112.05(9)°
	c = 12.267(4) Å γ = 117.42(8)°
Volume	1355.8(8) Å^3
Z	2
Density (calculated)	1.813 Mg/cm^3
Absorption coefficient(μ)	6.689 mm^{-1}
Crystal size	0.02 x 0.02 x 0.03 mm
Refinement method	Full-matrix least-squares on F^2
Goodness-of-fit on F^2	1.022
Final R indices [I>2sigma(I)]	R1 = 0.0402, wR2 = 0.0651
R indices (all data)	R1 = 0.0683, wR2 = 0.0730

Table 5.24. Crystallographic data for complex **5.18**.

[PtBrMe$_2$(CH$_2$-2-C$_6$H$_4$B{OH}$_2$)(DECBP)]	

Empirical formula	C$_{25}$H$_{30}$BBrN$_2$O$_6$Pt	
Formula weight	740.32	
Wavelength	0.71073 Å	
Crystal system	monoclinic	
Space group	P 2$_1$/c	
Unit cell dimensions	a = 20.654(4) Å	α = 90°
	b = 13.466(3) Å	β = 101.06(6)°
	c = 19.897(4) Å	γ = 90°
Volume	5431.(2) Å^3	
Z	8	
Density (calculated)	1.811 Mg/cm^3	
Absorption coefficient(μ)	6.680 mm^{-1}	
Crystal size	0.01 x 0.01 x 0.02 mm	
Refinement method	Full-matrix least-squares on F^2	
Goodness-of-fit on F^2	1.005	
Final R indices [I>2sigma(I)]	R1 = 0.0432, wR2 = 0.0677	
R indices (all data)	R1 = 0.0867, wR2 = 0.0809	

5.5 References

1. a) Haiduc, I.; Edelmann, F. T. *Supramolecular Organometallic Chemistry;* Wiley-VCH: Weinheim, Germany, **1999**. b) Atwood, J. L.; Steed, J. W. *Encyclopedia of Supramolecular Chemistry*, Marcel Dekker: New York, **2004**.

2. a) Jeffrey, G. A. *An Introduction to Hydrogen Bonding*. Oxford University Press: New York, **1997**. b) Desiraju, G. M.; Steiner, T. *The Weak Hydrogen Bond in Structural Chemistry and Biology*, Oxford University Press, **1999**.

3. a) Canty, A. J., Ed. *Comprehensive Organometallic Chemistry III; Elsevier*: Amsterdam, **2007**, Vol. 8. b) Seyferth, D. *Organometallics*, **2001**, 20, 2940.

4. a) Addicott, C.; Das, N.; Stang, P. J. *Inorg. Chem.* **2004**, 43, 5335. b) Au, R. H.; Jennings, M. C.; Puddephatt, R. J. *Organometallics*, **2009**, 28, 3754. c) Zheng, Y. R.; Yang, H. B.; Northrop, B. H.; Ghosh, K.; Stang, P. J. *Inorg. Chem.* **2008**, 47, 4706.

5. a) Au, R. H.; Jennings, M. C.; Puddephatt, R. J. *Organometallics*, **2009**, 28, 3734. b) Robin, A. Y.; Fromm, K. M. *Coord. Chem. Rev.* **2006**, 250, 2127. c) Braga, D.; Grepioni, F. *Coord. Chem. Rev.* **1999**, 183, 117.

6. Au, R. H.; Jennings, M. C.; Puddephatt, R. J. *Organometallics*, **2009**, 28, 5052.

7. a) Scott, J. D.; Puddephatt, R. J. *Organometallics*, **1983**, 2, 1643. b) Achar, S.; Scott, J. D.; Vittal, J. J.; Puddephatt, R. J. *Organometallics*, **1993**, 12, 4592. c) Achar, S.; Catalano, V. J. *Polyhedron*, **1997**, 16, 1555.

8. Fraser, C. S.; Eisler, D. J.; Puddephatt, R. J. *Polyhedron*, **2006**, 25, 266.

9. a) Au, R. H.; Jennings, M. C.; Puddephatt, R. J. *Dalton Trans*. **2009**, 3519. b) Reddy, K. L.; *Tet. Lett.*, **2003**, 44, 1453.

10. Sprintschnik, G.; Sprintschnik, H.; Kirsch, P.; Whitten, D. *J. Am. Chem. Soc.*, **1977**, 4947.

11. Hill, G.; Irwin, M. J.; Levy, C. J.; Rendina, L. M.; Puddephatt, R. J. *Inorganic Syntheses*, **1998**, 32, 149.

12. Zhang, F.; Broczkowski, M. E.; Jennings, M,. C.; Puddephatt, R. *J. Can. J. Chem.*, **2005**, 83, 595.

13. Nabavizadeh, S. M.; Hoseini, S. J.; Momeni, B. Z.; Shahabadi, N.; Rashidi, M.; Pakiari, A. H.; Eskandari, K. *Dalton Trans.*, **2008**, 2414.

14. Basch, A.; Hartl, M.; Behrens, P. *Microporous and Mesoporous Materials*, **2007**, 99, 244.

15. Zhang, F.; Prokopchuk, E. M.; Broczkowski, M. E.; Jennings, M,. C.; Puddephatt, R. *Organometallics*, **2006**, 25, 1583.

16. Taylor, R. A.; Law, D. J.; Sunley, G,. J.; White, A. J.; Britovsek, G. J. *Chem. Commun.*, **2008**, 24, 2800.

17. a) De Felice, V.; Giovannitti, B.; De Renzi, A.; Tesauro, D.; Panunzi, A. *J. Organomet. Chem.*, **2000**, 445, 593. b) Canty, A. J.; Jin, H.; Skelton, B. W.; White, A. H. *Inorg. Chem.*, **1998**, 37, 3975.

18. a) Hall, J. R.; Swile, G. A. *J. Organomet. Chem.*, **1976**, 122, C22. b) Agnew, H. N.; Appleton, T. G.; Hall, J. R. *Aust. J. Chem.*, **1982**, 35, 881.

19. Bernstein, J.; Davis, R. E.; Shimoni, L.; Chang, N. L. *Angew. Int. Ed. Engl.* **1995**, 34, 1555.

20. a) Bohm, H. J.; Klebe, G.; Brode, S.; Hesse, U. *Chem. Eur. J.*, **1996**, 2, 1509. b) Gleitsman, K. R.; Lester, H. A.; Dougherty, D. A. *ChemBioChem.*, **2009**, 10, 1385.

21. Dobrzanska, L. *Acta Crystallogr., Sect.*, E . **2005**, 61, m1625.

22. a) Allen, F. H.; Raithby, P. R.; Shields, G. P.; Taylor, R. *J. Chem. Soc., Chem. Commun.* **1998**, 1043. b) Davis, C. J.; Lewis, P. T.; Billodeax, D. R.; Fronczek, F. R.; Escobedo, J. O.; Strongin, R. M.; *Org. Lett.*, **2001**, 3, 2443.

23. Takeuchi, M.; Ikeda, M.; Sugasaki, A.; Shinkai, S. *Acc. Chem. Res.*, **2001**, 34, 865.

24. a) Fournier, J. H.; Maris, T.; Wuest, J. D.; Guo, W.; Galoppini, E. *J. Am. Chem. Soc.*, **2003**, 125, 1002. b) Hosseini, M. W. *Acc. Chem. Res.*, **2005**, 38, 313.

25. Cyranski, M. K.; Jezierska, A.; Klimentowska, P.; Panek, J. J.; Sporzynski, A. *J. Phys. Org. Chem.*, **2008**, 21, 472.

CHAPTER 6

General Conclusions

In this work, new mononuclear and binuclear organoplatinum complexes containing bidentate nitrogen donor ligands have been synthesized. The new platinum complexes were characterized by ^{1}H-NMR, ^{13}C-NMR, ^{19}F-NMR, IR, UV visible, mass spectrometry, and by elemental analysis. Several molecular structures were determined by X-ray crystallography. Reaction mechanisms and rates of exchange in a few cases were deduced using variable temperature ^{1}H-NMR spectroscopy.

Several new dimethylplatinum(II) complexes were prepared. These complexes undergo easy oxidative addition of alkyl halides, halogens, and peroxides, which resulted in the formation of novel platinum(IV) complexes. In some cases, the reverse process reductive elimination occurred. The oxidative addition and reductive elimination processes are vital to organometallic chemistry, and play a major role in catalytic cycles. Therefore, the results of our work provide a significant advancement in the understanding of the chemistry of organoplatinum complexes, and how the different designs of bidentate nitrogen ligands can be used to tune the reactivity of the platinum complexes.

Square planar platinum(II) complexes which form 5-membered chelating rings with bipyridine ligands were found to be unreactive in the activation of C-H bonds in hydrocarbons due to the steric effects caused by the *ortho* hydrogens on the pyridine rings. On the other hand, non planar platinum(II) complexes which form 6-membered chelating rings with bis-pyridine ligands were successful in activating C-H bonds in arenes, since the *ortho* hydrogen atoms of the pyridyl groups are moved out of the plane causing the complex to be more reactive due to less steric effects. In chapter 2, the plan was to test out the catalytic activity of a different ligand design with a potential complication due to the big chelate ring size, so a platinum(II) complex containing the bidentate nitrogen donor ligand 1,2-bis(2-pyridyl)ethane (dpe) which forms a 7-

membered chelating ring is synthesized. It is shown that the dimethylplatinum(II) complex [PtMe$_2$(dpe)] undergoes easy oxidative addition to give platinum(IV) complexes, but the octahedral platinum(IV) products have limited thermal stability. The ligand bpe forms stable complexes with square planar platinum(II), such as complexes [PtI$_2$(dpe)] and [PtBr$_2$(dpe)], in which the 7-membered Pt(bpe) chelate ring is in the boat conformation. The dimethylplatinum(II) complex reacts rapidly with MeI forming the known complex [PtIMe$_3$)$_4$]. The variable-temperature ^{1}H-NMR experiment for the reaction of CD$_3$I with [PtMe$_2$(dpe)] showed that platinum(II) complex is reactive to oxidative addition, but that the dpe ligand easily undergoes dissociation to form the known cubane structure. In reactions with bromine or iodine or HCl, the respective platinum(IV) complexes are formed initially but they decompose primarily via reductive elimination of MeX (X = Cl, Br or I) to give the platinum(II) complexes respectively. The reaction of [PtMe$_2$(dpe)] with hydrogen peroxide occurs with ligand loss to give [{PtMe$_2$(OH)$_2$}], but the reaction mixture then slowly yields crystals of [Pt$_4$(μ-OH)$_4$(μ_3-OH)$_2$Me$_{10}$], as a mixed complex with [PtMe$_2$(CO$_3$)(bpe)], while the reaction of the dimethylplatinum(II) complex with oxygen in methanol results in the formation of the complex [Pt$_4$(μ-OH)$_2$(μ-OMe)$_2$(μ_3-OMe)$_2$Me$_{10}$]. Both complexes are novel, in which the central cluster has unexpected structure based on a face-bridged double cubane. The easy dissociation of the chelate ring plays a major role in the reactivity of the platinum(II) complex, which results in unexpected discoveries.

In chapter 3, the synthesis and the reactions of the dimethylplatinum(II) complex [PtMe$_2$(bps)] are described. The 6-membered chelate ring was used to prevent easy dissociation of the ligand, while the idea of using a bigger silicon atom to bridge the two pyridyl groups instead of carbon was meant to increase the mean twist of the pyridyl groups from the square

plane which could potentially lead to a highly reactive platinum(II) complex. The platinum (II) complex was found to be highly reactive toward peroxides, halogens, organic halides, and alcohols. The reaction of [PtMe$_2$(bps)] with B(C$_6$F$_5$)$_3$ in trifluoroethanol in air occurred to give the unexpected novel binuclear complex [Me(bps)Pt-OSiMe(2-C$_5$H$_4$N)$_2$PtMe$_3$]$^+$ [B(OCH$_2$CF$_3$)(C$_6$F$_5$)$_3$]$^-$, containing a platinum(II) and platinum(IV) centers. The formation of binuclear platinum complex could be explained via the competitive methyl platinum group cleavage from [PtMe$_2$(bps)] by the acid H[B(OCH$_2$CF$_3$)(C$_6$F$_5$)$_3$] to give the platinum(II) fragment and oxidation by air to give the platinum(IV) fragment. Combination of the two units then gives the binuclear complex which involves a very easy methylsilicon group cleavage reaction. The oxidation of the complex [PtMe$_2$(bps)] by oxygen, hydrogen peroxide or dibenzoyl peroxide in the presence of water or alcohol gives the complex cation, [PtMe$_3$(κ^3-*N,N,O*-HOSiMe(2-C$_5$H$_4$N)$_2$)]+, in a reaction involving easy cleavage of a methylsilicon bond. The reaction of [PtMe$_2$(bps)] with MeOTf proceeds in acetone to produce [PtMe(OH$_2$)(bps)]$^+$[CF$_3$SO$_3$]$^-$ via oxidative addition. The two methylsilicon groups undergo fast exchange at room temperature, and also the three methyl-platinum groups, and such fast exchange probably occurs via a 5-coordinate platinum(IV) intermediate. The exchange can be stopped at lower temperatures. The use of a solvent that can coordinate very well to platinum(IV) complexes such as acetonitrile resulted in the formation of the complex [PtMe$_3$(NCCD$_3$)(bps)]$^+$ [CF$_3$SO$_3$]$^-$ which shows no fast methyl exchange at elevated temperatures.

Chapter 4 has dealt with incorporation of five-membered heterocyclic imidazole ligands that were chosen to vary the donor ability of the rings. The chosen imidazole ligands have potential in coordination chemistry as relatives of the planar 2,2'-bipyridyl. Both of the synthesized platinum(II) complexes containing imidazole ligands undergo oxidative addition

reactions with a broad variety of alkyl halides, peroxides, and halogens forming thermodynamically stable platinum(IV) complexes, which provide benchmark spectroscopic data. For example, the complex [PtMe$_2${(mim)$_2$C=CH$_2$}] reacts with MeI via oxidative addition reaction yielding the expected platinum(IV) complex. The platinum(II) complex is high reactive to benzyl bromide ligands, where all reactions results in the formation of the respective platinum(IV) complexes in two isomeric forms, *cis* and *trans*. The complex [PtMe$_2${(mim)$_2$C=CH$_2$}] is reactive toward halogenated solvents, which is shown through the oxidative of C-Cl bond of methylene chloride forming the platinum(IV) isomers *trans* and *cis* in an unexpected 1:2 ratio. The complex [PtMe$_2${(mim)$_2$C=CH$_2$}] reacts with H$_2$O$_2$ yielding the *trans* platinum(IV) complex as the only product, while it reacts with dibenzoyl peroxide forming the *cis* platinum(IV) complex as the only product. On the other hand, the complex [PtMe$_2${(mim)$_2$CHMe}] shows similar high reactivity toward organic halides, peroxides, and halogens. The presence of two different groups on the bridging carbon center yields two different *trans* isomer upon reaction with MeI, while it yields only one *trans* isomer upon reactions with iodine and hydrogen peroxide. The reactions with the bulkier benzyl bromide ligands showed only *trans* stereoselectivity with the methyl group on the bridging carbon and the benzyl group anti to each other. These ligands are shown to be highly reactive with potential to be capable of activation of inert bonds in hydrocarbons.

Finally, chapter 5 contains the reactions of the platinum(II) complex containing the ligand DECBP ligand which has two ester units, whose O=C carbonyl oxygen atoms can act as hydrogen bond acceptors. The main aim of this work was to develop the supramolecular chemistry of the complex [PtMe$_2$(DECBP)(LL)] by incorporating alkyl groups containing carboxylic acid, alcohols and amide units for hydrogen bonding. The complex [PtMe$_2$(DECBP)]

reactivity is studied first through various reactions with organic halide, peroxides, and halogens. The platinum(II) complex undergoes easy oxidative addition with alkyl bromides RCH₂Br, which have a carboxylic acid and amide functional groups in its R groups yielding stable platinum(IV) complexes. Those complexes self-assemble in the solid state to form supramolecular polymers through hydrogen bonding interactions and other weak interactions. Finally, the oxidative addition of *ortho-*, *meta-*, and *para-*(bromomethyl)phenyl boronic acids resulted in forming the *trans* isomers of the platinum(IV) complexes. The platinum(IV) complexes containing boronic acids self-assemble in the solid state to give supramolecular polymers through weak intermolecular secondary bonds. The obtained structures indicate the continued promise of interesting new structures in supramolecular organoplatinum complexes.

VITA

NAME:	Muhieddine Ahmad Safa
PLACE OF BIRTH:	Salmiyah, Hawalli, Kuwait
POST-SECONDARY	
EDUCATION AND	
DEGREES:	Ph.D. (Chemistry)
	The University of Western Ontario
	London, Ontario, Canada
	2007 – 2011
	H. BSc. (Chemistry)
	The University of Western Ontario
	London, Ontario, Canada
	2004 – 2007

PUBLICATIONS:

1. Safa, M.; Dong, Z.; Song, Y.; Huang, Y. "Examining the Structural Changes in $Fe_2(CO)_9$ Under High External Pressures by Raman Spectroscopy" *Can. J. Chem.*, **2007**, 85, 866.

2. Safa, M.; Jennings, M. C.; Puddephatt, R. J. "A Double Cubane Structure in Organoplatinum(IV) Chemistry" *Chem. Commun.*, **2009**, 1487.

3. Safa, M.; Jennings, M. C.; Puddephatt, R. "Easy Oxidatively Induced Silicon-Carbon Bond Activation in Organoplatinum Chemistry" *Chem. Commun.*, **2010**, 46, 2811.

4. Safa, M.; Jennings, M. C.; Puddephatt, R. J. "The Chemistry of [PtMe$_2$(1,2-bis(2-pyridyl)ethane)]: Remarkable Impact of an Easily Dissociated Chelate Ligand" *Organometallics*, **2011**, 30, 5625.

5. Safa, M.; Abo-Amer, A.; Puddephatt, R. J. "Self-Assembly of Organoplatinum(IV) Boronic Acids" *Organometallics*. Submitted.

PRESENTATIONS:

1. Safa, M. "Examining the structural change in Fe$_2$(CO)$_9$ under high external pressure by Raman spectroscopy " SOUSCC, UOIT, Oshawa, **2007.**

2. Safa, M. "C-H Bond Activation by a Derivatized Bis(pyridine) Platinum(II) Complex" 91st CSC meeting, Edmonton, Alberta, **2008**.

3. Safa, M. "The Chemistry of Platinum Complexes with Bidentate N-donor Ligand" 93rd CSC meeting, Toronto, Ontario, **2010**.

HONOURS AND AWARDS:

1. WGRS Scholarship (UWO)   May 2007 – April 2012
2. Dean's Honour List (UWO)   Sept 2006 – April 2007